ESTIMATION OF TWO-PHASE PETROLEUM RESERVOIR PROPERTIES

Thesis by

Albert Theodore Watson, Jr.

In Partial Fulfillment of the Requirements

for the Degree of

Doctor of Philosophy

California Institute of Technology
Pasadena, California

1980

(Submitted August 27, 1979)

ACKNOWLEDGMENTS

I would like to express my sincere appreciation to Professors J. H. Seinfeld and G. R. Gavalas for their guidance during the course of this research. The assistance by Dr. P. T. Woo is also gratefully acknowledged.

Financial support from the California Institute of Technology is gratefully acknowledged. Financial support, as well as various technical services, from Chevron Oil Field Research Company is also gratefully acknowledged.

The aid of Denise Heiman, Lenore Kerner and others who typed this thesis is acknowledged.

I would also like to thank my parents for their kind and understanding support, and encouragement, during my years as a student.

ABSTRACT

The estimation of petroleum reservoir properties on the basis of production rate and pressure observations at the wells is an essential component in the prediction of reservoir behavior. The reservoir properties to be estimated appear as parameters in the partial differential equations describing the flow of fluids in the reservoir. The estimation of these properties is referred to variously as the inverse or identification problem or as history matching. In this dissertation, new results have been obtained pertaining to the estimation of petroleum reservoir properties.

Most of the prior analysis of the reservoir parameter estimation problem has been confined to reservoirs containing a single fluid phase, e.g., oil. We consider here reservoirs that contain two fluid phases, e.g., oil and water. The parameters to be estimated in such a case are the porosity and permeability, which depend on spatial location, and the saturation-dependent relative permeabilities. In this work we treat two basic problems in reservoir parameter estimation: (1) establishing the ability to estimate the desired parameters (so-called identifiability), and (2) developing and testing a new algorithm, based on optimal control theory, to carry out the estimation.

In regard to problem (1), we have extended the classic analytical (Buckley-Leverett) solution for incompressible flow to heterogeneous reservoirs. Analysis for an incompressible water flooding situation shows that the spatially varying properties at locations behind the saturation front have an effect on the pressure solution. The spatially varying

properties can be uniquely determined based on data taken up to the time of water breakthrough. Only an integral value of the porosity can be determined from the water-oil ratio data alone; however, the spatially varying porosity may be determined when the initial saturation varies with location. The values of the relative permeabilities which are identifiable, and the information about the relative permeabilities obtained for other intervals of saturation, is established. Analytical expressions are derived for the sensitivity of the pressure and water-oil ratio observations to parameters appearing in functional forms of the relative permeabilities. When the relative permeabilities are represented as exponential functions, the coefficients and exponents can be uniquely determined.

For problem (2), an algorithm is developed for the estimation of porosity, permeability and the relative permeabilities for two-phase, compressible reservoirs. This work represents the first study for which relative permeabilities have been estimated based on a model generally used to represent fluid flow in petroleum reservoirs. An objective function, composed of the weighted sum of squares of the deviations between the observed and calculated values of pressure and water-oil ratio, is minimized by a first-order gradient method based on optimal control theory. The algorithm is tested for one- and two-dimensional hypothetical water floods. The algorithm performed well for problems in which the porosity, permeability and relative permeability exponents were simultaneously estimated. The increase from one to two spatial variables does not appear to change the properties of the estimation problem. Small observation errors are shown not to significantly affect the convergence of the estimates.

Table of Contents

Table of Contents (con't)

Table of Contents (con't)

List of Figures

List of Figures (con't)

List of Figures (con't)

List of Tables

1. INTRODUCTION

The flow of fluids in multi-phase petroleum reservoirs is described by a system of coupled, nonlinear, partial differential equations. Generally, the reservoir boundaries and initial pressure and relative distributions of the fluids (the saturations) are established through geological and drilling data. The estimation of porous rock properties on the basis of pressure and flow rate data taken during production is an integral part of the mathematical modeling of the reservoir. The reservoir parameters that are to be estimated are the porosity and permeability, which are spatially varying, and the relative permeabilities, which are nonlinear functions of the saturations of the reservoir fluids. Thus, the reservoir parameter estimation or identification problem is one in which the parameters to be estimated may depend on the spatial variables, or the state, of the system.

Due to the complexity of the equations governing reservoir behavior, the estimation of multi-phase reservoir properties has received little attention. The work developed for the estimation of reservoir properties on the basis of data taken during production has been for single-phase (e.g., oil) reservoirs, or multi-phase reservoirs in which the spatially varying properties are to be estimated on the basis of pressure data alone.

We consider here the general two-phase parameter estimation (history matching) problem for fluid phases. The transient pressure and saturation for a two-phase, immiscible reservoir model are described by two coupled, nonlinear, partial differential equations. When capillary pressure is neglected, the reservoir properties in this model are the spatially varying

porosity and permeability, and the saturation-dependent relative permeabilities. We investigate the estimation of these parameters on the basis of data usually available during production. The available data consist of the pressure at the injection and production wells, and a ratio of the flow rates of the two fluids at the producing wells. The total flow rate at the wells is assumed to be known exactly. These specifications are common ones in field applications.

Although the solution of the reservoir model equations must usually be carried out numerically, there is a particular reservoir model for which the equations can be solved analytically. In this model, the reservoir fluids are taken to be incompressible, and the fluid flow is described by one spatial dimension. The analytical solution provides a convenient means for studying the structure of the estimation problem. In this dissertation we use the model to investigate the effect of the spatially varying properties — the porosity and permeability — and the saturation-dependent relative permeabilities on the observable quantities. We then develop an algorithm for the estimation of two-phase petroleum properties for the more general reservoir model.

In Chapter 2, the equations that describe the flow of fluids in a two-phase reservoir are derived. The particular two-phase system investigated is specified, and the partial differential equations for compressible and incompressible flow are classified. In Chapter 3, the analytical solution for one-dimensional, incompressible flow is developed. The effects of the spatially varying properties and the relative permeabilities on the solution of this system are illustrated. In Chapter 4, the numerical solution of the compressible reservoir model by the method

of finite-differences is developed.

The identifiability of the reservoir parameters is investigated in Chapter 5. Based on the incompressible reservoir model, we establish the observations of pressure or the ratio of the flow rates over intervals of time which will be important in the determination of the reservoir parameters. The observability of the spatially varying and saturation-dependent parameters is established. In Chapter 6 an algorithm for the estimation of reservoir properties in a two-phase, compressible reservoir is developed. The performance of the algorithm is tested for one- and two-dimensional hypothetical reservoirs.

2. FLOW OF OIL AND WATER IN POROUS MEDIA

The partial differential equations used to describe the simultaneous flow of two fluid phases in porous media are presented in this chapter. In the first section, Darcy's law for single phase flow in porous media is given. This equation is extended to two-phase flow, and the particular form of the two-phase system which is investigated is presented in Subsection 2.1.3. Section 2.2 contains a general study of the nature of the governing partial differential equations.

2.1 Development of Equations for Oil-Water Flow in Porous Media

2.1.1 Single Phase Flow

The flow rate of a single phase through a horizontal porous material is represented by Darcy's law as:

$$Q = \frac{KA}{\mu} \frac{\Delta P}{L} \tag{2.1}$$

where Q is the volumetric flow rate of the fluid, μ is the viscosity of the fluid, A and L are the cross-sectional area and length of the system respectively, and ΔP is the pressure differential across the sample. The permeability K is a measure of the fluid conductivity of the porous material, and is typically given in units of darcies (or millidarcies). The unit of darcy is defined by Eq. 2.1 as follows: a porous material will have a permeability of one darcy if a pressure differential of 1 atm applied across a sample of the material with a cross-sectional area of 1 square cm and a length of 1 cm will produce a flow rate of 1 cubic cm per second when the fluid viscosity is 1 centipoise[1]. The unit darcy can be expressed as length squared.

The differential form of Darcy's law is

$$v = \frac{Q}{A} = - \frac{K}{\mu} \frac{\partial P}{\partial x} \tag{2.2}$$

where v is known as the superficial velocity, and the minus sign signifies that fluid flow is in the direction of decreasing pressure.

For multidimensional flow Darcy's law can be written as:

$$\underset{\sim}{v} = - \frac{\underset{\sim}{K}}{\mu} (\nabla P + \rho \underset{\sim}{g}) \tag{2.3}$$

where ρ is the density of the fluid, $\underset{\sim}{v}$ is the superficial velocity vector, and the vector $\underset{\sim}{g}$ denotes the magnitude and direction of the gravity force.

$\underset{\sim}{K}$ is a symmetric second rank tensor[2]. In this study we will make the usual assumption that the principal axes of permeability coincide with the directions of the coordinate system so that $\underset{\sim}{K}$ is diagonal.

2.1.2 Two-Phase, Immiscible Flow

To describe the simultaneous flow of two immiscible fluids in porous media, a Darcy equation is written to relate the superficial velocity of each phase to the pressure gradient of each phase:

$$\underset{\sim}{v}_w = - \frac{\underset{\sim}{K}_w}{\mu_w} (\nabla P_w + \rho_w \underset{\sim}{g}) \tag{2.4}$$

$$\underset{\sim}{v}_{nw} = - \frac{\underset{\sim}{K}_{nw}}{\mu_{nw}} (\nabla P_{nw} + \rho_{nw} \underset{\sim}{g}) \tag{2.5}$$

Due to the surface tension and curvature of the interphase between the two phases, one fluid, referred to as the wetting phase, tends to wet the porous medium more than the other fluid. The wetting fluid is denoted by the

subscript w, and the other fluid, referred to as the nonwetting phase, is denoted by the subscript nw. The saturation, or volumetric fraction of the void volume of the porous medium which is occupied by a particular fluid, is the measure of the relative amounts of each fluid which is present. Since the void volume is completely occupied by the two fluid phases, the following equation applies for the saturation S:

$$S_w + S_{nw} = 1 \tag{2.6}$$

The pressures of the two phases are related to each other by the capillary pressure P_c:

$$P_c = P_{nw} - P_w \tag{2.7}$$

Capillary pressure is empirically taken to be a function of the saturation of the wetting phase[1,3].

By relating the effective permeabilities $\underset{\sim}{K}_w$ and $\underset{\sim}{K}_{nw}$ to the single fluid permeability, $\underset{\sim}{K}$, the relative permeabilities k_{rw} and k_{rnw} can be defined:

$$k_{rw}\underset{\sim}{K} = \underset{\sim}{K}_w \tag{2.8}$$

$$k_{rnw}\underset{\sim}{K} = \underset{\sim}{K}_{nw} \tag{2.9}$$

The relative permeabilities are empirically taken to be functions of saturation and are assumed to be independent of direction[1]. Since the presence of one fluid tends to interfere with the flow of the other fluid, the relative permeabilities of each fluid should be less than or equal to one.

Two additional equations, the equations of continuity, can be written for each phase:

$$\frac{\partial(\phi\rho_w S_w)}{\partial t} = -\nabla\cdot(\rho_w \underset{\sim}{v}_w) + q_w \tag{2.10}$$

$$\frac{\partial(\phi\rho_{nw} S_{nw})}{\partial t} = -\nabla\cdot(\rho_{nw} \underset{\sim}{v}_{nw}) + q_{nw} \tag{2.11}$$

where ϕ is the porosity, or void fraction of the porous media, and q_w and q_{nw} represent source or sink terms.

Eqs. 2.4-7,10,11 represent the mathematical model for the flow of two immiscible phases in porous media. In order to solve these for the transient pressure and saturation of each phase, the following additional information is necessary: (1) appropriate boundary and initial conditions, (2) capillary pressure and relative permeabilities as functions of saturation, and (3) the porosity and fluid properties (densities and viscosities) as functions of pressure.

2.1.3 Simplified Model

We will confine our attention in this study to a less general model than that given above. Our model will be based upon petroleum reservoirs which can be represented by one or two horizontal dimensions. Since the areal dimensions in petroleum reservoirs are usually much greater than the thickness, and since reservoirs are usually more permeable in the horizontal direction than the vertical direction, many reservoirs are modeled as two-dimensional areal reservoirs[4]. The injection and production wells will be modeled as point sources or sinks in the continuity equations.

We will largely be concerned with water flooding problems. The two phases, oil and water, will be denoted by subscripts o and w, respectively. The effect of capillary pressure will be neglected as is often done in two-phase reservoir studies[5].

With these changes, the equations describing our system are:

$$\frac{\partial(\phi\rho_w S_w)}{\partial t} = -\nabla\cdot(\rho_w \underset{\sim}{v}_w) + \sum_{m=1}^{NW} q_{w_m}\delta(x_m - x)\delta(y_m - y) \tag{2.12}$$

$$\frac{\partial(\phi\rho_o S_o)}{\partial t} = -\nabla\cdot(\rho_o \underset{\sim}{v}_o) + \sum_{m=1}^{NW} q_{o_m}\delta(x_m - x)\delta(y_m - y) \tag{2.13}$$

$$\underset{\sim}{v}_w = -\frac{K\underset{\sim}{k}_{rw}}{\mu_w}\nabla P \tag{2.14}$$

$$\underset{\sim}{v}_o = -\frac{K\underset{\sim}{k}_{ro}}{\mu_o}\nabla P \tag{2.15}$$

$$S_o + S_w = 1 \tag{2.16}$$

where $\delta(x_m-x)$ is the Dirac delta function, NW is the number of wells, and x_m,y_m is the location of a single well. A positive value of q_{w_m} or q_{o_m} represents fluid injection, while a negative sign denotes production.

If the boundaries of the reservoir are taken to be impermeable, the necessary boundary condition on pressure and the initial conditions for pressure and saturation can be expressed as

$$\frac{\partial P}{\partial n} = 0 \quad \text{on } \partial \tag{2.17}$$

$$P(t=0) = P_{in} \tag{2.18}$$

$$S_w(t=0) = S_{in} \tag{2.19}$$

where n denotes the outward directed unit normal on the reservoir boundary ∂, and P_{in} and S_{in} denote the specified initial pressure and saturation. Rather than the no-flux boundary condition on pressure, values of pressure could be specified over some or all of the reservoir boundary.

In this study we will assume that fluid viscosities are independent of pressure. We will use the following relations to represent the fluid densities and porosity as functions of pressure:

$$c_w = \frac{1}{\rho_w} \frac{d\rho_w}{dP} \tag{2.20}$$

$$c_o = \frac{1}{\rho_o} \frac{d\rho_o}{dP} \tag{2.21}$$

$$c_r = \frac{1}{\phi} \frac{d\phi}{dP} \tag{2.22}$$

where constants c_w, c_o, and c_r are the compressibilities of water, oil, and the porous space, respectively.

When the rock properties, ϕ, $\underset{\sim}{K}$, k_{rw} and k_{ro}, and the well rates q_o and q_w are specified, Eqs. 2.12-22 can be solved for the transient pressure and saturation throughout the reservoir. These equations constitute the reservoir model. The remainder of this chapter, and Chapters 3 and 4, are devoted to the solution of these equations for transient pressure and saturation. Chapters 5 and 6 are concerned with the inverse problem - given portions of the solution, estimate the rock properties ϕ, K, k_{rw} and k_{ro}.

2.2 General Study of Oil-Water Flow Equations

In this section some preliminary remarks on the structure of the coupled partial differential equations 2.12-15 are made by deriving single partial differential equations for pressure and saturation[3]. For simplicity, in the following derivations we represent the source and sink terms in Eqs. 2.12 and 2.13 as simply q_w and q_o as was done in Eqs. 2.10 and 2.11.

2.2.1 Pressure Equation

By eliminating the flow velocities from Eqs. 2.12 and 2.13 and using Eqs. 2.16 to eliminate S_o from Eq. 2.13, the following set of coupled partial differential equations are obtained:

$$\frac{\partial(\phi\rho_w S_w)}{\partial t} = \nabla\cdot\left(\frac{K k_{rw}\rho_w}{\mu_w}\nabla P\right) + q_w \tag{2.23}$$

$$\frac{\partial[\phi\rho_o(1-S_w)]}{\partial t} = \nabla\cdot\left(\frac{K k_{ro}\rho_o}{\mu_o}\nabla P\right) + q_o \tag{2.24}$$

We will use the following steps to obtain a single partial differential equation for pressure: (1) expand the left hand sides of Eqs. 2.23 and 2.24, (2) use the compressibilities to eliminate the time derivatives of the porosity and densities, and (3) eliminate the time derivatives of saturation.

Expanding the left hand sides of Eqs. 2.23 and 2.24, we obtain:

$$\frac{\partial(\phi\rho_w S_w)}{\partial t} = \phi\rho_w\frac{\partial S_w}{\partial t} + S_w\left(\phi\frac{\partial\rho_w}{\partial t} + \rho_w\frac{\partial\phi}{\partial t}\right) \tag{2.25}$$

$$\frac{\partial[\phi\rho_o(1-S_w)]}{\partial t} = -\phi\rho_o \frac{\partial S_w}{\partial t} + (1-S_w)\left(\phi\frac{\partial \rho_o}{\partial t} + \rho_o \frac{\partial \phi}{\partial t}\right) \tag{2.26}$$

The following identities can be derived from Eqs. 2.20-22

$$\frac{\partial \rho_w}{\partial t} = \frac{d\rho_w}{dP}\frac{\partial P}{\partial t} = c_w\rho_w \frac{\partial P}{\partial t} \tag{2.27}$$

$$\frac{\partial \rho_o}{\partial t} = \frac{d\rho_o}{dP}\frac{\partial P}{\partial t} = c_o\rho_o \frac{\partial P}{\partial t} \tag{2.28}$$

$$\frac{\partial \phi}{\partial t} = \frac{d\phi}{dP}\frac{\partial P}{\partial t} = c_r\phi \frac{\partial P}{\partial t} \tag{2.29}$$

Using these relations to eliminate the derivatives of the density and porosity in Eq. 2.25, Eq. 2.23 can be written as:

$$\phi\rho_w\left[\frac{\partial S_w}{\partial t} + S_w(c_r+c_w)\frac{\partial P}{\partial t}\right] = \nabla\cdot\left[\frac{\underset{\sim}{K}k_{rw}}{\mu_w}\rho_w \nabla P\right] + q_w \tag{2.30}$$

Using a similar procedure, Eq. 2.24 becomes:

$$\phi\rho_o\left[-\frac{\partial S_w}{\partial t} + (1-S_w)(c_r+c_o)\frac{\partial P}{\partial t}\right] = \nabla\cdot\left[\frac{\underset{\sim}{K}k_{ro}}{\mu_o}\rho_o\nabla P\right] + q_o \tag{2.31}$$

Dividing Eq. 2.30 by ρ_w, Eq. 2.31 by ρ_o, and adding the two results we obtain

$$\phi\frac{\partial P}{\partial t}\left[c_r + c_o(1-S_w) + c_wS_w\right] = \frac{1}{\rho_w}\nabla\cdot\left[\frac{\underset{\sim}{K}k_{rw}}{\mu_w}\rho_w\nabla P\right] + \frac{1}{\rho_o}\nabla\cdot\left[\frac{\underset{\sim}{K}k_{ro}}{\mu_o}\rho_o\nabla P\right] + Q_t \tag{2.32}$$

where $Q_t = \frac{q_w}{\rho_w} + \frac{q_o}{\rho_o}$. The densities on the righthand side of Eq. 2.32 can be eliminated if the spatial variation of density is neglected[3]. A more precise statement can be made by making use of the following identities obtained from Eqs. 2.20 and 2.21:

$$\nabla\rho_w = \frac{d\rho_w}{dP}\nabla P = c_w\rho_w\nabla P \tag{2.33}$$

$$\nabla\rho_o = \frac{d\rho_o}{dP}\nabla P = c_o\rho_o\nabla P \tag{2.34}$$

By expanding the terms on the right hand side of Eq. 2.32 and using Eqs. 2.33 and 2.34 to eliminate the gradients of ρ_w and ρ_o, we obtain:

$$\phi\frac{\partial P}{\partial t}\left[c_r+c_o(1-S_w) + c_wS_w\right] =$$

$$\left(\frac{k_{rw}}{\mu_w}c_w + \frac{k_{ro}}{\mu_o}c_o\right)\underset{\sim}{K}(\nabla P\cdot\nabla P)$$

$$+ \nabla\cdot\left[\left(\frac{k_{rw}}{\mu_w} + \frac{k_{ro}}{\mu_o}\right)\underset{\sim}{K}\nabla P\right] + Q_t \tag{2.35}$$

By non-dimensionalizing this equation with respect to some characteristic reservoir pressure P* and length L, the conditions for neglecting the non-linear term are:

$$P^*c_w << 1$$

$$P^*c_o << 1$$

Neglecting this term we obtain the following equation for pressure:

$$C_t\phi\frac{\partial P}{\partial t} = \nabla\cdot\left[\left(\frac{k_{rw}}{\mu_w} + \frac{k_{ro}}{\mu_o}\right)\underset{\sim}{K}\nabla P\right] + Q_t \tag{2.36}$$

where

$$C_t = c_r + c_o(1-S_w) + c_w S_w$$

Eq. 2.36 is a parabolic partial differential equation.[3] If we are dealing with an incompressible system, then $C_t = 0$ and Eq. 2.36 becomes:

$$\nabla\cdot\left[\left(\frac{k_{rw}}{\mu_w} + \frac{k_{ro}}{\mu_o}\right)\underset{\sim}{K}\nabla P\right] + Q_t = 0 \tag{2.37}$$

Eq. 2.37 is an elliptic equation. For the incompressible problem, some value of pressure must be specified on the boundary ∂ in order to solve Eq. 2.37 uniquely for pressure. The initial condition given by Eq. 2.18 is no longer necessary.

2.2.2 Saturation Equation

To derive a single equation for saturation, we eliminate the pressure gradients from Eqs. 2.14 and 2.15 to obtain:

$$\underset{\sim}{v}_w = \frac{\lambda_w}{\lambda_o}\underset{\sim}{v}_o \tag{2.38}$$

where $\lambda_w = \frac{k_{rw}}{\mu_w}$ and $\lambda_o = \frac{k_{ro}}{\mu_o}$. The total velocity $\underset{\sim}{v}_t$ is given by:

$$\underset{\sim}{v}_t = \underset{\sim}{v}_o + \underset{\sim}{v}_w \tag{2.39}$$

We can define the fractional flow rate of water f_w by the relation:

$$\underset{\sim}{v}_w = f_w\underset{\sim}{v}_t \tag{2.40}$$

From Eqs. 2.38-40 we find that:

$$f_w = \frac{\lambda_w}{\lambda_o+\lambda_w} \tag{2.41}$$

Using Eq. 2.40, the flow velocity can be eliminated from Eq. 2.12 to obtain:

$$\frac{\partial[\phi\rho_w S_w]}{\partial t} = - \nabla\cdot(\rho_w f_w \underset{\sim}{v}_t) + q_w \tag{2.42}$$

If we assume that the reservoir fluids and rock are incompressible, we can divide Eq. 2.42 by ρ_w to obtain:

$$\phi \frac{\partial S_w}{\partial t} = - \nabla\cdot(f_w \underset{\sim}{v}_t) + \frac{q_w}{\rho_w} \tag{2.43}$$

Expanding the first term on the right hand side of Eq. 2.43, that equation can be written as:

$$\phi \frac{\partial S_w}{\partial t} = - f_w \nabla\cdot \underset{\sim}{v}_t - \underset{\sim}{v}_t\cdot\nabla f_w + \frac{q_w}{\rho_w} \tag{2.44}$$

Making use of the following identity

$$\nabla f_w = \frac{df_w}{dS_w} \nabla S_w \ , \tag{2.45}$$

Eq. 2.44 becomes:

$$\phi \frac{\partial S_w}{\partial t} = - f_w \nabla\cdot \underset{\sim}{v}_t - \underset{\sim}{v}_t \frac{df_w}{dS_w} \cdot\nabla S_w + \frac{q_w}{\rho_w} \tag{2.46}$$

If we are concerned with flow away from the boundaries and sources or sinks, then $q_w = 0$ and $\nabla\cdot \underset{\sim}{v}_t = 0$. Eq. 2.46 then becomes:

$$\phi \frac{\partial S_w}{\partial t} = - \underset{\sim}{v}_t \frac{df_w}{dS_w} \cdot \nabla S_w \qquad (2.47)$$

This is a first order hyperbolic equation.[3]

2.3 Summary

The particular reservoir model used in this study has been specified in Subsection 2.1.3. This model was obtained by first developing the general equations used to describe two-phase immiscible fluid flow in porous media, and then making the following assumptions: (1) the reservoir can be modeled with two horizontal dimensions and (2) capillary pressure can be neglected. The different forms of Darcy's equation used in this development are summarized in Table 2.1.

A general study of the structure of the model equations was made by deriving a single partial differential equation for pressure and a single equation for saturation. The pressure equation is shown to be parabolic if the fluids or reservoir are compressible, but is elliptic if the system is incompressible. The saturation equation is hyperbolic.

Table 2.1. Forms of Darcy's Equation Used in the Development of the Reservoir Model

EQUATION	SYSTEM
$\underset{\sim}{v} = -\frac{\underset{\sim}{K}}{\mu}(\nabla P + \rho \underset{\sim}{g})$	Single phase flow
$\underset{\sim}{v}_w = -\frac{\underset{\sim}{K}k_{rw}}{\mu_w}(\nabla P_w + \rho_w \underset{\sim}{g})$ $\underset{\sim}{v}_{nw} = -\frac{\underset{\sim}{K}k_{rnw}}{\mu_{nw}}(\nabla P_{nw} + \rho_{nw} \underset{\sim}{g})$ $P_c = P_{nw} - P_w$	Two-phase immiscible flow
$\underset{\sim}{v}_w = -\frac{\underset{\sim}{K}k_{rw}}{\mu_w}\nabla P$ $\underset{\sim}{v}_o = -\frac{\underset{\sim}{K}k_{ro}}{\mu_o}\nabla P$	Zero capillary pressure and gravity effect

3. ANALYTICAL SOLUTION FOR ONE-DIMENSIONAL INCOMPRESSIBLE FLOW

Assuming that the reservoir and fluids are incompressible and that the reservoir can be represented with a single spatial dimension, two equations can be derived from Eqs. 2.12-16 which can be solved analytically for the saturation and pressure. The saturation equation is the well known Buckley-Leverett equation[6] and can be solved by the method of characteristics.

Since the saturation equation is nonlinear, the solution of that equation by the method of characteristics becomes complicated because shocks, or discontinuities in the solution, must be constructed. There have been numerous studies of the solution for homogeneous reservoir models in the literature[1,6-9]. The solution by the method of characteristics can readily be extended to apply to heterogeneous reservoir models -- those for which the porosity and permeability vary spatially. This chapter contains a comprehensive review of the analytical solution for homogeneous models, as well as the extension to heterogeneous models.

In Section 3.1, the reservoir model is specified and the governing equations are derived. The solution of the saturation equation is discussed in Section 3.2. In Subsection 3.2.1 and 3.2.2, the analytical and graphical construction of shocks for homogeneous models is developed[1,6-10], and this is extended to heterogeneous models in 3.2.3. In Section 3.3, saturation and pressure solutions for example problems are presented, and the effect of different reservoir properties on the solutions are discussed.

3.1 Development of Equations

The decoupling of the saturation and pressure equations to obtain analytical solutions is similar to the derivations in Section 2.2. The saturation equation which will be derived is, in fact, Eq. 2.47 for one-dimensional flow. However, in order to unify the assumptions made in the model, the pressure and saturation equations will be derived below beginning with Eqs. 2.12-16.

We assume that fluid flow is along the single spatial dimension x. The reservoir model has a constant cross-sectional area A at all locations x, and the length is x_L. Water is injected at a specified volumetric flow rate Q at location x=0 and fluids are produced at $x=x_L$; the reservoir model is otherwise free of sources or sinks. This model is shown schematically in Fig. 3.1. We also assume that the fluids and reservoir rock are incompressible. Now, the equations describing our system, Eqs. 2.12-16, can be written as

$$\phi \frac{\partial S_w}{\partial t} = - \frac{\partial}{\partial x} v_w \tag{3.1}$$

$$\phi \frac{\partial S_o}{\partial t} = - \frac{\partial}{\partial x} v_o \tag{3.2}$$

$$v_w = - \frac{Kk_{rw}}{\mu_w} \frac{\partial P}{\partial x} \tag{3.3}$$

$$v_o = - \frac{Kk_{ro}}{\mu_o} \frac{\partial P}{\partial x} \tag{3.4}$$

$$S_o + S_w = 1 \tag{3.5}$$

Using Eq. 3.5 to eliminate S_o in Eq. 3.2, then adding Eqs. 3.1 and 3.2, we obtain:

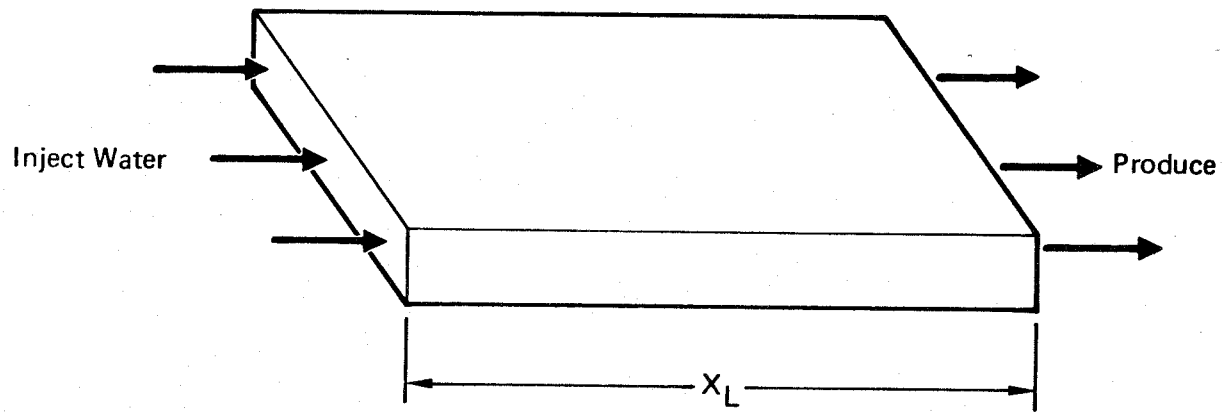

Figure 3.1
Schematic Reservoir Model

$$\frac{\partial}{\partial x}(v_w + v_o) = 0 \tag{3.6}$$

This means that the total superficial velocity is independent of location. Since the total superficial velocity v_t is known at x=0 ($v_t = \frac{Q}{A}$ by Eq. 2.2, where Q is the volumetric flow rate injected) the solution of Eq. 3.6 is:

$$v_t = v_o + v_w \tag{3.7}$$

The fractional flow of water f_w can be defined as:

$$f_w = v_w/v_t \tag{3.8}$$

Using Eq. 3.8, Eq. 3.1 can be written as:

$$\frac{\partial S_w}{\partial t} = -\frac{v_t}{\phi}\frac{\partial f_w}{\partial x} \tag{3.9}$$

Eliminating the pressure gradients in Eqs. 3.3 and 3.4 we obtain:

$$v_o = v_w \frac{k_{ro}}{\mu_o}\frac{\mu_w}{k_{rw}} \tag{3.10}$$

The following relation for f_w can be obtained from Eqs. 3.7,8,10:

$$f_w = \left(1 + \frac{\mu_w k_{ro}}{\mu_o k_{rw}}\right)^{-1} \tag{3.11}$$

Since the relative permeabilities are functions of saturation, Eq. 3.9 can be written as:

$$\frac{\partial S_w}{\partial t} = -\frac{v_t}{\phi}\frac{df_w}{dS_w}\frac{\partial S_w}{\partial x} \tag{3.12}$$

With an initial and boundary condition on saturation, Eq. 3.12 can be solved for the saturation distribution $S_w(x,t)$.

For simplicity, we will refer to the water saturation as simply S and use f to refer to the fractional flow of water. We will use f' to denote the derivative of the fractional flow with respect to saturation. With these changes, the equations which specify the saturation are:

$$\frac{\partial S}{\partial t} = - \frac{v_t}{\phi} f' \frac{\partial S}{\partial x} \tag{3.13}$$

$$S(x,0) = S_{in}(x) \tag{3.14}$$

$$S(0,t) = 1 - S_{ro} \tag{3.15}$$

Eqs. 3.14 and 3.15 are the initial and boundary conditions, respectively, where S_{ro} is the residual oil saturation.

Eq. 3.3 can be solved for the pressure P(x,t). Using the definition of f_w, Eq. 3.3 can be written as:

$$v_t f = - \frac{Kk_{rw}}{\mu_w} \frac{\partial P}{\partial x} \tag{3.16}$$

By specifying the pressure at x=0, the necessary boundary condition on pressure is:

$$P(0,t) = P_0(t) \tag{3.17}$$

The solution to Eqs. 3.16 and 3.17 is

$$P(x,t) - P_0(t) = v_t \mu_w \int_0^x \frac{f}{Kk_{rw}} dx \tag{3.18}$$

In this study we will confine our attention to the pressure drop, ΔP, across the reservoir model. Eq. 3.18 then becomes:

$$\Delta P(t) = P(x_L,t) - P_0(t) = v_t \mu_w \int_0^{x_L} \frac{f}{K k_{rw}} dx \tag{3.19}$$

3.2 Solution of the Saturation Equation

Eq. 3.13 is a nonlinear first order hyperbolic equation which can be solved analytically by the method of characteristics. This solution will be discussed in detail in this section.

The total derivative of saturation is

$$\frac{dS}{dt} = \frac{\partial S}{\partial t} + \frac{\partial S}{\partial x}\frac{dx}{dt} \tag{3.20}$$

By comparing this expression to the partial differential equation for saturation, Eq. 3.13, we see that solutions to the partial differential equation are equivalent to solutions of the following two ordinary differential equations:

$$\frac{dS}{dt} = 0 \tag{3.21}$$

$$\left.\frac{dx}{dt}\right|_S = \frac{v_t}{\phi} f'(S) \tag{3.22}$$

The solution to Eq. 3.13 can be given graphically as curves (called characteristic curves) in the (x,t) plane which satisfy Eqs. 3.21 and 3.22 and the initial and boundary conditions, Eqs. 3.14 and 3.15. Eq. 3.21 specifies that the value of saturation along one of these characteristic curves remains constant. Eq. 3.22 specifies the derivative along each

curve. The intersection of the characteristics with the x-axis satisfies the initial condition, 3.14, and the intersection with the t-axis satisfies the boundary condition, 3.15. If v_t is independent of t and ϕ is independent of x, the slope for each curve given by Eq. 3.22 is a constant, and hence the characteristics are straight lines.

We now consider an example problem. The velocity is taken to be independent of time, and the porosity is independent of location. For simplicity, we will define a dimensionless time τ and distance ξ such that

$$\tau = \frac{v_t t}{\phi x_L}$$

$$\xi = \frac{x}{x_L}$$

For the f and f' functions given in Fig. 3.2 and initial saturation profile shown in Fig. 3.3, the characteristic solution is plotted in Fig. 3.4.

The solution can be calculated analytically. If ϕ is independent of location and v_t is independent of time, Eq. 3.22 can be integrated to obtain

$$x(S,t) - x_0(S) = \frac{v_t t}{\phi} f'(S) \qquad (3.23)$$

where $x_0(S)$ is obtained by inverting the initial condition given by Eq. 3.14. The location of saturations at time t can be calculated by Eq. 3.23.

For the example problem considered above, S is plotted for three different times in Fig. 3.5. For time τ_3 the saturation curve becomes multivalued for some range of x. The reason for this is that the function f' has a maximum for some $S_c < S < 1 - S_{ro}$, where S_c is the connate water

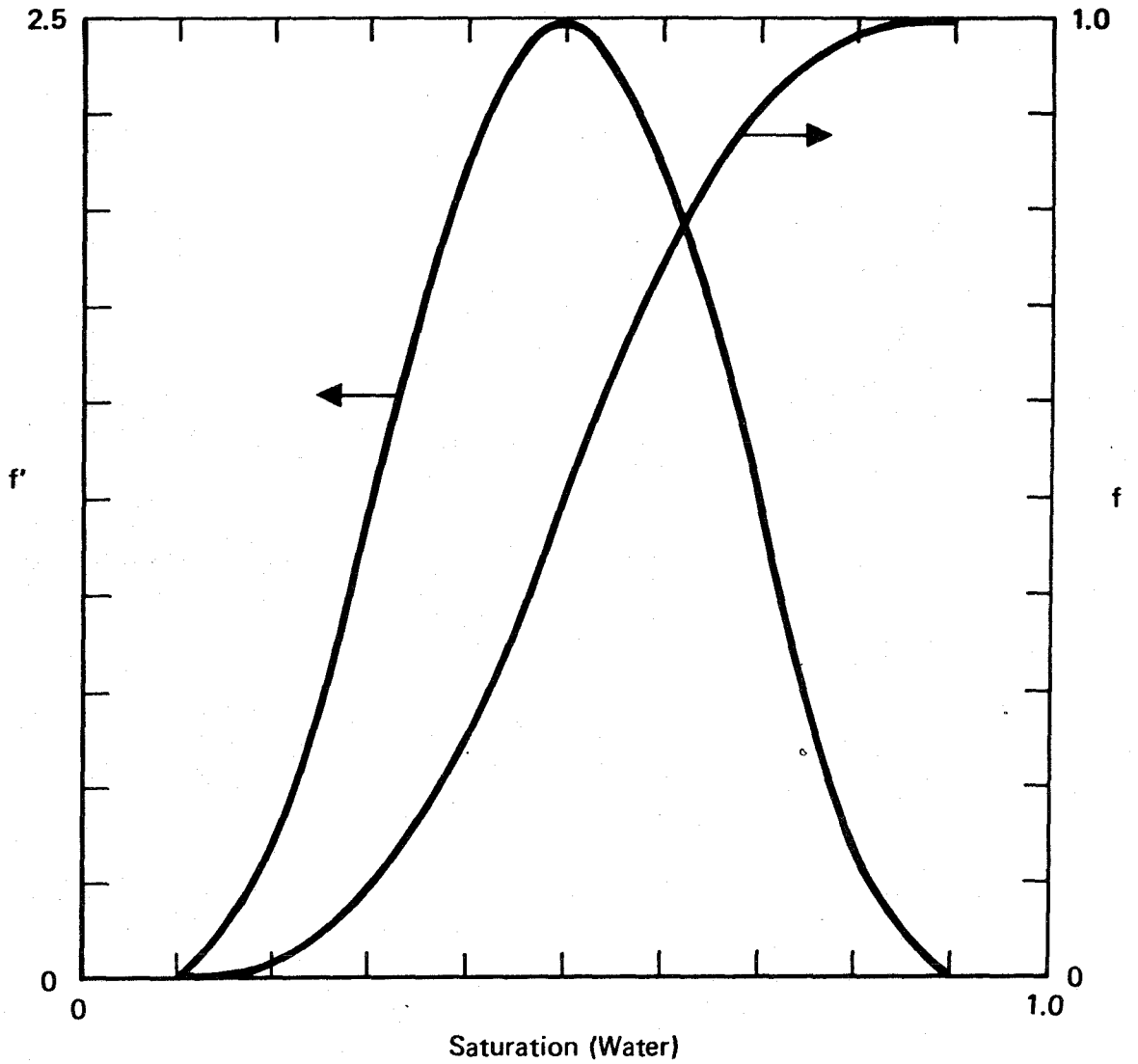

Figure 3.2
Fractional Flow for Example Problem

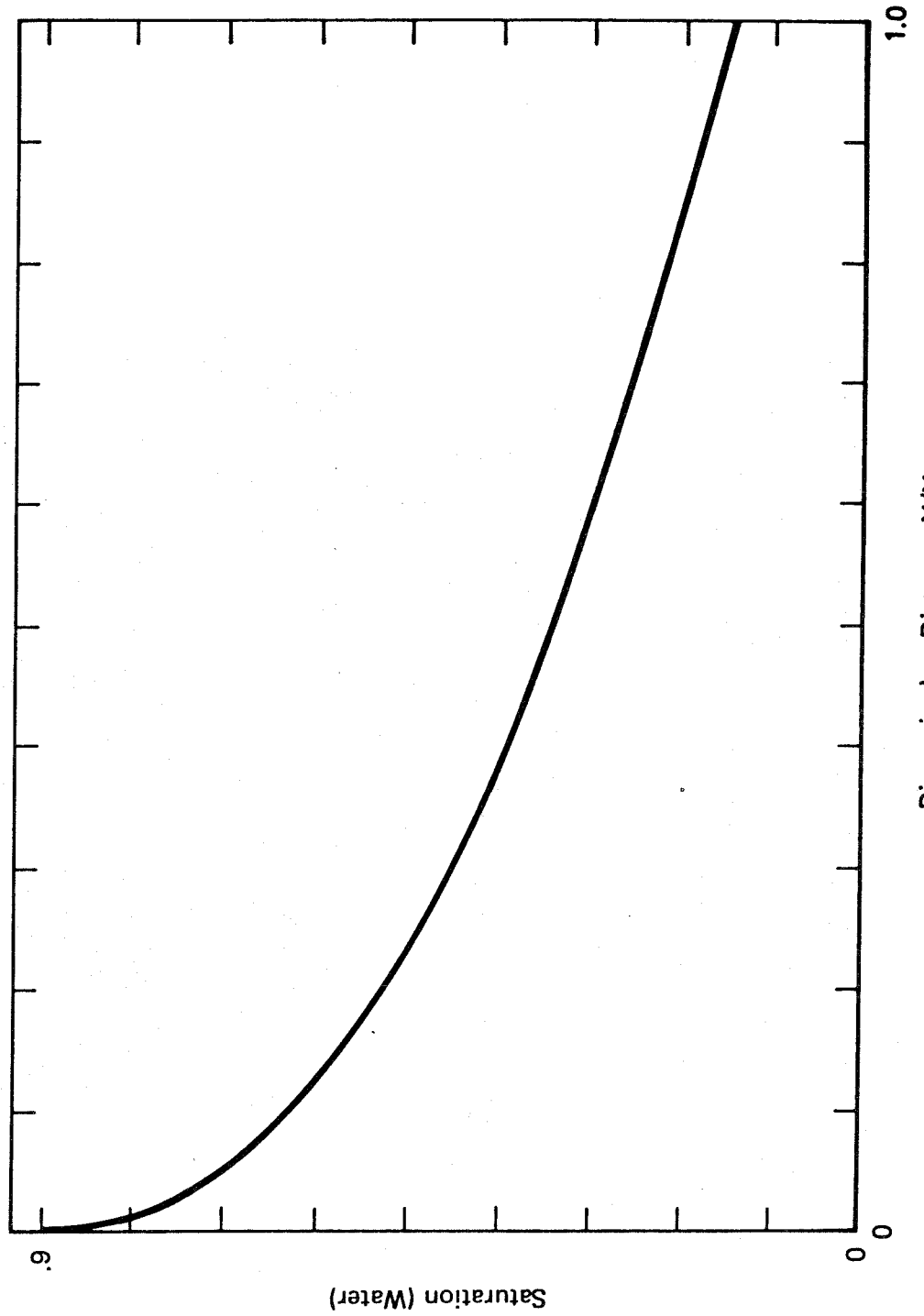

Figure 3.3
Initial Saturation for Example Problem

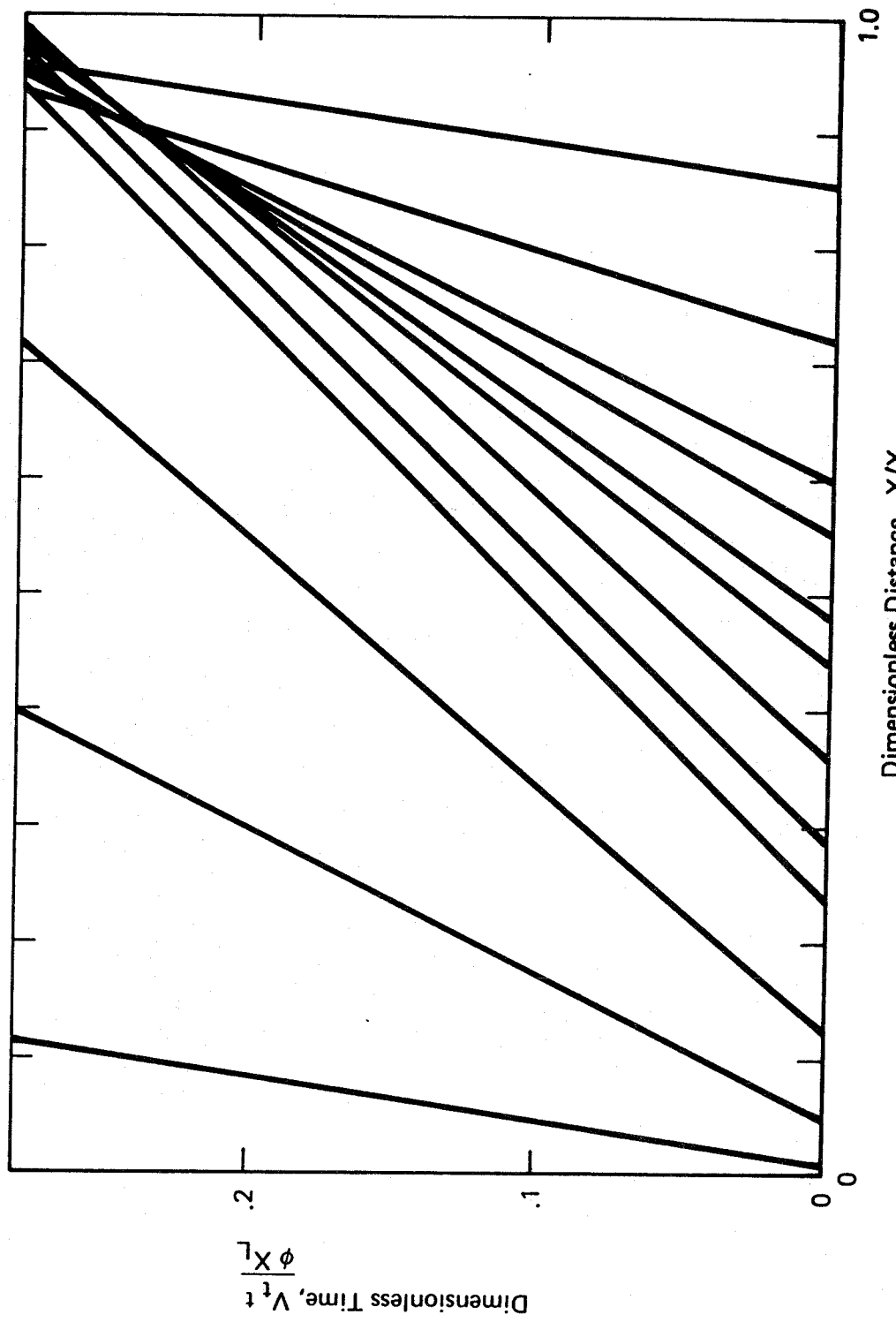

Figure 3.4
Characteristic Solution (Without Shocks) for Example Problem

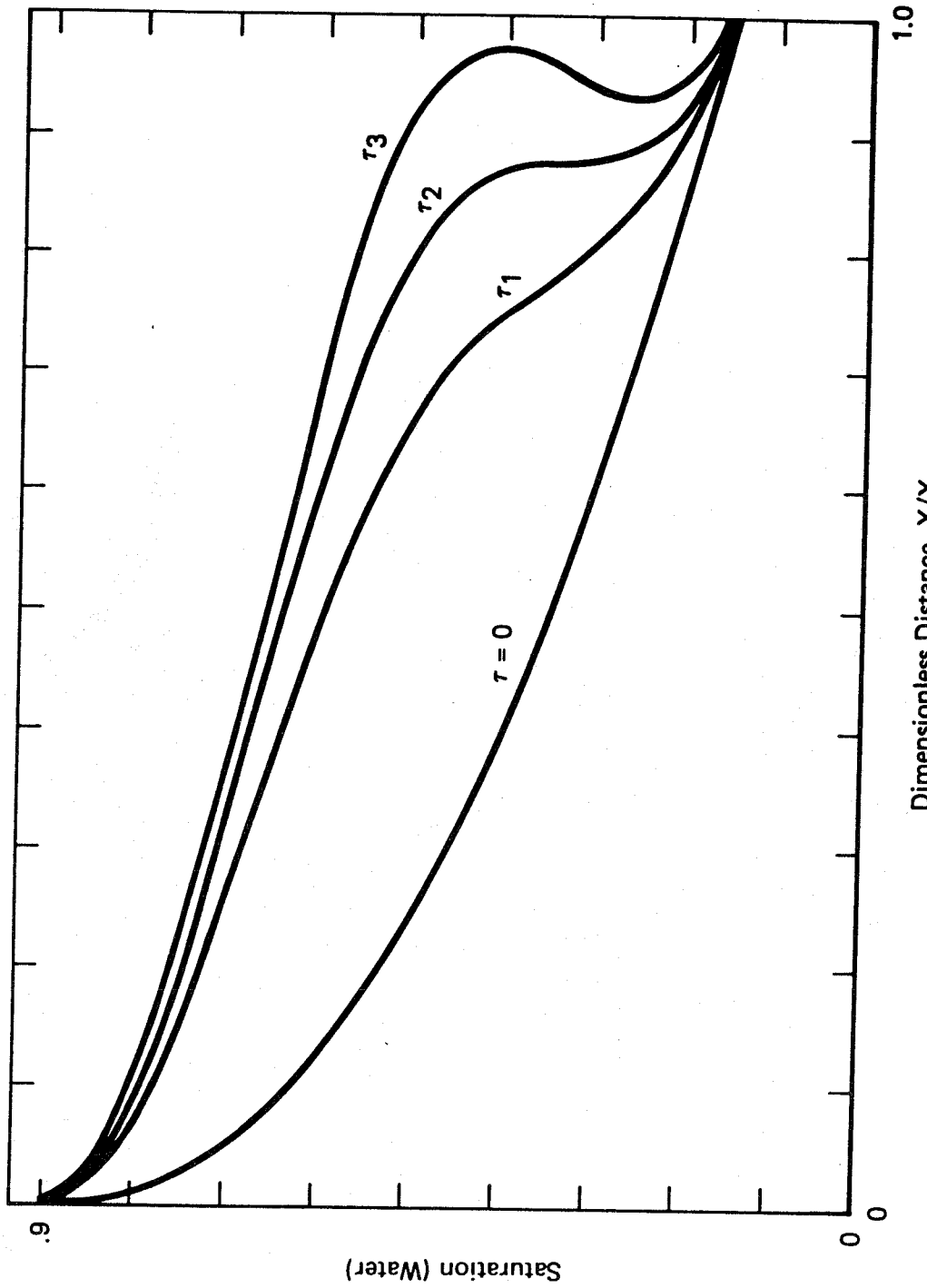

Figure 3.5
Saturation Solution (Without Shocks)
for Example Problem

saturation. That is, some intermediate saturations travel faster than saturations in the neighborhood of S_c and therefore overtake them. This feature can also be seen in the characteristic diagram Fig. 3.4. Multi-valued saturations occur where the characteristics intersect.

Obviously, the existence of more than one saturation at a particular position is physically impossible. Shocks, or discontinuities in saturation, are introduced to avoid these multi-valued saturations. Both the analytical and graphical construction of shocks will be presented.

For the example problem considered above, v_t was taken to be independent of t and ϕ was independent of x. Although the same principles of solution apply to the more general case of varying v_t and ϕ, the analytical solution becomes more difficult since certain explicit forms can not be obtained. Rather than obstruct certain features of the problem by studying only the more general case, we will first obtain the solution for constant v_t and ϕ, and later generalize it.

3.2.1 Analytical Construction of Shocks

At the time at which multi-valued saturations appear, the curve S as a function of x becomes vertical (time τ_2 in Fig. 3.5). Hence, at some value of x we have the following condition:

$$\frac{\partial S}{\partial x} \to \infty$$

The solution breaks down because the continuity equation 3.1 no longer applies since the saturation is not continuously differentiable there. However, material must still be conserved. The more general form of the continuity equation shown below applies regardless of the differentiability of saturation[10].

Consider a mass balance on water for some $x_a \leq x \leq x_b$. Then

$$\frac{d}{dt}\int_{x_a}^{x_b} \phi S dx = v_w(x_a,t) - v_w(x_b,t) \tag{3.24}$$

(If $S(x,t)$ has continuous derivatives, we obtain Eq. 3.1 in the limit as $x_a \to x_b$). Assume that the saturation is discontinuous at the point $x_d(t)$, and continuous elsewhere. Eq. 3.1 applies for $x < x_a$ and $x > x_b$. For $x_a \leq x \leq x_b$, Eq. 3.24 becomes

$$v_w(x_a,t) - v_w(x_b,t) = \frac{d}{dt}\left[\int_{x_a}^{x_d} \phi S dx + \int_{x_d}^{x_b} \phi S dx\right] \tag{3.25}$$

By carrying out the derivative in the right hand side, this equation becomes

$$v_w(x_a,t) - v_w(x_b,t) = \phi S(x_d^-,t)x_d' - \phi S(x_d^+,t)x_d' + \int_{x_a}^{x_d} \phi \frac{\partial S}{\partial t} dx + \int_{x_d}^{x_b} \phi \frac{\partial S}{\partial t} dx \tag{3.26}$$

where $x_d' = \frac{dx_d}{dt}$ and $S(x_d^-,t)$ and $S(x_d^+,t)$ are the values of S as $x \to x_d$ from $x < x_d$ and $x > x_d$, respectively. Since $\frac{\partial S}{\partial t}$ is bounded in each of the integrals in Eq. 3.26, in the limit as $x_a \to x_d^-$ and $x_b \to x_d^+$ these integrals tend to zero and Eq. 3.26 becomes:

$$v_w(x_d^-,t) - v_w(x_d^+,t) = \phi\left[S(x_d^-,t) - S(x_d^+,t)\right] x_d' \tag{3.27}$$

Denoting $S(x_d^-,t)$ and $S(x_d^+,t)$ by S^- and S^+, respectively, and applying the definition of f given by Eq. 3.8, Eq. 3.27 can be written, after rearranging, as:

$$\frac{dx_d}{dt} = \frac{v_t[f(S^-)-f(S^+)]}{\phi(S^--S^+)} \tag{3.28}$$

This equation gives the velocity of the shock if the saturations are known on either side of the shock. An equivalent form for Eq. 3.28 is

$$\frac{dx_d}{dt} = \frac{v_t}{\phi}\,\overline{f'(S^-,S^+)} \tag{3.29}$$

where

$$\overline{f'(S^-,S^+)} = \frac{\int_{S^+}^{S^-} f'dS}{S^--S^+}$$

From Eq. 3.29 we see that the shock moves with a velocity which is proportional to the average velocity of all saturations $S^- \geq S \geq S^+$.[8]

In order to find the time t_c at which the first shock is formed, we find an expression for $\frac{\partial S}{\partial x}$ and determine the first time at which $\frac{\partial S}{\partial x} \to \infty$.[10] Taking the derivative with respect to x in Eq. 3.23 we obtain:

$$1 - \frac{dx_0}{dS}\frac{\partial S}{\partial x} = \frac{v_t}{\phi}\,tf''\,\frac{\partial S}{\partial x} \tag{3.30}$$

After rearranging, we obtain the following expression for $\frac{\partial S}{\partial x}$:

$$\frac{\partial S}{\partial x} = \left[\frac{dx_0}{dS} + \frac{v_t}{\phi}\,tf''\right]^{-1} \tag{3.31}$$

Investigating the conditions for which $\frac{\partial S}{\partial x} \to \infty$, we see that t_c is given by:

$$t_c = \left|\frac{dx_0/dS}{\frac{v_t}{\phi}\,f''}\right|_{min} \tag{3.32}$$

Once a shock is formed, the location of the shock x_d and the values of saturation at either side of the discontinuity, S^- and S^+, can be found by using the following argument. Since both the multi-valued curve and the discontinuous curve of S satisfy conservation of mass, then the area $\int_0^{x_L} S dx$ must be identical for both curves[6,10]. Hence, the shock is constructed on the multi-valued curve at the location which cuts off lobes of equal area (see Fig. 3.6). Since x is a function of saturation over the range $S^- \geq S \geq S^+$, this condition can be derived more easily by considering the area given by $\int x(S)\, dS$. The equal area requirement then becomes:

$$\int_{S^+}^{S^-} x(S) dS = (S^- - S^+)\, x_d \tag{3.33}$$

Using Eq. 3.22 in the integral, we obtain:

$$\int_{S^+}^{S^-} x_0(S)\, dS + t \frac{v_t}{\phi} \int_{S^+}^{S^-} f' dS = (S^- - S^+)\, x_d \tag{3.34}$$

Since the saturations to the left and right of the shock must satisfy the continuity Eq. 3.1, we have from Eq. 3.23 two expressions for x_d:

$$x_d = x_0(S^+) + \frac{v_t t}{\phi} f'(S^+) \tag{3.35}$$

$$x_d = x_0(S^-) + \frac{v_t t}{\phi} f'(S^-) \tag{3.36}$$

Substituting Eq. 3.35 into 3.34 for x_d and rearranging, we obtain:

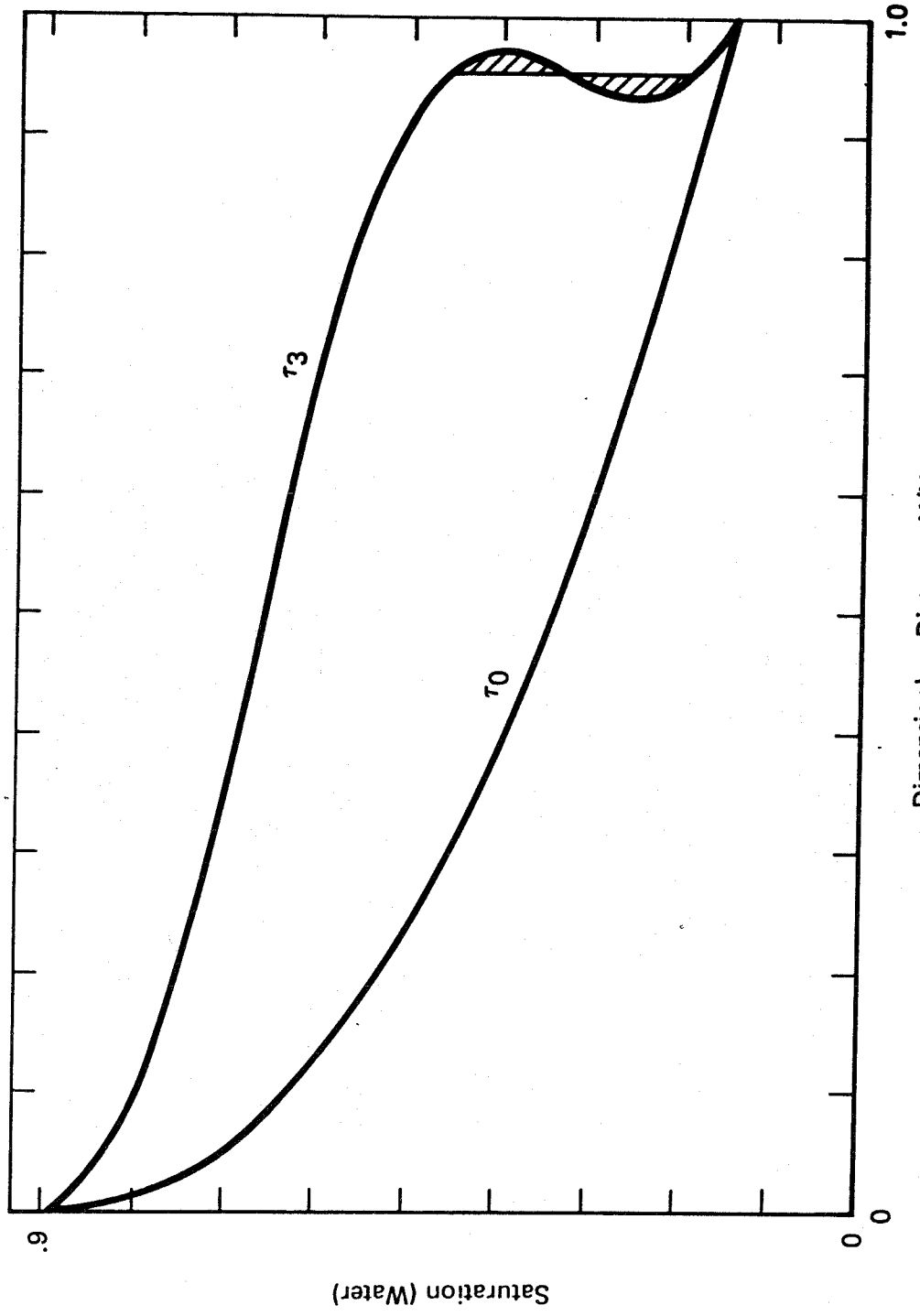

Figure 3.6
Saturation Solution (With Shock) for Example Problem

$$\frac{\int_{S^+}^{S^-} x_0(S)dS-(S^--S^+)x_0(S^+)}{(S^--S^+)f'(S^+)-\int_{S^+}^{S^-} f'dS} = \frac{v_t t}{\phi} \tag{3.37}$$

Treating Eqs. 3.36 and 3.34 similarly, we obtain:

$$\frac{\int_{S^+}^{S^-} x_0(S)dS-(S^--S^+)x_0(S^-)}{(S^--S^+)f'(S^-)-\int_{S^+}^{S^-} f'dS} = \frac{v_t t}{\phi} \tag{3.38}$$

Equating Eqs. 3.37 and 3.38 and evaluating the integral in the denominators, the following equation, which appears in Cardwell[8], is obtained:

$$\frac{\int_{S^+}^{S^-} x_0(S)dS-(S^--S^+)x_0(S^+)}{(S^--S^+)f'(S^+)-[f(S^-)-f(S^+)]} = \frac{\int_{S^+}^{S^-} x_0(S)dS-(S^--S^+)x_0(S^-)}{(S^--S^+)f'(S^-)-[f(S^-)-f(S^+)]} \tag{3.39}$$

After the time of shock formation, the shock can be constructed by finding pairs of saturations S^- and S^+ which satisfy Eq. 3.39. The time at which a particular pair S^-, S^+ exist is given by

$$t(S^-,S^+) = \frac{x_0(S^-)-x_0(S^+)}{\frac{v_t}{\phi}\left[f'(S^+)-f'(S^-)\right]} \tag{3.40}$$

Eq. 3.40 is found by eliminating x_d between Eqs. 3.35 and 3.36 and rearranging. The position of the shock for the particular time is then given by Eq. 3.35 or 3.36 evaluated at $t(S^-,S^+)$.

For arbitrary initial conditions, the construction of shocks in the saturation solution is complicated since not only does the position of a shock and saturation values on either side of the shock vary with time, but there may be multiple shocks as well as merging of shocks.[10] An important limiting case of the Buckley-Leverett problem has the following initial condition for the saturation:

$$S(x,0) = S_c \tag{3.41}$$

where S_c is the connate water saturation. For this case, a single shock is formed immediately (i.e., $x=0^+$, $t=0^+$). It is not convenient to use Eq. 3.39 to construct the shock analytically since $x_0(S)$ is no longer a function. Welge[7] proposed a graphical method to determine the upper value of the shock S^- for this limiting case. It consists of plotting f vs. S. A straight line is drawn from $S=S_c$, $f=0$, such that it is tangent to the f curve. S^- is given by the value of saturation corresponding to the intersection of the line with the f curve, and $S^+ = S_c$. The values of the shock are independent of time. Construction of the shock graphically provides an important insight into the Welge solution.

3.2.2 Graphical Construction of Shocks

Graphical construction of the solution by characteristics is often used to determine approximate solutions to the problem and determine the general nature of the solution. In the previous section it was shown that

shocks must be constructed in the solution when multi-valued saturations are calculated. In this section the graphical construction of shocks will be discussed[9].

Multi-valued saturation solutions correspond to regions in the characteristic diagram for which characteristic curves intersect. The characteristic solution for the example problem in the previous section (see Fig. 3.4) is plotted with shocks in Fig. 3.7. The position of the shock in the (ξ,τ) plane is denoted by a broken line. The characteristics first interesect at the point $(\bar{\xi},\bar{\tau})$ in Fig. 3.7. The values of saturation for the characteristic curves which meet at this point correspond to S^- and S^+. Theoretically, these values should be only infinitesimally different. However, when graphing the characteristics the first intersection will generally be at some time greater than t_c and S^- and S^+ will have finitely different values. To find the position of the shock at $\bar{\tau} + \Delta\tau$ where $\Delta\tau$ is some small increment of time, a straight line can be extended from $(\bar{\xi},\bar{\tau})$ with a slope given by

$$\frac{d\xi_d}{d\tau} = \frac{[f(S^-)-f(S^+)]}{S^- - S^+} \tag{3.42}$$

This is the dimensionless form of Eq. 3.28, the equation for the velocity of the shock. The point at which two characteristics intersect at $\bar{\tau} + \Delta\tau$ can be found by trial and error. This point will be in the neighborhood of the intersection of the straight line extended from $(\bar{\xi},\bar{\tau})$ and the line with zero slope given by $(\xi,\bar{\tau} +\Delta\tau)$. The new values of saturation across the shock, S^- and S^+, belong to the two characteristics which intersect at this point. This process can be extended to trace the development of the shock with time.

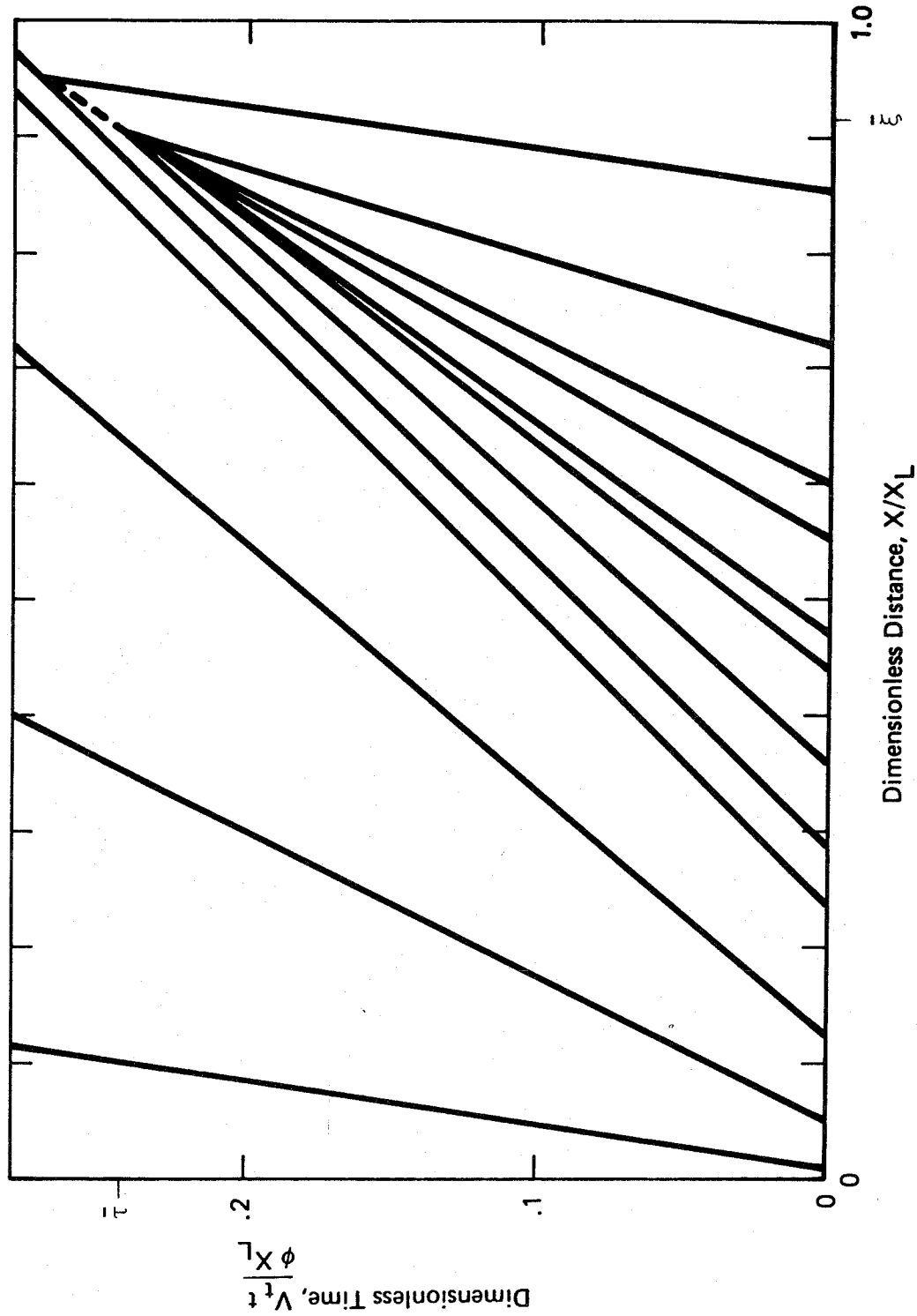

Figure 3.7
Characteristic Solution (With Shocks) for Example Problem

The characteristic diagram for the initial condition given by Eq. 3.41 consists of vertical lines along the x-axis and a "fan" at x = 0 (see Fig. 3.8). For this case, $S^+ = S_c$, but the upper value of the saturation across the discontinuity cannot be found directly from Fig. 3.8.

Sheldon, et al.[9] considered initial saturations of the type given by Fig. 3.3 (i.e., concave) for a typical function f. By plotting the characteristic solution they show that S^- and S^+ approach limiting values as t increases. The steeper the initial profile is, the more quickly this limiting value is attained. For the limiting case given by Eq. 3.41, the proper solution is that $S^+ = S_c$ for all time and S^- is constant for all time. Hence, graphically the proper solution can be chosen by considering these steeper initial saturation profiles. This shows the uniqueness of the Welge solution.

If S_d is the saturation S^- corresponding to the limiting characteristic, then the velocity of the shock is given by Eq. 3.29 evaluated at S_d and S_c:

$$\frac{dx_d}{dt} = \frac{v_t}{\phi} \overline{f'(S_d,S_c)} \tag{3.43}$$

where

$$\overline{f'(S_d,S_c)} = \frac{f(S_d)-f(S_c)}{S_d-S_c}$$

Evaluating Eq. 3.22 at the saturation S_d gives us another expression for the velocity of the shock:

$$\frac{dx_d}{dt} = \frac{v_t}{\phi} f'(S_d) \tag{3.44}$$

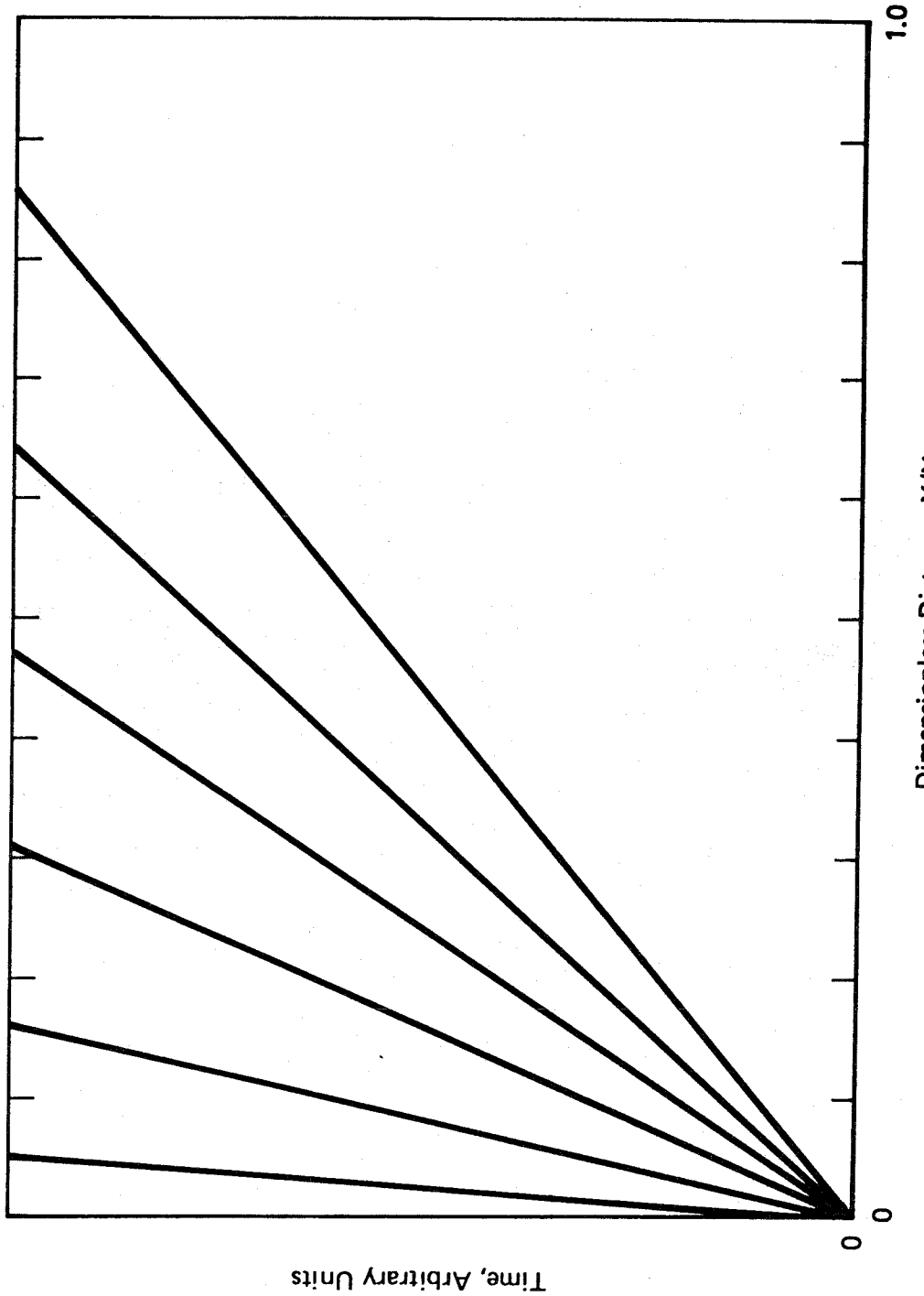

Figure 3.8
Characteristic Solution for $S_{IN} = S_C$

The following relation can then be obtained by equating the right hand side of Eqs. 3.43 and 3.44:

$$f'(S_d) = \overline{f'(S_d,S_c)} \tag{3.45}$$

Since geometrically the average slope of a curve between two points is given by a straight line joining those points, Eq. 3.45 is an analytical statement of the Welge solution.

To obtain a single shock with constant values S^-, S^+, it is not necessary that the initial saturation be the connate water saturation S_c. The initial saturation can be any constant value $S_\alpha < S_m$ such that $f'(S_m) = \max f'(S)$ for all $S_c \leq S \leq 1 - S_{ro}$. Then S^- is found by drawing a straight line from $S = S_\alpha$, $f = f(S_\alpha)$ so that it is tangent to the f curve on the plot of f vs. S. If $S_\alpha \geq S_m$, then no shock is formed.

3.2.3 Solution of the Saturation Equation for $\phi(x)$ and $v_t(t)$

Although the solution of Eqs. 3.21 and 3.22 is more difficult for spatially varying porosity and temporally varying velocity, the derivation closely parallels that for the less general case. The chief difference in the solution is that Eq. 3.22 can no longer be integrated to give x(S,t) as an explicit function of saturation and time. Instead, Eq. 3.22 can be solved as

$$\int_{x_0(S)}^{x(S,t)} \phi(x)dx = f'(S) \int_0^t v_t(t)\, dt \tag{3.46}$$

For any time t, Eq. 3.46 gives x implicitly as a function of S. For convenience, we will write Eq. 3.46 as:

$$\Phi(x) = V(t)f'(S) \tag{3.47}$$

where

$$\Phi(x) = \int_{x_0(S)}^{x(S,t)} \phi(x)dx$$

and

$$V(t) = \int_0^t v_t(t)dt$$

The derivation of Eq. 3.28, which gives the velocity of the shock, is identical to the previous derivation since ϕ was not taken outside of the integrals in Eqs. 3.24-26. By noting the functional dependence of v_t and ϕ, we can write Eq. 3.28 as:

$$\frac{dx_d}{dt} = \frac{v_t(t)}{\phi(x_d)} \overline{f'(S^-,S^+)} \tag{3.48}$$

To obtain an expression for t_c which corresponds to Eq. 3.32, we differentiate Eq. 3.46 with respect to x to obtain:

$$\phi(x) - \phi(x_0) \frac{dx_0}{dS} \frac{\partial S}{\partial x} = V(t)f''(S) \frac{\partial S}{\partial x} \tag{3.49}$$

Rearranging, we obtain the following expression for $\frac{\partial S}{\partial x}$:

$$\frac{\partial S}{\partial x} = \frac{\phi(x)}{\phi(x_0)x_0'+V(t)f''(S)} \tag{3.50}$$

where $x_0' = \frac{dx_0}{dS}$. The time at which the first shock forms, t_c, is given implicitly by:

$$V(t_c) = \left| \frac{x_0'(S)\phi(x_0)}{f''(S)} \right|_{min} \tag{3.51}$$

The condition that both the discontinuous and continuous saturation profiles conserve mass, which is analogous to Eq. 3.33, is:

$$\int_{S^+}^{S^-} \phi x dS = \phi(x_d)(S^- - S^+)x_d \tag{3.52}$$

where $x(S,t)$ is given implicitly by Eq. 3.47. The saturations S^- and S^+ satisfy Eq. 3.47:

$$\Phi(x_d) = V(t)f'(S^-) \tag{3.53}$$

$$\Phi(x_d) = V(t)f'(S^+) \tag{3.54}$$

For $t > t_c$, Eqs. 3.52-54 must be solved for the functions $S^-(t)$, $S^+(t)$, and $x_d(t)$.

The graphical construction of shocks is identical to the method outlined in Section 3.2.2 for constant porosity and velocity since the velocity of the shock (given by Eq. 3.28) is the same for both cases. The characteristics will now be curves rather than straight lines.

For the limiting initial condition given by Eq. 3.41, the following derivation shows that the Welge condition given by Eq. 3.45 applies to a heterogeneous reservoir. Consider a mass balance on water for time $\bar{t}$, such that $\bar{t} < t_B$, where t_B is the breakthrough time, or time at which water is

first produced. The volume of water in the reservoir at time $\bar{t}$ is then equal to the volume of water initially in the reservoir plus the volume of water injected. The mathematical statement of this is:

$$A\left\{S_c \int_0^{x_L} \phi dx + V(\bar{t})\right\} = A \int_0^{x_L} \phi S dx \tag{3.55}$$

Eliminating the area A from both sides and rewriting the integral, Eq. 3.55 can be written as:

$$S_c \int_0^{x_L} \phi dx + V(\bar{t}) = \int_0^{x_d} \phi S dx + S_c \int_{x_d}^{x_L} \phi dx \tag{3.56}$$

The first integral on the right hand side of Eq. 3.56 can be transformed to an integral over S. By taking the derivative with respect to S of Eq. 3.47 evaluated at time $\bar{t}$, we obtain

$$\phi(x) \frac{\partial x}{\partial S} = V(\bar{t}) f''(S) \tag{3.57}$$

Then, the integral can be transformed as follows:

$$\int_0^{x_d} \phi S dx = \int_{1-S_{ro}}^{S_d} \phi S \frac{\partial x}{\partial S} dS = V(\bar{t}) \int_{1-S_{ro}}^{S_d} S f'' dS \tag{3.58}$$

Here we have assumed that the value $S = 1-S_{ro}$ occurs only at $x = 0$ -- i.e., we have taken $f'(1-S_{ro}) = 0$, as is usually done. The integral in Eq. 3.58 can be integrated by parts to obtain:

$$\int_{1-S_{ro}}^{S_d} S f'' ds = S_d f'(S_d) - \left[f(S_d) - 1\right] \tag{3.59}$$

where $f(1-S_{ro})$ has been evaluated as 1 and $f'(1-S_{ro})$ has been evaluated as 0.

Using Eq. 3.59, and rearranging, Eq. 3.56 can be written as:

$$S_c\left[\int_0^{x_L}\phi dx - \int_{x_d}^{x_L}\phi dx\right] = V(\bar{t})\left[S_d f'(S_d) - f(S_d)\right] \tag{3.60}$$

The two integrals on the left hand side of Eq. 3.60 can be written as a single integral, and then simplified by Eq. 3.46, as follows:

$$S_c\left[\int_0^{x_L}\phi dx - \int_{x_d}^{x_L}\phi dx\right] = S_c\left[\int_0^{x_d}\phi dx\right] = S_c V(\bar{t}) f'(S_d) \tag{3.61}$$

After rearranging, Eq. 3.60 becomes:

$$f'(S_d) = \frac{f(S_d)}{(S_d - S_c)} \tag{3.62}$$

Since $f(S_c) = 0$, this is identical to the Welge solution given by Eq. 3.45.

3.3 Example Problems and Discussion

In this section the effect of different reservoir and fluid properties on the pressure and saturation solutions are discussed. A computer program was written to solve Eqs. 3.19 and 3.22 with the following boundary and initial conditions:

$$S(0,t) = 1 - S_{ro} \tag{3.63}$$

$$S(x,0) = S_c \tag{3.64}$$

The superficial velocity was taken to be constant.

The relative permeabilities were represented as follows:

$$k_{rw}(S) = a_w \left(\frac{S-S_c}{1-S_{ro}-S_c} \right)^{b_w} \tag{3.65}$$

$$k_{ro}(S) = a_o \left(\frac{1-S_{ro}-S}{1-S_{ro}-S_c} \right)^{b_o} \tag{3.66}$$

For each set of relative permeabilities and viscosity ratios used, the upper value of the saturation at the shock, S_d, was determined analytically using Eq. 3.45. A detailed description of the computer program is given in Appendix A.

Nine cases were run using the data given in Table 3.1. These cases are divided into three groups. In the first group the effect of different relative permeabilities and viscosity ratios on the solution is investigated. The effect of spatially varying permeability is investigated in the second group, and the effect of spatially varying porosity is investigated in the third group.

Table 3.1. Specification of Reservoir Properties Used for the Example Problems

$v_t = 5 \times 10^{-3}$ ft/hr $\mu_w = 1$ cp

$x_L = 1 \times 10^4$ ft

GROUP I:

K = 0.2737 darcy $\phi = 0.3$

Case	Relative Permeability Set Used(1)	μ_o(cp)
1	A	1
2	B	1
3	C	1
4	A	10

GROUP II:

Relative Permeability Set A, Fig. 3.9 $\phi = 0.3$

$\mu_o = 1$ cp

Case	Permeability Set Used(2)
1	a
5	b
6	c
7	d

GROUP III:

Relative Permeability Set A, Fig. 3.9 K = 0.2737 darcy

Case	Porosity Set Used(2)
1	a
8	b
9	c

(1) See Figs. 3.9-3.11

(2) See Fig. 3.15

The three different sets of relative permeabilities used for the cases studied are given in Figs. 3.9-11. The four permeability profiles and three porosity profiles used are shown in Fig. 3.12. The graphs of the calculated saturation and pressure drop are plotted in terms of a dimensionless distance X, a dimensionless time T, and a dimensionless pressure $\Delta P^*(t)$ defined as

$$X = x/x_L \tag{3.67}$$

$$T = t/t_B \tag{3.68}$$

$$\Delta P^*(t) = \Delta P(t)/\Delta P(0) \tag{3.69}$$

where t_B is the time of water breakthrough. The calculated values of $\Delta P(0)$ and t_B for each case are given in Table 3.2.

3.3.1 Relative Permeability and Viscosity Ratio

A constant permeability and porosity profile were used for these four cases. Three different sets of relative permeabilities were used for Cases 1-3. The parameters used in Case 4 were the same as Case 1 except for $\mu_o = 10$ (see Group I in Table 3.1).

For Case 1, the pressure solution in shown in Fig. 3.13, and the saturation solution is shown in Fig. 3.14. The functions f and f' which correspond to the relative permeabilities in Set A are shown in Fig. 3.15. The pressure solution $\Delta P^*(t)$ for constant v_t, K, and ϕ have this same form for different relative permeabilities: The pressure drop is linear with time for $t \leq t_B$, and then it asymptotically approaches the limiting value

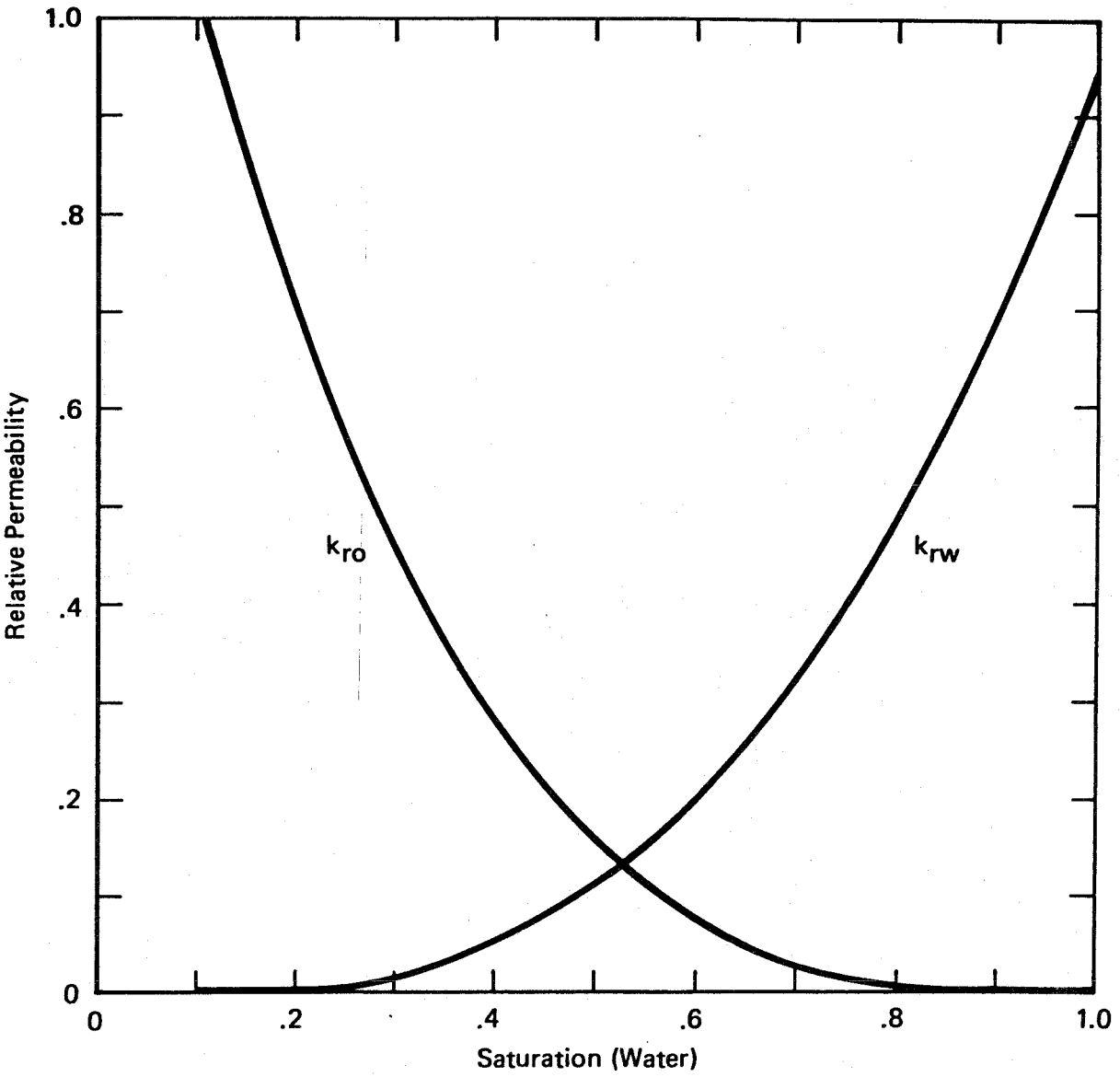

Figure 3.9
Relative Permeabilities — Set A

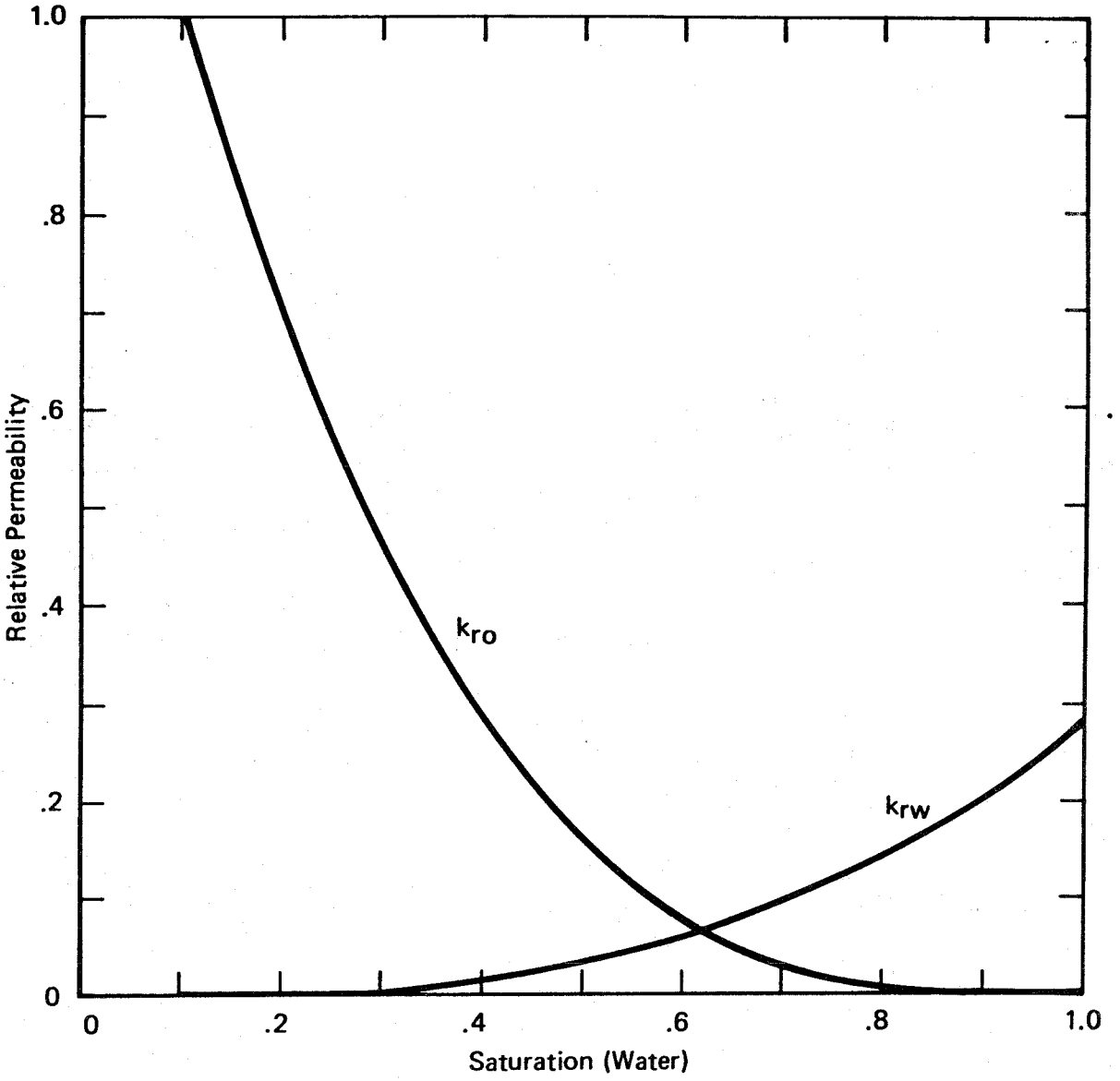

Figure 3.10
Relative Permeabilities — Set B

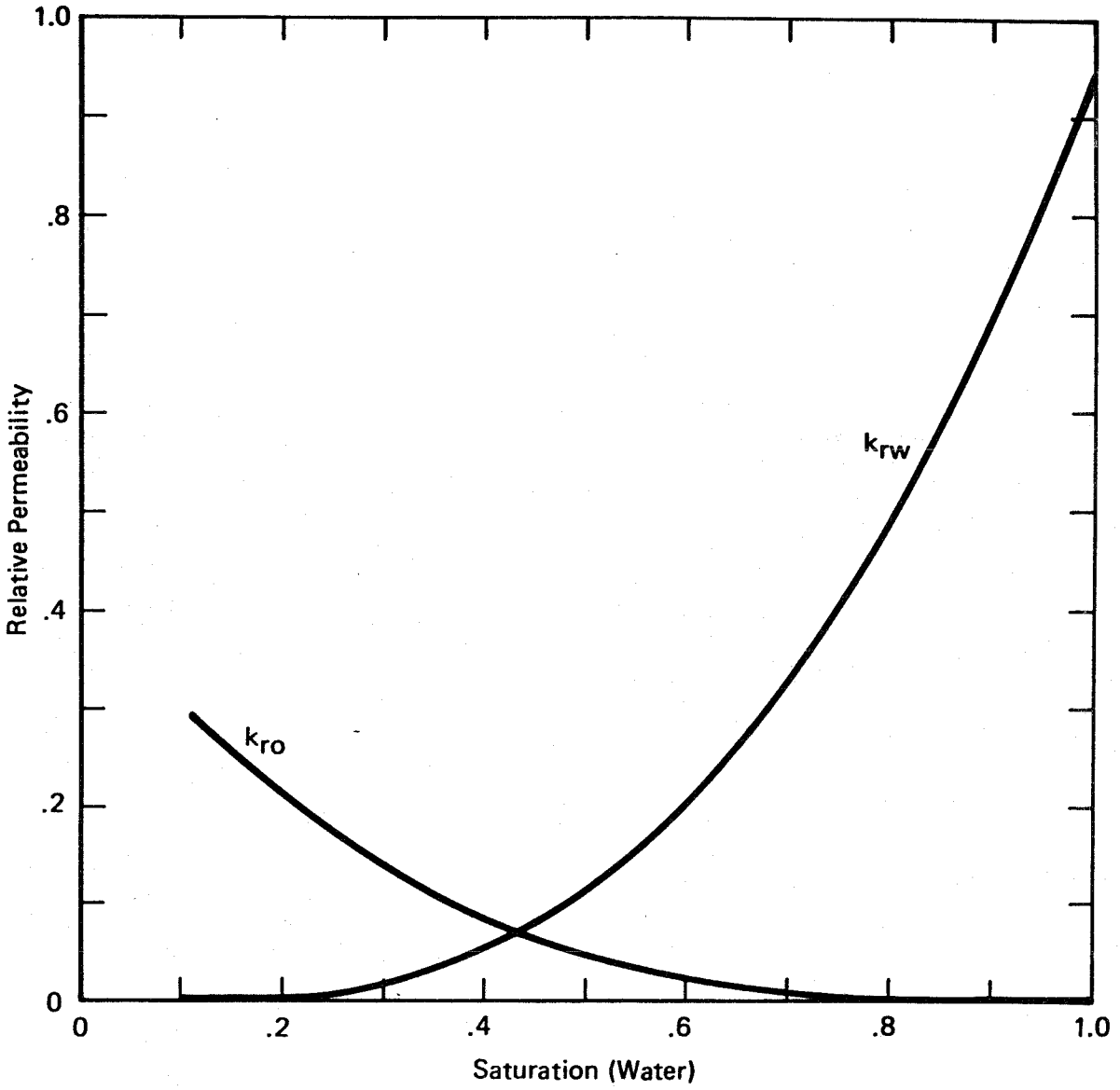

Figure 3.11
Relative Permeabilities - Set C

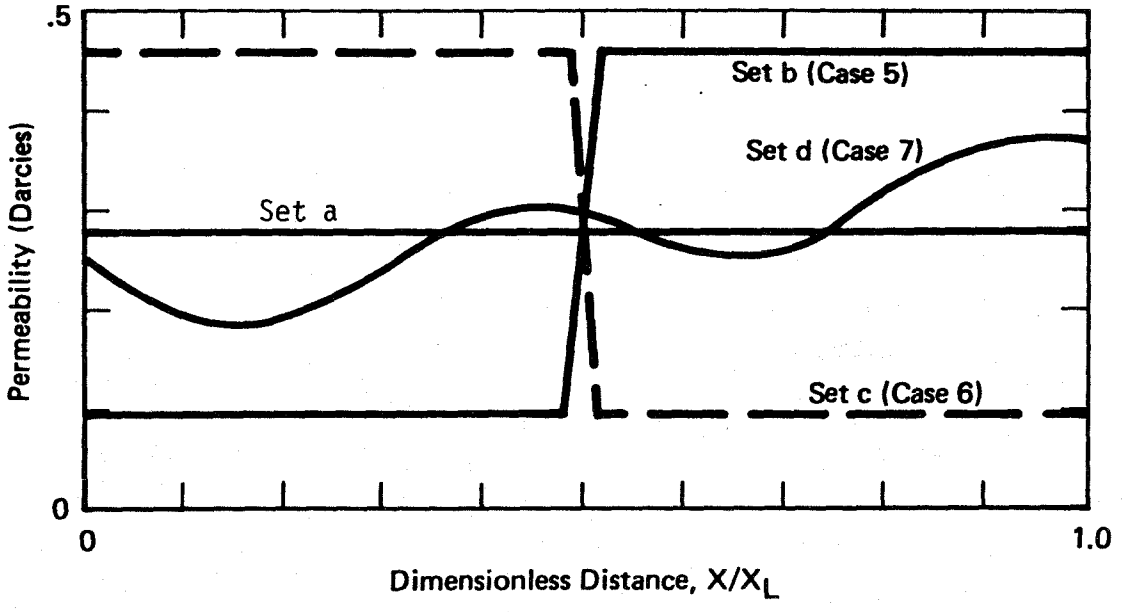

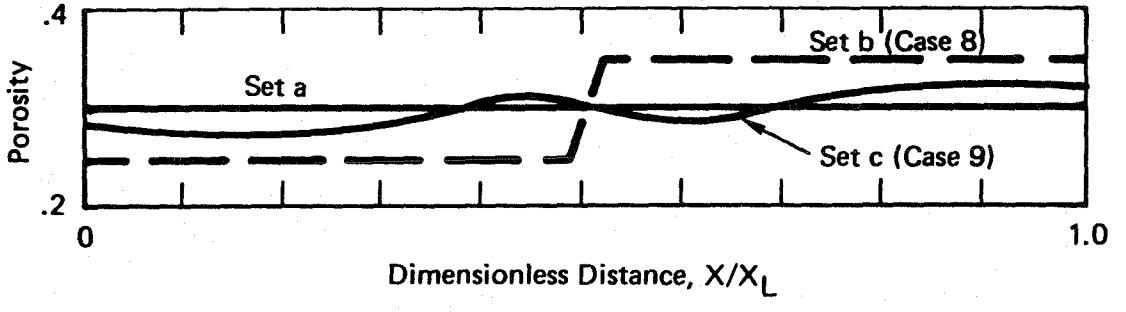

Figure 3.12
Permeability and Porosity Profiles

Table 3.2. Calculated Data for the Example Problems

Case	Initial Pressure Drop (atm)	Breakthrough Time (days)	S_d	$\beta^{(1)}$	$\int_0^1 \frac{f}{k_{rw}} dS^{(1)}$
1	4.8	1610	0.672	1.33	2.37
2	4.8	1820	0.777	4.67	5.77
3	16.0	1340	0.552	0.12	3.80
4	48.0	1080	0.443	-0.34	6.78
5	8.6	1610	0.672		
6	8.6	1610	0.672		
7	5.0	1610	0.672		
8	4.8	1610	0.672		
9	4.8	1610	0.672		

(1) See Eqs. 3.65 and 3.66

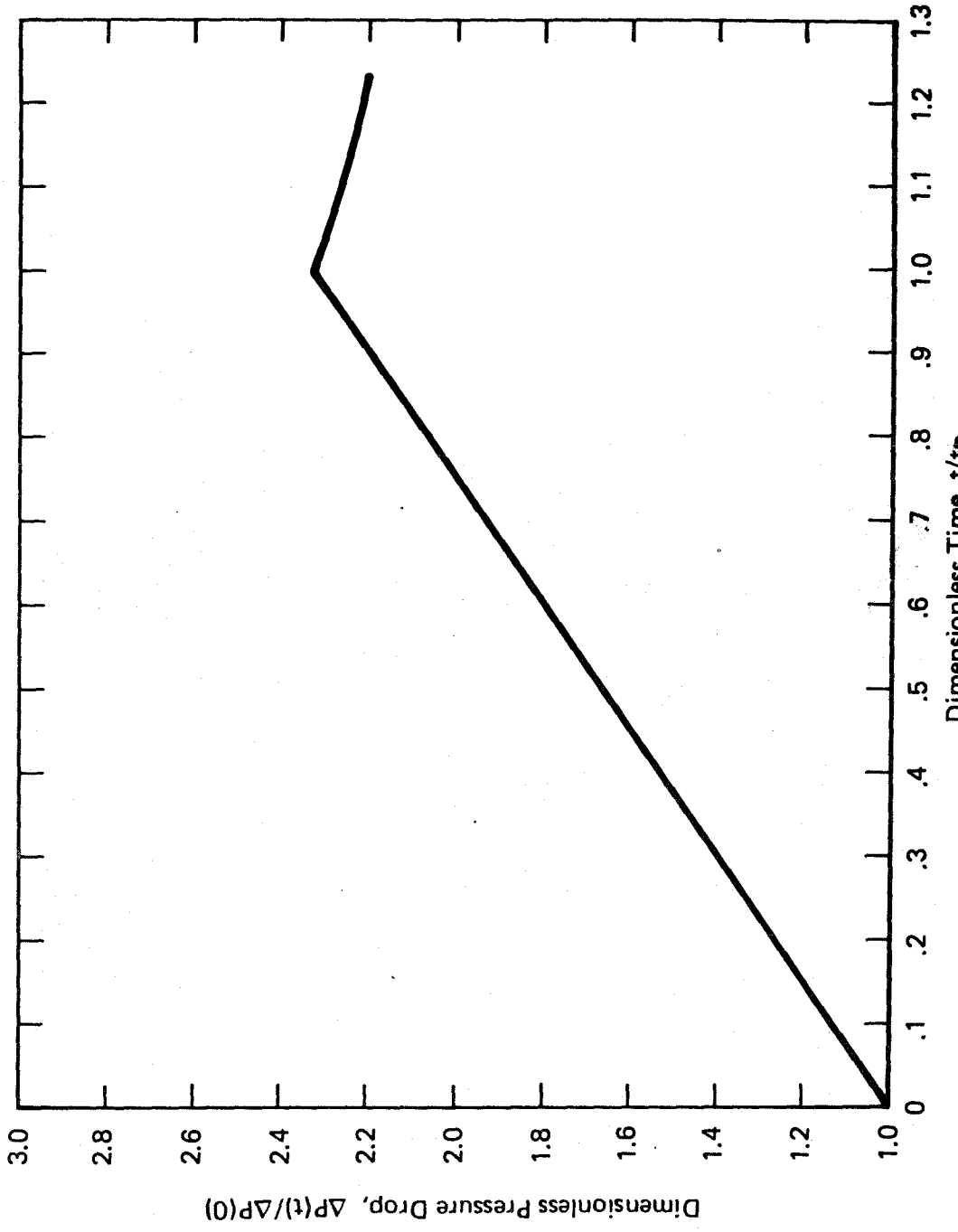

Figure 3.13
Transient Pressure Drop — Case 1

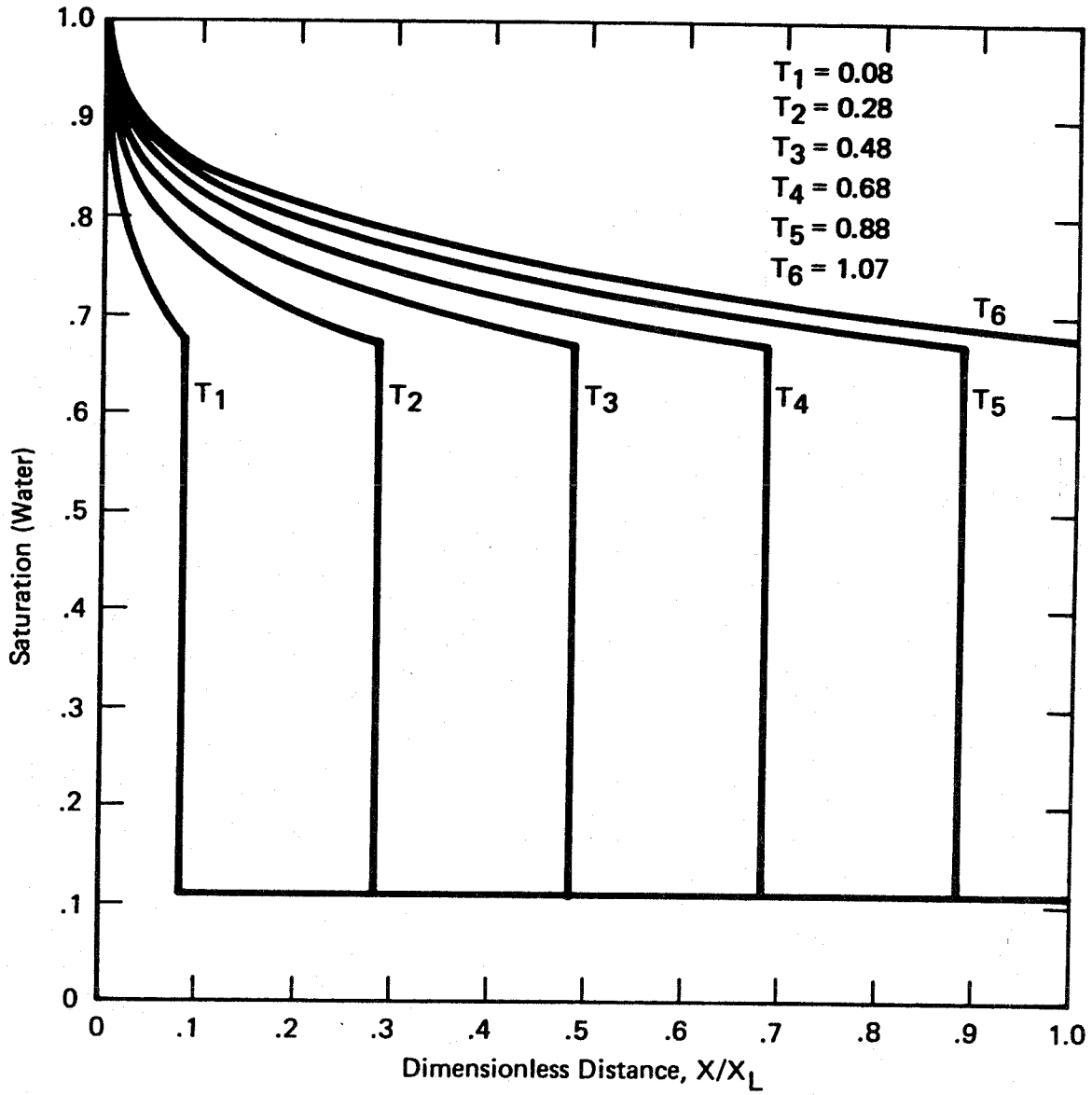

Figure 3.14
Saturation Solution — Case 1

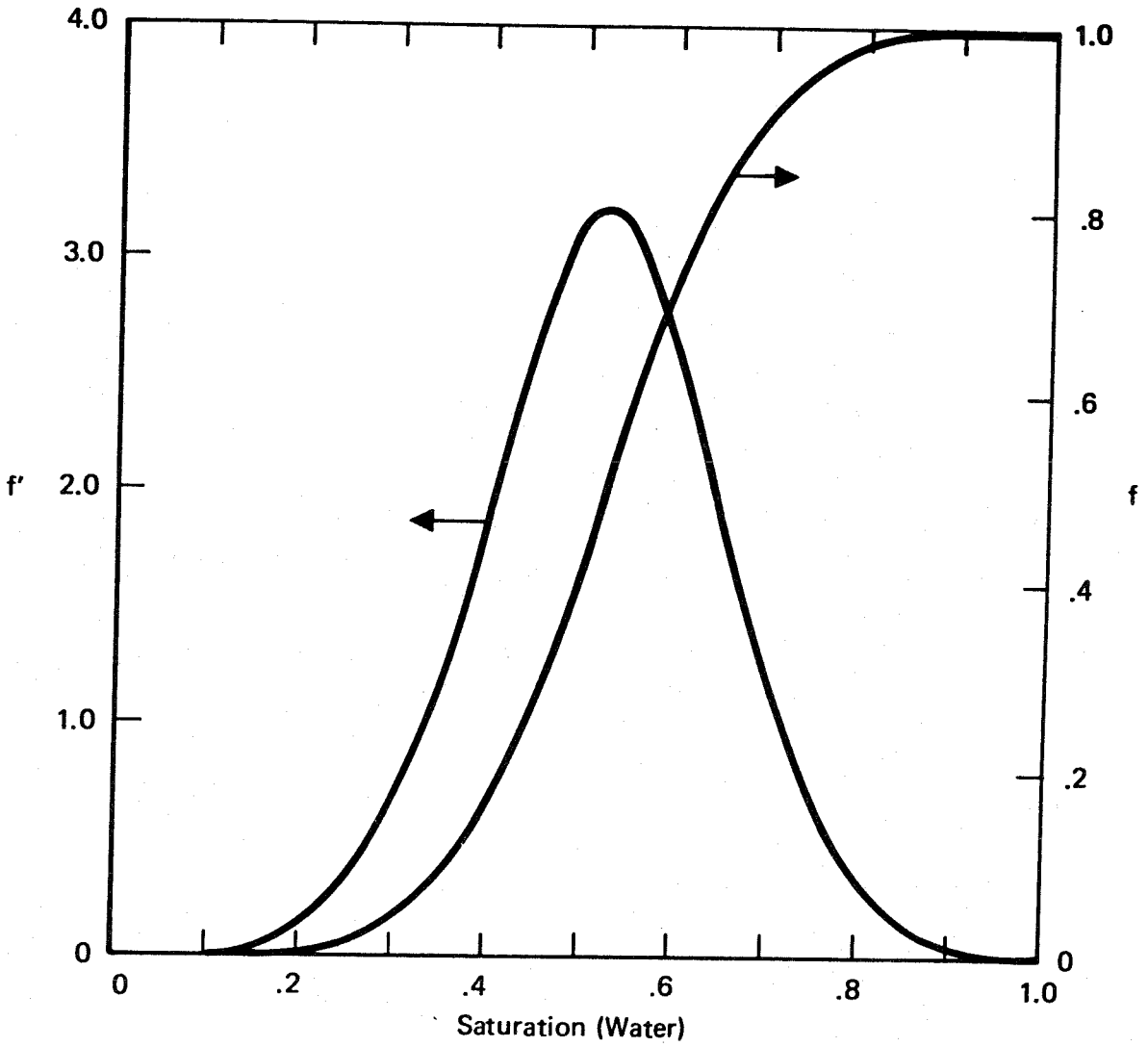

Figure 3.15
Fractional Flow — Set A, $\frac{\mu_o}{\mu_w} = 1$

$$\Delta P^*(\infty) = \frac{\mu_w k_{ro}(S_c)}{\mu_o k_{rw}(1-S_{ro})} \quad , \tag{3.70}$$

which is a measure of the driving force required for the flow of water at saturation $S = 1-S_{ro}$ relative to that required for the flow of oil at $S = S_c$.

Using the pressure equation 3.19, we can show that $\Delta P^*(t)$ is linear with respect to t for $0 \leq t \leq t_B$. This development does not depend upon the particular shapes of the relative permeabilities represented by Eqs. 3.65 and 3.66. Since the saturation for $x > x_d$ is S_c, and since K is constant for these cases, Eq. 3.19 can be written as:

$$\Delta P(t) = \frac{v_t}{K}\left[\mu_w \int_0^{x_d} \frac{f}{k_{rw}}\,dx + \frac{\mu_o}{k_{ro}(S_c)}\,(x_L - x_d)\right] \tag{3.71}$$

For $t = 0$, $x_d = 0$, we obtain the following expression for the initial pressure drop:

$$\Delta P(0) = \frac{v_t}{K}\,\frac{\mu_o}{k_{ro}(S_c)}\,x_L \tag{3.72}$$

The equation for the normalized pressure drop is obtained from Eqs. 3.69,71,72:

$$\Delta P^*(t) = \frac{k_{ro}(S_c)}{x_L}\left[\frac{\mu_w}{\mu_o}\int_0^{x_d} \frac{f}{k_{rw}}\,dx + \frac{1}{k_{ro}(S_c)}\,(x_L - x_d)\right] \tag{3.73}$$

For constant porosity and velocity and the initial and boundary conditions given by Eqs. 3.63 and 3.64, the saturation equation 3.22 can be integrated to:

$$x(S) = \frac{v_t t}{\phi}\,f'(S) \tag{3.74}$$

We will define a new variable ξ by:

$$\xi = \frac{x}{x_d} \tag{3.75}$$

Now the integral in Eq. 3.73 can be expressed as:

$$\int_0^{x_d} \frac{f}{k_{rw}}\, dx = x_d \int_0^1 \frac{f}{k_{rw}}\, d\xi \tag{3.76}$$

Using this form of the integral in Eq. 3.73 and replacing x_d with its equivalent given by Eq. 3.74, Eq. 3.73 can be written as:

$$\Delta P^*(t) = \frac{k_{ro}(S_c)}{x_L}\left[\frac{\mu_w}{\mu_o} v_t \frac{f'(S_d)}{\phi} t\left(\int_0^1 \frac{f}{k_{rw}}\, d\xi - \frac{\mu_o}{k_{ro}(S_c)\mu_w}\right) + \frac{x_L}{k_{ro}(S_c)}\right] \tag{3.77}$$

Using Eqs. 3.74 and 3.75, the variable ξ can be expressed as a function of saturation:

$$\xi = \frac{f'(S)}{f'(S_d)} \tag{3.78}$$

Since S_d is independent of time, Eq. 3.78 implies that the integral in Eq. 3.77 is independent of time for $t \leq t_B$, and the normalized pressure drop is a linear function of time.

Eq. 3.77 can be further simplified by writing it in terms of the dimensionless time defined by Eq. 3.68. The time of breakthrough can be found by evaluating Eq. 3.74 at $x = x_d$ and $S = S_d$ and rearranging:

$$t_B = \frac{\phi x_L}{v_t f'(S_d)} \tag{3.79}$$

Using Eqs. 3.79 and 3.68 to eliminate t from Eq. 3.77, that equation can be written as:

$$\Delta P^*(T) = \beta T + 1 \tag{3.80}$$

where

$$\beta = \frac{k_{ro}(S_c)\mu_w}{\mu_o} \int_0^1 \frac{f}{k_{rw}} d\xi - 1 \tag{3.81}$$

Using Eq. 3.11 for f, the integrand in Eq. 3.77 can be expressed as:

$$\frac{f}{k_{rw}} = \left(k_{rw} + \frac{\mu_w}{\mu_o} k_{ro}\right)^{-1} \tag{3.82}$$

The quantity ΔP^* is the measure of the driving force required to maintain the water flood at a fixed velocity relative to that required for the flow of oil at that same velocity, and the quantity β shows the effect of the relative permeabilities and fluid viscosities on that driving force. Although in Eq. 3.81 these effects are not independent, they can be illustrated by considering two examples.

The first example is the limiting case represented by a moving saturation boundary (or infinitely steep saturation front) first described by Muskat[11]. Assume that the saturation at locations behind the front (i.e. $x < x_d$) is $1-S_{ro}$, and the saturation before the front is S_c. This case would correspond to the following relative permeabilities:

$$\begin{aligned} k_{rw}(S) &= k_{rw}(1-S_{ro}) && S = 1-S_{ro} \\ &= 0 && S \neq 1-S_{ro} \\ k_{ro}(S) &= k_{ro}(S_c) && S = S_c \\ &= 0 && S \neq S_c \end{aligned}$$

The discontinuity in saturation is bounded by $S^- = 1-S_{ro}$, $S^+ = S_c$, and moves with velocity $v_t/(1-S_{ro}-S_c)$. For this case the normalized pressure drop is given by Eq. 3.80 and β is:

$$\beta = \frac{k_{ro}(S_c)\mu_w}{k_{rw}(1-S_{ro})\mu_o} - 1 \tag{3.83}$$

If we further assume that $k_{ro}(S_c) = k_{rw}(1-S_{ro})$, then β is simply

$$\beta = \frac{\mu_w}{\mu_o} - 1 \tag{3.84}$$

If $\mu_w < \mu_o$, the slope of $\Delta P^*(T)$ vs. T is negative, and less pressure is required to maintain the waterflood as the more viscous fluid (oil) is displaced. Thus, in the absence of relative permeability effects, the pressure drop which characterizes the flood is a function of the viscosities. If $\mu_w = \mu_o$ and $k_{ro}(S_c) = k_{rw}(1-S_{ro}) = 1$, the pressure drop corresponds to that for a single phase fluid flow, and $\Delta P^*(T) = 1$.

We can also consider the effect of relative permeabilities in the absence of the viscosity effects. If $\mu_w = \mu_o$, and $k_{ro}(S_c) = 1$, then β is

$$\beta = \int_0^1 \frac{f}{k_{rw}}\, d\xi - 1 \tag{3.85}$$

Almost invariably when oil and water are the two phases in a reservoir, the sum $(k_{rw} + k_{ro}) < 1$, except perhaps at $S = S_c$ or $S = 1-S_{ro}$. Since the integrand in Eq. 3.85 is given by this sum (see Eq. 3.82), β is greater than 1. That is, the pressure drop necessary for the simultaneous flow of two fluids is greater than that for a single fluid. In fact, we might

expect that this integral represents a measure of the degree of nonlinearity (or concavity) in the relative permeability curves since by decreasing the relative permeabilities, the term given by Eq. 3.82 is increased. However, since changing the relative permeabilities also changes the f and f' curves, and hence the relation of S as a function of ξ, the effect of different relative permeabilities on this integral is not so obvious. For Cases 1-4, the values for the integral and β in Eq. 3.81 and the values for S_d are given in Table 3.2.

In Case 2, the relative permeability of oil is the same as that used in Case 1, and the relative permeability of water is three-tenths that of Case 1. The pressure for Case 2 is shown in Fig. 3.16. The slope β in Eq. 3.80 for the pressure profile for this case is greater than that of Case 1, as is the integral in Eq. 3.81.

The saturation solution for Case 2 is shown in Fig. 3.17. Since the fractional flow is different from Case 1, a different value of S_d is obtained. This value is greater than that obtained for the first case, and the saturation profile more nearly approximates piston-like displacement. Since the porosity and velocity are identical to Case 1, the time of breakthrough is later than Case 1. The f and f' curves for Case 2 are shown in Fig. 3.18, and the values for S_d and t_B are given in Table 3.2.

In Case 3, the relative permeability of water is identical to that used in Case 1, and the relative permeability of oil is three-tenths that of Case 1. The pressure solution for this case is shown in Fig. 3.19. If we compare the values of the integral and β given by Eq. 3.81 to those for Case 1 (see Table 3.2), we find that the value of the integral is larger, but β is smaller for this case. The reason is that the value of $k_{ro}(S_c)$

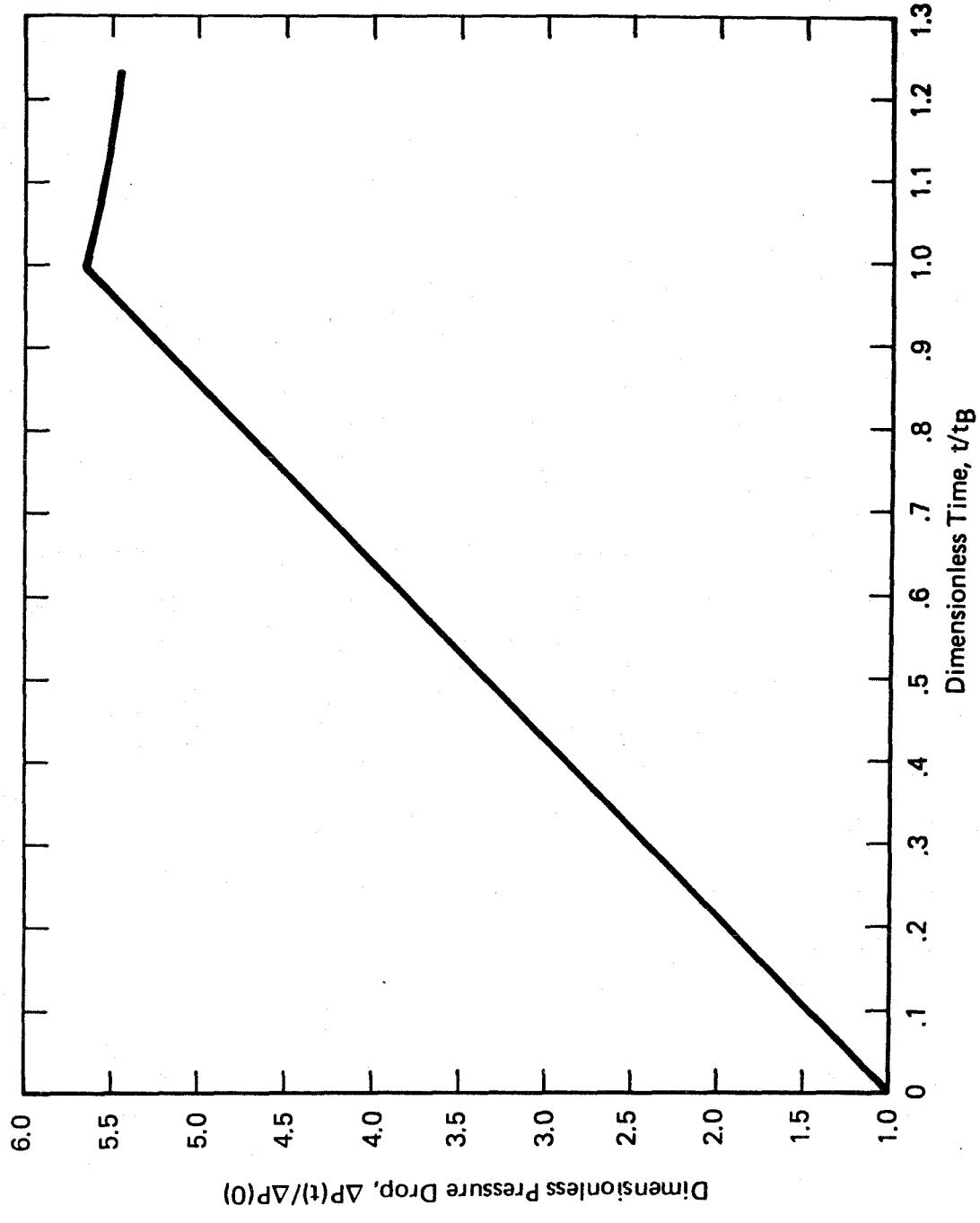

Figure 3.16
Transient Pressure Drop — Case 2

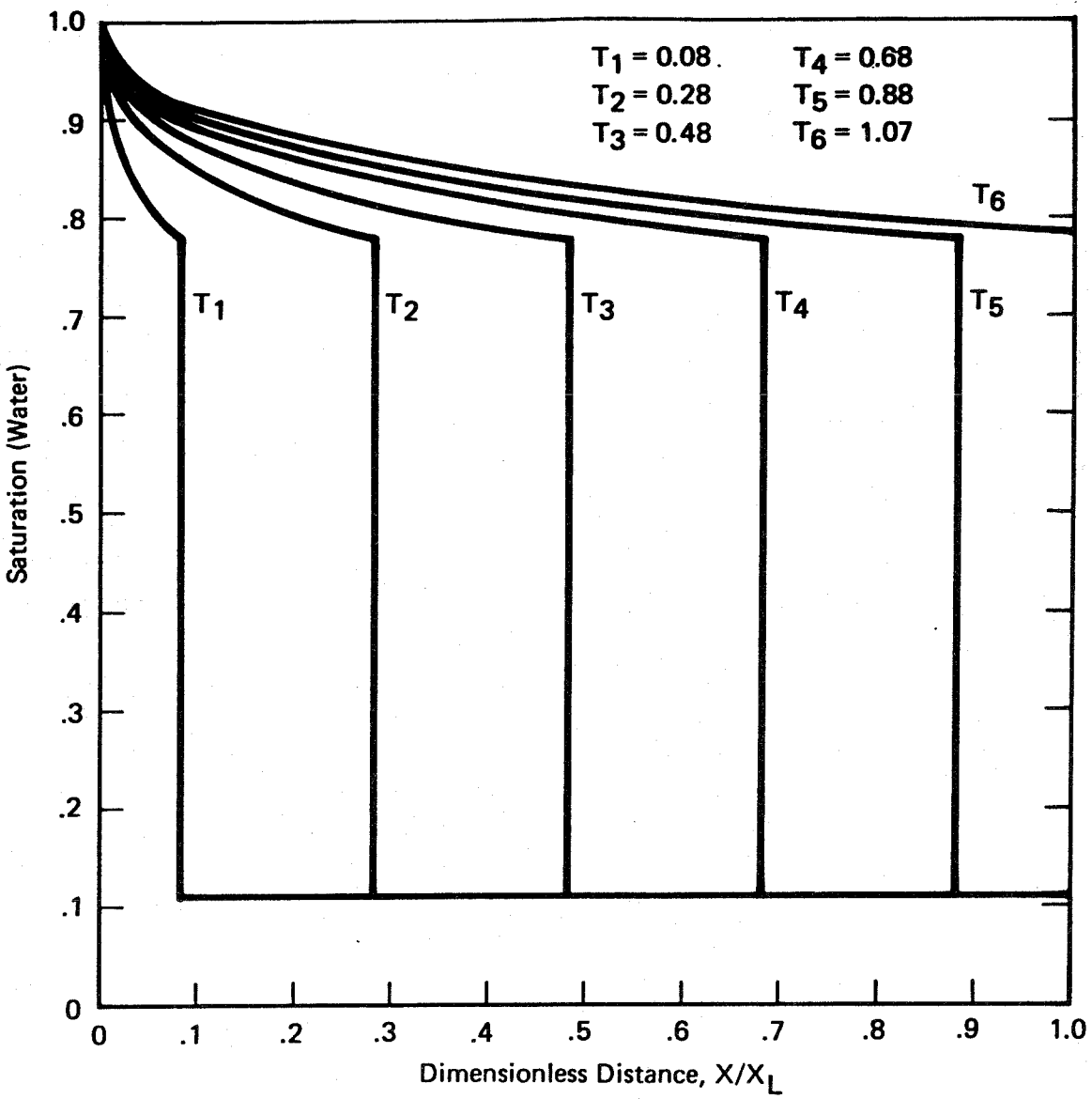

Figure 3.17
Saturation Solution — Case 2

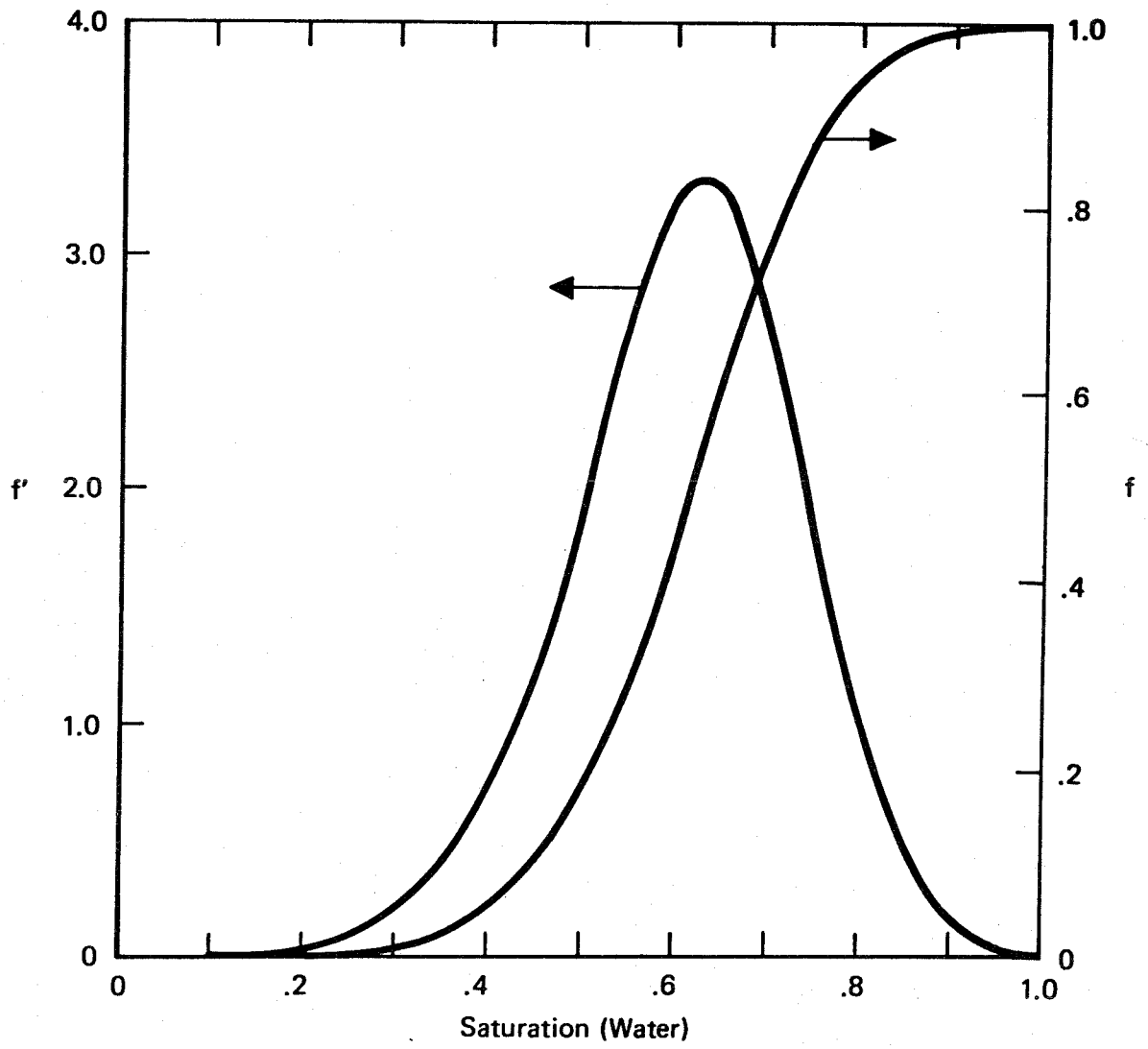

Figure 3.18
Fractional Flow – Set B, $\frac{\mu_o}{\mu_w} = 1$

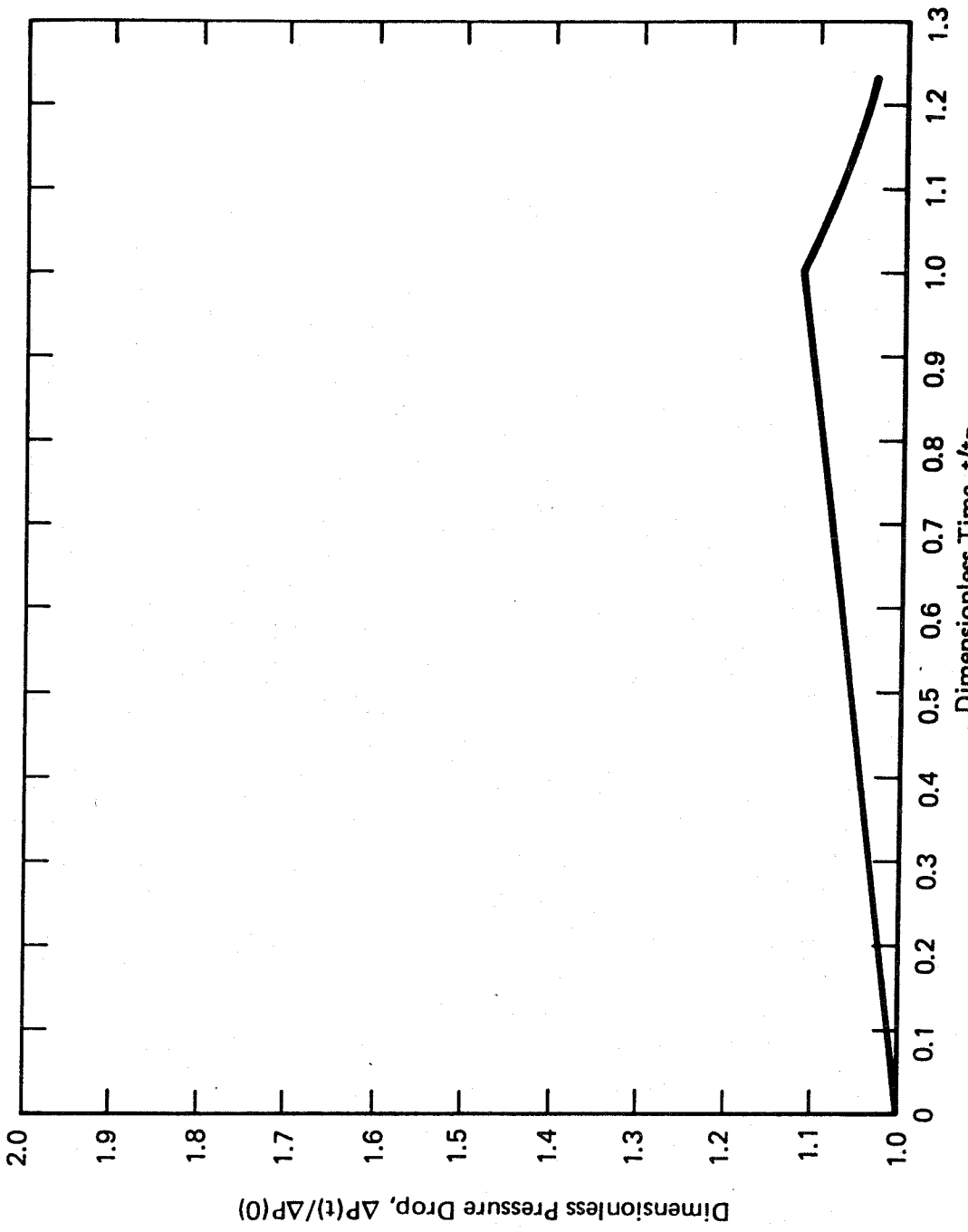

Figure 3.19
Transient Pressure Drop – Case 3

is much smaller for Case 3. This value has the inverse effect of μ_o in the moving boundary problem discussed above (see Eq. 3.83) and appears explicitly in the value of β given by Eq. 3.81.

The saturation solution for Case 3 is shown in Fig. 3.20. For this case the value calculated for S_d is smaller than that in Case 1, and water breakthrough is earlier.

The parameters used in Case 4 are identical to those used for Case 1, except that $\mu_o = 10$. The effect of increasing the oil viscosity is similar to that of decreasing the relative permeability of oil, as was done in Case 3. This can be seen by examining Eqs. 3.81-83. For this case the value of the integral in Eq. 3.81 is larger than Cases 1-3, and the slope β is smaller, and in fact negative as shown in Fig. 3.21. The saturation solution is shown in Fig. 3.22. The value for S_d is smaller for this case than the previous case, and the water breakthrough time is earlier. Comparison of Figs. 3.15, 18 and 23 shows the effect that changing the relative permeability and viscosity parameters has on the values of S_d that were obtained.

3.3.2 Permeability

Here we consider the effect of spatially varying permeability on the solution. The parameters used are given in Table 3.1. In Cases 5-7 we used the same parameters as Case 1, except that different absolute permeability profiles, shown in Fig. 3.12, were used.

For times $t \leq t_B$, the pressure equation 3.19 can be written as:

$$\Delta P(t) = v_t \left[\mu_w \int_0^{x_d} \frac{f}{K k_{rw}} dx + \frac{\mu_o}{k_{ro}(S_c)} \int_{x_d}^{x_L} \frac{1}{K} dx \right] \qquad (3.86)$$

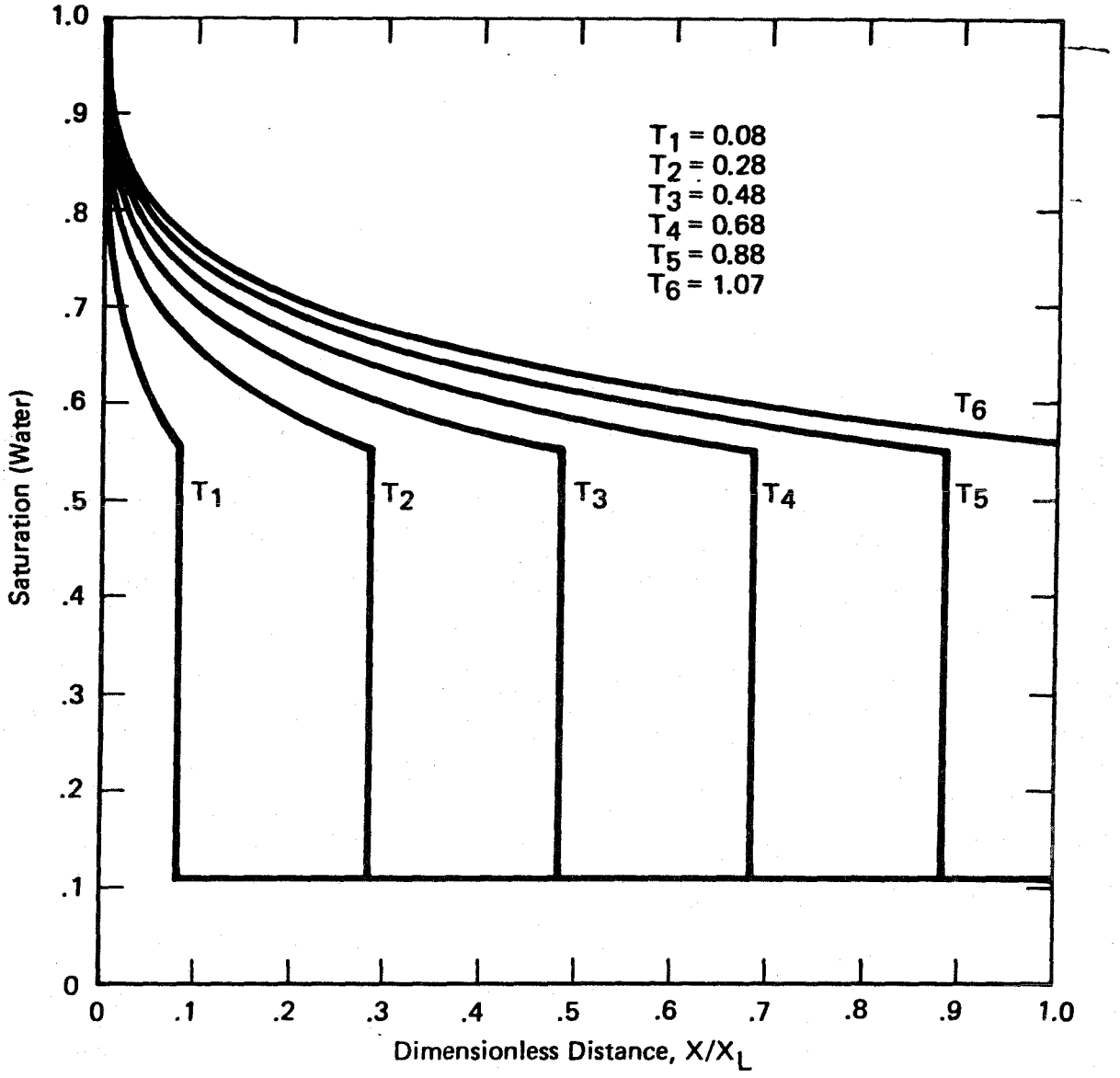

Figure 3.20
Saturation Solution — Case 3

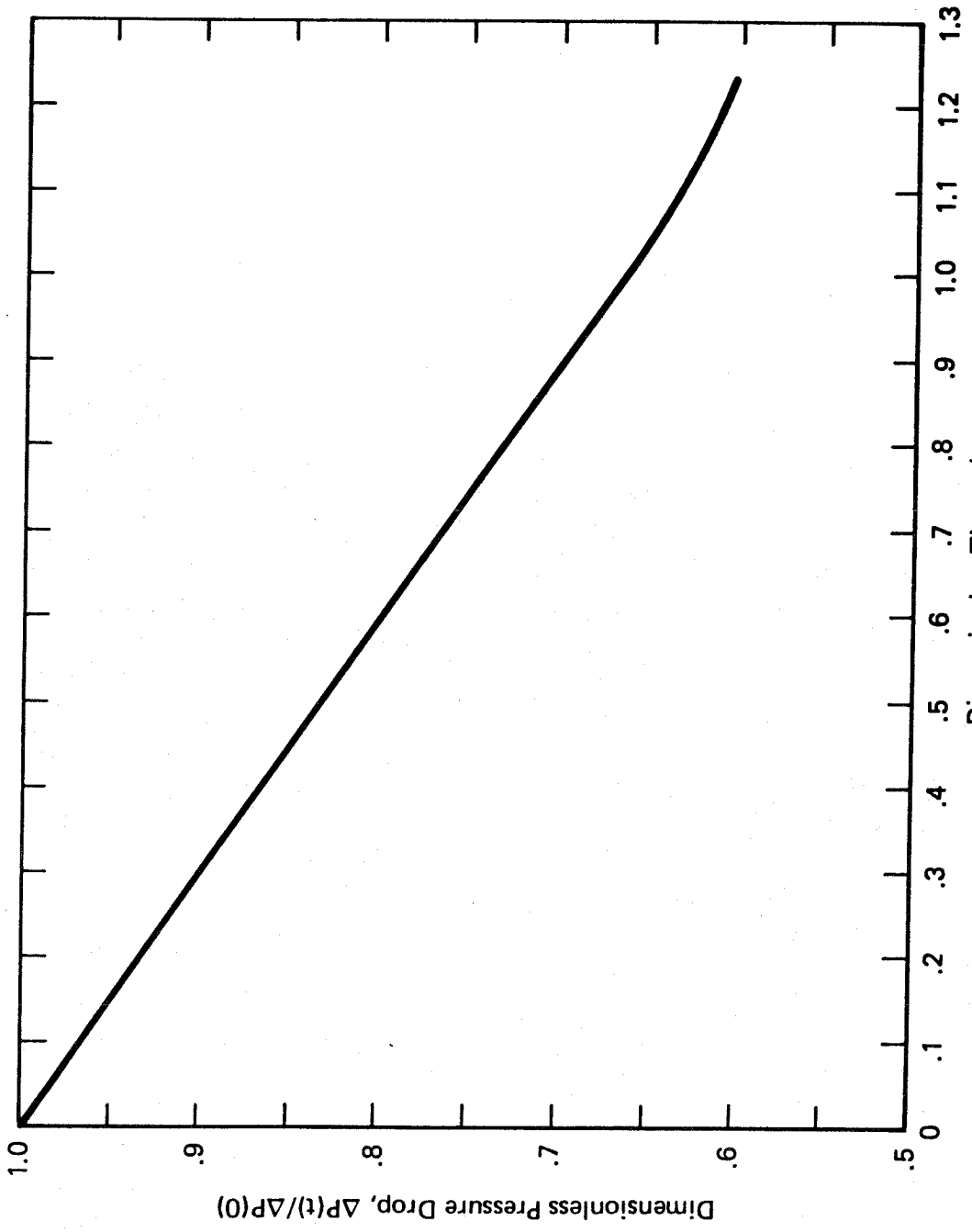

Figure 3.21
Transient Pressure Drop – Case 4

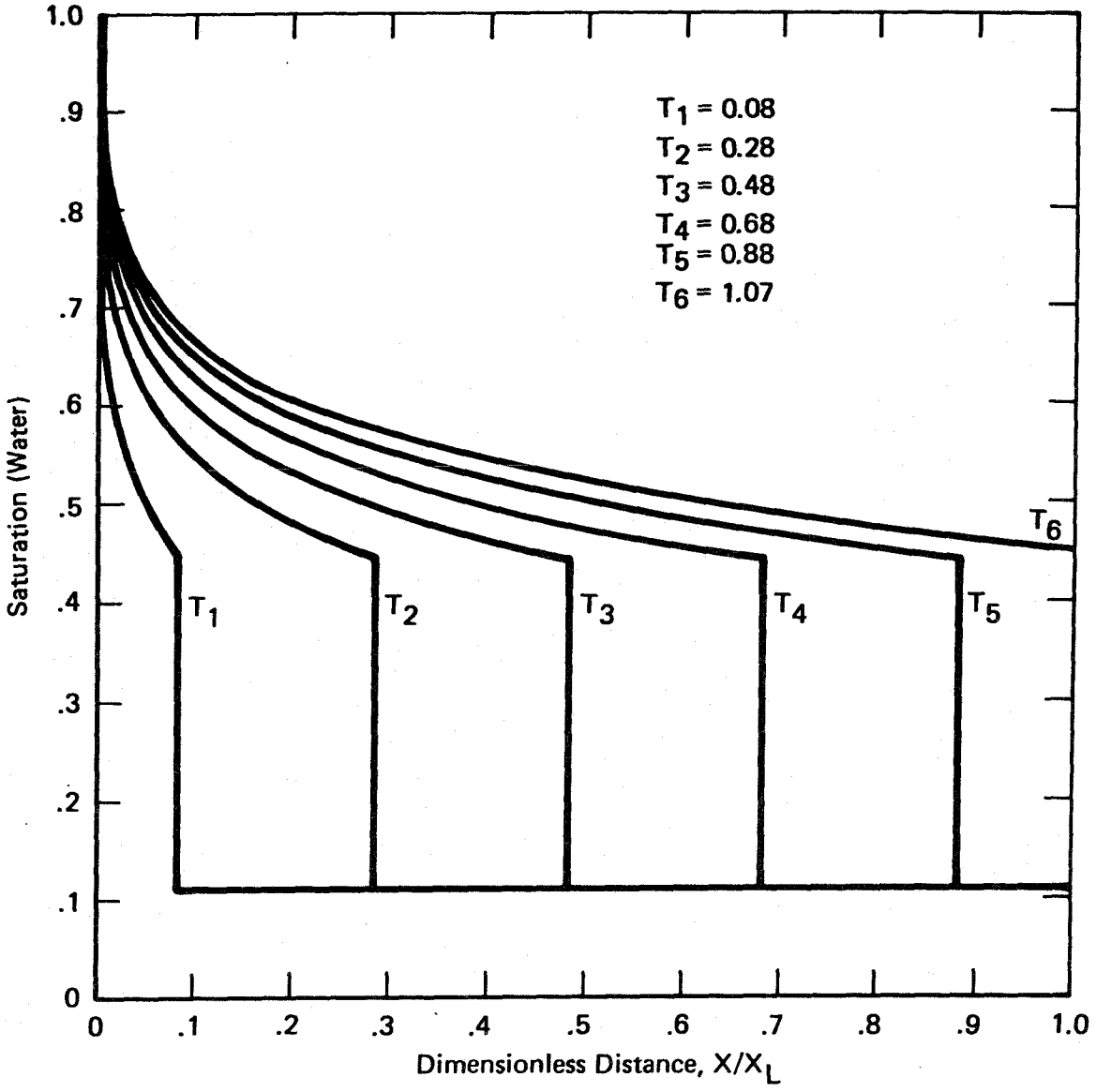

Figure 3.22
Saturation Solution — Case 4

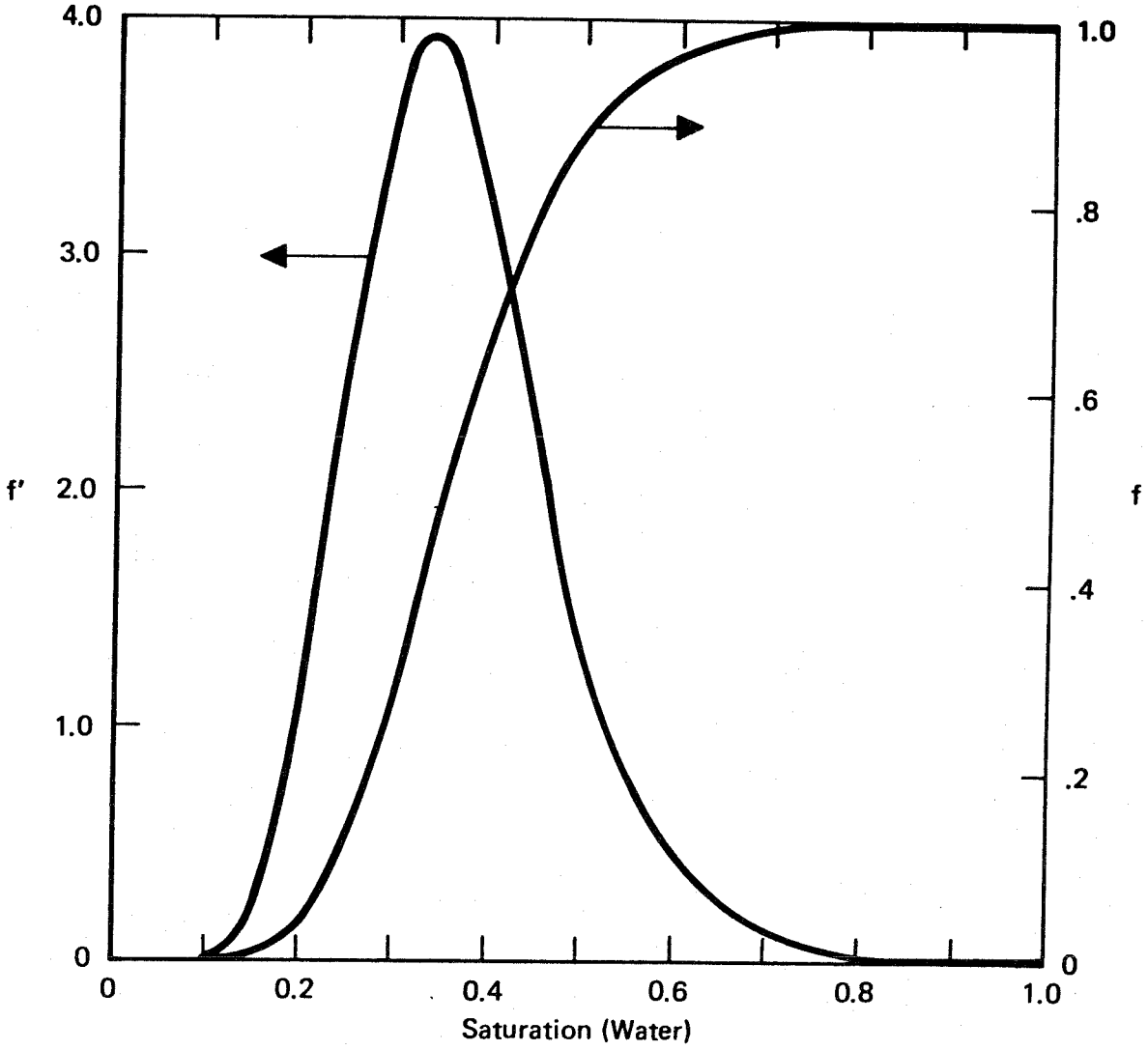

Figure 3.23
Fractional Flow – Set A, $\frac{\mu_o}{\mu_w} = 10$

Investigation of the effect of relative permeabilities in Section 3.3.1 showed the importance of the saturation solution, and consequently the integral in Eq. 3.71, on the pressure solution. Now the spatially varying permeability appears in that integral, and the relation of the saturation profile relative to the absolute permeability profile is important.

The pressure solution for Cases 1, 5-7 are shown in Fig. 3.24. The initial pressure drop for these cases is given by

$$\Delta P(0) = \frac{v_t \mu_o x_L}{k_{ro}(S_c)} \int_0^{x_L} \frac{1}{K}\, dx \qquad (3.87)$$

The saturation solution is independent of the permeability, so the saturation solution for these cases are identical to that of Case 1, which is shown in Fig. 3.14.

Since v_t and ϕ are constant and the dimensionless X and T were chosen as in Eqs. 3.67 and 3.68, the location of the shock at time $T \leq 1$ is given by T (i.e. $X_d(T) = T$, $T \leq 1$). The permeability profiles for Cases 5 and 6 are constant for $X \leq 0.483$. The pressure solutions for $T \leq 0.483$ are linear with respect to time for these cases. This can be shown by considering some permeability profile K such that

$$\begin{aligned} K &= K_m \qquad & x &\leq x_m \\ K &= K(x) \qquad & x &> x_m \end{aligned}$$

For $x_d \leq x_m$, Eq. 3.86 can be written as:

$$\Delta P(t) = v_t \left\{ \frac{\mu_w}{K_m} \left[\int_0^{x_d} \frac{f}{k_{rw}}\, dx + \frac{\mu_o}{k_{ro}(S_c)\mu_w}(x_m - x_d) \right] + \frac{\mu_o}{k_{ro}(S_c)} \int_{x_m}^{x_L} \frac{1}{K}\, dx \right\} \qquad (3.88)$$

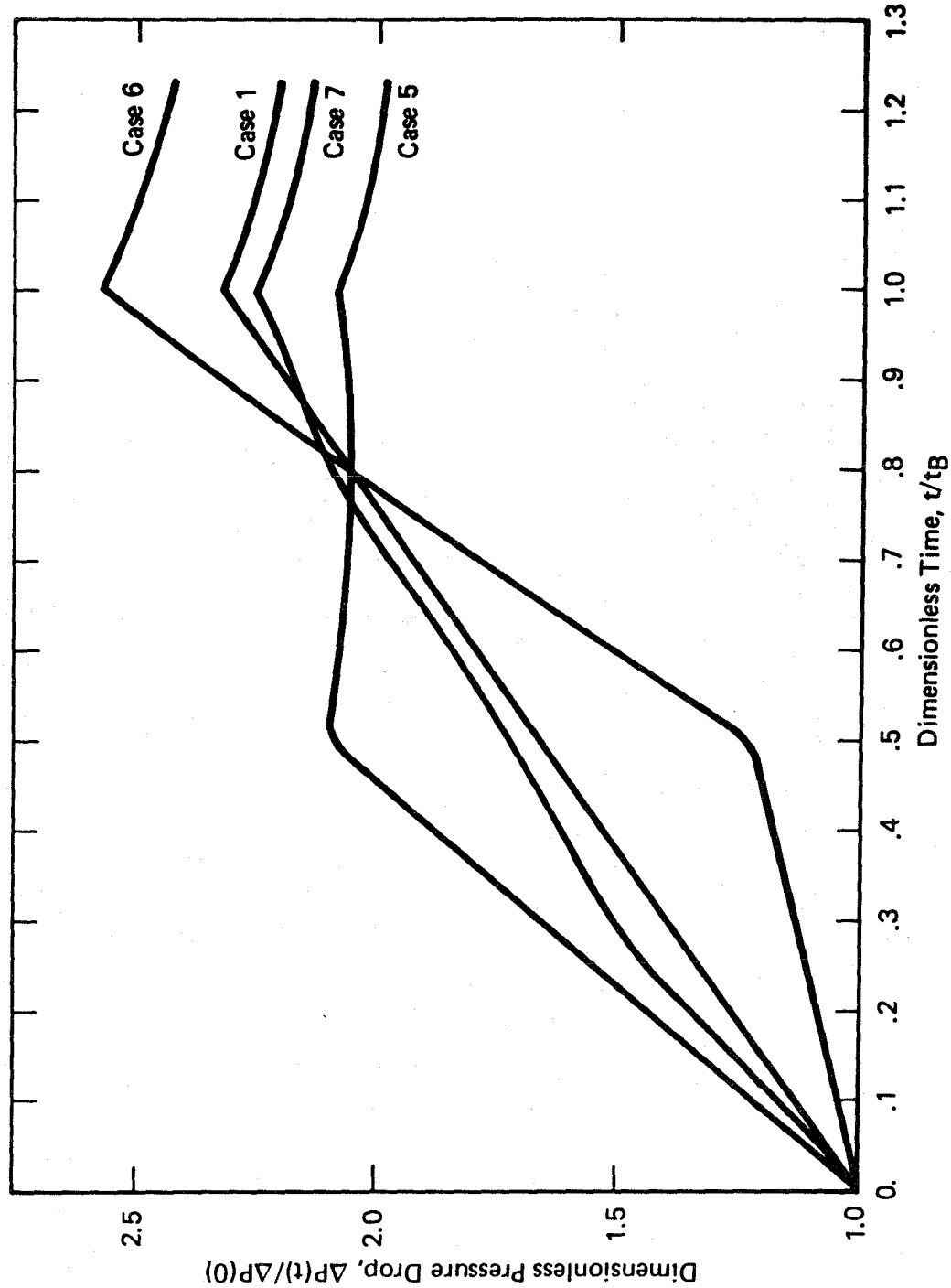

Figure 3.24
Transient Pressure Drop for Spatially Varying Permeability

Comparing Eq. 3.88 to Eq. 3.71, we note that the parameters which are functions of time (i.e. x_d and $\int_0^{x_d} \frac{f}{k_{rw}}\,dx$) appear in the same way in both equations. By an analysis similar to that used to show that Eq. 3.71 is a linear function of time, it can be shown that Eq. 3.88 is linear with respect to time.

Once the saturation front has passed into a region for which the permeability varies, then the spatial distribution K(x) for $x \leq x_d$ enters into the solution for the pressure drop (through the first integral in Eq. 3.86), but only an average of K(x) for $x > x_d$ (the second integral in that equation).

The importance of the characteristics of two-phase flow in the calculated pressure drop for spatially varying permeability can be illustrated by examining the moving boundary problem which was considered in the discussion of relative permeability in Section 3.3.1. For this limiting case, the pressure equation 3.19 can be written as:

$$\Delta P(t) = v_t \left[\frac{\mu_w}{k_{rw}(1-S_{ro})} \int_0^{x_d} \frac{1}{K}\,dx + \frac{\mu_o}{k_{ro}(S_c)} \int_{x_d}^{x_L} \frac{1}{K}\,dx \right] \tag{3.89}$$

If $\mu_w = \mu_o$ and $k_{rw}(1-S_{ro}) = k_{ro}(S_c) = 1$, then Eq. 3.89 becomes

$$\Delta P(t) = v_t \int_0^{x_L} \frac{1}{K}\,dx$$

This solution is identical to the solution for the single phase flow problem (see Eq. 2.2). The pressure drop is a constant which only

depends upon an integral of the spatially varying permeability. The calculated pressure drop would be identical for permeability profiles b and c in Fig. 3.12, and the normalized pressure drop would be equal to one for all times. If $\frac{\mu_w}{k_{rw}(1-S_{ro})} \neq \frac{\mu_o}{k_{ro}(S_c)}$, the pressure solutions given by Eq. 3.89 would be different for the two permeability profiles for $t < t_B$.

3.3.3 Porosity

The parameters used in Cases 8 and 9 are the same as Case 1, except that different porosity profiles were used (see Fig. 3.12). The saturation solution is different for these cases; the saturation solutions for Cases 8 and 9 are given in Figs. 3.25 and 3.26. However, the time of breakthrough for these cases is the same since the value of $\int_0^{x_L} \phi dx$ is the same for each case.

A smaller porosity has the effect of increasing the velocity at which a given saturation travels (see Eq. 3.11). Since the porosity profiles for Cases 8 and 9 are not constant, the value of X_d no longer corresponds to T. By comparing the saturation solution for Cases 1 and 8 (see Figs. 3.14 and 3.25), we see that the times for which the front x_d is at a particular location are different for these two cases. Careful examination of Fig. 3.25 shows that there is a kink in the saturation profiles for T_4, T_5, and T_6 at approximately X = 0.5 which corresponds to the change in the porosity profile b at that location.

The pressure solutions for Cases 1, 8, and 9 are shown in Fig. 3.27. Note that for Case 8 the slope of ΔP^* is linear for $T \leq 0.4$. Since the porosity for profile b is a constant for $X \leq 0.483$, Eq. 3.74 can be used

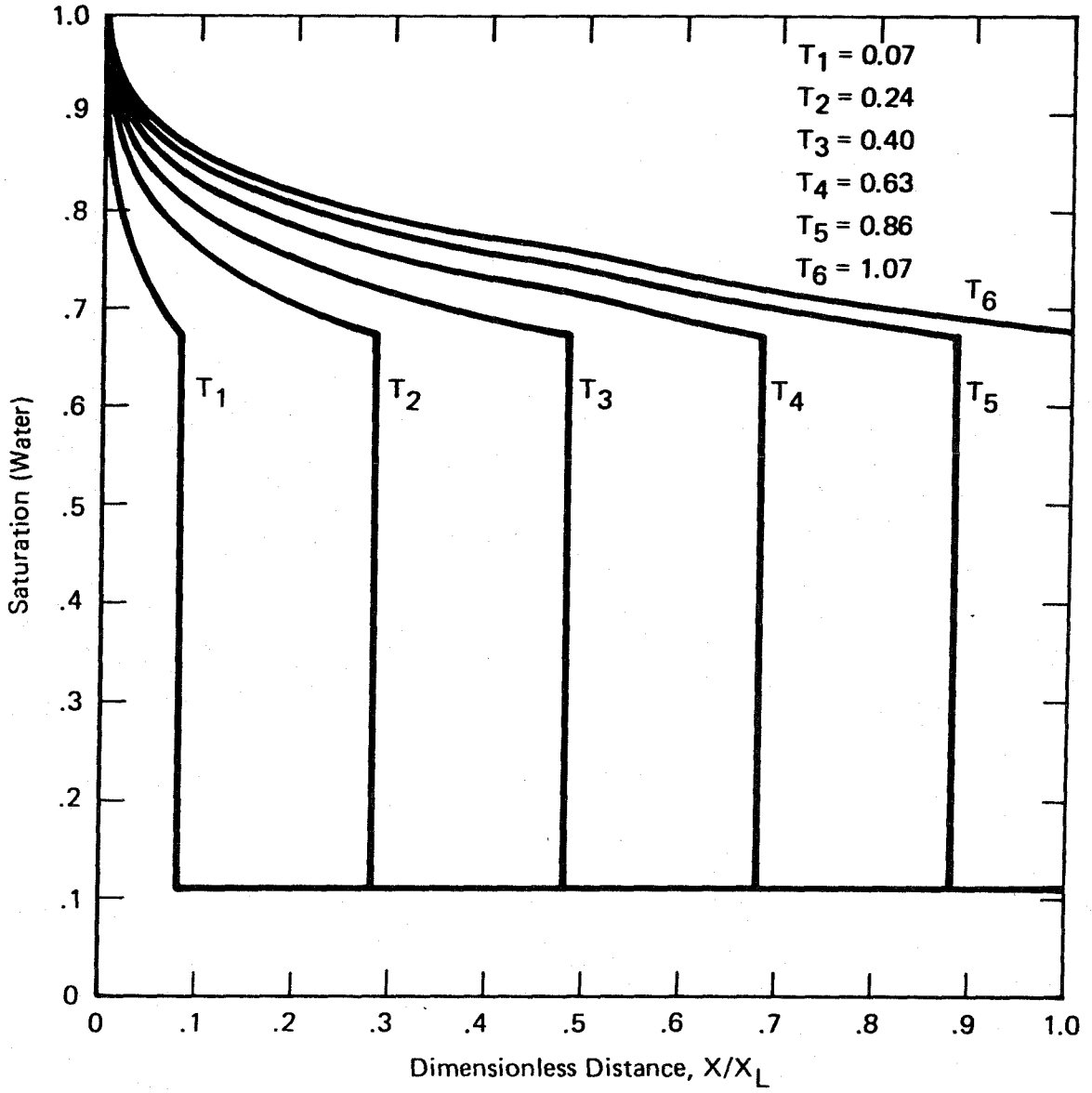

Figure 3.25

Saturation Solution for Spatially Varying Porosity – Case 8

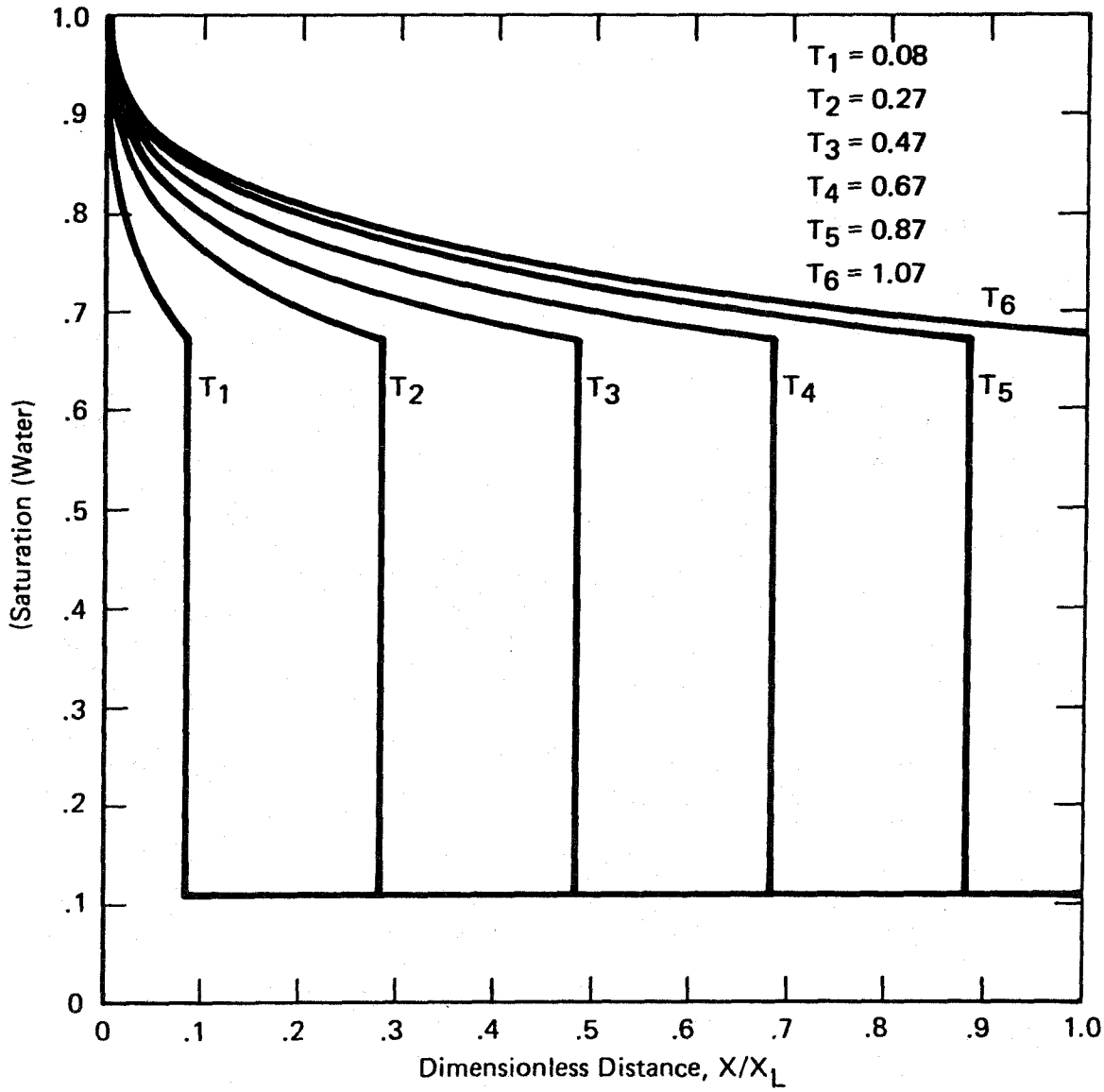

Figure 3.26

Saturation Solution for Spatially Varying Porosity — Case 9

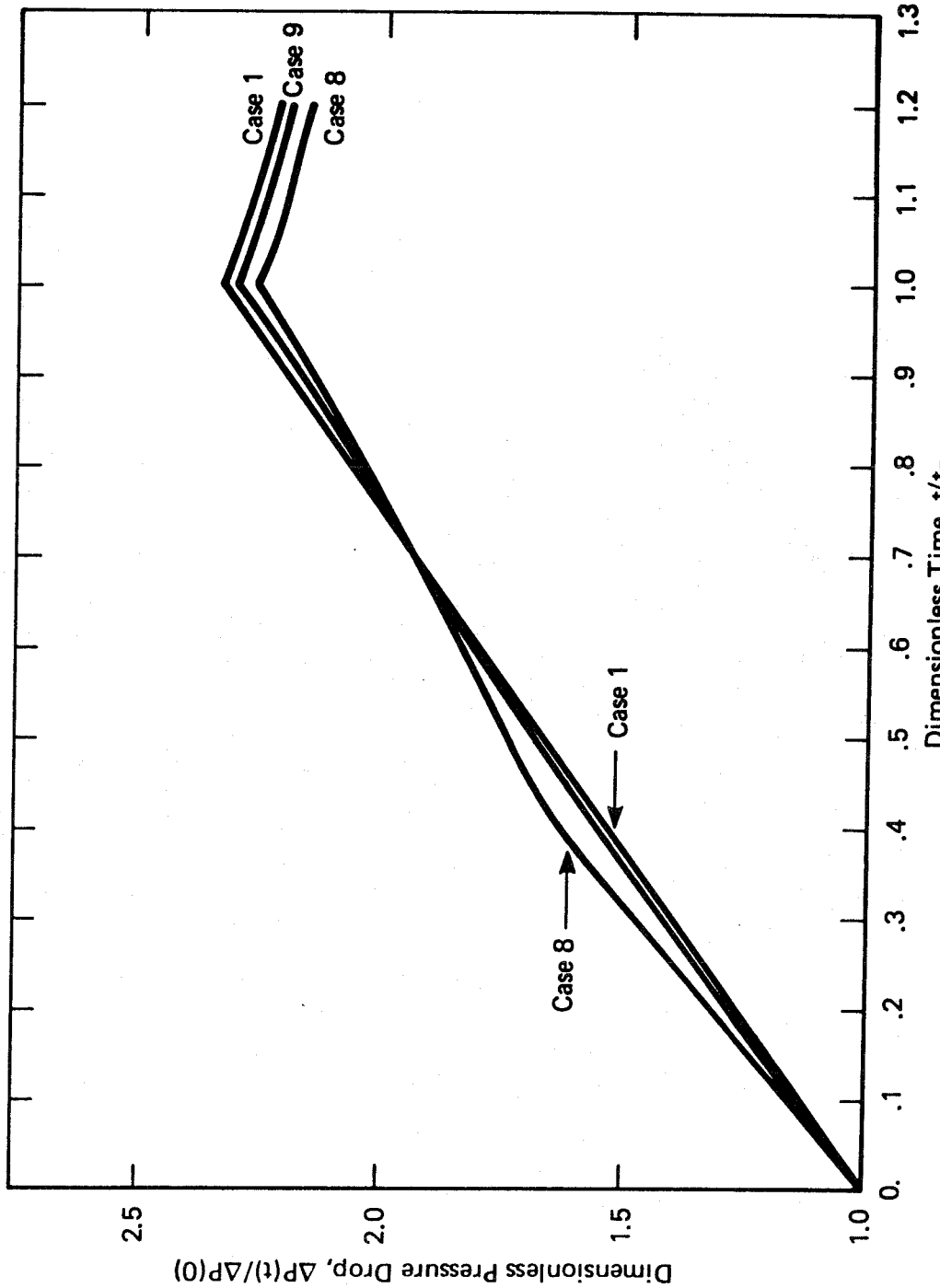

Figure 3.27
Transient Pressure Drop for
Spatially Varying Porosity

to construct the saturation solution for $X \leq 0.483$. In particular, if we use that equation to compare the times for which the shock is at location X_d for Case 1 and Case 8, we find that

$$T_{[\text{Case 8}]} = \left(\frac{.25}{.3}\right) T_{[\text{Case 1}]}$$

where 0.3 and 0.25 are the porosities for $X \leq 0.483$ for Cases 1 and 8, respectively. That is, for Case 8 the shock is at the location of the change in the porosity profile at $T = 0.4$.

3.4 Summary and Conclusions

In Section 3.1 a model was specified for which an analytical solution of Eqs. 2.12-16 can be obtained. In Subsections 3.2.1 and 3.2.2 the solution of the saturation equation for homogeneous reservoir models by the method of characteristic was developed. Both the analytical and graphical construction of shocks in the saturation equation were discussed.[1,6-10] The solution was extended to heterogeneous reservoir models in Subsection 3.2.3. It was shown that the Welge solution[7] also applies to heterogeneous models.

The effects of reservoir model properties on the saturation and pressure drop solution for a water flooding problem were examined in Section 3.3. In Subsection 3.3.1 it was shown that the pressure drop is linear with respect to time before breakthrough for a constant flow rate and homogeneous reservoir properties.

The effect of spatially varying permeability on the pressure drop solution was illustrated in Subsection 3.3.2. For single phase incompressible flow, the pressure drop depends upon an integral of the permeability. Any

permeability profiles which have the same harmonic average will have the same pressure drop response. For two-phase flow, the pressure drop at any time depends upon the position of the saturation profile. The spatially varying profile of permeability at locations behind the saturation discontinuity (i.e., for locations for which the water saturation is greater than the connate water saturation) affects the pressure drop solution.

The effect of spatially varying porosity was discussed in Subsection 3.3.3. Porosity appears explicity in the saturation equation and implicitly in the pressure equation. At any time, the saturation value calculated at a particular location depends upon an integral value of the porosity behind that location. Spatially varying porosity indirectly affects the pressure drop since the calculated pressure drop is a function of the saturation profile.

4. NUMERICAL SOLUTION FOR COMPRESSIBLE OIL-WATER RESERVOIRS

In order to simulate multi-dimensional, compressible two-phase reservoir flow described by Eqs. 2.12-22, it has been necessary to resort to numerical techniques. Although different numerical techniques have been investigated, the method now used universally in the production industry is finite-differences.

Formulation of a finite-difference procedure for these equations is made difficult by the presence of nonlinear relative permeability terms and the mixed nature of the coupled partial differential equations illustrated in Section 2.2. There is in fact a variety of ways in which the nonlinear terms can be handled and the method chosen usually depends upon the particular application[4].

In Section 4.1 the finite-difference equations used are developed[3,4,13]. The stability and truncation error associated with this finite-difference form is examined in the second section[3,14]. Some solutions to test problems which indicate the effects of truncation error on the pressure and saturation solutions are presented in Section 4.3.

4.1 Finite-Difference Equations

In this section we develop the finite-difference equations used to solve the system described by Eqs. 2.12-22. The spatial domain is represented by a Cartesian coordinate system with axes x and y. In this development, we make the following assumptions regarding the geometry of the reservoir: (1) the boundaries can be represented, or approximated, as a rectangle bounded by $x = 0$, x_B and $y = 0$, y_B, (2) the boundaries are impermeable to fluid flow, and (3) the thickness of the reservoir is independent of location.

The manner by which assumptions (1) and (2) can be relaxed will be discussed later in this section. Although assumption (3) is not necessary since reservoirs which have a thickness that depends upon location can readily be handled, that case was not considered in this study.

Using Eqs. 2.14 and 2.15 to eliminate the flow velocities $\underset{\sim}{v}_w$ and $\underset{\sim}{v}_o$ in Eqs. 2.12 and 2.13, the partial differential equations describing our system can be written as:

$$\frac{\partial(\phi\rho_w S_w)}{\partial t} = \frac{\partial}{\partial x}\left[\frac{K_x\rho_w}{\mu_w} k_{rw} \frac{\partial P}{\partial x}\right] + \frac{\partial}{\partial y}\left[\frac{K_y\rho_w}{\mu_w} k_{rw} \frac{\partial P}{\partial y}\right] + \sum_{m=1}^{NW} q_{w_m} \delta(x-x_m)\delta(y-y_m) \tag{4.1}$$

$$\frac{\partial(\phi\rho_o S_o)}{\partial t} = \frac{\partial}{\partial x}\left[\frac{K_x\rho_o}{\mu_o} k_{ro} \frac{\partial P}{\partial x}\right] + \frac{\partial}{\partial y}\left[\frac{K_y\rho_o}{\mu_o} k_{ro} \frac{\partial P}{\partial y}\right] + \sum_{m=1}^{NW} q_{o_m} \delta(x-x_m)\delta(y-y_m) \tag{4.2}$$

The no-flux boundary conditions (see Fig. 4.1) are:

$$\frac{\partial P}{\partial x} = 0 \qquad x = 0,\ x_B \tag{4.3}$$

$$\frac{\partial P}{\partial y} = 0 \qquad y = 0,\ y_B \tag{4.4}$$

We will introduce into Eqs. 4.1 and 4.2 the formation volume factors B_w and B_o, the ratio of the volume of a fluid at local reservoir conditions of pressure and temperature to that at standard temperature and pressure (60^o F and 1 atm.). The formation volume factor for a fluid can be expressed as

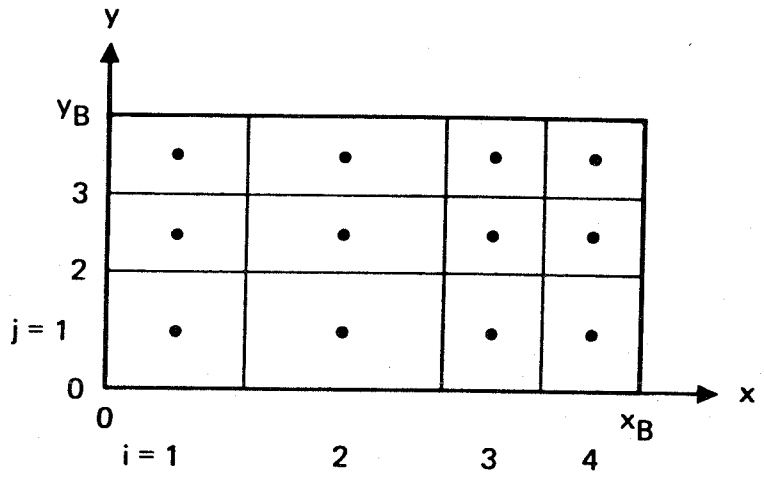

Figure 4.1

Finite–Difference Grid

$$B_\ell = \frac{\rho_\ell^{St}}{\rho_\ell^{Res}} \tag{4.5}$$

where the subscript ℓ denotes that the equation applies to either reservoir fluid and the superscripts St and Res refer to standard and local reservoir conditions, respectively. By dividing Eq. 4.1 by ρ_w^{St} and Eq. 4.2 by ρ_o^{St} and using Eq. 4.5 to eliminate the densities and Eq. 2.16 to eliminate S_o, Eqs. 4.1 and 4.2 become

$$\frac{\partial}{\partial t}\left(\frac{\phi S}{B_w}\right) = \frac{\partial}{\partial x}\left[\frac{K_x k_{rw}}{B_w \mu_w}\frac{\partial P}{\partial x}\right] + \frac{\partial}{\partial y}\left[\frac{K_y k_{rw}}{B_w \mu_w}\frac{\partial P}{\partial y}\right] + \sum_{m=1}^{NW} \bar{q}_{w_m}\delta(x-x_m)\delta(y-y_m) \tag{4.6}$$

$$\frac{\partial}{\partial t}\left[\frac{\phi(1-S)}{B_o}\right] = \frac{\partial}{\partial x}\left[\frac{K_x k_{ro}}{B_o \mu_o}\frac{\partial P}{\partial x}\right] + \frac{\partial}{\partial y}\left[\frac{K_y k_{ro}}{B_o \mu_o}\frac{\partial P}{\partial y}\right] + \sum_{m=1}^{NW} \bar{q}_{o_m}\delta(x-x_m)\delta(y-y_m) \tag{4.7}$$

where S refers to the water saturation and $\bar{q}_\ell = q_\ell/\rho_\ell^{St}$.

We will divide the spatial domain into a block-centered finite-difference grid as is shown in Fig.4.1. The grid points, or block centers, are at locations x_i, i = 1,..., NX in the x-direction and locations y_j, j = 1,...,NY in the y-direction. The time domain is divided into discrete times t^n, n = 0,...., NT. At time $t^{n+1/2}$, the derivatives in Eqs. 4.6 and 4.7 are approximated at each grid point i,j with the following first order time and second order space differences

$$\frac{\partial}{\partial t}\left(\frac{\phi S}{B_w}\right) \simeq \frac{1}{t^{n+1}-t^n}\left[\left(\frac{\phi S}{B_w}\right)^{n+1} - \left(\frac{\phi S}{B_w}\right)^{n}\right] \tag{4.8}$$

$$\frac{\partial}{\partial x}\left[M\frac{\partial P}{\partial x}\right] \simeq \frac{1}{\Delta x_i}\left[M_{i+1/2}^{n+1/2}\frac{(P_{i+1,j}-P_{i,j})^{n+1}}{\Delta x_{i+1/2}} - M_{i-1/2}^{n+1/2}\frac{(P_{i,j}-P_{i-1,j})^{n+1}}{\Delta x_{i-1/2}}\right] \tag{4.9}$$

where the subscript i+1/2 refers to the block boundaries, so that $\Delta x_{i+1/2} = x_{i+1}-x_i$ and $\Delta x_i = x_{i+1/2}-x_{i-1/2}$. Justification for the implicit evaluation of pressure in Eq. 4.9 is given in the next section.

In order to express the production terms as standard volumetric flow rates, we will multiply the finite-difference equations by the volume of the block $V_{i,j} = \Delta x_i \, \Delta y_j h$, where h is the reservoir thickness. For convenience the following difference operators are defined:

$$\Delta_t(u) = \frac{1}{t^{n+1}-t^n}\,(u^{n+1} - u^n) \tag{4.10}$$

$$\Delta_x(T_\ell \Delta P) = (T^\ell_{i+1/2,j})^{n+1/2}(P_{i+1,j}-P_{i,j})^{n+1}-(T^\ell_{i-1/2,j})^{n+1/2}(P_{i,j}-P_{i-1,j})^{n+1} \tag{4.11}$$

Our finite-difference equations for grid point i,j can thus be written

$$v\Delta_t\left(\frac{\phi S}{B_w}\right) = \Delta_x(T_w\Delta P) + \Delta_y(T_w\Delta P) + \sum_{m=1}^{NW} Q_{w_m}^{n+1/2}\,\delta(i,i_m)\delta(j,j_m) \tag{4.12}$$

$$v\Delta_t\left(\frac{\phi(1-S)}{B_o}\right) = \Delta_x(T_o\Delta P) + \Delta_y(T_o\Delta P) + \sum_{m=1}^{NW} Q_{o_m}^{n+1/2}\,\delta(i,i_m)\delta(j,j_m) \tag{4.13}$$

where v refers to $V_{i,j}$, $\delta(i,i_m)$ is the Kronecker delta function, (i_m,j_m) is the grid block location of well m, and

$$\left(T^\ell_{i+1/2,j}\right)^{n+1/2} = \frac{\Delta y_j\, h}{\Delta x_{i+1/2}}\left(\frac{K_x k_{r\ell}^{n+1/2}}{\mu_\ell^{n+1/2} B_\ell^{n+1/2}}\right)_{i+1/2,j} \tag{4.14}$$

Eqs. 4.12 and 4.13 written for the grid blocks which are adjacent to the boundary contain fictitious values of pressure. These values $P_{0,j}$ and $P_{NX+1,j}$, $j = 1,\ldots, NY$, and $P_{i,0}$ and $P_{i,NY+1}$, $i = 1,.. NX$, can be eliminated by applying the following reflection boundary conditions:

$$P_{0,j} = P_{1,j}$$

$$P_{NX+1,j} = P_{NX,j} \qquad j = 1,\ldots, NY \tag{4.15}$$

$$P_{i,0} = P_{i,1}$$

$$P_{i,NY+1} = P_{i,NY} \qquad i = 1,\ldots, NX \tag{4.16}$$

The initial conditions, Eqs. 2.18 and 2.19, can be written as:

$$P^0_{i,j} = P_{in}(x_i,y_j) \tag{4.17}$$

$$S^0_{i,j} = S_{in}(x_i,y_j) \qquad i = 1,\ldots, NX,\ j = 1,\ldots, NY$$

Eqs. 4.13-17 represent the basic form of the finite-difference equations we will use. Before our system is completely specified, the following will be done: (1) the method of handling the source and sink terms must be specified, (2) a time derivative with respect to pressure will be introduced into the left hand sides of Eqs. 4.12 and 4.13 through the use of the compressibilities, (3) the way in which the nonlinear terms are handled must be specified. The production terms require special treatment. The flow rate $Q_{\ell m}$ can be assigned at the injection wells. However, the fraction of each fluid flowing at the production wells is a function of the relative permeabilities, and hence the saturation of the grid block at which the

well is situated. Therefore both flow rates cannot be specified at the producing wells. We will specify the total production Q_T at those wells and derive a function of saturation which relates Q_w and Q_o to the total flow rate.

At a producing well, the volumetric flow rates at reservoir conditions Q_ℓ^{Res} are related to the fractional flow f_w as[3]:

$$\begin{aligned} Q_w^{Res} &= f_w Q_T^{Res} \\ Q_o^{Res} &= (1 - f_w) Q_T^{Res} \end{aligned} \tag{4.18}$$

The flow rates Q_{ℓ_m} in Eqs. 4.12 and 4.13 are expressed as volumetric flow rates at standard conditions. A function g_w such that

$$Q_w = g_w Q_T \tag{4.19}$$

$$Q_o = (1 - g_w) Q_T \tag{4.20}$$

can be derived by algebraic manipulation of Eq. 4.18 and the following relations:

$$Q_\ell = Q_\ell^{Res} / B_\ell \tag{4.21}$$

$$Q_T = Q_w + Q_o \tag{4.22}$$

That function is:

$$g_w = \left(1 + \frac{B_w \mu_w k_{ro}}{B_o \mu_o k_{rw}} \right)^{-1} \tag{4.23}$$

The source term in Eq. 4.12 can then be expressed as

$$\sum_{m=1}^{NW} Q_T g_w \delta(i,i_m)\delta(j,j_m) \tag{4.24}$$

and the corresponding term in Eq. 4.13 becomes:

$$\sum_{m=1}^{NW} Q_T (1-g_w)\delta(i,i_m)\delta(j,j_m) \tag{4.25}$$

A time difference with respect to pressure is introduced into Eqs. 4.12 and 4.13 through the use of compressibilities in the accumulation terms in the conservation equations. The following derivation will be carried out for the accumulation term in Eq. 4.12. For consistent differencing of a product, we can write

$$\Delta_t(uv) = \frac{1}{\Delta t_n}\left[u^{n+1}(v^{n+1}-v^n) + v^n(u^{n+1}-u^n)\right] \tag{4.26}$$

where $\Delta t_n = t^{n+1} - t^n$.

The following identity for the accumulation term in Eq. 4.12 can be written by using Eq. 4.26 and rearranging:

$$\Delta_t\left(\frac{\phi S}{B_w}\right) = \left(\frac{\phi}{B_w}\right)^{n+1}\Delta_t(S) + S^n\left[\phi^{n+1}\Delta_t\left(\frac{1}{B_w}\right) + \frac{1}{B_w^n}\Delta_t(\phi)\right] \tag{4.27}$$

The following difference equations can be written from the definitions of the compressibilities, Eqs. 2.20-22:

$$B_w^{n+1} - B_w^n = - B_w^{n+1/2} c_w (p^{n+1} - p^n) \tag{4.28}$$

$$\phi^{n+1} - \phi^n = \phi^{n+1/2} c_r (p^{n+1} - p^n) \tag{4.29}$$

Using Eqs. 4.28 and 4.29, Eq. 4.27 becomes:

$$\Delta_t\left(\frac{\phi S}{B_w}\right) = \left(\frac{\phi}{B_w}\right)^{n+1}\Delta_t(S) + S^n\left[\frac{\phi^{n+1}}{B_w^{n+1/2}}c_w + \frac{\phi^{n+1/2}}{B_w^n}c_r\right]\Delta_t(P) \qquad (4.30)$$

By a similar analysis, the accumulation term in Eq. 4.13 can be written as:

$$\Delta_t\left(\frac{\phi(1-S)}{B_o}\right) = -\left(\frac{\phi}{B_o}\right)^{n+1}\Delta_t(S) + (1-S^n)\left[\frac{\phi^{n+1}}{B_o^{n+1/2}}c_o + \frac{\phi^{n+1/2}}{B_o^n}c_r\right]\Delta_t(P) \qquad (4.31)$$

These relations could have been derived more directly from the forms of the accumulation terms given in Eqs. 2.30 and 2.31. However, the derivation from those equations would call for dating of the parameters in Eqs. 4.30 and 4.31 at different time levels, the important difference being that the saturation in the second terms of Eqs. 4.30 and 4.31 would be dated at time $S^{n+1/2}$, where saturation is unknown.

Now the method of treating the nonlinear terms must be specified. Settari and Aziz[12] have reviewed the various techniques of handling these terms. The nonlinear terms can be categorized as weak or strong nonlinearities. If the porosity, viscosities, or formation volume factors are functions of pressure, they represent weak nonlinearities in that their value would change very little over any time step. The usual method of treating these terms which are evaluated at times $t^{n+1/2}$ and t^{n+1} in Eqs. 4.14,30,31 is by approximating them as their values at time t^n.

The relative permeabilities, which appear in the term T in Eq. 4.14 and in the function g_w represent strong nonlinearities. It can be shown that implicit evaluation of these terms in the finite-difference equations results in unconditional stability[3]. However, the finite-difference

equations are nonlinear and special techniques must be used to solve the finite difference system. Evaluation of the relative permeabilities explicitly yields a linear finite difference system which is conditionally stable when upstream weighting is used, but unstable for mid-point or downstream weighting. This is explained further in the next section. While for certain problems it has been found that an implicit procedure is necessary, many reservoir problems can be simulated using explicit relative permeabilities with upstream weighting[3]. In this work the relative permeabilities are evaluated explicitly using upstream weighting. In order to avoid oscillations in the solution near the producing wells[3], the production terms are semi-implicit. With these specifications the difference equations 4.12 and 4.13 used in this study can now be written as

$$\left(\frac{\phi}{B_w}\right)^n \Delta_t(S) + C_w\Delta_t(P) = \Delta_x(T^w\Delta P) + \Delta_y(T^w\Delta P) + \sum_{m=1}^{NW} Q_{T_m}^{n+1}\left[g_w^n + \left(\frac{dg_w}{dS}\right)^n (S^{n+1}-S^n)\right]\delta(i,i_m)\delta(j,j_m) \qquad (4.32)$$

$$-\left(\frac{\phi}{B_o}\right)^n \Delta_t(S) + C_o\Delta_t(P) = \Delta_x(T^o\Delta P) + \Delta_y(T^o\Delta P) + \sum_{m=1}^{NW} Q_{T_m}^{n+1}\left[1-g_w^n - \left(\frac{dg_w}{dS}\right)^n (S^{n+1}-S^n)\right]\delta(i,i_m)\delta(j,j_m) \qquad (4.33)$$

where

$$C_w = S^n\left(\frac{\phi}{B_w}\right)^n (c_w + c_r) \qquad (4.34)$$

$$C_o = (1-S^n)\left(\frac{\phi}{B_o}\right)^n (c_o + c_r) \qquad (4.35)$$

For this study, the viscosities are taken to be independent of pressure. The formation volume factors at the grid block boundaries which appear in Eq. 4.14 were evaluated as arithmetic averages:

$$B_{\ell_{i+1/2}} = \frac{1}{2}\left(B_{\ell_{i+1}} + B_{\ell_i}\right)^n \tag{4.36}$$

The relative permeabilities in Eq. 4.14 can be expressed as:

$$k_{r\ell_{i+1/2}} = k^n_{r\ell_{i+1}} \quad \text{if } P^n(i+1,j) \geq P^n(i,j) \tag{4.37}$$

$$= k^n_{r\ell_i} \quad \text{if } P^n(i+1,j) < P^n(i,j)$$

The permeabilities in Eq. 4.14 can be expressed as arithmetic or geometric averages of the grid block permeabilities. In this study, the permeabilities were defined at the grid block boundaries.

The finite-difference relations needed to simulate the two-dimensional reservoir are given by Eqs. 4.32-37, with boundary and initial conditions Eq. 4.15-17. Given the solution for the pressure and saturation at time t^n (or t^0), these relations represent a linear system of equations which can be solved for the pressure and saturation at times t^{n+1}. The method of solving the system is given in Appendix B. Although only rectangular reservoir boundaries were used in this study, more arbitrary reservoir boundaries can be specified by assigning the permeability or porosity of certain grid blocks to be zero[3,13].

4.2 Analysis of the Finite-Difference Method

An analysis of the stability and truncation error associated with the finite difference solution of Eqs. 2.12-16 has been made by analyzing the solution of single equations for pressure and saturation which are obtained from the coupled system[3,14]. Here, this analysis is illustrated using the pressure and saturation equations derived in Subsections 2.2.1 and 2.2.2.

4.2.1 Pressure Equation

For one-dimensional flow without sources or sinks, the parabolic pressure equation 2.36 can be written as

$$C_t\phi \frac{\partial P}{\partial t} = \frac{\partial}{\partial x}\left(\frac{k_{ro}}{\mu_w} + \frac{k_{ro}}{\mu_o}\right) K \frac{\partial P}{\partial x} \tag{4.38}$$

where $C_t = c_r + c_o(1-S) + c_w S$. If it assumed that S, ϕ, and K are constants, Eq. 4.38 can be written as

$$\alpha \frac{\partial P}{\partial t} = \frac{\partial^2 P}{\partial x^2} \tag{4.39}$$

where α can be determined by comparison with Eq. 4.38.

It has been well established that an explicit finite-difference solution of Eq. 4.39 is conditionally stable and an implicit solution is unconditionally stable[3,4,13]. For most reservoir problems, the conditional stability requirement is too restrictive[13], and hence pressure is usually evaluated implicitly as done in Eq. 4.9. The truncation error associated with the finite-difference approximations given by Eqs. 4.8 and 4.9 can be shown to be first order with respect to time and second order with respect to space[3,13].

4.2.2 Saturation Equation

The first order hyperbolic equation for saturation, Eq. 2.47, imposes a greater limitation on the quality of finite-difference solution than does the pressure equation. Defining a dimensionless time τ and distance ξ as

$$\tau = \frac{v_t t}{x_L \phi}$$

$$\xi = \frac{x}{x_L}$$

Eq. 2.47 can be written for one-dimensional flow as:

$$\frac{\partial S}{\partial \tau} = - \frac{\partial f}{\partial \xi} \tag{4.40}$$

The following explicit finite-difference solution of this problem can be considered:

$$\frac{S_i^{n+1} - S_i^n}{\Delta \tau} = - \frac{1}{\Delta \xi} \left[W(f_i^n - f_{i-1}^n) + (1-W)(f_{i+1}^n - f_i^n) \right] \tag{4.41}$$

where we have assumed equal grid point spacing in ξ and W is a weighting parameter. A value of W=1 corresponds to upstream weighting, W=1/2 is midpoint weighting, and W=0 is downstream weighting. If it is assumed that f is a linear function of saturation, Eq. 4.41 can be put in the following form which is convenient for analysis:

$$\frac{S_i^{n+1} - S_i^n}{\Delta \tau} = - \frac{f'}{\Delta \xi} \left[W(S_i^n - S_{i-1}^n) + (1-W)(S_{i+1}^n - S_i^n) \right] \tag{4.42}$$

It can be shown by a von Neumann stability analysis that Eq. 4.42 is unstable for downstream and mid-point weighting. For upstream weighting, or W=1, Eq. 4.42 is conditionally stable[3]. The condition for stability is:

$$\frac{f'\Delta\tau}{\Delta\xi} \leq 1 \tag{4.43}$$

The truncation error associated with Eq. 4.42 with upstream weighting can be quantitatively assessed[14]. This derivation is shown in Appendix C; it shows that the truncation error, or numerical dispersion, is controlled by the following term:

$$f'(\Delta\xi - f'\Delta\tau)/2 \tag{4.44}$$

While the truncation error associated with the pressure equation is second order in space, the corresponding error associated with the saturation equation is first order.

A similar truncation analysis for an implicit finite-difference approximation to Eq. 4.40 using upstream weighting yields an expression identical to Eq. 4.44, except that the space and time truncation contributions are additive[14]. While the explicit formulation is less stable than the implicit formulation, the explicit formulation exhibits a smaller truncation error. This trade off of stability and truncation error can be seen in a more complete analysis of the various time and distance weightings which could be used with the finite-difference solution of Eq. 4.40[3].

4.3 Test Problems

The finite-difference model developed in Section 4.1 can be used to approximate the reservoir model developed in Section 3.1 for which analytical solutions were obtained. Comparison of the finite-difference solutions to the analytical solutions provides a practical test of the simulator. In this section, the method used to approximate the model developed in Section 3.1 is described, and the effects of the truncation error on the pressure drop and saturation solutions are illustrated.

The matrix formed in the solution of the finite-difference equations (see Appendix B) is singular when the compressibilities of the reservoir formation and fluids are zero. In this case, as shown in Subsection 2.2.1, some pressure on the boundary must be specified. Incompressible flow can be approximated by specifying a small, non-zero value of compressibility. For these problems the fluid compressibilities were assigned to be zero, and the reservoir formation is taken to be slightly compressible.

The finite-difference grid consists of a single row of blocks centered at equally spaced points x_i, i=1,..., NX. Injection and production are specified at grids blocks 1 and NX, and the length $x_{NX}-x_1$ is given by x_L, the length of the reservoir model shown in Fig. 3.1. The boundary conditions used in Chapter 3 are approximated by assigning the blocks centered at x_1 and x_{NX} one-half the pore volume of the other blocks while specifying the total pore volume of the finite-difference model to be the same as that for the model shown in Fig. 3.1.

Using the guidelines given above, Case 1 in Section 3.3 was simulated using the finite-difference model. With a spatial grid consisting of

twenty-five blocks, three cases using different time steps were run. The data used for each of these cases are given in Table 4.1.

The pressure drop across the reservoir model as a function of time for Cases 1-3 are shown in Fig. 4.2 along with the pressure drops calculated analytically for Case 1 in Section 3.3. This figure illustrates the effect of the truncation error given by Eq. 4.44 on the pressure solution. As the time step Δt is increased from 20 to 40 days, the difference between the numerical and analytical pressure drop is decreased. As the time step is further increased from 40 to 50 days, oscillations in the numerical solution become larger. We can reason that as Δt is increased from 20 to 50 days, the numerical dispersion term given by Eq. 4.44 was initially positive and has passed through a minimum at approximately $\Delta t = 40$, and it has become negative for $\Delta t = 50$. Peaceman[3] showed that a negative numerical dispersion is usually associated with instability. For $\Delta t = 50$ we can expect that the stability requirement given by the linear analysis of the saturation equation 4.43 has been violated.

For Cases 1 and 2, the saturation profile at $t = 1080$ days is plotted with the Buckley-Leverett solution in Fig. 4.3. This figure illustrates the degree of smearing of the saturation discontinuity and the decrease of the numerical dispersion with the increase in the step size.

Table 4.1. Specification of Data Used for Test Problems

Reservoir Properties and Fluid Properties

$K = 0.2737$ darcy	$\mu_o = 1$ cp
$\phi = 0.3$	$\mu_w = 1$ cp
$c_r = 4 \times 10^{-6}$ atm^{-1}	$c_o = c_w = 0$
$P_{in} = 20$ atm	$S_{in} = 0.11$

Relative Permeability Parameters

$a_w = 0.9458$	$a_o = 0.9814$
$b_w = 2.557$	$b_o = 3.163$
$S_c = 0.11$	$S_{ro} = 0.0$

Model Dimensions

$h = 1$ cm	$\Delta x = 41.7$ ft
$y_B = 100$ ft	NX = 25

Injection/Production Rate

$Q_T = 0.07$ bbl/day

Time Step Size

Case	Δt (days)
1	20
2	40
3	50

---

(1) See Eqs. 3.65 and 3.66

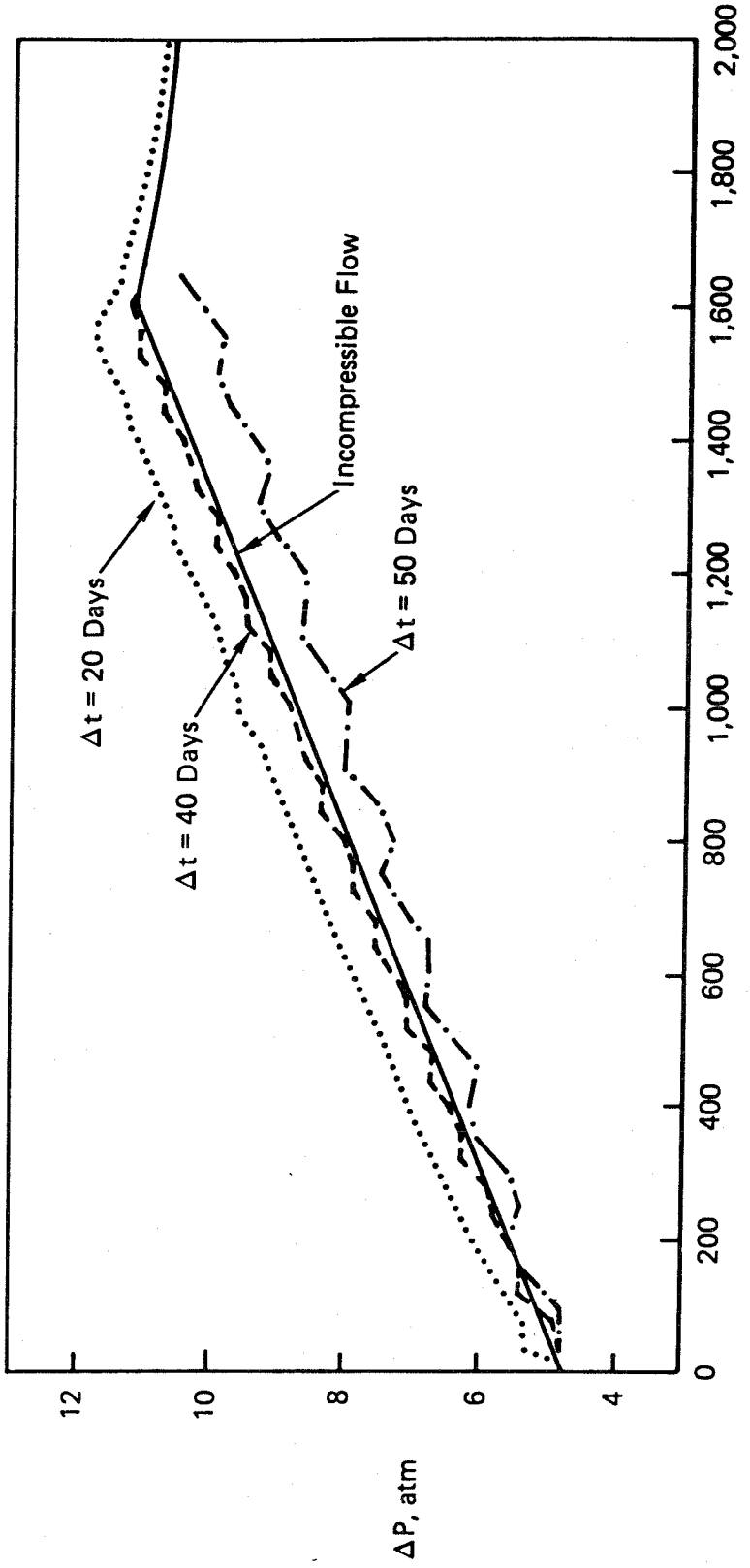

Figure 4.2
Pressure Drop Across Reservoir Model for Test Problems

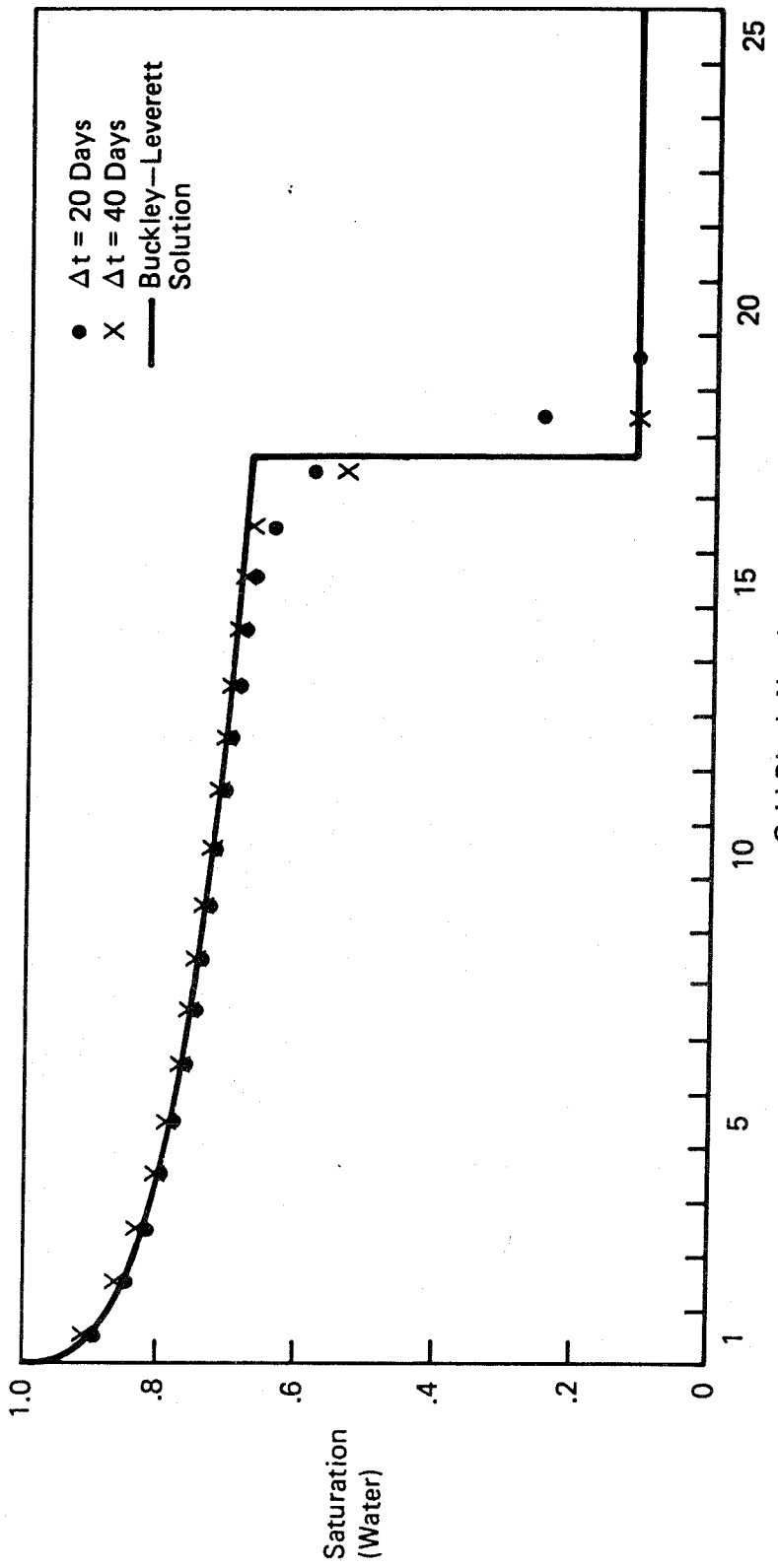

Figure 4.3

Saturation Solution for Test Problems

4.4 Summary

In the first section the numerical finite-difference scheme used to solve Eqs. 2.12-22 is developed. The method used here is the simultaneous solution. The relative permeabilities in the transmissibility terms are explicit, pressure is implicit, and the production terms are semi-implicit. The total production rates at the wells are specified.

The stability and truncation error associated with the finite-difference method is analyzed in Section 4.2. It is shown that the hyperbolic saturation equation presents the greatest problems in the numerical solution.[3,14]

In Section 4.3, some numerical results are presented. The effects of truncation error on the pressure drop and saturation solutions are illustrated.

5. IDENTIFIABILITY IN INCOMPRESSIBLE RESERVOIRS

In this chapter we investigate the estimation of reservoir properties from flow data based on the incompressible, linear, two-phase reservoir model developed in Chapter 3. Although the numerical solution developed in Chapter 4 must be used for solving the general history matching problem, certain features inherent to parameter estimation in two-phase flow can be elucidated by studying this simplified problem.

The reservoir model considered is shown schematically in Fig. 3.1. Water is injected at a specified rate at $x = 0$, and production takes place at $x = x_L$. Unless otherwise stated, the initial saturation is taken to be the connate water saturation so that a single shock is formed in the saturation solution at the saturation S_d.

We assume that the measurements of the dependent variables pressure and saturation available to use are the pressure drop across the reservoir , $\Delta P(t)$, and the relative rates of flow of the two fluids, oil and water, at the producing end. The measurement of the relative rates of flow can be expressed as either the ratio of the flow of water to oil, designated as WOR (water-oil ratio), or as the fractional flow of water f. The two quantities are related by:

$$f = \frac{WOR}{1 + WOR} \tag{5.1}$$

This measurement represents an indirect measurement of saturation since, if the relative permeabilities are known, the saturation at that location can be calculated from Eq. 3.11.

Three estimation problems are considered separately. In Section 5.1 the porosity and relative permeabilities are taken to be known, and the estimation of spatially varying absolute permeability is investigated. In Section 5.2 the estimation of spatially varying porosity is considered. The relative and absolute permeabilities are taken to be known. The estimation of the relative permeabilities assuming that the other reservoir properties are known is investigated in Section 5.3.

5.1 Estimation of K(x)

The porosity and relative permeabilities are assumed to be known, and we consider here the problem of estimating the spatially varying absolute permeability. For simplicity we assume that the superficial velocity v_t is independent of time, and that the porosity is independent of location. Eq. 3.74, repeated below, can be solved for the saturation solution at any time t :

$$x(S) = \frac{v_t t}{\phi} f'(S) \tag{5.2}$$

Since this equation is independent of the absolute permeability, measurements of the fractional flow at $x = x_L$ give no information about the absolute permeability. Eq. 3.19 relates the permeability to the pressure drop across the reservoir:

$$\Delta P(t) = v_t \mu_w \int_0^{x_L} \frac{f}{K k_{rw}} dx \tag{5.3}$$

The inverse problem we consider here is the estimation of $K(x)$ given $\Delta P(t)$ in Eq. 5.3.

A general approach to estimating the permeability if we are given q measurements of ΔP at times t_i, $i = 1,\ldots,q$, can be made by defining a performance index J as:

$$J = \sum_{i=1}^{q} [\Delta P^{obs}(t_i) - \Delta P^{c}(t_i)]^2 \tag{5.4}$$

where the superscript obs refers to the observed (or measured) pressure drop and c refers to the pressure drop calculated by Eq. 5.3. We would choose $K(x)$ so that J is minimized. In Appendix D an analytical minimization procedure based on calculus of variations is formulated. An iterative procedure has also been formulated by Van den Bosch and Seinfeld[15] based on the analytical solution of the two-phase problem in radial geometry.

In the following subsections we consider the explicit estimation of the unknown absolute permeability for two simplified problems. In Subsection 3.3.1 we showed the effects of viscosities and relative permeabilities on the pressure drop calculated from two-phase flow by analyzing two special problems: (1) the moving boundary problem, and (2) relative permeabilities given by the functional forms in Eqs. 3.65 and 3.66. Here we consider these two problems and show the important effect that the characteristics of two-phase flow has on the estimation of spatially varying absolute permeability.

5.1.1 Moving Boundary Problem

For the limiting case of a moving saturation boundary or infinitely steep saturation front (see p. 57), the location of the saturation discontinuity is given by:

$$x_d = \frac{v_t t}{\phi(1-S_{ro}-S_c)} \tag{5.5}$$

For $t \leq t_B$, the breakthrough time, the pressure equation 5.3 can be written as:

$$\Delta P(t) = v_t \left[\frac{\mu_w}{k_{rw}(1-S_{ro})} \int_0^{x_d} \frac{1}{K}\, dx + \frac{\mu_o}{k_{ro}(S_c)} \int_{x_d}^{x_L} \frac{1}{K}\, dx \right] \tag{5.6}$$

Assume that the reservoir consists of n discrete zones over which the absolute permeability is constant. That is, the absolute permeability can be expressed as :

$$K(x) = K_i \qquad x_{i-1} < x \leq x_i \qquad i = 1,\ldots,n \tag{5.7}$$

Assume that we are given the values of ΔP corresponding to the n times that the saturation discontinuity is at the location of the zone boundaries. Since the porosity is known, these times are given by Eq. 5.5 as:

$$t_i = \frac{\phi(1-S_{ro}-S_c)x_i}{v_t} \qquad i = 1,\ldots,n \tag{5.8}$$

At time t_i, Eq. 5.6 can be written, after rearranging, as:

$$\frac{\Delta P(t_i)k_{ro}(S_c)}{v_t\mu_o} = \frac{\mu_w k_{ro}(S_c)}{\mu_o k_{rw}(1-S_{ro})} \sum_{j=1}^{i} u_j\Delta x_j + \sum_{j=i+1}^{n} u_j\Delta x_j \qquad (5.9)$$

where u, known as the reservoir resistivity, is given by $u_j = \frac{1}{K_j}$.

For the n times t_i, i = 1,...,n, Eq. 5.9 can be written as the following linear system:

$$\underset{\sim}{A}\ \underset{\sim}{u} = \underset{\sim}{b} \qquad (5.10)$$

where $\underset{\sim}{u}$ is an n-vector $\underset{\sim}{u} = [u_1\ u_2 \ldots u_n]^T$, $\underset{\sim}{b}$ is an n-vector with elements

$$b_i = \frac{\Delta P(t_i)k_{ro}(S_c)}{v_t\mu_o}\ , \qquad (5.11)$$

and elements of the nxn matrix $\underset{\sim}{A}$ are given by:

$$A_{i,j} = \begin{cases} m\Delta x_j\ , & i \geq j \\ \Delta x_j\ , & i < j \end{cases} \qquad (5.12)$$

where $m = \frac{\mu_w k_{ro}(S_c)}{\mu_o k_{rw}(1-S_{ro})}$.

If the matrix $\underset{\sim}{A}$ is nonsingular, then each of the n values of the resistivity can be obtained by solving Eq. 5.10. It will be shown below that the matrix $\underset{\sim}{A}$ given by Eq. 5.12 is nonsingular for $m \neq 1$ (m = 0 is not physically meaningful for two-phase flow, and $x \neq 0$ by definition of the zonation).

Assertion: The determinant of the nxn matrix $\underset{\sim}{A}$ given by Eq. 5.12 in nonsingular for $m \neq 1$.

Proof: The proof is by induction. For simplicity, we will let $a_i = \Delta x_i$.

For n = 2, $\underset{\sim}{A}$ becomes

$$\underset{\sim}{A} = \begin{bmatrix} ma_1 & a_2 \\ ma_1 & ma_2 \end{bmatrix}$$

Then $\det\underset{\sim}{A} = ma_1a_2(m-1) \neq 0$.

Given that $\det(\underset{\sim}{A}_{n,n}) \neq 0$, we show that $\det(\underset{\sim}{A}_{n+1,n+1}) \neq 0$. The matrix $\underset{\sim}{A}_{n+1,n+1}$ can be written in abbreviated form as:

$$\underset{\sim}{A} = \begin{bmatrix} ma_1 & a_2 & a_3 & \cdots & a_{n+1} \\ ma_1 & ma_2 & a_3 & \cdots & a_{n+1} \\ \vdots & & & & \vdots \\ ma_1 & \cdots & & & ma_{n+1} \end{bmatrix}$$

Subtracting the second row from the first row, and then expanding the determinant by the first row, we obtain

$$\det\underset{\sim}{A} = -a_2(1-m)\det \begin{bmatrix} ma_1 & a_3 & a_4 & & a_{n+1} \\ ma_1 & ma_3 & a_4 & \cdots & a_{n+1} \\ & & & & \\ ma_1 & ma_3 & \cdots & & ma_{n+1} \end{bmatrix}$$

The determinant of the matrix in brackets is nonzero since, by renumbering the indices, that matrix is equivalent to the nxn matrix defined by Eq. 5.12; therefore, $\det(\underset{\sim}{A}_{n+1,n+1}) \neq 0$.

Note that for m = 1, the matrix $\underset{\sim}{A}$ is singular. When $\mu_o = \mu_w = \mu$ and $k_{rw}(1-S_{ro}) = k_{ro}(S_c) = 1$, the pressure solution for Eq. 5.6 is equivalent to the solution of the pressure drop for the single phase flow problem, which can be obtained by integrating Eq. 2.2. In that case, the n values of u_i cannot be uniquely determined.

A second example of the moving boundary problem can be considered. Assume that we are given continuous measurements of $\Delta P(t)$ for times $0 \leq t \leq t_B$. Taking the derivative of Eq. 5.6 with respect to time, we obtain :

$$\frac{d\Delta P(t)}{dt} = v_t \frac{dx_d}{dt}\left[\frac{\mu_w}{k_{rw}(1-S_{ro})} - \frac{\mu_o}{k_{ro}(S_c)}\right] \frac{1}{K(x_d)} \qquad (5.13)$$

An expression for $\frac{dx_d}{dt}$ can be obtained by differentiating Eq. 5.5 with respect to time. Eliminating that term from Eq. 5.13 we obtain:

$$\frac{d\Delta P(t)}{dt} = \frac{v_t^2}{\phi(1-S_{ro}-S_c)}\left[\frac{\mu_w}{k_{rw}(1-S_{ro})} - \frac{\mu_o}{k_{ro}(S_L)}\right] \frac{1}{K(x_d)} \qquad (5.14)$$

The spatially varying permeability can then be calculated provided that $\frac{\mu_w}{k_{rw}(1-S_{ro})} \neq \frac{\mu_o}{k_{ro}(S_c)}$.

If the pressure drop data are available for only $0 \leq t \leq \bar{t}$, where $\bar{t} < t_B$, then the permeability $K(x)$ can be calculated from Eq. 5.14 for $0 \leq x \leq x_d(\bar{t})$, where $x_d(\bar{t})$ is obtained from Eq. 5.5. The values of $K(x)$ in $x_d(\bar{t}) \leq x \leq x_L$ cannot be obtained, although the integral

$$\int_{x_d(\bar{t})}^{x_L} \frac{1}{K}\, dx$$ can be calculated from Eq. 5.6.

5.1.2 Unit Viscosity Ratio

As in the previous subsection we will consider a problem which allows us to express the pressure drop as a linear function of the resistivity. For unit viscosity ratio and with certain assumptions about the form of the relative permeability functions, we will show that the n values K_i can be uniquely determined.

For times $t \leq t_B$, the pressure Eq. 5.3 can be written as:

$$\Delta P(t) = v_t \left[\mu_w \int_0^{x_d} \frac{f}{K k_{rw}}\, dx + \frac{\mu_o}{k_{ro}(S_c)} \int_{x_d}^{x_L} \frac{1}{K}\, dx \right] \qquad (5.15)$$

Similarly to the moving boundary problem, we note that if only the values $\Delta P(t)$ for $0 \leq t \leq \bar{t}$, where $\bar{t} < t_B$, are available, we would not be able to determine $K(x)$ for $x > x_d(\bar{t})$. The best we would be able to do is to determine an average for that range--the value $\int_{x_d(\bar{t})}^{x_L} \frac{1}{K}\, dx$. We need to investigate the effect that the saturation dependent terms in the first integral in Eq. 5.15 has on the determination of spatially varying permeability.

As in Subsection 5.1.1, assume that the reservoir consists of n discrete zones over which the permeability is constant (see Eq. 5.7) and that we are given n values of ΔP at the times for which the position of the saturation discontinuity coincides with the zone boundaries. These times are given by Eq. 5.2 as:

$$t_i = \frac{\phi x_i}{v_t} f'(S_d) \qquad i = 1,\ldots,n \tag{5.16}$$

For time t_i, Eq. 5.15 can be written as

$$\frac{\Delta P(t_i) k_{ro}(S_c)}{\mu_o v_t} = \frac{\mu_w}{\mu_o} k_{ro}(S_c) \sum_{j=1}^{i} u_j \int_{x_{j-1}}^{x_j} g(t_i)dx + \sum_{j=i+1}^{n} u_j \Delta x_j \tag{5.17}$$

where $g = \frac{f}{k_{rw}}$, $u_j = \frac{1}{K_j}$, and $\Delta x_j = x_j - x_{j-1}$.

The n equations for times t_i, $i = 1,\ldots,n$, can be written as the following linear system:

$$\underset{\sim}{A}\ \underset{\sim}{u} = \underset{\sim}{b}$$

where the i^{th} element of $\underset{\sim}{b}$ is

$$b_i = \frac{\Delta P(t_i)}{v_t} k_{ro}(S_c) \tag{5.18}$$

Elements of the nxn matrix $\underset{\sim}{A}$ are given by

$$A_{i,j} = k_{ro}(S_c) \int_{x_{j-1}}^{x_j} g(t_i)dx \qquad i \geq j \tag{5.19}$$

To further investigate this linear system, we must determine some properties of the integrals in the matrix given by Eq. 5.19. Assuming that the relative permeabilities can be represented by the parametrizations given by Eqs. 3.65 and 3.66, with b_w, $b_o > 1$ (which gives the typical concave shape of the relative permeabilities), we will show that

$$\int_{x_{j-1}}^{x_j} g(t_{i+1})dx > \int_{x_{j-1}}^{x_j} g(t_i)dx > k_{rw}(1-S_{ro})\Delta x_j \qquad i \geq j \qquad (5.20)$$

Verification. The first inequality can be verified in two steps: (1) show that $S(x,t_{i+1}) > S(x,t_i)$, $x_{j-1} \leq x \leq x_j$, and (2) show that $g(S)$ is a strictly decreasing function of saturation for $S_d \leq S \leq 1-S_{ro}$, which is the range of all possible saturations in the integrals given by Eq. 5.19. The second inequality is then easily verified. The following verification applies for the general case of arbitrary viscosities.

(1) In Section 3.2 it was shown that a single shock in the saturation solution is formed at S_d for the initial condition that $S_{in}(x) = S_c$. It is necessary that the function $f'(S)$ be strictly decreasing with saturation over the interval $S_d \leq S \leq 1-S_{ro}$, since otherwise multiple saturations for $x < x_d$ would be calculated by Eq. 5.2. Since $f'(S)$ is strictly decreasing with saturation, it follows from Eq. 5.2 that $S(x,t_{i+1}) > S(x,t_i)$ for $x \leq x_d(t_{i+1})$.

(2) The function $g(S)$ is given by

$$g(S) = \frac{1}{(k_{rw}+mk_{ro})} \qquad (5.21)$$

where $m = \frac{\mu_w}{\mu_o}$, and f is defined by Eq. 3.11. To show that g(S) is strictly decreasing with saturation over the range of interest, we can show that

$$g'(S) < 0 \qquad S_d \leq S \leq 1-S_{ro}$$

We can investigate the function g(S) by examining its derivative with respect to saturation. The derivative of Eq. 5.21 is

$$g'(S) = \frac{-(k'_{rw}+mk'_{ro})}{(k_{rw}+mk_{ro})^2} \tag{5.22}$$

The derivatives of the relative permeabilities given by Eqs. 3.65 and 3.66 are:

$$k'_{rw} = a_w b_w (S-S_c)^{b_w-1}\left(\frac{1}{1-S_{ro}-S_c}\right)^{b_w} \tag{5.23}$$

$$k'_{ro} = -a_o b_o (1-S_{ro}-S)^{b_o-1}\left(\frac{1}{1-S_{ro}-S_c}\right)^{b_o} \tag{5.24}$$

Since b_w, $b_o > 1$, the function k'_{rw} is strictly increasing with saturation from $k'_{rw}(S_c) = 0$. The function k'_{ro} is also strictly increasing from a negative value at S_c to $k_{ro}(1-S_{ro}) = 0$. Since Eq. 5.22 is positive at $S = S_c$, negative at $S = 1-S_{ro}$, and continuous, that function must be zero at some point S_m in the interval $S_d < S < 1-S_{ro}$. There must be only one

point at which Eq. 5.22 is zero since Eqs. 5.23 and 5.24 are monotonically increasing functions. At the point S_m, the second derivative of Eq. 5.21 is

$$g''(S_m) = - \frac{(k''_{rw}+mk''_{ro})}{(k_{rw}+mk_{ro})^2} \tag{5.25}$$

Since b_w, $b_o > 1$, the second derivatives of the relative permeabilities are positive, $g''(S_m) > 0$, and the function g(S) has a maximum at the point S_m.

We have shown that the function g(S) has a single stationary point, which is a maximum, in the interval $S_d < S < 1-S_{ro}$. If we show that $g'(S_d) < 0$, it follows that $g'(S) < 0$, $S_d \leq S \leq 1-S_{ro}$.

The equation for the analytical determination of S_d (see Section 3.2) is

$$\frac{f(S_d)}{(S_d-S_c)} = f'(S_d) \tag{5.26}$$

This can equivalently be written in terms of the function g as:

$$\frac{k_{rw}(S_d)g(S_d)}{(S_d-S_c)} = k'_{rw}(S_d)g(S_d) + k_{rw}(S_d)g'(S_d) \tag{5.27}$$

Rearranging this expression, we obtain:

$$\left[\frac{k'_{rw}(S_d)}{k_{rw}(S_d)} + \frac{g'(S_d)}{g(S_d)}\right] (S_d-S_c) = 1 \tag{5.28}$$

From Eqs. 3.55 and 5.23, the following identity is obtained:

$$\frac{k'_{rw}(S_d)}{k_{rw}(S_d)} = \frac{b_w}{(S_d-S_c)} \tag{5.29}$$

Eq. 5.28 can now be written as

$$b_w + \frac{g'(S_d)}{g(S_d)} (S_d-S_c) = 1 \tag{5.30}$$

Since $b_w > 1$, $g(S_d) > 0$, and $S_d > S_c$, it follows that $g'(S_d) > 0$. The second inequality is easily verified. We have shown that $g'(S) < 0$, $S_d \leq S \leq 1-S_{ro}$. It follows from Eq. 5.21 evaluated at $S = 1-S_{ro}$ that $g(S) > k_{rw}(1-S_{ro})$, $S_d \leq S < 1-S_{ro}$, and consequently

$$\int_{x_{j-1}}^{x_j} g(t_i)dx > k_{rw}(1-S_{ro})\Delta x_j, \quad i \geq j.$$

The matrix given by Eq. 5.19 can be written in abbreviated form as:

$$\underset{\sim}{A} = \begin{bmatrix} a_{11} & a_2 & a_3 & \cdots & a_n \\ a_{21} & a_{22} & a_3 & & \vdots \\ \vdots & & & & a_n \\ a_{n1} & a_{n2} & \cdots & & a_{nn} \end{bmatrix} \tag{5.31}$$

where

$$a_{i,j} = k_{ro}(S_c)\int_{x_{j-1}}^{x_j} g(t_i)dx \qquad i \geq j$$

$$a_j = \Delta x_j \qquad j = 2,\ldots,n$$

It if is assumed that $k_{ro}(S_c) \geq k_{rw}(1-S_{ro})$, then this matrix has the following properties:

$$a_{i,j} > a_{i+1,j} > a_j > 0 \qquad \begin{matrix} i = 1,\ldots,n-1 \\ j = 1,\ldots,n-1 \end{matrix} \tag{5.32}$$

It will now be shown that $\underset{\sim}{A}$ is nonsingular, and hence we can solve for the n values of u_i.

Assertion: The determinant of the matrix given by Eq. 5.31, with the properties given by Eq. 5.32, is positive.

Proof: The proof is by induction. For n = 2, $\underset{\sim}{A}$ is

$$\underset{\sim}{A} = \begin{bmatrix} a_{11} & a_2 \\ a_{21} & a_{22} \end{bmatrix}$$

$\text{Det}\underset{\sim}{A} = a_{11}a_{22}-a_{21}a_2$. Since, by Eq. 5.32, $a_{11} > a_{21}$ and $a_{22} > a_2$, it follows that

$$\det \underset{\sim}{A} > a_{21}(a_{22}-a_2) > 0$$

Now, given that $\underset{\sim}{A}_{nxn}$ is nonsingular, we show that $\underset{\sim}{A}_{(n+1)x(n+1)}$ is nonsingular. The matrix $A_{(n+1)x(n+1)}$ can be written as:

$$\underset{\sim}{A} = \begin{bmatrix} a_{11} & a_2 & \cdots & a_{n+1} \\ a_{21} & a_{22} & a_3\cdot\cdot & a_{n+1} \\ \vdots & & & \vdots \\ & & & a_{n+1} \\ a_{n+1,1} & & & a_{n+1,n+1} \end{bmatrix}$$

By subtracting the second row from the first row and then expanding the determinant about the first row, we obtain:

$$\det\underset{\sim}{A} = (a_{11}-a_{21}) \det\begin{bmatrix} a_{22} & a_3 & \cdots & a_{n+1} \\ a_{32} & a_{33} & a_4 & a_{n+1} \\ \vdots & & & \\ & & & a_{n+1} \\ a_{n+1,2} & \cdots & & a_{n+1,n+1} \end{bmatrix}$$

$$- (a_2-a_{22}) \begin{bmatrix} a_{21} & a_3 & \cdots & a_{n+1} \\ a_{31} & a_{33} & a_4 \cdots & a_{n+1} \\ \vdots & & & \vdots \\ & & & a_{n+1} \\ a_{n+1,1} & & \cdots & a_{n+1,n+1} \end{bmatrix}$$

The determinants of the two matrices in brackets are positive since by renumbering the indices, they are nxn matrices with the properties given by Eq. 5.32. Since $a_{11} > a_{21}$ and $a_{22} > a_2$, $\det\underset{\sim}{A}_{(n+1)x(n+1)} > 0$.

We note that the restrictions of unit viscosity ratio and $k_{ro}(S_c) \geq k_{rw}(1-S_{ro})$ can be replaced with a more general statement. The properties of $\underset{\sim}{A}$ given by Eq. 5.32, and hence the demonstration of the ability to solve the linear system given by Eqs. 5.17 and 5.18, follow by specifying that

$$M = \frac{k_{rw}(1-S_{ro})\mu_o}{k_{ro}(S_c)\mu_w} \leq 1$$

where M is the mobility ratio.[1]

5.2 Estimation of $\phi(x)$

In this section, we consider the estimation of the spatially varying porosity assuming that the relative permeabilities and absolute permeability are known. The pressure solution is given by Eq. 5.3. The saturation is governed by Eq. 3.22; the integrated form given by Eq. 5.2 no longer applies since ϕ varies spatially.

Since the saturation solution depends upon the porosity, we expect to obtain information about the porosity from measurements of the fractional flow as well as from measurements of the pressure drop. The identifiability of the porosity with respect to these two types of data will be considered separately.

5.2.1 Fractional Flow Data

The fractional flow of water is zero until breakthrough. For $t \geq t_B$, Eq. 3.22 can be integrated to obtain:

$$\int_0^{x_L} \phi dx = v_t t f'(S_L) \qquad (5.33)$$

where S_L is the saturation at the production location x_L at time t. The saturation S_L at any time can be determined from the fractional flow data

by Eq. 3.11. Only the integral value of the porosity given by the left hand side of Eq. 5.33 can be determined from the measurement of the fractional flow. That is, given the fractional flow at any time t, $t \geq t_B$, the average value of the porosity can be calculated. The fractional flow at any other time gives no additional information.

It is possible to obtain more information about the porosity from fractional flow data for problems with an initial saturation profile which varies with x. If we consider initial saturation profiles which can be inverted to obtain functions $x_0(S)$ (note that the initial condition $S_{in}(x) = S_c$ cannot be inverted to obtain a function $x_0(S)$), the equation for the saturation at the production location x_L can be obtained by integrating Eq. 3.22:

$$\int_{x_0(S_L)}^{x_L} \phi(x)dx = v_t t f'(S_L) \tag{5.34}$$

We can consider two examples for which information about the spatially varying porosity, rather than just the average porosity, can be obtained. Since the saturation S_L can be obtained directly from fractional flow data from Eq. 3.11, we can consider S_L rather than the fractional flow to be the observed quantity.

Example 1.

Assume that we are given an initial saturation $S_{in}(x)$ which is a monotonically decreasing function such that no shocks are formed in the saturation solution. That is, all saturations S_L, where $S_{in}(x_L) \leq S_L \leq S_{in}(0)$, are represented in the continuous fractional flow data for all times $t > 0$.

For this case, the porosity can be calculated at all locations in the reservoir since, by Eq. 5.34, the integral $\int_{x}^{x_L} \phi dx$ can be calculated for all x, $0 < x < x_L$. If n discrete measurements were available which correspond to the saturations S_i, $i = 1,...n$, then the following integrated values of the porosity can be obtained from the application of Eq. 5.34:

$$\int_{x(S_1)}^{x_L} \phi dx$$

$$\int_{x(S_i)}^{x(S_{i-1})} \phi dx \qquad i = 1,...,n$$

Example 2.

Assume that we are given an initial saturation $S_{in}(x)$ which is a monotonically decreasing function such that a single shock is formed in the saturation solution at some $t > 0$. The continuous fractional flow data for all times would represent the saturations S_L for $S_{in}(x_L) \leq S_L \leq S_1$ and $S_2 \leq S_L \leq S_{in}(0)$, where S_1 and S_2 are upper and lower saturation bounds of the shock when it is at the location x_L. As in the previous example, the porosity can be calculated at all locations x such that $x_0(S_1) < x < x_L$ and $0 < x < x_0(S_2)$. However, in the range $x_0(S_2) < x < x_0(S_1)$, only the integral value $-\int_{x_0(S_2)}^{x_0(S_1)} \phi(x)dx-$ can be calculated.

5.2.2 Pressure Drop Data

In Subsection 3.3.3, the pressure drop was calculated for several different porosity profiles. Although the porosity does not appear explicitly in the pressure equation 5.3, the term $\frac{f}{k_{rw}}$ in the integrand is a function of saturation, which is related to the variable of integration x and the spatially varying porosity $\phi(x)$ through the saturation equation 3.22 When the pressure equation is written as Eq. 5.15 for $t \leq t_B$, we note that no information about $\phi(x)$ for $x_d(\bar{t}) < x \leq x_L$ can be obtained from a measurement of the pressure drop at time $\bar{t} < t_B$. Consequently, the porosity for all x can not be determined from data taken before breakthrough.

Further analysis of the identifiability of the porosity by explicit means is difficult due to the implicit dependence of the pressure solution on the porosity. An additional difficulty is that the location of the saturation discontinuity for times before breakthrough cannot be calculated directly as in the case when the porosity is specified. However, the moving boundary problem can be investigated analytically.

For $t \leq t_B$, the pressure is governed by Eq. 5.6 and the equation for the saturation boundary is:

$$\frac{dx_d}{dt} = \frac{v_t}{\phi(x_d)(1-S_{ro}-S_c)} \tag{5.35}$$

If the absolute permeability is independent of position, the pressure solution can be written as:

$$b(t) = x_L + x_d(t)(m-1) \tag{5.36}$$

where $b(t) = \dfrac{\Delta P(t) K k_{ro}(S_c)}{v_t \mu_o}$ and $m = \dfrac{\mu_w k_{ro}(S_c)}{\mu_o k_{rw}(1-S_{ro})}$.

If the pressure drop is given for all times $t \leq t_B$, the location of the saturation discontinuity at any time can be calculated from Eq. 5.36 provided that $m \neq 1$. By differentiating Eq. 5.36 with respect to time and using Eq. 5.35 to eliminate the term $\dfrac{dx_d}{dt}$, the following expression is obtained:

$$b'(t) = \frac{v_t(m-1)}{\phi(x_d)(1-S_{ro}-S_c)} \tag{5.37}$$

The porosity throughout the reservoir can then be determined with Eqs. 5.36 and 5.37 provided that $m \neq 1$. If $m = 1$, the pressure drop is constant for all times and the porosity cannot be determined.

5.3 Estimation of the Relative Permeabilities

A method for determining relative permeabilities from pressure and flow rate data obtained from laboratory water floods was reported by Johnson et al.[16] Their derivation of the relations used to calculate the relative permeabilities (see also Appendix E) shows that the relative permeabilities for a particular range of saturation values can be explicitly calculated using both pressure and flow rate data. While the water flooding of laboratory cores are generally taken to the point that nearly all of the moveable oil is expelled from the core, the water flooding of petroleum reservoirs are not taken to completion. In Subsection 5.3.1, we specify the range of saturations for which the relative permeabilities could be explicitly calculated for a water flood which is not taken to completion. The information which can then be obtained from the pressure and flow data for the relative permeabilities at other saturation values is specified. In the remainder of the section we investigate the estimation of coefficients in parametrizations of the relative permeabilities. This serves as an introduction to the approach used for the history matching method developed in Chapter 6 for compressible two-phase flow.

For simplicity, the reservoir model used in this section is taken to be homogeneous and the superficial velocity is independent of time. The pressure drop is related to the relative permeabilities by the following equation:

$$\Delta P(t) = \frac{v_t \mu_w}{K} \int_0^{x_L} \frac{f}{k_{rw}} \, dx \tag{5.38}$$

The saturation is related to the variable of integration x through the saturation equation 5.2, and integrand is given by:

$$\frac{f}{k_{rw}} = \frac{1}{k_{rw} + \frac{\mu_w}{\mu_o} k_{ro}}$$

The fractional flow at the producing location is a function of the relative permeabilities evaluated at the saturation S_L (see Eq. 3.11).

The parametrizations we investigate are given by the following functional forms:

$$k_{rw}(S) = a_w \left(\frac{S-S_c+\varepsilon}{1-S_{ro}-S_c+\varepsilon} \right)^{b_w} - a_w \left(\frac{\varepsilon}{1-S_{ro}-S_c+\varepsilon} \right)^{b_w} \qquad (5.39)$$

$$k_{ro}(S) = a_o \left(\frac{1-S_{ro}-S_c+\varepsilon}{1-S_{ro}-S_c+\varepsilon} \right)^{b_o} - a_o \left(\frac{\varepsilon}{1-S_{ro}-S_c+\varepsilon} \right)^{b_o} \qquad (5.40)$$

where ε is equal to 10^{-3}. For $\varepsilon = 0$, Eqs. 5.39 and 5.40 are identical to Eqs. 3.65 and 3.66. The specification of a small, positive value for ε changes the shape of the relative permeabilities only slightly, but is necessary to avoid singularities in the derivatives of these equations with respect to b_o or b_w at certain saturations. The advantage of the functional forms 5.39 and 5.40 is that, although they contain only four adjustable constants, they give the typically concave, or bowed, shape of the relative permeability curves for b_w, $b_o > 1$.

In Subsection 5.3.1, we make some general comments about the identifiability of the relative permeabilities corresponding to certain ranges of saturation. This investigation applies to general relative permeability curves, and does not depend on the particular functional forms

given by Eqs. 5.39 and 5.40. We then specify the identifiability of the parameters in the functional forms 5.39 and 5.40 based on data taken before water breakthrough. In Subsection 5.3.2 we use a sensitivity analysis to investigate the determination of the relative permeability parameters based on data taken after breakthrough.

5.3.1 Pre-Breakthrough Data and General Considerations

Data taken before the time of water breakthrough are of limited use in determining the relative permeabilities. Since the fractional flow is zero for $t < t_B$, we obtain no information from the fractional flow during that period. Multiplying Eq. 3.77, which was developed in Section 3.3.1 for the normalized pressure drop defined by Eq. 3.69, by the initial pressure drop (given by Eq. 3.72), the following equation is obtained for the pressure drop for $t < t_B$

$$\Delta P(t) = \frac{v_t}{K}\left[\mu_w v_t \frac{f'(S_d)}{\phi} t\left(\int_o^1 \frac{f}{k_{rw}}\, d\xi - \frac{\mu_o}{\mu_w k_{ro}(S_c)}\right) + \frac{x_L \mu_o}{k_{ro}(S_c)}\right] \qquad (5.41)$$

Using the definition of ξ given by Eq. 3.78, Eq. 5.41 can be written as:

$$\Delta P(t) = \frac{v_t}{K}\left[\frac{v_t}{\phi}\left(\mu_w \int_{1-S_{ro}}^{S_d} \frac{ff''}{k_{rw}}\, dS - \frac{\mu_o f'(S_d)}{k_{ro}(S_c)}\right)t + \frac{x_L \mu_o}{k_{ro}(S_c)}\right] \qquad (5.42)$$

This relationship, which is linear with respect to time, can be specified by any two exact measurements of pressure at times t_1, $t_2 < t_B$; no additional information is obtained by measurements at other times before breakthrough. The following values can be calculated from Eq. 5.42 when at least two values of the pressure drop are specified:

(1) $k_{ro}(S_c)$

(2) $\frac{1}{f'(S_d)} \int_{1-S_{ro}}^{S_d} \frac{ff''}{k_{rw}} dS$

Alternatively, $k_{ro}(S_c)$ can be calculated from the single observation of the initial pressure drop given by Eq. 3.72. If the time of breakthrough is known, the value of $f'(S_d)$ can be calculated by the following relation obtained from Eq. 5.2:

$$f'(S_d) = \frac{\phi x_L}{v_t t_B} \tag{5.43}$$

With this additional information the value of the integral in (2) above can be calculated. The value of S_d is unknown, but is related nonlinearly to the relative permeabilities by Eq. 3.45.

Based on the derivation of the relations used to calculate the relative permeabilities from laboratory water floods by Johnson et al[16], the values $k_{ro}(S)$ and $k_{rw}(S)$ for $S \geq S_d$ are determinable from pressure drop and flow rate data. If data are available for only the range of time $t \leq t_f$, where $t_f \geq t_B$, then the relative permeabilities of oil and water can be calculated for the saturations $S_d \leq S \leq S_f$, where S_f is the saturation at the producing location at time t_f. This follows directly from the analysis by Johnson et al[16] (see Appendix E). The information about the relative permeabilities for $S > S_f$ is given by the following integral which can be obtained directly from Eq. E.15:

$$\Delta P(t) = \frac{v_t^2 t_f \mu_w}{K\phi} \int_{1-S_{ro}}^{S_f} \frac{ff''}{k_{rw}} \, dS \qquad (5.44)$$

In summary, based on the pressure drop and fractional flow solution for $t \leq t_f$, the values of the relative permeabilities which are identifiable are

(1) $k_{ro}(S_c)$

(2) $k_{ro}(S)$, $S_d \leq S \leq S_f$

(3) $k_{rw}(S)$, $S_d \leq S \leq S_f$

In addition, we have certain information about the relative permeabilities for the range $S \geq S_f$ given by an integral of the values of the relative permeabilities in Eq. 5.44. The values of S_d and S_f are determinable (see Appendix E), and the information which can be obtained about the relative permeabilities for the range $S_c < S < S_d$ is contained in the relation given by Eq. 3.45, which relates the value of S_d to a function of the relative permeabilities. While this additional information does not allow us to determine the individual values of the relative permeabilities, it may be of some consequence in determining coefficients in a parametrization of the relative permeabilities. Thus, in the next subsection we consider the analysis of the determination of the relative permeability parameters given by the functional forms 5.39 and 5.40. This analysis is based on data taken after breakthrough. We note that the observability of the

relative permeability value $k_{ro}(S_c)$ from the pressure drop data taken before breakthrough gives information about the value a_o, since, with $\varepsilon = 0$ in Eq. 5.40, we obtain

$$k_{ro}(S_c) = a_o$$

Hence, the value a_o is observable from pre-breakthrough data.

5.3.2 Analysis for Data Taken after Breakthrough

In this subsection we investigate the estimation of the relative permeability parameters in Eqs. 5.39 and 5.40 using pressure drop and flow data taken after breakthrough. In Subsection 5.3.2.1 we derive the sensitivity coefficients $\frac{\partial \Delta P}{\partial \gamma_j}$ and $\frac{\partial f}{\partial \gamma_j}$, $j = 1,\ldots,4$, where γ_j, $j = 1,\ldots,4$, refer to b_w, b_o, a_w, and a_o in Eqs. 5.39 and 5.40. The information that is obtained from examination of the sensitivity coefficients is discussed. In 5.3.2.2, the sensitivity coefficients are used in the calculation of the covariance matrix associated with parameter estimates. In that subsection confidence intervals are compared for the estimates of the relative permeability parameters in Eqs. 5.39 and 5.40 based on pressure data alone, flow data alone, and pressure and flow data combined. Confidence intervals for the estimates of the parameters b_o and b_w (i.e. we assume that the endpoints $k_{ro}(S_c)$ and $k_{rw}(1-S_{ro})$ are specified) are also given.

5.3.2.1 Sensitivity Coefficients

The quantities $\frac{\partial \Delta P}{\partial \gamma_j}$ and $\frac{\partial f}{\partial \gamma_j}$, $j = 1,\ldots,4$, are called sensitivity coefficients.[17] These quantities give us a measure of the change in the calculated quantities with respect to perturbations in the parameters. If, for example, the sensitivities of the quantities ΔP and f with respect to one of the parameters γ_j were small for all observation times, this parameter could not be determined very accurately, since large changes in its value would produce only small changes in the observed quantities.

In this subsection, we derive expressions that are used to calculate the sensitivity coefficients for specified values of the relative permeability parameters and viscosity ratio.

We define a dimensionless time τ, the moveable pore volume injected, as:

$$\tau = \frac{v_t t}{\phi x_L (1-S_{ro}-S_c)} \tag{5.45}$$

The sensitivity coefficients will be calculated as functions of the dimensionless times τ_i, rather than t_i.

Using Eqs. 5.39 and 5.40 to eliminate the relative permeabilities in Eq. 3.11, the fractional flow at time τ_i can be calculated from the relative permeability parameters γ_j, $j = 1,\ldots,4$, and the calculated value of S_L at time τ_i. We denote this functional dependence of the fractional flow as:

$$f(\tau_i) = f(\Gamma, S_L) \tag{5.46}$$

where we have used Γ to refer to γ_j, $j = 1,\ldots,4$. The saturation S_L at time τ_i can be calculated using Eq. 5.45 and the following relation obtained directly from Eq. 5.2:

$$x_L = \frac{v_t t}{\phi} f'(S_L) \tag{5.47}$$

Using Eq. 5.45 to eliminate t in Eq. 5.47, and evaluating that expression at time τ_i, we obtain:

$$\tau_i = \left[f'(\Gamma,S_L)(1-S_{ro}-S_c)\right]^{-1} \tag{5.48}$$

The prime denotes the derivative of fractional flow with respect to saturation. The functional dependence of S_L given by Eq. 5.48 can be expressed as:

$$S_L = S_L(\Gamma,\tau_i) \tag{5.49}$$

The sensitivity of the fractional flow with respect to γ_j is given by:

$$\frac{\partial f(\tau_i)}{\partial \gamma_j} = \frac{\partial f(\Gamma,S_L)}{\partial \gamma_j} + \frac{\partial f(\Gamma,S_L)}{\partial S_L} \frac{\partial S_L}{\partial \gamma_j} \tag{5.50}$$

An expression for $\frac{\partial S_L}{\partial \gamma_j}$ is obtained by taking the derivative of Eq. 5.48 with respect to γ_j and rearranging:

$$\frac{\partial S_L}{\partial \gamma_j} = - \frac{\partial f'(\Gamma, S_L)}{\partial \gamma_j} \Big/ \frac{\partial f'(\Gamma, S_L)}{\partial S_L} \tag{5.51}$$

Substituting Eq. 5.51 into 5.50, we obtain the following expression for the sensitivity coefficient:

$$\frac{\partial f(\tau_i)}{\partial \gamma_j} = \frac{\partial f(\Gamma, S_L)}{\partial \gamma_j} - \frac{\partial f'(\Gamma, S_L)}{\partial \gamma_j} f'(\Gamma, S_L) \Big/ f''(\Gamma, S_L) \tag{5.52}$$

The sensitivity coefficients for the water-oil ratio can be obtained directly from the sensitivity coefficients given by Eq. 5.52. Rearranging Eq. 5.1, the following expression is obtained for the value of WOR calculated at time τ_i:

$$WOR(\tau_i) = \frac{f(\tau_i)}{[1-f(\tau_i)]} \tag{5.53}$$

The sensitivity of WOR with respect to γ_j can then be calculated by the following equation:

$$\frac{\partial WOR(\tau_i)}{\partial \gamma_j} = [1-f(\tau)]^{-2} \frac{\partial f(\tau_i)}{\partial \gamma_j} \tag{5.54}$$

In order to obtain the sensitivity coefficients of the pressure drop, we use the following change of variables in the integral in the pressure equation 5.38:

$$\int_0^{x_L} \frac{f}{k_{rw}}\, dx = \int_{1-S_{ro}}^{S_L} \frac{f}{k_{rw}} \frac{\partial x}{\partial S}\, dS \tag{5.55}$$

The following relation can be obtained from Eq. 5.2:

$$\frac{\partial x}{\partial S} = \frac{v_t t}{\phi} f''(S) \tag{5.56}$$

so that the pressure equation can be written as:

$$\Delta P(t_i) = \frac{v_t^2 t_i \mu_w}{\phi K} \int_{1-S_{ro}}^{S_L} \frac{ff''}{k_{rw}}\, dS \tag{5.57}$$

Using the dimensionless time defined by Eq. 5.45, the pressure drop at τ_i is:

$$\Delta P(\tau_i) = \frac{v_t \tau_i \mu_w x_L (1-S_{ro}-S_L)}{K} \int_{1-S_{ro}}^{S_L} g(\Gamma,S)\, dS \tag{5.58}$$

where $g(\Gamma,S) = \dfrac{ff''}{k_{rw}}$.

The sensitivity of the pressure drop with respect to γ_j is given by:

$$\frac{\partial \Delta P(\tau_i)}{\partial \gamma_j} = \frac{v_t \tau_i \mu_w x_L (1-S_{ro}-S_L)}{K} \left[\int_{1-S_{ro}}^{S_L} \frac{\partial}{\partial \gamma_j} g(\Gamma,S)\, dS + g(\Gamma,S_L) \frac{\partial S_L}{\partial \gamma_j} \right] \tag{5.59}$$

The quantity $\frac{\partial S_L}{\partial \gamma_j}$ is given by Eq. 5.51. Dividing Eq. 5.59 by the initial pressure drop $\Delta P(0)$ given by Eq. 3.72, and using Eq. 5.48 to eliminate τ_i on the right hand side, we obtain:

$$\frac{1}{\Delta P(0)} \frac{\partial \Delta P(\tau_i)}{\partial \gamma_j} = \frac{\mu_w}{\mu_o} \frac{k_{ro}(S_c)}{f'(S_L)} \left[\int_{1-S_{ro}}^{S_L} \frac{\partial g(\Gamma,S)}{\partial \gamma_j} dS + g(\Gamma,S_L) \frac{\partial S_L}{\partial \gamma_j} \right] \tag{5.60}$$

The normalized sensitivities can thus be calculated when Γ and the viscosity ratio are specified.

The sensitivities of the fractional flow and normalized pressure drop can be exhibited for a specified value of Γ and viscosity ratio. Choosing the relative permeability parameters as $a_o = a_w = 1$, $b_o = 3$, $b_w = 2$, and $\frac{\mu_w}{\mu_o} = 1$, we plot the sensitivities for dimensionless times $\tau \leq 10$. The sensitivities $\frac{\partial f}{\partial a_w}$ and $\frac{\partial f}{\partial a_o}$ are shown in Fig. 5.1, and $\frac{\partial f}{\partial b_w}$ and $\frac{\partial f}{\partial b_o}$ are shown in Fig. 5.2. The corresponding sensitivities for the pressure drop are shown in Figs. 5.3 and 5.4. We see from these figures that both fractional flow and pressure drop are sensitive to changes in each of the four relative permeability parameters.

Note from Fig. 5.1 that $\frac{\partial f}{\partial a_o} = -\frac{\partial f}{\partial a_w}$ for all times τ. These sensitivities are thus linearly dependent for all times τ, and consequently both quantities a_o and a_w can not be determined from fractional flow data

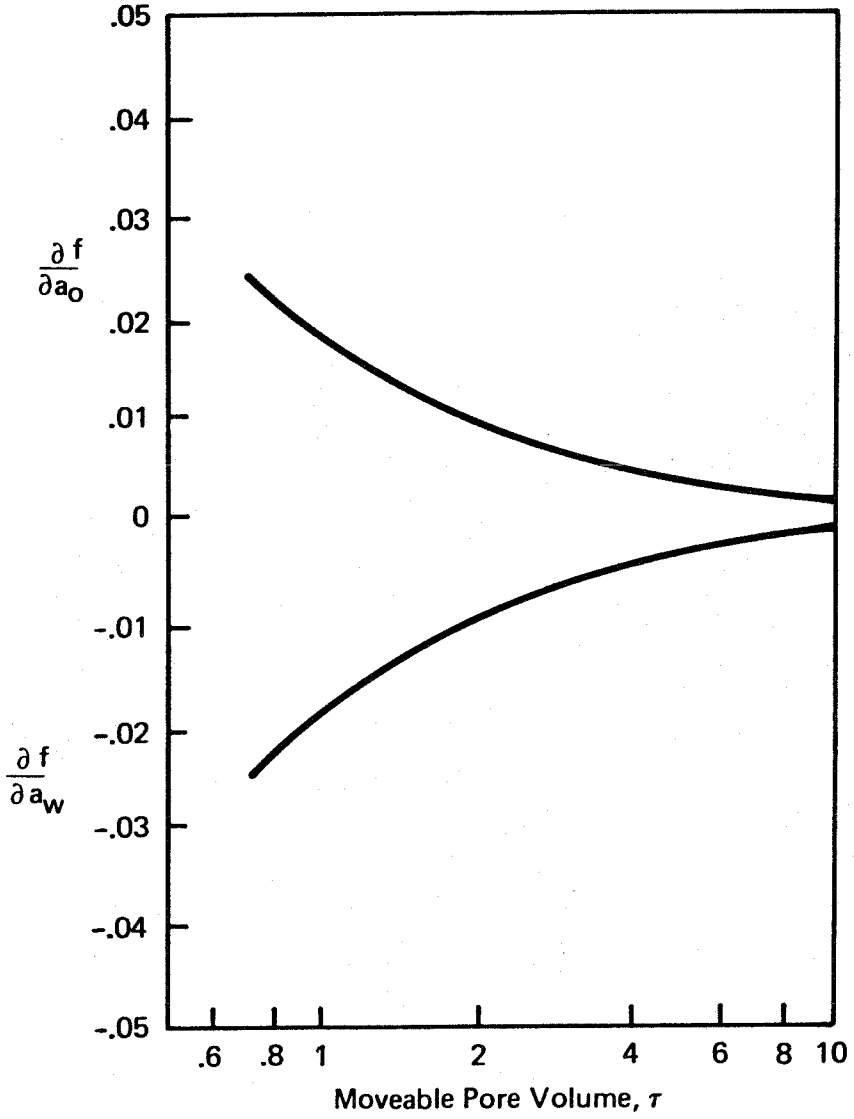

Figure 5.1

Sensitivity Coefficients $\frac{\partial f}{\partial a_o}$ and $\frac{\partial f}{\partial a_w}$

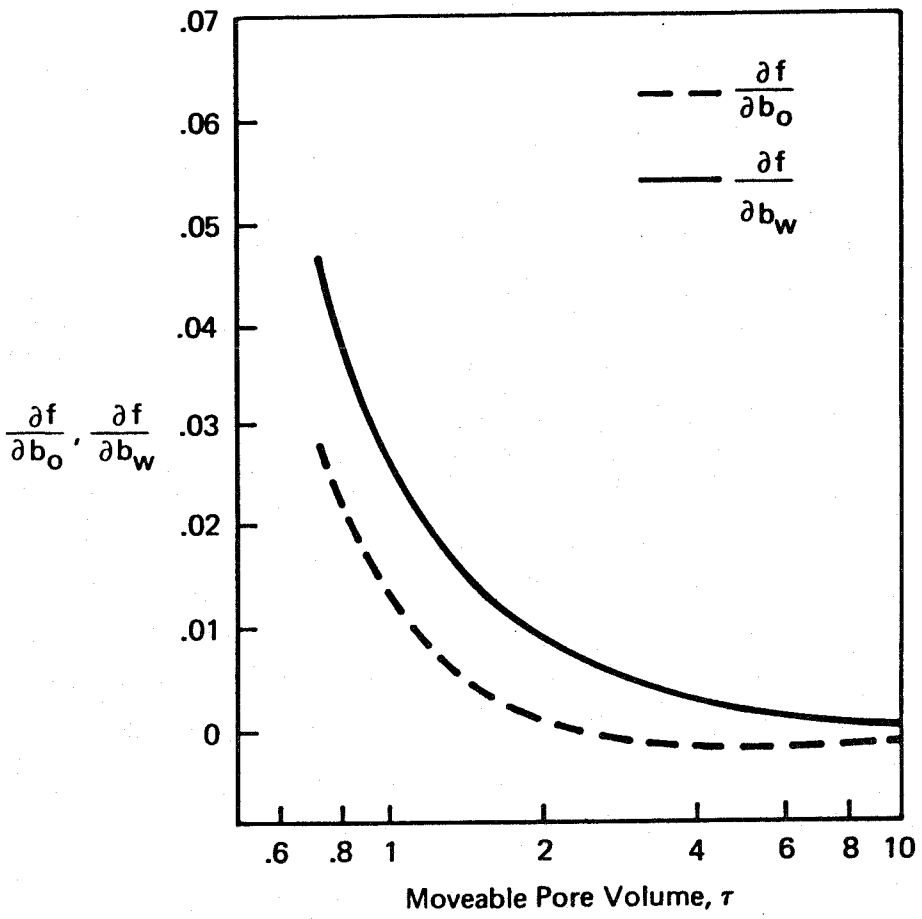

Figure 5.2

Sensitivity Coefficients $\frac{\partial f}{\partial b_o}$ and $\frac{\partial f}{\partial b_w}$

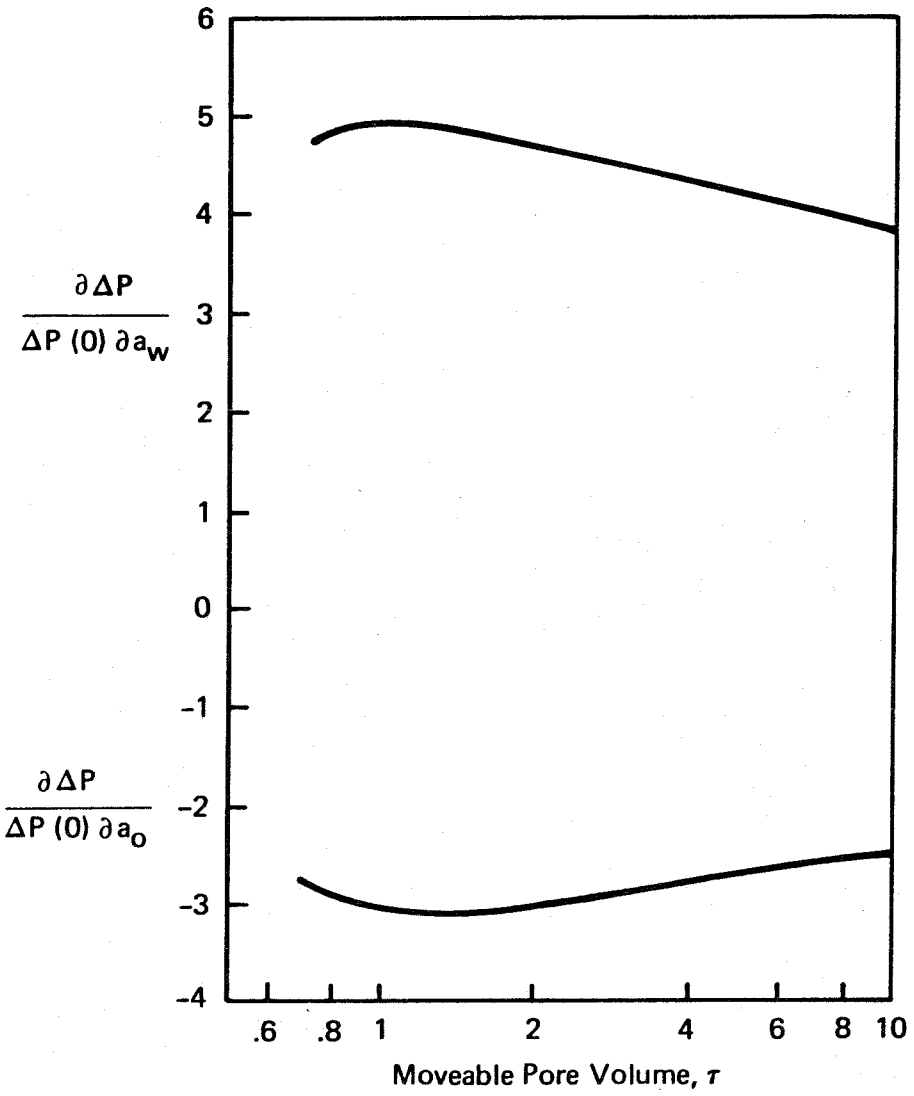

Figure 5.3

Sensitivity Coefficients $\frac{\partial \Delta P}{\Delta P(0)\partial a_o}$ **and** $\frac{\partial \Delta P}{\Delta P(0)\partial a_w}$

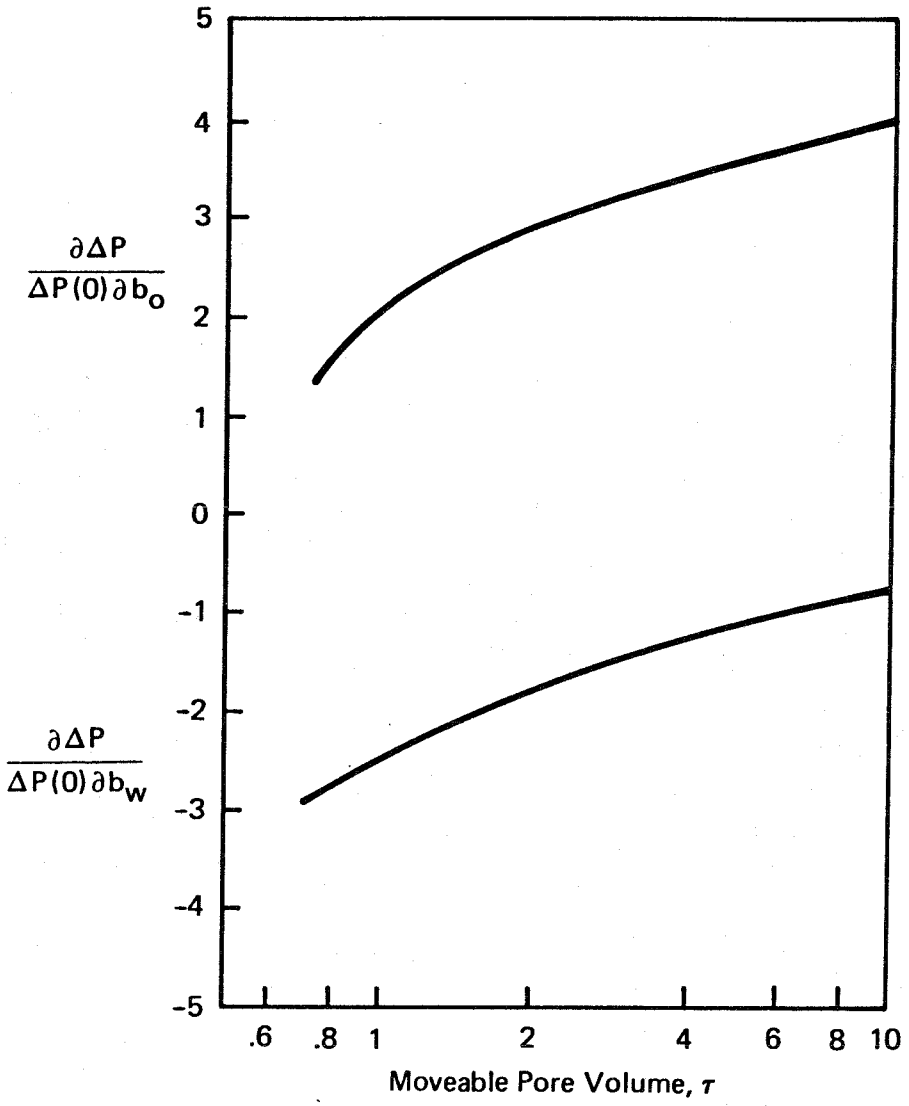

Figure 5.4

Sensitivity Coefficients $\frac{\partial \Delta P}{\Delta P(0) \partial b_o}$ **and** $\frac{\partial \Delta P}{\Delta P(0) \partial b_w}$

alone.[17] This fact can also be established by simply noting that the quantities a_o and a_w appear as a ratio in Eq. 3.11 for the fractional flow when the relative permeabilities are expressed by the functional forms 5.39 and 5.40.

5.3.2.2 Analysis of the Covariance Matrix

In this section we present an analysis of the accuracy associated with estimates of the relative permeability parameters based on observations of the pressure drop and water-oil ratio containing random error. Now that we are considering observations which have error associated with them, we use the water-oil ratio rather than the fractional flow since the former quantity is generally used in petroleum reservoir studies. It is assumed that the errors associated with the measurements of the pressure drop have a Gaussian distribution with zero mean and variance σ_p^2. Similarly, the errors associated with measurements of the water-oil ratio have zero mean and variance σ_w^2.

Assume that we are given estimates $\bar{\Gamma}$ of the true relative permeability parameters Γ which minimize the function

$$J = \sum_{i=1}^{n} \underset{\sim}{y}_i^T \underset{\sim}{W}_i \underset{\sim}{y}_i \tag{5.61}$$

where the vector $\underset{\sim}{y}_i$ is given by

$$\underset{\sim}{y}_i = \left[\frac{\Delta P^{obs}(\tau_i) - P^c(\tau_i)}{\Delta P(0)} \quad WOR^{obs}(\tau_i) - WOR^c(\tau_i) \right]^T$$

The superscripts obs and c refer to the observed and calculated quantities respectively, and n is the number of discrete times τ_i at which measurements are taken. The 2x2 matrix $\underset{\sim}{W}_i$ is the inverse of the covariance of the measurements.[18,19] The quantity $\Delta P(0)$ is assumed to be exactly known. The pressure drop is normalized so that our analysis will not depend upon specification of all the reservoir properties (see Eqs. 5.59 and 5.60). Thus, the variance associated with $\frac{\Delta P^{obs}}{\Delta P(0)}$ is $\left(\frac{\sigma_P}{\Delta P(0)}\right)^2$, and the weighting $\underset{\sim}{W}_i$ is given by:

$$\underset{\sim}{W}_i = \begin{bmatrix} \left(\frac{P(0)}{\sigma_P}\right)^2 & 0 \\ 0 & \left(\frac{1}{\sigma_w}\right)^2 \end{bmatrix} \tag{5.62}$$

If we assume that the difference between the true and estimated values of γ_j, given by α_j, is small, the distribution of the error in the parameter estimates can be calculated. The probability density for $\underset{\sim}{\alpha} = [\alpha_1\ \alpha_2\ \alpha_3\ \alpha_4]^T$ will be Gaussian with mean zero and covariance $\underset{\sim}{C}$.[18,19] That is,

$$\underset{\sim}{C} = E\left[\underset{\sim}{\alpha}\ \underset{\sim}{\alpha}^T\right]$$

where E denotes the expected value. The inverse of the covariance matrix $\underset{\sim}{C}^{-1}$, which we denote here as $\underset{\sim}{H}$, is given by

$$\underset{\sim}{H} = \sum_{i=1}^{n} \underset{\sim}{D}_i^T \underset{\sim}{W}_i \underset{\sim}{D}_i \tag{5.63}$$

where $\underset{\sim}{D}_i$ is the following 2x4 matrix of sensitivity coefficients:

$$\underset{\sim}{D}_i = \begin{bmatrix} \frac{\partial \Delta P^c(\tau_i)}{\Delta P(0) \partial \gamma_1} & \frac{\partial \Delta P^c(\tau_i)}{\Delta P(0) \partial \gamma_2} & \cdots & \frac{\partial \Delta P^c(\tau_i)}{\Delta P(0) \partial \gamma_4} \\ \\ \frac{\partial WOR^c}{\partial \gamma_1} & \cdots & & \frac{\partial WOR^c}{\partial \gamma_4} \end{bmatrix} \tag{5.65}$$

The sensitivity coefficients are derived in Subsection 5.3.2.1. The eigenvalues of the covariance matrix $\underset{\sim}{C}$, which are the variances of certain linear combinations of the errors α_j, give us a measure of how well the parameters can be determined.[17]

The covariance matrix was calculated for the set of relative permeability parameters, measurement variances, initial pressure drop, and viscosity ratio given in Table 5.1. These values might correspond to a typical water flooding problem, although the discrete times at which measurements are taken are arbitrary. The range for τ is appropriate, however, since water breakthrough corresponds to $\tau = 0.75$, and $\tau = 2.0$ is a reasonable upper bound for a water flood. The eigenvalues of the covariance matrix, λ_i, are given as Case 1 in Table 5.3. The largest eigenvalue has the value 0.83, which is of the same order of magnitude as the parameters that are to be estimated. Consequently, we would not expect to be able to determine all four parameters very accurately. However, the inverse of $\underset{\sim}{C}$, given by $\underset{\sim}{H}$, is nonsingular, and so the four parameters are observable.[18]

We now consider several cases specified in Table 5.2 all based on the parameter values of Table 5.1. Case 2 corresponds to the estimation of the four relative permeability parameters based on pressure drop data only.

Table 5.1 Specification of Properties Used in the Calculation of the Covariance Matrix

Relative Permeability Parameters:

$a_o = 1$ $a_w = 1$ $S_c = 0.1$

$b_o = 3$ $b_w = 2$ $S_{ro} = 0.1$

Viscosity Ratio: $\mu_o/\mu_w = 1$

Initial Pressure Drop: $\Delta P(0) = 20$ atm

Measurement Times: $\tau_i = 0.8 + (i-1)\ 0.1$ $i = 1,\ldots, 13$

Measurement Variances: $\sigma_p^2 = 0.5\ atm^2$ $\sigma_w^2 = 0.5$

Table 5.2 Specification of Cases for Which the Covariance Matrix is Calculated

Cases	Estimated Parameters	Data Used
1	a_o, a_w, b_o, b_w	ΔP, WOR
2	a_o, a_w, b_o, b_w	ΔP
3	a_o, a_w, b_o, b_w	WOR
4	b_o, b_w	ΔP, WOR
5	b_o, b_w	ΔP
6	b_o, b_w	WOR

Table 5.3 Eigenvalues of the Calculated Covariance Matrix

Case	λ_1	λ_2	λ_3	λ_4
1	8×10^{-1}	7×10^{-3}	2×10^{-4}	1×10^{-6}
2	5×10^{1}	2×10^{-1}	2×10^{-4}	1×10^{-6}
3†				
4	2×10^{-4}	4×10^{-6}		
5	2×10^{-4}	4×10^{-6}		
6	8×10^{-2}	1×10^{-3}		

†$\underset{\sim}{H}$ is singular

The eigenvalues for this problem are given in Table 5.3. The largest eigenvalue has the value 50, which is much larger than the corresponding value for Case 1 for which both flow and pressure data were used. Case 3 corresponds to the estimation of the relative permeability parameters based on WOR data only. As noted in Subsection 5.3.2.1, all four relative permeability parameters are not observable; $\underset{\sim}{H}$ is singular in this case.

In Cases 4, 5, and 6 we assume that the endpoints values $k_{rw}(1-S_{ro})$ and $k_{rw}(S_c)$ are known, thus specifying the values a_o and a_w. The covariance matrix calculated for these cases corresponds to the error in the estimates of the exponents b_o and b_w. In Case 4, both pressure drop data and water-oil ratio data are used. The largest eigenvalue of the covariance matrix for this case is several orders of magnitude smaller than the values of the exponents, and consequently we expect that the exponents b_o and b_w can be accurately estimated. Case 5 is based on pressure drop data alone, and Case 6 is based on WOR data alone. The eigenvalues of the covariance matrix for both of these cases are small, and hence it appears that the exponents b_o and b_w can be determined accurately from either pressure data or water-oil ratio data.

5.4 Summary and Conclusions

In this chapter we have investigated the identifiability of reservoir parameters in a two-phase, incompressible, one-dimensional reservoir model. The analytical solution for this problem provides a convenient means for studying the structure of the parameter estimation problem.

In Section 5.1, it was shown that the fractional flow data do not depend upon the spatially varying permeability, and thus only the pressure drop is used in the estimation of the permeability. The pressure drop solution does not depend upon the spatially varying permeability at locations in the reservoir ahead of the saturation discontinuity. Hence, the spatially varying permeability throughout the reservoir cannot be determined from pressure drop data taken before the time of breakthrough. The pressure drop does depend upon the spatially varying permeability at locations in the reservoir behind the saturation discontinuity. The identifiability of the spatially varying permeability was established for two limiting cases of two-phase flow — the moving boundary problem and the representation of the relative permeabilities by the functional forms 5.39 and 5.40.

The spatially varying porosity has an effect on both the saturation and pressure solutions. The identifiability of the spatially varying porosity based on fractional flow data alone, and pressure drop data alone, was considered in Subsections 5.2.1 and 5.2.2. Similar to the case for the absolute permeability, it was shown that the pressure drop solution for times before water breakthrough does not depend upon the spatially varying porosity at locations ahead of the saturation discontinuity. The

identifiability of the spatially varying porosity based on pressure drop data taken through the time of breakthrough was established for the moving boundary problem. The fractional flow depends only upon the average porosity, and not the spatially varying porosity. Consequently, if the initial saturation in the reservoir is the connate water saturation, only the average value of the porosity can be obtained from fractional flow data. It was shown in Subsection 5.2.1 that the spatially varying porosity may be identifiable when the initial saturation profile varies with location in the reservoir.

Both pressure and saturation solutions depend upon the relative permeabilities. In Subsection 5.3.1, the identifiability of the relative permeabilities was investigated. It was shown that the pressure solution before breakthrough depends on the value $k_{ro}(S_c)$ and a single value of an integral of the relative permeabilities over the range of saturation $S_d \leq S \leq 1-S_{ro}$. If the water flood is taken to completion (i.e. the water saturation value $1-S_{ro}$ is attained at all locations in the reservoir), the relative permeability values of oil and water are identifiable, based on the pressure drop and fractional flow data, for all saturation $S \geq S_d$. Based on data taken for times $t \leq t_f$, the relative permeabilities for the range $S_d \leq S \leq S_f$, where S_f corresponds to the saturation value at the producing location at time t_f, are identifiable. An integral value of the relative permeabilities for the range of saturation $S > S_f$ can be obtained.

The determination of the coefficients in a parametrization of the relative permeabilities, given by Eqs. 5.39 and 5.40, based on data taken after breakthrough was investigated in Subsection 5.3.2. Sensitivity coefficients were derived for the four parameters in those functional forms.

An analysis of the covariance matrix of the error in the estimates based on noisy observations of the pressure drop and water-oil ratio was presented. From this analysis, it was concluded that the four parameters could not be determined accurately from measurements taken for a limited range of time after breakthrough, although they are observable. If the endpoints of the relative permeabilities are exactly known, and hence the values a_o and a_w specified in the functional forms 5.39 and 5.40, the values of the exponents b_o and b_w can be accurately determined. These values can also be accurately determined from either pressure drop data alone, or water-oil ratio data alone.

6. ESTIMATION OF TWO-PHASE RESERVOIR PROPERTIES

The use of an algorithm which proceeds systematically from an initial set of reservoir parameter guesses to one that minimizes an objective function is commonly called automatic history matching. Most of the published work to date on automatic history matching has been devoted to single phase reservoirs in which the unknown parameters to be estimated are the reservoir porosity and absolute permeability. In the single phase problem the objective function usually consists of the deviations between the predicted and measured reservoir pressures at the wells. Parameter estimation, or history matching, in multiphase reservoirs is fundamentally a more difficult problem than that in single phase reservoirs. The multiphase equations are nonlinear, and in addition to the porosity and absolute permeability, the relative permeabilities of each phase may be unknown and subject to estimation Measurements of the relative rates of flow of oil, water and gas at the wells may also be available for the objective function.

The aspect of the reservoir history matching problem that distinguishes it from other parameter estimation problems in science and engineering is the large dimensionality of both the system state and the unknown parameters. As a result of this large dimensionality, computational efficiency becomes a prime consideration in the implementation of an automatic history matching method. In all parameter estimation methods a trade-off exists between the amount of computation performed per iteration and the speed of convergence of the method. An important savings in computing time was realized in single phase automatic history matching through the introduction of optimal control theory as a method for calculating the gradient of the objective function

with respect to the unknown parameters.[20,21] This technique is currently limited to first-order gradient methods. First-order gradient methods generally converge more slowly than those of higher order. Nevertheless, the amount of computation required per iteration is significantly less than that required for higher order optimization methods, and thus, first-order methods are attractive for automatic history matching. The optimal control algorithm for automatic history matching has been shown to produce excellent results when applied to field problems.[22] Therefore, the first approach to the development of a general automatic history matching algorithm for multiphase reservoirs would seem to proceed through the development of an optimal control approach for calculating the gradient of the objective function with respect to the parameters for use in a first-order method.

In this chapter a new algorithm based on optimal control theory is presented for the estimation of absolute permeability, porosity, and relative permeability in two-phase reservoirs using pressure and production rate data. In Section 6.1, the algorithm is summarized. In Section 6.2, detailed results are presented for test problems for one- and two-dimensional water flooding situations.

6.1 Summary of the Algorithm

In this section, the basic algorithm developed in this work is outlined. An objective function J is defined as the weighted sum of the squares of the differences between the observed and calculated values of the reservoir pressure and flow rate data at the wells:

$$J = \sum_i \omega_i^P (P^{obs}-P^{cal})_i^2 + \sum_j \omega_j^R (R^{obs}-R^{cal})_j^2 \qquad (6.1)$$

where P is the pressure, R represents the flow rate data, and ω_i is a weighting factor for data element i. The production rate data consist of the production rate of one of the phases, or a ratio of the flow rates. In most simulation of two-phase reservoirs, either the total flow rate of the two fluids, or the flow rate of oil, is specified at each production well. If the total flow rate is specified, either the oil production rate or the water-oil ratio may be used as the rate data in Eq. 6.1. The water-oil ratio may be used if the oil production is specified. For the test problems presented in this study, the total production is specified, and the water-oil ratio is used as the flow data.

The reservoir properties to be estimated are the porosity and absolute permeability and the saturation-dependent relative permeabilities. Porosity and absolute permeability may vary spatially throughout the reservoir. The most detailed spatial resolution available corresponds to the finite-difference grid of the simulator. The algorithm developed here allows each of the unknown parameters associated with each grid block to be estimated. The technique of zonation or specification of regions of the reservoir within which a property is assumed to be constant is easily included within the present development. The relative permeabilities are represented by the functional forms specified by Eqs. 5.39 and 5.40. Thus, the relative permeability estimation problem we consider is that of estimating coefficients a_o and a_w, and the exponents b_o and b_w.

The history matching problem consists of determining the unknown reservoir properties so that J is minimized. The first-order gradient method requires that we calculate the partial derivatives of the objective function with respect to each of the unknown reservoir parameters. These derivatives can be calculated most efficiently through the use of optimal control theory. The detailed derivation of the equations used to evaluate the derivatives of the performance index are given in Appendices F and G. In Appendix F, the derivation is based on the partial differential equation formulation of the reservoir model developed in Subsection 2.1.3. In Appendix G, the derivation is based on the finite-difference formulation of the reservoir model which was developed in Section 4.1. Using this derivation, no approximations are made in the solution of the adjoint system which is used to calculate the partial derivatives of the objective function. This is discussed further in Appendix G. Finally, in Appendix H, the gradient method used in this study is specified.

The objective function in Eq. 6.1 is written in a general form that allows each data point to be weighted separately. Considerations on an analysis of confidence intervals for estimated parameters shows that the weighting should be chosen to reflect the relative uncertainty of each measurement.[18] However, a priori information usually will not be available to warrant weighting individual pressure and flow rate measurements differently. In this study, a single weighting is used for all pressure measurements, and another weighting is used for all rate measurements. Since the objective function J can be multiplied by any positive constant without changing the problem, only the relative weighting between the two terms in the objective function is important. With these simplifications, Eq. 6.1 can be written as

$$J = J_p + \omega J_R \tag{6.2}$$

where J_p refers to the sum of the squared differences between the observed and calculated pressures, and J_R is the corresponding sum for the water-oil ratio data. Given a variance σ_p^2 associated with the pressure measurements, and variance σ_R^2 associated with the rate measurements, ω would be specified as the ratio σ_p^2/σ_R^2. The selection of the weighting factor in the objective function if no estimate of the relative errors in the data is available is discussed in the following section.

6.2 Test Problems

In this section, we present several test problems to illustrate the use of the automatic history matching method developed. All the cases correspond to the water flooding of hypothetical reservoirs initially at the connate water saturation. The "observed data" were generated by exercising the simulator developed in Chapter 4 with the true, but presumed unknown, parameter values. In all except one of the cases, the data consist of the pressure in the injection and production grid blocks and the water-oil ratio in the producing grid block at each time step in the simulation. In the final case, errors generated by a Gaussian random number generator with specified variances were added to the observed data.

In practical or field history matching problems, the test of the quality of the match is given by the magnitude of the objective function at the conclusion of the estimation. For a hypothetical history matching problem the true but presumed unknown parameter values are available so that the quality of the match can be determined by comparing not only the initial and final values of the objective function but also the estimated and true parameter

values. A question related to the quality of the match is that of the rate of convergence of the algorithm, that is, the number of iterations required to achieve an acceptably low value of the objective function. Although we do not assign acceptable minimum values for the objective function, the quantities J_p and J_R for several iterations will be presented for each problem. These quantities serve as a measure of how well the data have been matched.

From Eq. 6.2, we note that for a given set of estimated reservoir parameters, the value of the performance index J will depend upon the weighting ω. When the weighting is specified as the ratio of the variances of the pressure and water-oil ratio measurements, the quantities J_p and ωJ_R are expressed in the same units. When no estimate of relative error is available, the choice of ω is somewhat arbitrary. For the problems in which the relative permeabilities were estimated, the rate of convergence generally improved when J_p and ωJ_R were of comparable orders of magnitude based on the initial parameter guesses. For the cases in which exact data were used as the observed data, ω was set to 10. For the case in which the simulated data were corrupted with noise, ω was set to the ratio σ_p^2/σ_R^2.

6.2.1 One-Dimensional Water Flood

To explore the properties and performance of the algorithm, it is desirable to study a one-dimensional hypothetical reservoir. Therefore, five cases based on a water flooding situation are presented. The reservoir dimensions, injection and production rates, and relative permeabilities are the same for all cases; only different sets of reservoir parameters are estimated in each case. The water flooding problem is specified in Table 6.1, and the set of parameters estimated in each case are given in Table 6.2.

Table 6.1. Specification of Water Flood Cases

Fluid and Reservoir Properties

$K = 0.08\ d$[1]	$\mu_o = 5$ cp	$c_w = 1\times10^{-4}\ atm^{-1}$
$\phi = 0.3$[2]	$\mu_w = 1$ cp	$c_o = 1\times10^{-4}\ atm^{-1}$
Initial P = 50 atm	Initial $S_w = S_{wc}$	$c_r = 0$

Relative Permeability Parameters

$a_o = 1$	$b_o = 2$	$S_{wc} = 0.1$
$a_w = 1$	$b_w = 3$	$S_{ro} = 0.1$

Model Specification

	1-D	2-D
Model Dimensions (Length/Width):	10/3	1
Grid Blocks:	10	10x10
Inj/Prod Rate (PV/Time Step):	0.0137	0.0107[3] (Avg.)
Number of Time Steps:	60	89

(1) Step function was used in Case 1
(2) Sine function was used in Case 2
(3) Variable time steps were used to control ΔS at each time step to approximately 0.1.

Table 6.2. Parameters Estimated in Test Problems

Case	Dimensions	Parameters Estimated
1	1	Step function of K
2	1	Sine function of ϕ
3	1	a_o, a_w, b_o, b_w
4	1	b_o, b_w
5	1	K, ϕ, b_o, b_w
6	2	b_o, b_w
7	2	K, ϕ, b_o, b_w
8(1)	2	K, ϕ, b_o, b_w

(1) A Gaussian random error term was added to the "observed data"

In Case 1, the unknown parameter values are the nine harmonic-average values of the absolute permeability. The true harmonic-average permeabilities form a step function with the discontinuity occurring between grid blocks 5 and 6. An initial guess of 0.2 darcy is used for each of these parameters. The estimated values after 11 iterations of the algorithm and after 48 iterations are shown in Fig. 6.1. The quantity J_p at several iterations is summarized in Table 6.3 For Case 1 J_R is zero and consequently does not provide information about the parameters. Note from Table 6.3 that the objective function at the 11th iteration is less than one percent of its initial value. More iterations lead to further reductions in the objective function, although the rate of reduction is much slower than during the initial iterations. After 48 iterations the objective function is less than 1 atm^2. The corresponding root mean square deviation is less than 0.1 atm, which represents a smaller tolerance than one might require for a practical problem. We note from Fig. 6.1 that a reduction of the objective function from 15 to 1 atm^2 (which corresponds to the 11th and 48th iterations, respectively) does not lead to a significant improvement in the parameter estimates.

In Case 1 we note that at a low value of J (1 atm^2 based on the root mean square deviation of less than 0.1 atm) the correct values of the harmonic-average permeabilities have not been attained. In fact, the estimates have not moved appreciably from their values when J equaled 15 atm^2. This behavior, noted frequently in the estimation of spatially varying properties, is a result of an attempt to estimate too many parameters on the basis of the available data leading to a very shallow minimum in the objective function surface.[23] Because our main interest here is not the uniqueness problem

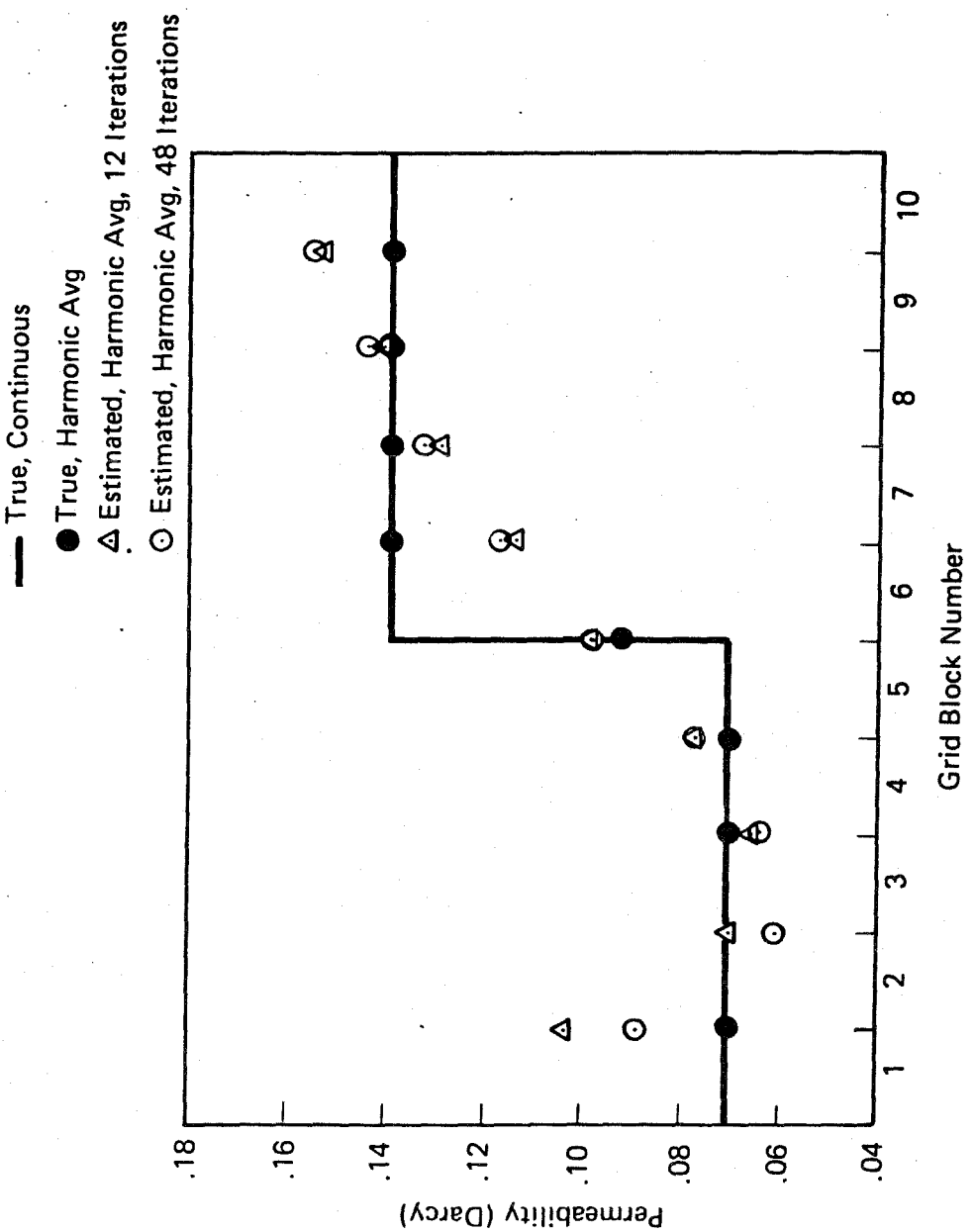

Figure 6.1

Estimation of Permeability, 1–D Model, With Initial Guess K = 0.2 Darcy

Table 6.3. Summary of the Objective Function as a Function of Iteration Number for the Eight Cases Presented

Case No.		Iteration Number					
		0	5	10	20	40	Final
1.	J_P[1]	2900	660	33	1.9	1.1	0.96(48)[2]
	J_R	0					
2.	J_P	360	35	3			0.75(15)
	J_R	560	0.57	0.32			0.015
3.	J_P	3000	620	190	25	7.1	0.33(76)
	J_R	190	150	58	5.7	1.3	0.06
4.	J_P	3000	1300	31			0.40(13)
	J_R	190	98	2.2			0.03
5.	J_P	3400	430	64	3.8		0.12(32)
	J_R	64	44	10	0.84		0.057
6.	J_P	4800	2300	3.5			2.4(11)
	J_R	230	100	0.25			0.01
7.	J_P	10,000	1600	130	3.8		3.2(24)
	J_R	52	57	17	0.31		0.16
8.	J_P	12,000	1420	310	170	165	165(60)
	J_R	91	65	22	12	11	11

(1) J_P has dimensions atm^2

(2) The value of the performance index at the final iteration taken. The corresponding iteration number is given in parentheses.

of history matching we will not pursue this aspect further here. The interested reader is referred to Shah et al.[23] for such a discussion for single phase reservoirs. The algorithm developed here does perform as desired in that J is significantly reduced.

In Case 2 the unknown parameters to be estimated are the values of porosity of each grid block. The true porosities are assumed to be a sine function, and the initial guess is the uniform value of 0.18. The estimated values after 15 iterations are shown in Figure 6.2. The value of J_p that corresponds to this estimate is 0.75 atm^2. As in Case 1 the correct values have not been attained, although the true profile is represented.

The values of J_p and J_R for several iterations are shown in Table 6.3. While the initial value of J_p is approximately one-tenth of that for the previous Case 1, J_R is now nonzero. In Section 5.2 it was shown exactly that the water-oil ratio is a function of the average porosity but not of the individual grid block porosities. For this case, the value of J_R decreases as the difference between the true average of the porosity and the average of the estimated values decreases. The true average is 0.25; the average of the estimates for the first five iterations is successively 0.197, 0.215, 0.236, 0.256, and 0.246. The corresponding values of J_R are 273, 97, 12, 6.6, and 0.57.

In Cases 3 and 4 we assume that the porosity and absolute permeability are known and the parameters in the relative permeability functions of Eqs. 5.39 and 5.40 are to be estimated. We consider in Case 3 the estimation of all four parameters, a_o, a_w, b_o, and b_w. In Case 4 we assume a_o and a_w are known and attempt to estimate the exponents b_o and b_w.

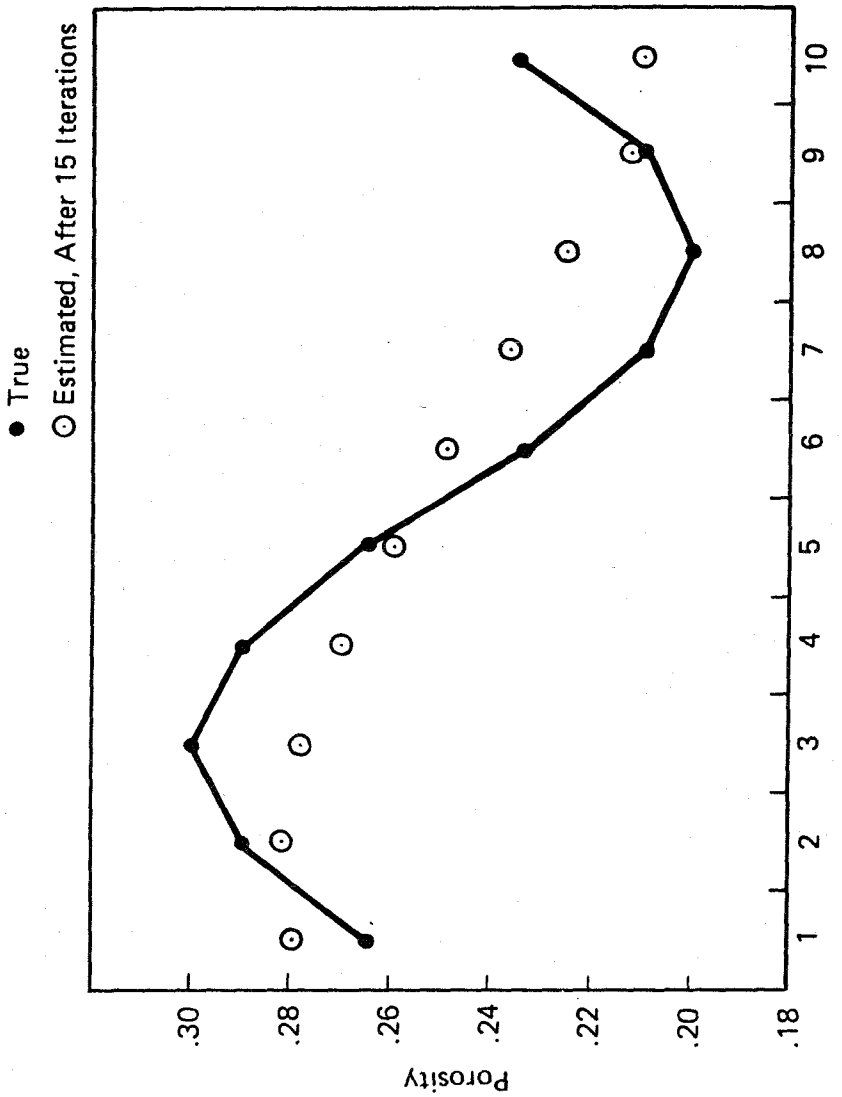

Figure 6.2

Estimation of Porosity, 1–D Model,
With Initial Guess $\phi = .18$

In Case 3 the true values of a_o and a_w are 1, and the true values of b_o and b_w are 2 and 3, respectively. An initial guess of 1 is used for all the parameters. The iterative estimates for this case are shown in Fig. 6.3. While the parameter estimates do converge to the true values, the rate of convergence is slow particularly for parameters a_w and b_w. The values of the objective function for different numbers of iterations is shown in Table 6.3.

A qualitative understanding of this case can be obtained by first examining the relative permeability functions given by Eqs. 5.39 and 5.40 with ε set to zero. The endpoints of the relative permeability curves are given by

$$k_{ro}(S_c) = a_o \tag{6.3}$$

$$k_{rw}(1-S_{ro}) = a_w \tag{6.4}$$

Thus, if the relative permeabilities are known at the endpoints, the two curves are completely specified by b_o and b_w.

For this case, the endpoints are not specified. The initial guess for the relative permeabilities correspond to straight line functions. With the exceptions of $k_{ro}(S_c)$ and $k_{rw}(1-S_{ro})$, the true values of the relative permeability curves are less than those represented by the straight lines. Convergence towards the true curves is accomplished by either decreasing the coefficients a_o and a_w or increasing the exponents b_o and b_w. Note from Fig. 6.3 that in the early iterations, both a_o and a_w have decreased, even though the initial guesses for a_o and a_w were the true values. Note also that the values for J_p and J_R shown in Table 6.3 have, in fact, been reduced. Consequently, the pairs of parameters a_o, b_o and a_w, b_w appear to be correlated.

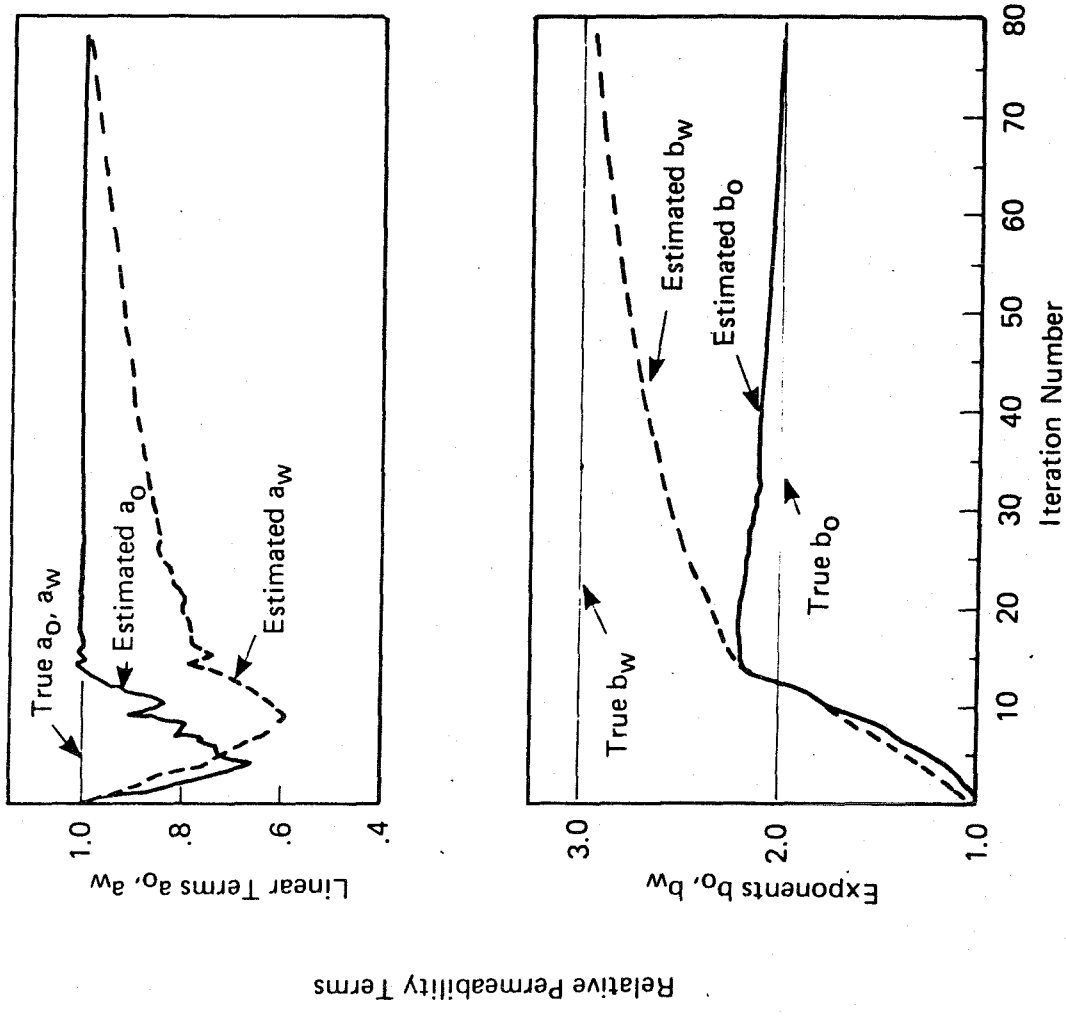

Figure 6.3

Estimation of Relative Permeabilities, 1–D Model

The fact that the estimates of the oil relative permeability parameters converge to their true values before those for the water relative permeability can be reasoned by investigating the effect that the end point values $k_{ro}(S_c)$ and $k_{rw}(1-S_{ro})$ have on the pressure and saturation solutions for the reservoir model. For the incompressible case, it was shown in Subsection 5.3.1 that the pressure drop solution before water breakthrough does depend upon the value of $k_{ro}(S_c)$. However, the reservoir saturations must reach the residual oil saturation before $k_{rw}(1-S_{ro})$ will have an effect on the solution.

In Fig. 6.3 we note that after 15 iterations, the estimates for a_o are its correct value. Thus, although the pairs of parameters values in Eqs. 5.39 and 5.40 are correlated, the additional information about a_o which is obtained from the dependence of the observed data upon the endpoint permeability of oil appears to significantly improve the estimation of oil permeability parameters.

In Case 4, the values a_o and a_w are specified. Fig. 6.4 shows the parameter estimates as a function of iteration for Case 4. Convergence is seen to be much faster than in Case 3. After 11 iterations both parameters are within five percent of the true values and J_p and J_R are both less than one. Thus, specification of the endpoints of the relative permeability curves markedly increases the rate of convergence. Since good estimates for the relative permeability endpoints may often be obtained from core flood data, it appears most advantageous to determine the coefficients a_o and a_w separately and estimate only the exponents b_o and b_w.

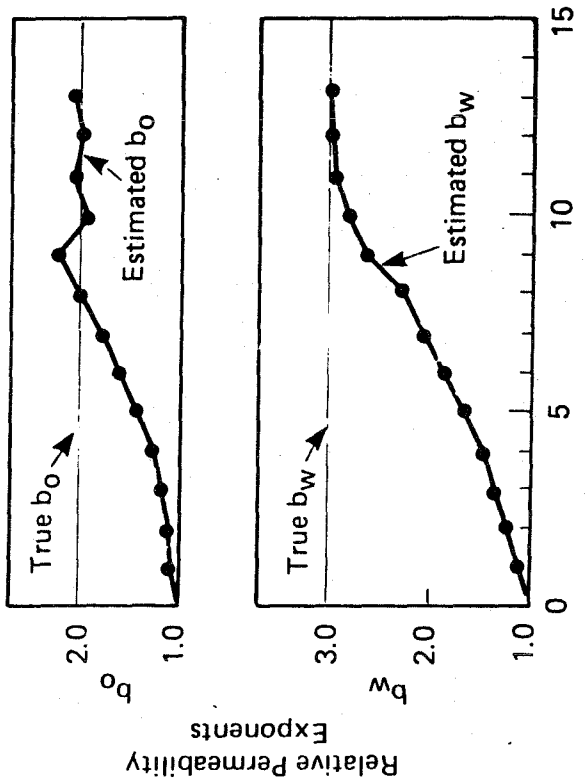

Figure 6.4

Estimation of Relative Permeabilities, 1–D Model

In Case 5, the porosity and absolute and relative permeabilities are to be estimated. Here the porosity and absolute permeabilities are represented by a single zone. The parameters to be estimated are thus the single value of porosity and permeability, and the relative permeability exponents b_o and b_w. The iterative estimates for this case are shown in Fig. 6.5. While some parameter values converge to the true values before others, all the parameter estimates are within 5% of the true values after 20 iterations. This test case demonstrates that porosity, permeability, and relative permeabilities can be jointly estimated.

6.2.2 Two-Dimensional Water Flood

Three cases based on the water flooding of a hypothetical quarter of a five-spot are presented here. The properties used for these three cases are summarized in Table 6.1. In Case 6, the parameters to be estimated are the relative permeability exponents b_o and b_w. In Case 7, we estimate the porosity and absolute and relative permeabilities. The porosity and absolute permeability are represented by a single zone. For these cases, the observed data correspond to the pressures at the injection and production grid blocks and the water-oil ratio at the production grid block for each step in the simulation. The final case presented is similar to Case 7, with the exception that the observed data have been corrupted with Gaussian error.

The iterative estimates for Cases 6 and 7 are shown in Figs. 6.6 and 6.7, and the quantities J_p and J_R for several iterations are given in Table 6.3. For both problems, the parameter estimates converge to the true values. The

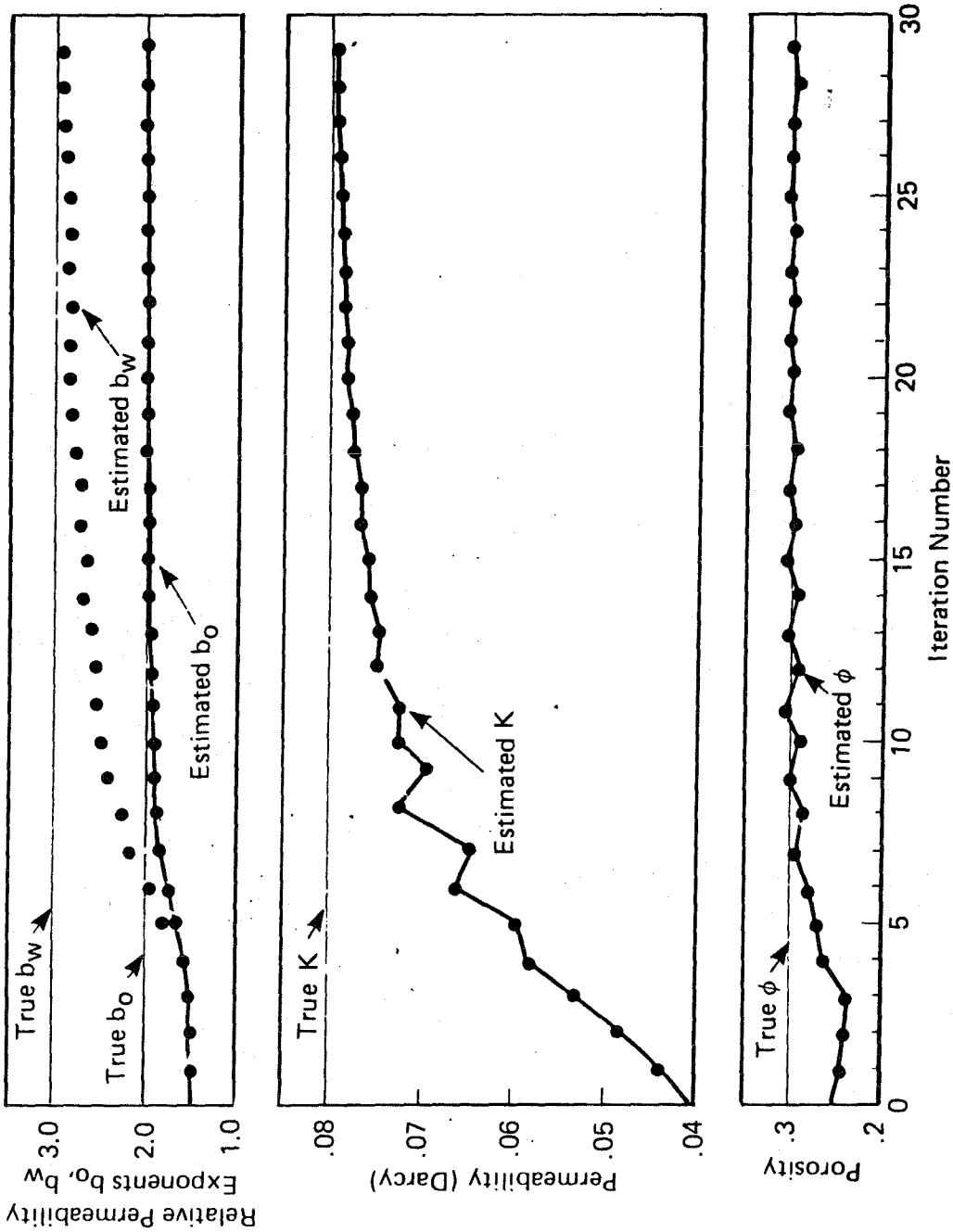

Figure 6.5

Estimation of Porosity and Absolute and Relative Permeabilities, 1–D Model

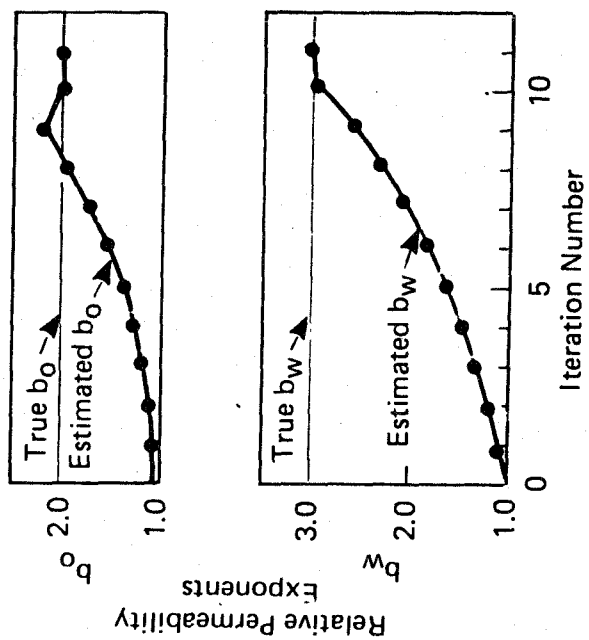

Figure 6.6

Estimation of Relative Permeabilities, 2–D Model

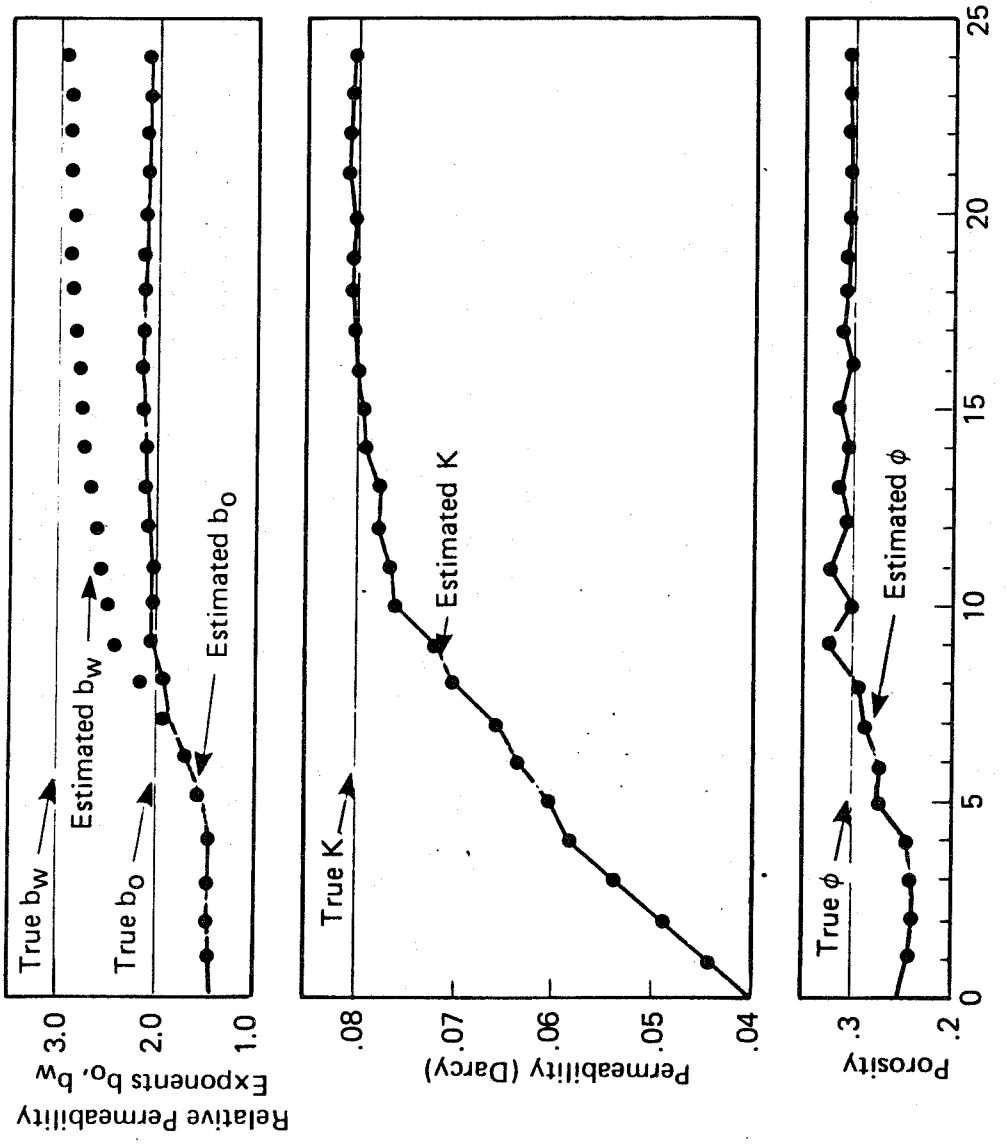

Figure 6.7

Estimation of Porosity and Absolute and Relative Permeabilities, 2–D Model

number of iterations required in each case is about the same as for the corresponding one-dimensional problems. This suggests that an additional space dimension does not change the characteristics of the estimation problem.

In Case 8, the observed data correspond to the simulated data to which a random error term have been added. The error was obtained by a Gaussian random number generator with mean zero and specified standard deviations. The standard deviation used for the pressure and water-oil ratio measurements was one atmosphere and 0.5, respectively. The weighting factor ω used in this case was 4, which is equal to the ratio of the variances of the pressure and water-oil ratio. The parameter estimates for several iterations are given in Table 6.4, and the corresponding values of J_p and J_R are given in Table 6.3. Comparison of the iterative parameter estimates for Cases 7 and 8 shows no significant differences. After 20 iterations, all estimated values are within 10% of the true values. The introduction of Gaussian error to this problem has not affected the performance of the algorithm.

6.3 Summary and Conclusions

An automatic history matching algorithm based on an optimal control approach has been developed to estimate porosity, permeability, and saturation-dependent relative permeability curves in two-phase reservoirs. Both pressure and water-oil ratio data are used in the objective function. The algorithm was tested for one- and two-dimensional hypothetical reservoirs.

When the relative permeabilities are expressed as exponential functions, the exponents can be determined readily if the endpoints of the

Table 6.4. Parameter Estimates for Case 8

Parameter	Iteration Number 0	5	10	15	20	40	60
K (Darcy)	0.04	0.063	0.075	0.081	0.081	0.081	0.081
ϕ	0.25	0.29	0.33	0.32	0.32	0.31	0.31
b_o	1.5	1.6	2.2	2.2	2.2	2.1	2.1
b_w	1.5	1.5	2.4	2.6	2.7	2.8	2.9

relative permeability curves are specified. If the endpoints of the relative permeability curves are not specified, the coefficients and exponents of the functional forms can be determined, but convergence is slow.

The algorithm works well for the cases in which the permeability, porosity, and relative permeability exponents are determined simultaneously. The spatially varying properties were represented by single zones in these cases.

There were no significant differences in performance for one- and two-dimensional cases in which the same parameters are estimated. Small measurement errors did not cause any significant differences in the convergence of the estimates.

7. CONCLUSIONS

In this dissertation several new results have been obtained pertaining to the estimation of petroleum reservoir properties.

For one-dimensional, incompressible flow of oil and water, analytical solutions for the pressure and saturation can be obtained. The saturation solutions consists of the well-known Buckley-Leverett equation.[6] Chapter 3 contains a comprehensive review of the solution of the saturation equation for homogeneous reservoir models by the method of characteristics.[1,6-9] These techniques are then extended to heterogeneous models. When the initial water saturation is the connate water saturation, it is shown that the Welge technique[7] for the determination of the saturation discontinuity also applies to the heterogeneous reservoir model.

Before water breakthrough, the pressure drop solution across the one-dimensional reservoir is linear with respect to time for a constant, specified injection rate and homogeneous reservoir properties. When the reservoir properties vary spatially, the pressure solution is nonlinear. The spatially varying permeability at locations behind the saturation front has an effect on the pressure drop solution, while only an integral (the harmonic average) of the permeability corresponding to the locations ahead of the saturation front affects the pressure drop. The saturation solution is independent of the spatially varying permeability, and hence observations of the fractional flow rate at the producing location give no information about that property. The identifiability of the spatially varying permeability based on the pressure drop solution for the range of time up to the breakthrough time is established in Chapter 5. The spatially varying

porosity at locations behind the saturation front has an effect on both the pressure and saturation solutions. The information that can be obtained about the porosity from observations of the fractional flow rate at the producing location depends upon the initial saturation profile. In Chapter 5 it is shown that only the average value can be obtained when the initial saturation is the connate water saturation. The spatially varying porosity for portions of the reservoir may be identifiable when the initial saturation profile varies with location in the reservoir. The identifiability of the spatially varying porosity on the basis of the pressure drop solution is established for the moving boundary problem.

The identifiability of the relative permeabilities is investigated in Chapter 5. It is shown that the value of $k_{ro}(S_c)$, and an integral of the relative permeabilities for water saturations greater than the value at the saturation discontinuity S_d, is identifiable from pressure drop data taken before the time of water breakthrough. The relative permeabilities for the range of water saturation $S_d \leq S \leq S_f$, where S_f corresponds to the saturation at the producing location at the final time for which pressure drop and fractional flow rate data are taken, are identifiable. Only an integral value of the relative permeabilities for water saturations greater than S_f is identifiable.

In Chapter 6, an algorithm is developed for the estimation of properties based on a two-phase, compressible reservoir model. The objective function, composed of a weighted sum of the squares of the differences between the observed and calculated values of the pressure and water-oil ratio, is minimized by the method of steepest descent. An optimal control approach is used to calculate the gradient of the objective function.

The algorithm is tested for one- and two-dimensional hypothetical water floods. When the relative permeabilities are expressed as exponential functions, the coefficients and exponents of the functional forms can be determined, but convergence is slow. The exponents can be determined readily when the end points of the relative permeability curves are specified. The algorithm performed well for problems in which the porosity, permeability and relative permeability exponents were estimated simultaneously. The porosity and permeability in these problems were represented by single zones. There were no significant differences in the convergence of the estimates for one- and two-dimensional problems. It is shown that small measurement errors would not affect the convergence of the estimates.

NOMENCLATURE

A	— cross sectional area
a_o, a_w, b_o, b_w	— relative permeability parameters given in Eqs. 5.39 and 5.40
B_o, B_w	— formation volume factors
c_o, c_w, c_r	— compressibilities of oil, water and rock
f, f_w	— fractional flow of water
g, g_w	— function defined by Eq. 4.23
h	— reservoir thickness
J	— objective function
J_P	— sum of squares of the deviations between observed and calculated pressures (atm^2)
J_R	— sum of squares of the deviations between observed and calculated water-oil ratio
K	— permeability
k_{ro}	— relative permeability of oil
k_{rw}	— relative permeability of water
N	— time index corresponding to the final time in the simulation
NX	— number of grid blocks in the x-direction
NY	— number of grid blocks in the y-direction
P	— pressure
P_{in}	— initial pressure
ΔP	— pressure drop across one-dimensional reservoir
ΔP^*	— normalized pressure drop defined by Eq. 3.69
q_o, q_w	— volumetric flow rate/unit volume
Q_o, Q_w	— volumetric flow rate
Q_T	— total volumetric flow rate

Nomenclature (con't)

R — water-oil ratio

S, S_w — saturation of water

S_c — connate water saturation

S_d — upper value of water saturation at discontinuity

S_{in} — initial water saturation

S_L — water saturation at location x_L

t — time

t_B — time of water breakthrough

T — dimensionless time defined by Eq. 3.68

v — volume of grid block (Ch. 4)

v_o, v_w — superficial velocity

v_t — total superficial velocity

x, y — spatial coordinates

x_B — length of reservoir in x-direction

x_d — location of saturation discontinuity

x_L — length of one-dimensional reservoir

$x_0(S)$ — function which is the inverse of $S_{in}(x)$

X — dimensionless distance defined by Eq. 3.67

y_B — length of reservoir in y-direction

WOR — water-oil ratio

γ_i — relative permeability parameter

Γ — refers to all relative permeability parameters considered

λ_1, λ_2 — adjoint variables

μ_o, μ_w — viscosities

ρ_o, ρ_w — densities

Nomenclature (con't)

Operators

δ — variation, or perturbation

$\delta(\cdot \sim \cdot)$ — Dirac delta function

$\delta(\cdot,\cdot)$ — Kronecker delta function

Δ_t — difference operator defined by Eq. 4.10

Δ_x, Δ_y — difference operators defined by Eq. 4.11

REFERENCES

1. Collins, R. E.: Flow of Fluids through Porous Materials, Petroleum Publishing Co., Tulsa (1976).
2. Bear J.: Dynamics of Fluids in Porous Media, American Elsevier Publishing Co., Inc., New York (1972).
3. Peaceman, D. W.: Fundamentals of Numerical Reservoir Simulation, Elsevier Scientific Publishing Co., Amsterdam, Netherlands (1977).
4. Crichlow, H. B.: Modern Reservoir Engineering - A Simulation Approach, Prentice-Hall, Englewood Cliffs, New Jersey (1977).
5. Conversation with P. T. Woo, Chevron Oil Field Research Co., La Habra, Cal.
6. Buckley, S. E. and Leverett, M. C.: "Mechanism of Fluid Displacement in Sands," Trans. AIME (1942) Vol. 146, 139-148.
7. Welge, H. J.: "A Simplified Method for Computing Oil Recovery by Gas and Water Drive," Trans. AIME (1952) Vol. 195, 91-98.
8. Cardwell, Jr., W. T.: "The Meaning of the Triple Value in Noncapillary Buckley-Leverett Theory," Trans. AIME (1959) Vol. 216, 271-176.
9. Sheldon, J. W., Zondek, B. and Cardwell, Jr., W. T.: "One Dimensional, Incompressible, Noncapillary Two-Phase Fluid Flow in a Porous Medium," Trans. AIME (1959) Vol. 216, 290-296.
10. Whitham, G. B.: Linear and Nonlinear Waves, John Wiley and Sons, New York (1974).
11. Muskat, M.: The Flow of Homogeneous Fluids Through Porous Media, J. W. Edwards, Ann Arbor, Michigan (1946).

12. Settari, A. and Aziz, K.: "Treatment of Nonlinear Terms in the Numerical Solution of Partial Differential Equations for Multiphase Flow in Porous Media," Int. J. Multiphase Flow, Vol. 1, 817-844.

13. Thomas, G. W.: Principles of Hydrocarbon Reservoir Simulation, University of Trondheim (1977).

14. Lantz, R. B.: "Quantitative Evaluation of Numerical Diffusion (Truncation Error)," Trans. AIME (1971) Vol. 251, Sect. 2, 315-320.

15. Van den Bosch, B. and Seinfeld, J. H.: "History Matching in Two-Phase Petroleum Reservoirs: Incompressible Flow," Soc. Petrol. Eng. J., (Dec. 1977), 398-406.

16. Johnson, E. F., Bossler, D. P. and Naumann, V. O.: "Calculation of Relative Permeability From Displacement Experiments," Trans. AIME (1959) Vol. 216, 370-372.

17. Beck, J. V. and Arnold, K. J.: Parameter Estimation in Engineering and Science, John Wiley and Sons, New York (1977).

18. Rosenbrock, H. H. and Storey, C.: Computational Techniques for Chemical Engineers, Pergamon Press Ltd, Oxford (1966).

19. Seinfeld, J. H. and Lapidus, L.: Process Modeling, Estimation, and Identification, Prentice-Hall, Englewood Cliffs, New Jersey (1974).

20. Chen, W. H., Gavalas, G. R., Seinfeld, J. H. and Wassermann, M. L.: "A New Algorithm for Automatic History Matching," Soc. Petrol. Eng. J., (Dec. 1974), 593-608.

21. Chavent, G. Dupuy, M. and Lemonnier, P.: "History Matching by Use of Optimal Theory," Soc. Petrol. Eng. J., (Feb. 1975), 74-86.

22. Wasserman, M. L., Emanuel, A. S. and Seinfeld, J. H.: "Practical Applications of Optimal-Control Theory to History-Matching Multiphase Simulator Models," Soc. Petrol. Eng. J., (Aug. 1975), 347-355.

23. Shah, P. C., Gavalas, G. R. and Seinfeld, J. H.: "Error Analysis in History Matching: The Optimum Level of Parameterization," Soc. Petrol. Eng. J., (Jun. 1978), 219-228.

24. Jahns, H.P.: "A Rapid Method for Obtaining a Two-Dimensional Reservoir Description from Well Pressure Response Data," Trans. AIME (1966) Vol. 237, 315-327.

25. Schechter, R. S.: The Variational Method in Engineering, McGraw-Hill, Inc., New York (1967).

APPENDIX A. Solution of Equations for the Incompressible Reservoir Model

A computer code was written in Fortran to solve Eqs. 3.19 and 3.22 with boundary and initial conditions given by Eqs. 3.63 and 3.64. Relative permeabilities were input with the parametrization given by Eqs. 3.65 and 3.66. For each set of relative permeabilities and viscosity ratios used, the upper value of the saturation at the shock, S_d, was determined analytically using Eq. 3.45. The superficial velocity was independent of time. The method of solution after breakthrough was slightly different than that before breakthrough, and both methods will be discussed below.

Solution for $t \leq t_B$

A dimensionless distance X and time T were defined as:

$$X = x/x_L \tag{A.1}$$

$$T = t/t_B \tag{A.2}$$

In terms of these variables, the solution to Eq. 3.22 is:

$$\Phi(x) = \left(\frac{v_t t_B}{x_L}\right) T\, f'(S) \tag{A.3}$$

where

$$\Phi(x) = \int_0^{X(S)} \phi\, dx$$

For $t \leq t_B$, Eq. 3.19 can be written as

$$\Delta P(T) = v_t x_L \left[\mu_w \int_0^{X_d} \frac{f}{k_{rw} K}\, dX + \frac{\mu_o}{k_{ro}(S_c)} \int_{X_d}^{1} \frac{1}{K}\, dX\right] \tag{A.4}$$

The spatial grid was divided into n discrete blocks with length $\Delta X = 1/n$. The absolute permeability and porosity were assigned at points centered within each discrete block, and the permeability and porosity at all locations were then obtained by linear interpolation. To solve Eqs. A.3 and A.4, X, rather than time, was chosen independently. The integrations in those equations were carried out numerically using trapezoids.

The following steps were taken in the solution of Eqs. A.3 and A.4:

1. Using the values $X = 1$, $T = 1$, and $S = S_d$, solve Eq. A.3 for t_B.
2. For $X_d = 0$, $T = 0$, solve Eq. A.4 for $\Delta P(0)$.
3. Set $\ell = 1$.
4. Calculate $(X_d)_\ell = \ell \frac{\Delta X}{2}$.
5. Solve Eq. A.3 for T_ℓ, the time at which the shock is at location $(X_d)_\ell$.
6. Set $m = \ell$.
7. Calculate $X_j = j \frac{(X_d)_\ell}{m}$, $j = 0,1,\ldots, m$.
8. Use Eq. A.3 to calculate $(f'(S))_j$ at the $m + 1$ values of X_j.
9. Invert $(f'(S))_j$ to obtain S_j.
10. Use Eq. A.4 to calcualte $\Delta P(T_\ell)$ (the $m + 1$ values of S_j are used in the evaluation of the first integral in the equation).
11. Set $m = 2m$ and repeat steps 7 - 10.

If the difference between the value of $\Delta P(T_\ell)$ just calculated and the previously calculated value meet some tolerance test, set $\ell = \ell + 1$ and return to step 4 (provided that $\ell \leq 2n$, which is equivalent to $t \leq t_B$). Otherwise, set $m = 2m$, repeat steps 7-10, and check the new tolerance. Continue to double m until the tolerance is met.

Solution for $t > t_B$

There are two differences in the solution for $t > t_B$: (1) the equation for pressure is different from Eq. A.4, and (2) time, rather than X_d, was chosen independently. In terms of the dimensionless distance and time defined by Eqs. A.1 and A.2, Eq. 3.19 for $t > t_B$ can be written as:

$$\Delta P(T) = v_t x_L \mu_w \int_0^1 \frac{f}{k_{rw} K} \, dX \qquad (A.5)$$

Times $t_i > 1$ were chosen for which the solution was desired. For each time T_i the following steps were taken:

1. Set $m = n$.
2. Calculate $X_j = \frac{j}{m}$, $j = 0,1,\ldots,m$.
3. Use Eq. A.3 to calculate $(f'(S))_j$ at the $m+1$ values of X_j.
4. Invert $(f'(S))_j$ to obtain S_j
5. Use Eq. A.5 to calculate $\Delta P(T_i)$.
6. Set $m = 2m$ and repeat steps 2-5. Apply some tolerance test to these two values of $\Delta P(T_i)$. If they do not meet the tolerance, then set $m = 2m$, repeat steps 2-5, and check the new tolerance. Continue doubling m until the tolerance is met.

APPENDIX B. Linear System Used for the Solution of the Compressible Reservoir Model

Here we outline the method used to solve the finite-difference equations for two-phase flow developed in Chapter 4. Writing Eqs. 4.32 and 4.33 for each grid block, a linear system is constructed which can be solved for the pressure and saturation at time t^{n+1} given the solution at time t^n (or initial conditions at time t^0).

The reservoir grid consists of NXY blocks, where NXY is the product of NX and NY, the number of blocks in the x and y directions, respectively (see Fig. 4.1). We use the single index k to refer to the grid block at location i,j, where k is defined as:

$$k = (i-1)NX + j \quad i = 1,\ldots, NX, \quad j = 1,\ldots, NY \qquad (B.1)$$

Using the index k, the finite difference equations given by Eqs. 4.32 and 4.33 can be written as:

$$CB_{k-NX}P_{k-NX}^{n+1} + CB_{k-1}P_{k-1}^{n+1} + CA_kS_k^{n+1} + CB_kP_k^{n+1} + CB_{k+1}P_{k+1}^{n+1} + CB_{k+NX}P_{k+NX}^{n+1} = E_k \qquad (B.2)$$

$$DB_{k-NX}P_{k-NX}^{n+1} + DB_{k-1}P_{k-1}^{n+1} + DA_kS_k^{n+1} + DB_kP_k^{n+1} + DB_{k+1}P_{k+1}^{n+1} + DB_{k+NX}P_{k+NX}^{n+1} = F_k \qquad (B.3)$$

Two letters are used to refer to the coefficients which multiply the unknown terms -- the saturation and pressure at the time level n+1 -- in those equations. The first letter, C or D, refers to Eq. B.2 or B.3, respectively.

The second letter, A or B, refers to the unknown which the coefficient multiplies; A refers to saturation and B refers to pressure.

Using the reflection boundary conditions given by Eqs. 4.15 and 4.16, Eqs. B.2 and B.3 apply for all k, k = 1,..., NXY. These 2NXY equations can be written as:

$$\underset{\sim}{A}\underset{\sim}{u} = \underset{\sim}{b} \tag{B.4}$$

where the solution vector $\underset{\sim}{u}$ is given by:

$$\underset{\sim}{u} = \left[S_1^{n+1} \; P_1^{n+1} \; S_2^{n+1} \; \cdots \; S_k^{n+1} \; P_k^{n+1} \; \cdots \; S_{NXY}^{n+1} \; P_{NXY}^{n+1} \right]^T$$

The (2NXY) x (2NXY) matrix $\underset{\sim}{A}$ can be written as:

$$\underset{\sim}{A} = \begin{bmatrix} \alpha_{1,1} & \alpha_{1,2} & \cdots & \alpha_{1,NXY} \\ \alpha_{2,1} & & & \vdots \\ \vdots & & & \vdots \\ \alpha_{NXY,1} & & & \alpha_{NXY,NXY} \end{bmatrix}$$

where each $\alpha_{k,\ell}$ is a 2x2 matrix defined as:

$$\alpha_{k,\ell} = \begin{bmatrix} CA_k & CB_k \\ DA_k & DB_k \end{bmatrix} \quad \text{for } \ell = k$$

$$= \begin{bmatrix} 0 & CB_\ell \\ 0 & DB_\ell \end{bmatrix} \quad \text{for } \ell = k+1,\ k-1,\ k+NX,\ \text{or } k-NX$$

$$= \begin{bmatrix} 0 & 0 \\ 0 & 0 \end{bmatrix} \quad \text{otherwise}$$

The vector $\underset{\sim}{b}$ can be written as

$$\underset{\sim}{b} = \left[\beta_1\ \beta_2 \cdots\ \beta_{NXY}\right]^T$$

where the β_k are vectors with dimension 2x1 defined as:

$$\beta_k = \begin{bmatrix} E_k \\ F_k \end{bmatrix}$$

Eq. B.4 was solved by a direct method for sparse matrices. The algorithm used was supplied by Chevron Oil Field Research Company.

APPENDIX C. Truncation Error in the Finite-Difference Solution of the Saturation Equation

The truncation error associated with the explicit, backwards difference approximation to Eq. 4.40 is derived. The procedure used in the analysis is outlined by Lantz[14]. The resulting equation from this analysis, Eq. C.9, is also given by Lantz, although the actual derivation is not presented.

Since the term f in Eq. 4.40 is a function of saturation, that equation can be written as

$$\frac{\partial S}{\partial \tau} = - f' \frac{\partial S}{\partial \xi} \tag{C.1}$$

where the prime denotes the derivative with respect to saturation. The standard backwards difference approximation to C.1 is:

$$\frac{S(\tau+\Delta\tau)-S(\tau)}{\Delta\tau} = - f' \frac{[S(\xi)-S(\xi-\Delta\xi)]}{\Delta\xi} \tag{C.2}$$

The following expression for the difference terms in Eq. C.3 can be obtained from Taylor series expansions for $S(\tau+\Delta\tau)$ and $S(\xi-\Delta\xi)$:

$$\frac{S(\tau+\Delta\tau)-S(\tau)}{\Delta\tau} = \frac{\partial S}{\partial \tau} + \frac{\partial^2 S}{\partial \tau^2} \frac{(\Delta\tau)}{2} + O(\Delta\tau)^2 \tag{C.3}$$

$$\frac{S(\xi)-S(\xi-\Delta\xi)}{\Delta\xi} = \frac{\partial S}{\partial \xi} - \frac{\partial^2 S}{\partial \xi^2} \frac{(\Delta S)}{2} + O(\Delta\xi)^2 \tag{C.4}$$

Substituting Eqs. C.3 and C.4 into Eq. C.2 and omitting the second order terms, we obtain the following differential equation:

$$\frac{\partial S}{\partial \tau} = - \frac{\partial^2 S}{\partial \tau^2} \frac{(\Delta\tau)}{2} - f' \left[\frac{\partial S}{\partial \xi} - \frac{\partial^2 S}{\partial \xi^2} \frac{(\Delta\xi)}{2} \right] \tag{C.5}$$

To second order in space and time, Eq. C.5 is the differential equation actually being solved by the finite difference approximation given by Eq. C.2.

This equation can be written in a different form by establishing an equivalence between time and space derivatives. Taking the derivative of Eq. C.1 with respect to time we obtain:

$$\frac{\partial^2 S}{\partial \tau^2} = - f'' \frac{\partial S}{\partial \tau} \frac{\partial S}{\partial \xi} - f' \frac{\partial^2 S}{\partial \xi \partial \tau} \tag{C.6}$$

The derivative of Eq. C.1 with respect to space is:

$$\frac{\partial^2 S}{\partial \tau \partial \xi} = - f'' \left(\frac{\partial S}{\partial \xi} \right)^2 - f' \frac{\partial^2 S}{\partial \xi^2} \tag{C.7}$$

Using Eq. C.7 to eliminate the second derivative of saturation on the right hand side of Eq. C.6, the following is obtained:

$$\frac{\partial^2 S}{\partial \tau^2} = (f')^2 \frac{\partial^2 S}{\partial \xi^2} - f'' \left[\frac{\partial S}{\partial \tau} \frac{\partial S}{\partial \xi} - f' \left(\frac{\partial S}{\partial \xi} \right)^2 \right] \tag{C.8}$$

Using this equation to eliminate the second derivative of saturation with respect to time in Eq. C.5, we obtain:

$$\frac{\partial S}{\partial \tau} = - f' \frac{\partial S}{\partial \xi} + f' \left[\frac{\Delta \xi - f'(\Delta \tau)}{2} \right] \frac{\partial^2 S}{\partial \xi^2} + \frac{\Delta \tau}{2} f'' \left[\frac{\partial S}{\partial \tau} \frac{\partial S}{\partial \xi} - f' \left(\frac{\partial S}{\partial \xi} \right)^2 \right] \tag{C.9}$$

If we assume that the function f is linear, or that the second derivative of f is small, Eq. C.9 can be written as:

$$\frac{\partial S}{\partial \tau} = - f' \frac{\partial S}{\partial \xi} + f' \left[\frac{\Delta \xi - f'(\Delta \tau)}{2} \right] \frac{\partial^2 S}{\partial \xi^2} \tag{C.10}$$

By analogy of this equation with the convection - diffusion equation, the truncation error associated with the finite difference solution of Eq. C.1 is called numerical dispersion, and the term which multiplies the second derivative in Eq. C.10 is known as the numerical dispersion coefficient.

APPENDIX D. Formulation of Algorithm to Estimate Permeability for Incompressible Reservoir Model

Using the analytical formulation developed in Chapter 3 for the two-phase flow problem, a system is formulated here to estimate the absolute permeability from measurements of the pressure drop, assuming that the porosity and relative permeabilities are known. This system is based upon the Ritz method.[25]

Given q measurements of the pressure drop at times t_ℓ, a performance index J can be defined as:

$$J = \sum_{\ell=1}^{q} W_\ell \left[\Delta P^o(t_\ell) - \Delta P^c(t_\ell)\right]^2 \qquad (D.1)$$

where the superscript o refers to the observed (or measured) pressure drop at time t_ℓ, W_ℓ is a weighting coefficient associated with that measurement, and the superscript c refers to the calculated pressure drop. The pressure drop is calculated from Eq. 3.19 evaluated at time t_ℓ:

$$\Delta P(t_\ell) = v_t \mu_w \int_0^{x_L} g(t_\ell) u \, dx \qquad (D.2)$$

where $g = f/k_{rw}$ and $u = 1/K$. Eq. 5.2 must be solved to determine $g(t_\ell)$ as a function of x.

The estimation problem is to choose the absolute permeability (or alternatively the conductivity u) so that J is minimized. We will assume that the conductivity can be approximated as the following sum of specified functions $\Phi_i(x)$

$$u(x) = \sum_{i=1}^{n} c_i \Phi_i(x) \qquad (D.3)$$

where the c_i are constants which are to be determined. The necessary conditions for the minimization of Eq. D.1 are:

$$\frac{\partial J}{\partial c_i} = 0 \qquad i = 1,\ldots, n \tag{D.4}$$

These n equations can be written as the following matrix equation:

$$\underset{\sim}{A}\underset{\sim}{c} = \underset{\sim}{b} \tag{D.5}$$

where $\underset{\sim}{c} = [c_1\ c_2 \ldots\ c_n]^T$, the $\underline{i}$th element of $\underset{\sim}{b}$ is

$$b(i) = \frac{1}{v_t \mu_w} \sum_{\ell=1}^{q} W_\ell \Delta P^o(t_\ell) \int_0^{x_L} g(t_\ell)\Phi_i \, dx$$

and the i,j element of the nxn matrix A is:

$$A(i,j) = \sum_{\ell=1}^{q} W_\ell \int_0^{x_L} (t_\ell)\Phi_i \, dx \int_0^{x_L} g(t_\ell)\Phi_i \, dx$$

The matrix $\underset{\sim}{A}$ is symmetric. If that matrix is nonsingular, Eq. D.5 can be solved for the unknown constant c_i.

APPENDIX E. Determination of Relative Permeabilities by the JBM Method

The method of Johnson et al[16] to determine relative permeabilities of oil and water from laboratory water floods on reservoir cores has become a standard technique used by the production industry. Their derivation is somewhat difficult to follow since much of the nomenclature and derivation is contained within a paper by Welge[7]. Also, some of the assumptions, as well as the conclusion that the relative permeabilities for a certain range of saturations are not determinable by this method, are not stated. Here we have augmented, and attempted to clarify, the derivation by Johnson et al.[16]

It is assumed that the one-dimensional, analytical solution developed in Chapter 3 can be used to describe the water flood. The initial saturation of the core is the connate water saturation, S_c. Water is injected at x=0, and fluids are produced at $x=x_L$. It is further assumed that:

1. The core is homogeneous
2. ϕ, x, μ_o, μ_w, and K are known, and $k_{ro}(S_c)$ is taken to be 1.

The following equations can then be used to describe the water flood:

$$\Delta P(t) = v_t \frac{\mu_w}{K} \int_0^{x_L} \frac{f}{k_{rw}}\, dx \tag{E.1}$$

$$\left.\frac{dx}{dt}\right|_S = \frac{v_t}{\phi} f'(S) \tag{E.2}$$

$$f = \left(1 + \frac{\mu_w k_{ro}}{\mu_o k_{rw}}\right)^{-1} \tag{E.3}$$

The following data are taken during the water flood:

i) $\Delta P(t)$ for $t \geq t_B$

ii) The cumulative effluent $V_t(t) = \int_0^t v_t \, dt$

iii) The volumetric fraction of each phase in the cumulative effluent as a function of time.

The volume of oil produced V_o can be calculated using ii) and iii). Then, using a mass balance, the average saturation S_{av} can be calculated:

$$S_{av} = \frac{\phi x_L (1-S_c) - V_o(t)}{\phi x_L} \tag{E.4}$$

Integrating Eq. E.2, we obtain:

$$x\Big|_S = \frac{V_t}{\phi} f'(S) \tag{E.5}$$

From this equation we obtain the following expression for the saturation at the production end, S_L, at time $t \geq t_B$:

$$x_L = \frac{V_t}{\phi} f'(S_L) \tag{E.6}$$

The cumulative effluent in pore volumes, W(t), is:

$$W(t) = \frac{V_t(t)}{\phi x_L} = \frac{1}{f'(S_L)} \tag{E.7}$$

The average saturation in the reservoir is:

$$S_{av} = \frac{\int_0^{x_L} S \, dx}{x_L} \tag{E.8}$$

Using the following expression obtained from Eq. E.2:

$$dx = \frac{V_t}{\phi} df' \tag{E.9}$$

the integral in Eq. E.8 can be written as:

$$\int_0^{x_L} S\, dx = \frac{V_t}{\phi} \int_{1-S_{ro}}^{S_L} S\, df' \tag{E.10}$$

This can be integrated by parts to obtain:

$$\int_0^{x_L} S\, dx = \frac{V_t}{\phi} \left[S_L f'(S_L) - f(S_L) + 1\right] \tag{E.11}$$

where $f'(1-S_{ro})$ and $f(1-S_{ro})$ are evaluated as 0 and 1, respectively. Substituting Eq. E.11 into Eq. E.8 we obtain the following expression for S_{av}:

$$S_{av} = \frac{V_t}{\phi x_L} \left[S_L f'(S_L) - f(S_L) + 1\right] \tag{E.12}$$

Using Eq. E.6 to eliminate the term $V_t/\phi x_L$, the following is obtained:

$$S_{av} = S_L + \frac{[1-f(S_L)]}{f'(S_L)} \tag{E.13}$$

The following expression is obtained by taking the derivative of Eq. E.13 with respect to W(t) and rearranging:

$$f(S_L) = 1 - \frac{dS_{av}}{dW} \tag{E.14}$$

The following can then be calculated for any time $t \geq t_B$:

1. $f(S_L)$ using Eq. E.14
2. $f'(S_c)$ using Eq. E.7
3. S_L using Eq. E.13.

Using Eq. E.9, the pressure equation E.1 can be written for $t \geq t_B$ as:

$$\frac{\Delta P(t)}{v_t} = \frac{\mu_w}{K} \frac{V_t}{\phi} \int_0^{x_L} \frac{f}{k_{rw}} df' \tag{E.15}$$

Define I_r as

$$I_r = \frac{\Delta P(0)/v_t(0)}{\Delta P(t)/v_t(t)} \tag{E.16}$$

The numerator in Eq. E.16 is obtained from Eq. E.1 as:

$$\frac{\Delta P(0)}{v_t(0)} = \frac{\mu_o}{K} x_L \tag{E.17}$$

The following can be obtained using Eqs. E.15-17 and Eq. E.7:

$$\frac{1}{W(t) I_r} = \frac{\mu_w}{\mu_o} \int_0^{x_L} \frac{f}{k_{rw}} df' \tag{E.18}$$

Taking the derivative of Eq. E.18 with respect to 1/W(t), we obtain:

$$\frac{d(1/WI_r)}{d(1/W)} = \frac{\mu_w}{\mu_o} \frac{f(S_L)}{k_{rw}(S_L)} \tag{E.19}$$

The relative permeability of water can be determined from this equation since $f(S_L)$ and S_L have been determined independently by Eqs. E.14 and E.13. Then $k_{ro}(S_L)$ can be calculated from the following expression obtained from Eq. E.3:

$$k_{rw}(S_L) = \frac{\mu_w}{\mu_o} k_{ro}(S_L) \frac{f(S_L)}{1-f(S_L)} \tag{E.20}$$

The relative permeabilities can thus be determined for the range of saturation which are at the production location. The relative permeabilities for $S \leq S_d$ are not determinable.

APPENDIX F. Derivatives of the Objective Function with Respect to the Reservoir Parameters - Derivation for Partial Differential Equation Model

In this appendix we derive expressions for the derivatives of the objective function with respect to the reservoir properties based on the formulation of the state equations as partial differential equations. The state equations are given by Eqs. 4.1 and 4.2. Before proceeding, we make the following changes in those equations: (1) Eq. 2.16 is used to eliminate S_o, (2) S is used to refer to the water saturation, (3) the flow rate of water at well m, q_{w_m}, is given by the product of the total flow rate q_m and the fractional flow f, and (4) the flow rate of oil at well m is given by $q_{o_m} = q_m(1-f)$. With these changes, the state equations are:

$$\frac{\partial(\phi\rho_w S)}{\partial t} = \frac{\partial}{\partial x}\left[\frac{K_x\rho_w}{\mu_w} k_{rw} \frac{\partial P}{\partial x}\right] + \frac{\partial}{\partial y}\left[\frac{K_y\rho_w}{\mu_w} k_{rw} \frac{\partial P}{\partial y}\right] + \sum_m q_m f \, \delta(x-x_m)\delta(y-y_m) \tag{F.1}$$

$$\frac{\partial[\phi\rho_o(1-S)]}{\partial t} = \frac{\partial}{\partial x}\left[\frac{K_x\rho_o}{\mu_o} k_{ro} \frac{\partial P}{\partial x}\right] + \frac{\partial}{\partial y}\left[\frac{K_y\rho_o}{\mu_o} k_{ro} \frac{\partial P}{\partial y}\right] + \sum_m q_m(1-f)\delta(x-x_m)\delta(y-y_m) \tag{F.2}$$

The boundary and initial conditions (see Eqs. 4.3, 4.4, 2.18, and 2.19) are:

$$\frac{\partial P}{\partial x} = 0, \; x = 0, \; x_B \tag{F.3}$$

$$\frac{\partial P}{\partial y} = 0, \; y = 0, \; y_B \tag{F.4}$$

$$P(t=0) = P_{in} \tag{F.5}$$

$$S(t=0) = S_{in} \tag{F.6}$$

The objective function given by Eq. 6.2 can be written as the following integral:

$$J = \int_0^T \int_0^{y_B} \int_0^{x_B} \left\{ \sum_\xi \sum_\theta \sum_\tau \left[P^{obs}(x_\xi, y_\theta, t_\tau) - P(x_\xi, y_\theta, t_\tau) \right]^2 \delta(x-x_\xi)\delta(y-y_\theta)\delta(t-t_\tau) \right.$$

$$\left. + \sum_\beta \sum_\nu \sum_\eta \omega \left[R^{obs}(x_\beta, y_\nu, t_\eta) - R(x_\beta, y_\nu, t_\eta) \right]^2 \delta(x-x_\beta)\delta(y-y_\nu)\delta(t-t_\eta) \right\} dxdydt \tag{F.7}$$

The subscripted values of x, y, and t refer to the location and time of each observation.

Using an optimal control formulation, the problem is stated as follows: choose the reservoir parameters (or control variables) so that Eq. F.7 is minimized, subject to constraints F.1-6. The derivatives of the objective function are derived using a variational approach.

Estimation of the Absolute Permeability

Here, we specify that the quantity to be estimated is the spatially varying permeability. Our objective is to relate perturbations in K_x, δK_x, and K_y, δK_y, to a variation in J, δJ. First, we consider perturbations, which are functions of the location (x,y), about some nominal, or specified, values $\bar{K}_x$ and $\bar{K}_y$:

$$K_x = \bar{K}_x + \delta K_x \tag{F.8}$$

$$K_y = \bar{K}_y + \delta K_y \tag{F.9}$$

We then relate these perturbations to variations in the state variables P and S through Eqs. F.1 and F.2. The perturbation equations are

$$\frac{\partial[\phi\rho_w(\bar{S}+\delta S)]}{\partial t} = \frac{\partial}{\partial x}\left[\frac{(\bar{K}_x+\delta K_x)}{\mu_w}\rho_w(\bar{k}_{rw}+\delta k_{rw})\frac{\partial(\bar{P}+\delta P)}{\partial x}\right]$$

$$+\frac{\partial}{\partial y}\left[\frac{(\bar{K}_y+\delta K_y)}{\mu_w}\rho_w(\bar{k}_{rw}+\delta k_{rw})\frac{\partial(\bar{P}+\delta P)}{\partial y}\right]$$

$$+\sum_m q_m(\bar{f}+\delta f)\delta(x-x_m)\delta(y-y_m) \qquad (F.10)$$

$$\frac{\partial[\phi\rho_o(1-\bar{S}-\delta S)]}{\partial t} = \frac{\partial}{\partial x}\left[\frac{(\bar{K}_x+\delta K_x)}{\mu_o}\rho_o(\bar{k}_{ro}+\delta k_{ro})\frac{\partial(\bar{P}+\delta P)}{\partial x}\right]$$

$$+\frac{\partial}{\partial y}\left[\frac{(\bar{K}_y+\delta K_y)}{\mu_o}\rho_o(\bar{k}_{ro}+\delta k_{ro})\frac{\partial(\bar{P}+\delta P)}{\partial y}\right]$$

$$+\sum_m q_m(1-\bar{f}-\delta f)\delta(x-x_m)\delta(y-y_m) \qquad (F.11)$$

To first order, the variations of the nonlinear functions of saturation are related to variations in the saturation by:

$$\delta k_{rw} = k'_{rw}\delta S \qquad (F.12)$$

$$\delta k_{ro} = k'_{ro}\delta S \qquad (F.13)$$

$$\delta f = f'\delta S \qquad (F.14)$$

where the primes denote the derivative with respect to saturation. The first order variational equations are given by:

$$\frac{\partial(\phi\rho_w\delta S)}{\partial t} = \frac{\partial}{\partial x}\left[\frac{\rho_w k_{rw}}{\mu_w}\left(K_x\frac{\partial\delta P}{\partial x} + \delta K_x\frac{\partial P}{\partial x}\right)\right.$$

$$\left. + \frac{\rho_w k'_{rw}}{\mu_w} K_x\frac{\partial P}{\partial x}\delta S\right]$$

$$+ \frac{\partial}{\partial y}\left[\frac{\rho_w k_{rw}}{\mu_o}\left(K_y\frac{\partial\delta P}{\partial y} + \delta K_y\frac{\partial P}{\partial y}\right)\right.$$

$$\left. + \frac{\rho_w k'_{rw}}{\mu_w} K_y\frac{\partial P}{\partial y}\delta S\right]$$

$$+\sum_m q_m\, f'\delta S\delta(x-x_m)\delta(y-y_m) \qquad \text{(F.15)}$$

$$-\frac{\partial(\phi\rho_o\delta S)}{\partial t} = \frac{\partial}{\partial x}\left[\frac{\rho_o k_{ro}}{\mu_o}\left(K_x\frac{\partial\delta P}{\partial x} + \delta K_x\frac{\partial P}{\partial x}\right)\right.$$

$$\left. + \frac{\rho_o k'_{ro}}{\mu_o} K_x\frac{\partial P}{\partial x}\delta S\right]$$

$$+ \frac{\partial}{\partial y}\left[\frac{\rho_o k_{ro}}{\mu_o}\left(K_y\frac{\partial\delta P}{\partial y} + \delta K_y\frac{\partial P}{\partial y}\right)\right.$$

$$\left. + \frac{\rho_o k'_{ro}}{\mu_o} K_y\frac{\partial P}{\partial y}\delta S\right] - \sum_m q_m\, f'\delta S\delta(x-x_m)\delta(y-y_m) \qquad \text{(F.16)}$$

For convenience we have omitted the bars used in Eqs. F.10 and F.11.

To simplify notation, we introduce the following variables:

$$d_w = \phi\rho_w \qquad d_o = \phi\rho_o$$

$$D_w = \frac{\rho_w k_{rw}}{\mu_w} \qquad D_o = \frac{\rho_o k_{ro}}{\mu_o}$$

$$C_w = \frac{\rho_w k'_{rw}}{\mu_w} \qquad C_o = \frac{\rho_o k'_{ro}}{\mu_o}$$

$$h_m = f' q_m$$

We now multiply Eqs. F.15 and F.16 by adjoint variables λ_1 and λ_2, respectively. The left hand side of Eq. F.15 can be written as:

$$\lambda_1 \frac{\partial(d_w \delta S)}{\partial t} = \frac{\partial(\lambda_1 d_w \delta S)}{\partial t} - d_w \delta S \frac{\partial \lambda_1}{\partial t} \tag{F.17}$$

Similarly, the left hand side of Eq. F.16 can be written as

$$- \lambda_2 \frac{\partial(d_o \delta S)}{\partial t} = - \frac{\partial(\lambda_2 d_o \delta S)}{\partial t} + d_o \delta S \frac{\partial \lambda_2}{\partial t} \tag{F.18}$$

We now develop an identity for the first term on the right hand side of Eq. F.15. That term is:

$$\lambda_1 \frac{\partial}{\partial x} \left[D_w \left(K_x \frac{\partial \delta P}{\partial x} + \delta K_x \frac{\partial P}{\partial x} \right) + C_w K_x \frac{\partial P}{\partial x} \delta S \right]$$

$$= \lambda_1 \frac{\partial}{\partial x} \left(D_w K_x \frac{\partial \delta P}{\partial x} \right) + \lambda_1 \frac{\partial}{\partial x} \left(D_w \delta K_x \frac{\partial P}{\partial x} \right) + \lambda_1 \frac{\partial}{\partial x} \left(C_w K_x \frac{\partial P}{\partial x} \delta S \right) \tag{F.19}$$

The first term on the right hand side of Eq. F.19 can be written as:

$$\lambda_1 \frac{\partial}{\partial x} \left(D_w K_x \frac{\partial \delta P}{\partial x} \right) = \frac{\partial}{\partial x} \left(\lambda_1 D_w K_x \frac{\partial \delta P}{\partial x} \right)$$

$$- \frac{\partial}{\partial x} \left(D_w K_x \delta P \frac{\partial \lambda_1}{\partial x} \right) + \delta P \frac{\partial}{\partial x} \left(D_w K_x \frac{\partial \lambda_1}{\partial x} \right) \tag{F.20}$$

The following identities can be written for the second and third terms in Eq. F.19:

$$\lambda_1 \frac{\partial}{\partial x}\left(D_w \delta K_y \frac{\partial P}{\partial x}\right) = \frac{\partial}{\partial x}\left(\lambda_1 D_w \delta K_x \frac{\partial P}{\partial x}\right)$$

$$- D_w \frac{\partial P}{\partial x}\frac{\partial \lambda_1}{\partial x}\delta K_x \qquad \text{(F.21)}$$

$$\lambda_1 \frac{\partial}{\partial x}\left(C_w K_x \frac{\partial P}{\partial x}\delta S\right) = \frac{\partial}{\partial x}\left(\lambda_1 C_w K_x \frac{\partial P}{\partial x}\delta S\right)$$

$$- C_w K_x \frac{\partial P}{\partial x}\frac{\partial \lambda_1}{\partial x}\delta S \qquad \text{(F.22)}$$

The second term on the right hand side of Eq. F.15 can be written in a form analogous to Eqs. F.20-22, as can the first and second terms on the right hand side of Eq. F.16.

Combining Eqs. F.15 and F.16, using the identities specified by Eqs. F.17-22, the following equation can be obtained:

$$\frac{\partial(\lambda_1 d_w \delta S)}{\partial t} - \frac{\partial(\lambda_2 d_o \delta S)}{\partial t} = \left[d_w \frac{\partial \lambda_1}{\partial t} - d_o \frac{\partial \lambda_2}{\partial t}\right.$$

$$+ \sum_m h_m(\lambda_1 - \lambda_2)\delta(x-x_m)(y-y_m) - C_w K_x \frac{\partial P}{\partial x}\frac{\partial \lambda_1}{\partial x}$$

$$- C_w K_y \frac{\partial P}{\partial y}\frac{\partial \lambda_1}{\partial y} - C_o K_x \frac{\partial P}{\partial x}\frac{\partial \lambda_2}{\partial x}$$

$$\left. - C_o K_y \frac{\partial P}{\partial y}\frac{\partial \lambda_2}{\partial y}\right]\delta S + \left[\frac{\partial}{\partial x}\left(D_w K_x \frac{\partial \lambda_1}{\partial x} + D_o K_x \frac{\partial \lambda_2}{\partial x}\right)\right.$$

$$\left. + \frac{\partial}{\partial y}\left(D_w K_y \frac{\partial \lambda_1}{\partial y} + D_o K_y \frac{\partial \lambda_2}{\partial y}\right)\right] \delta P$$

$$+ \frac{\partial}{\partial x}\left(\lambda_1 D_w K_x \frac{\partial \delta P}{\partial x} - D_w K_x \delta_P \frac{\partial \lambda_1}{\partial x}\right.$$

$$+ \lambda_1 D_w \delta K_x \frac{\partial P}{\partial x} + \lambda_1 C_w K_x \frac{\partial P}{\partial x}\delta S$$

$$+ \lambda_2 D_o K_x \frac{\partial \delta P}{\partial x} - D_o K_x \delta P \frac{\partial \lambda_2}{\partial x}$$

$$+ \lambda_2 D_o \delta K_x \frac{\partial P}{\partial x} + \lambda_2 C_o K_x \frac{\partial P}{\partial x} \delta S \Bigg)$$

$$+ \frac{\partial}{\partial y} \Bigg(\lambda_1 D_w K_y \frac{\partial \delta P}{\partial y} - D_w K_y \delta P \frac{\partial \lambda_1}{\partial y}$$

$$+ \lambda_1 D_w \delta K_y \frac{\partial P}{\partial y} + \lambda_1 C_w K_y \frac{\partial P}{\partial y} \delta S$$

$$+ \lambda_2 D_o K_y \frac{\partial \delta P}{\partial y} - D_o K_y \delta P \frac{\partial \lambda_2}{y}$$

$$+ \lambda_2 D_o \delta K_y \frac{\partial P}{\partial y} + \lambda_2 C_o K_y \frac{\partial P}{\partial y} \delta S \Bigg)$$

$$- \left(D_w \frac{\partial P}{\partial x} \frac{\partial \lambda_1}{\partial x} + D_o \frac{\partial P}{\partial x} \frac{\partial \lambda_2}{\partial x} \right) \delta K_x$$

$$- \left(D_w \frac{\partial P}{\partial y} \frac{\partial \lambda_1}{\partial y} + D_o \frac{\partial P}{\partial y} \frac{\partial \lambda_2}{\partial y} \right) \delta K_y \qquad \text{(F.23)}$$

Note that certain terms can be omitted by use of the boundary conditions given by Eqs. F.3 and F.4.

We now integrate Eq. F.23 over the spatial domain $[0,x_B]$ and $[0,y_B]$, and time domain $[0,T]$. After evaluating the explicit integrations, the following equation is obtained:

$$\int_0^{y_B} \int_0^{x_B} (\lambda_1 d_w \delta S - \lambda_2 d_o \delta S) \Big|_0^T dxdy = \int_0^T \int_0^{x_B} \int_0^{y_B} \Bigg[d_w \frac{\partial \lambda_1}{\partial t} - d_o \frac{\partial \lambda_2}{\partial t}$$

$$+ \sum_m h_m (\lambda_1 - \lambda_2) \delta(x - x_m) \delta(y - y_m) - C_w K_x \frac{\partial P}{\partial x} \frac{\partial \lambda_1}{\partial x} - C_w K_y \frac{\partial P}{\partial y} \frac{\partial \lambda_1}{\partial y}$$

$$- C_o K_x \frac{\partial P}{\partial x} \frac{\partial \lambda_2}{\partial x} - C_o K_y \frac{\partial P}{\partial y} \frac{\partial \lambda_2}{\partial y} \Bigg] \delta S \, dxdydt$$

$$+ \int_0^T \int_0^{y_B} \Bigg[\lambda_1 D_w K_x \frac{\partial \delta P}{\partial x} - D_w K_x \frac{\partial \lambda_1}{\partial x} \delta P + \lambda_1 D_w \frac{\partial P}{\partial x} \delta K_x + \lambda_1 C_w K_x \frac{\partial P}{\partial x} \delta S$$

$$+ \lambda_2 D_o K_x \frac{\partial \delta P}{\partial x} - D_o K_x \frac{\partial \lambda_2}{\partial x} \delta P + \lambda_2 D_o \frac{\partial P}{\partial x} \delta K_x + \lambda_2 C_o K_x \frac{\partial P}{\partial x} \delta S \Big]\Big|_0^{x_B} dydt$$

$$+ \int_0^T \int_0^{x_B} \Big[\lambda_1 D_w K_x \frac{\partial \delta P}{\partial y} - D_w K_y \frac{\partial \lambda_1}{\partial y} \delta P + \lambda_1 D_w \frac{\partial P}{\partial y} \delta K_y$$

$$+ \lambda_1 C_w K_y \frac{\partial P}{\partial y} \delta S + \lambda_2 D_o K_y \frac{\partial \delta P}{\partial y} - D_o K_x \frac{\partial \lambda_2}{\partial y} \delta P \Big]\Big|_0^{y_B} dxdt$$

$$- \int_0^T \int_0^{y_B} \int_0^{x_B} \Big[\Big(D_w \frac{\partial P}{\partial x} \frac{\partial \lambda_1}{\partial x} + D_o \frac{\partial P}{\partial x} \frac{\partial \lambda_2}{\partial x} \Big) \delta K_x$$

$$+ \Big(D_w \frac{\partial P}{\partial y} \frac{\partial \lambda_1}{\partial y} + D_o \frac{\partial P}{\partial y} \frac{\partial \lambda_2}{\partial y} \Big) \delta K_y \Big] dxdydt \qquad \text{(F.24)}$$

We will add Eq. F.24 to the variation in the objective function. The first order variation of Eq. F.7 is

$$\delta J = -2 \int_0^T \int_0^{t_B} \int_0^{x_B} \Big\{ \sum_\xi \sum_\theta \sum_\tau \Big[P^{obs}(x_\xi, y_\theta, t_\tau) - P(x_\xi, y_\theta, t_\tau) \Big] \delta P \delta(x - x_\xi) \cdot$$

$$\delta(y - y_\theta) \delta(t - t_\tau) + \sum_\beta \sum_\nu \sum_\eta \omega \Big[R^{obs}(x_\beta, y_\nu, t_\eta)$$

$$- R(x_\beta, y_\nu, t_\eta) \Big] R' \delta S \delta(x - x_\beta) \delta(y - y_\nu) \delta(t - t_\eta) \Big\} dxdydt \qquad \text{(F.25)}$$

Eq. F.23 can be simplified after obtaining the variations of P and S at the boundaries and initial time. From Eqs. F. 3-6, we obtain the following relation:

$$\frac{\partial \delta P}{\partial x} = 0 , \qquad x = 0, x_B \qquad \text{(F.26)}$$

$$\frac{\partial \delta P}{\partial y} = 0 \qquad y = 0, y_B \qquad \text{(F.27)}$$

$$\delta P(t=0) = 0 \tag{F.28}$$

$$\delta S(t=0) = 0 \tag{F.29}$$

Using Eqs. F.3, F.4, and F.26-29 to simplify Eq. F.24, and adding the resultant equation to Eq. F.25, the following relation is obtained:

$$\delta J + \int_0^{y_B}\int_0^{x_B}\left[\lambda_1 d_w - \lambda_2 d_o\right]\delta S\Big|_{t=T} dxdy$$

$$= \int_0^{T}\int_0^{y_B}\int_0^{x_B}\Bigg\{ d_w \frac{\partial \lambda_1}{\partial t} - d_o \frac{\partial \lambda_2}{\partial t} + \sum_m h_m(\lambda_1-\lambda_2)\delta(x-x_m)\delta(y-y_m)$$

$$- C_w K_x \frac{\partial P}{\partial x}\frac{\partial \lambda_1}{\partial x} - C_w K_y \frac{\partial P}{\partial y}\frac{\partial \lambda_1}{\partial y} - C_o K_x \frac{\partial P}{\partial x}\frac{\partial \lambda_2}{\partial x} - C_o K_y \frac{\partial P}{\partial y}\frac{\partial \lambda_2}{\partial y}$$

$$- 2\sum_\beta\sum_\nu\sum_\eta \omega\left[R^{obs}(x_\beta,y_\nu,t_\eta) - R(x_\beta,y_\nu,t_\eta)\right] R'\delta(x-x_\beta)\delta(y-y_\nu)$$

$$\delta(t-t_\eta)\Bigg\}\,\delta S\; dxdydt$$

$$+ \int_0^{T}\int_0^{y_B}\int_0^{x_B}\Bigg\{\frac{\partial}{\partial x}\left(D_w K_x \frac{\partial \lambda_1}{\partial x}\right) + \frac{\partial}{\partial y}\left(D_w K_y \frac{\partial \lambda_1}{\partial y}\right)$$

$$+ \frac{\partial}{\partial x}\left(D_o K_x \frac{\partial \lambda_2}{\partial x}\right) + \frac{\partial}{\partial y}\left(D_o K_y \frac{\partial \lambda_2}{\partial y}\right)$$

$$- \sum_\xi\sum_\theta\sum_\tau\left[P^{obs}(x_\xi,y_\theta,t_\tau) - P(x_\xi,y_\theta,t_\tau)\right]\Bigg\}\delta P\; dxdydt$$

$$- \int_0^{T}\int_0^{y_B}\left[D_w K_x \frac{\partial \lambda_1}{\partial x} + D_o K_x \frac{\partial \lambda_2}{\partial x}\right]\delta P\Big|_0^{x_B} dydt$$

$$- \int_0^{T}\int_0^{x_B}\left[D_w K_y \frac{\partial \lambda_1}{\partial y} + D_o K_y \frac{\partial \lambda_2}{\partial y}\right]\delta P\Big|_0^{y_B} dxdt$$

$$- \int_0^T \int_0^{y_B} \int_0^{x_B} \left[\left(D_w \frac{\partial P}{\partial x} \frac{\partial \lambda_1}{\partial x} + D_o \frac{\partial P}{\partial x} \frac{\partial \lambda_2}{\partial x} \right) \delta K_x + \left(D_w \frac{\partial P}{\partial y} \frac{\partial \lambda_1}{\partial y} \right. \right.$$

$$\left. \left. + D_o \frac{\partial P}{\partial y} \frac{\partial \lambda_2}{\partial y} \right) \delta K_y \right] dxdydt \qquad (F.30)$$

We now specify that λ_1 and λ_2 satisfy the following partial differential equations:

$$d_w \frac{\partial \lambda_1}{\partial t} - d_o \frac{\partial \lambda_2}{\partial t} + \sum_m h_m(\lambda_1 - \lambda_2)\delta(x-x_m)\delta(y-y_m)$$

$$- C_w K_x \frac{\partial P}{\partial x} \frac{\partial \lambda_1}{\partial x} - C_w K_y \frac{\partial P}{\partial y} \frac{\partial \lambda_1}{\partial y} - C_o K_x \frac{\partial P}{\partial x} \frac{\partial \lambda_1}{\partial x} - C_o K_y \frac{\partial P}{\partial y} \frac{\partial \lambda_2}{\partial y}$$

$$- 2 \sum_\beta \sum_\nu \sum_\eta \omega \left[R^{obs}(x_\beta, y_\nu, t_\eta) - R(x_\beta, y_\nu, t_\eta) \right] R' \delta(x-x_\beta)\delta(y-y_\nu)$$

$$\delta(t-t_\eta) = 0 \qquad (F.31)$$

$$\frac{\partial}{\partial x} \left(D_w K_x \frac{\partial \lambda_1}{\partial x} + D_o K_x \frac{\partial \lambda_2}{\partial x} \right) + \frac{\partial}{\partial y} \left(D_w K_y \frac{\partial \lambda_1}{\partial y} + D_o K_y \frac{\partial \lambda_2}{\partial y} \right)$$

$$- 2 \sum_\xi \sum_\theta \sum_\tau \left[P^{obs}(x_\xi, y_\theta, t_\tau) - P(x_\xi, y_\theta, t_\tau) \right] \delta(x-x_\xi)\delta(y-y_\theta)\delta(t-t_\tau) = 0$$

$$(F.32)$$

The boundary conditions for λ_1 and λ_2 are specified as:

$$\frac{\partial \lambda_1}{\partial x} = \frac{\partial \lambda_2}{\partial x} = 0, \qquad x = 0, x_B \qquad (F.33)$$

$$\frac{\partial \lambda_1}{\partial y} = \frac{\partial \lambda_2}{\partial y} = 0, \qquad y = 0, y_B \tag{F.34}$$

and the final conditions are given by

$$\lambda_1(T) = \lambda_2(T) = 0 \tag{F.35}$$

With these specifications, the variation in the objective function resulting from perturbations in the absolute permeability are given by:

$$\delta J = -\int_0^T \int_0^{y_B} \int_0^{x_B} \left[\left(D_w \frac{\partial \lambda_1}{\partial x} + D_o \frac{\partial \lambda_2}{\partial x} \right) \frac{\partial P}{\partial x} \delta K_x + \left(D_w \frac{\partial \lambda_1}{\partial y} + D_o \frac{\partial \lambda_2}{\partial y} \right) \frac{\partial P}{\partial y} \delta K_y \right] dx dy dt \tag{F.36}$$

Finally, the functional derivatives of the objective function with respect to the absolute permeability are given by the following expressions:

$$\frac{\delta J}{\delta K_x} = \int_0^T \left[\left(D_w \frac{\partial \lambda_1}{\partial x} + D_o \frac{\partial \lambda_2}{\partial x} \right) \frac{\partial P}{\partial x} \right] dt \tag{F.37}$$

$$\frac{\delta J}{\delta K_y} = \int_0^T \left[\left(D_w \frac{\partial \lambda_1}{\partial y} + D_o \frac{\partial \lambda_2}{\partial y} \right) \frac{\partial P}{\partial y} \right] dt \tag{F.38}$$

If it is assumed that the reservoir is isotropic (i.e. $K_x = K_y = K$) then the functional derivative of the objective function with respect to the absolute permeability is given by the following relation obtained from Eq. F.36:

$$\frac{\delta J}{\delta K} = \int_0^T \left[\left(D_w \frac{\partial \lambda_1}{\partial x} + D_o \frac{\partial \lambda_2}{\partial x} \right) \frac{\partial P}{\partial x} + \left(D_w \frac{\partial \lambda_1}{\partial y} + D_o \frac{\partial \lambda_2}{\partial y} \right) \frac{\partial P}{\partial y} \right] dt \qquad (F.39)$$

Estimation of the Porosity

Here we outline the derivation of the relations that are used to calculate the derivatives of the objective function with respect to the porosity.

$$\phi = \bar{\phi} + \delta\phi \qquad (F.40)$$

Analogous to the steps used to obtain Eqs. F.15 and F.16, the following first order variational equations are obtained:

$$\frac{\partial(\phi\rho_w \delta S)}{\partial t} + \frac{\partial(S\rho_w \delta\phi)}{\partial t} = \frac{\partial}{\partial x}\left[\frac{\rho_w K_x}{\mu_w}\left(k_{rw}\frac{\partial \delta P}{\partial x} + k'_{rw}\frac{\partial P}{\partial x}\delta S\right)\right] + \frac{\partial}{\partial y}\left[\frac{\rho_w K_y}{\mu_w}\left(k_{rw}\frac{\partial \delta P}{\partial y} + k'_{rw}\frac{\partial P}{\partial y}\delta S\right)\right]$$

$$+ \sum_m q_m f' \delta S \delta(x-x_m)\delta(y-y_m) \qquad (F.41)$$

$$\frac{\partial(\phi\rho_o \delta S)}{\partial t} + \frac{\partial[(1-S)\rho_o \delta\phi]}{\partial t} = \frac{\partial}{\partial x}\left[\frac{\rho_o K_x}{\mu_o}\left(k_{ro}\frac{\partial \delta P}{\partial x} + k'_{ro}\frac{\partial P}{\partial x}\delta S\right)\right] + \frac{\partial}{\partial y}\left[\frac{\rho_o K_y}{\mu_o}\left(k_{ro}\frac{\partial \delta P}{\partial y} + k'_{ro}\frac{\partial P}{\partial y}\delta S\right)\right]$$

$$- \sum_m q_m f' \delta S \delta(x-x_m)\delta(y-y_m) \qquad (F.42)$$

With the exception of the terms in Eqs. F.41 and F.42 that contain $\delta\phi$, and the terms in Eqs. F.15 and F.16 that contain δK_x and δK_y, Eq. F.41 is identical to Eq. F.15, and Eq. F.42 is identical to F.16. The derivation can be carried out analogous to the previous derivation given by Eqs. F.17-30. With the specification that λ_1 and λ_2 satisfy Eqs. F.31-35, the following relation is obtained for the variation in the objective function:

$$\delta J = \int_0^T \int_0^{y_B} \int_0^{x_B} \left[S\rho_w \frac{\partial \lambda_1}{\partial t} + (1-S)\rho_o \frac{\partial \lambda_2}{\partial t} \right] \delta\phi \, dx dy dt \qquad (F.43)$$

Thus, the functional derivative of the objective function is given by the following equation:

$$\frac{\delta J}{\delta \phi} = \int_0^T \left[S\rho_w \frac{\partial \lambda_1}{\partial t} + (1-S)\rho_o \frac{\partial \lambda_2}{\partial t} \right] dt \qquad (F.44)$$

Estimation of Relative Permeabilities

We assume that the relative permeabilities are given as functions of unknown coefficients γ_j:

$$k_{rw} = k_{rw}(S;\gamma_j) \qquad (F.45)$$

$$k_{ro} = k_{ro}(S;\gamma_j) \qquad (F.46)$$

We consider perturbations in each coefficient γ_j, such that

$$\gamma_j = \bar{\gamma}_j + \delta\gamma_j \qquad (F.47)$$

Perturbations in the nonlinear functions of saturation are now given by:

$$\delta k_{rw} = k'_{rw}\,\delta S + \sum_j \left(\frac{\partial k_{rw}}{\partial \gamma_j}\,\delta\gamma_j\right) \tag{F.48}$$

$$\delta k_{ro} = k'_{ro}\delta S + \sum_j \left(\frac{\partial k_{ro}}{\partial \gamma_j}\,\delta\gamma_j\right) \tag{F.49}$$

$$\delta f = f'\delta S + \sum_j \left(\frac{\partial f}{\partial \gamma_j}\,\delta\gamma_j\right) \tag{F.50}$$

The first order variational equations are:

$$\begin{aligned}\frac{\partial(\phi\rho_w\delta S)}{\partial t} = {} & \frac{\partial}{\partial x}\left\{\frac{\rho_w K_x}{\mu_w}\left[k_{rw}\frac{\partial\delta P}{\partial x} + k'_{rw}\frac{\partial P}{\partial x}\,\delta S\right.\right. \\ & \left.\left. + \frac{\partial P}{\partial x}\sum_j\left(\frac{\partial k_{rw}}{\partial\gamma_j}\,\delta\gamma_j\right)\right]\right\} + \frac{\partial}{\partial y}\left\{\frac{\rho_w K_y}{\mu_w}\left[k_{rw}\frac{\partial\delta P}{\partial y} + k'_{rw}\frac{\partial P}{\partial y}\,\delta S\right.\right. \\ & \left.\left. + \frac{\partial P}{\partial y}\sum_j\left(\frac{\partial k_{rw}}{\partial\gamma_j}\,\delta\gamma_j\right)\right]\right\} \\ & + \sum_m q_m\left[f'\delta S + \sum_j\left(\frac{\partial f}{\partial\gamma_j}\,\delta\gamma_j\right)\right]\delta(x-x_m)\delta(y-y_m)\end{aligned} \tag{F.51}$$

$$\begin{aligned}-\frac{\partial(\phi\rho_o\delta S)}{\partial t} = {} & \frac{\partial}{\partial x}\left\{\frac{\rho_o K_x}{\mu_o}\left[k_{ro}\frac{\partial\delta P}{\partial x} + k'_{ro}\frac{\partial P}{\partial x}\,\delta S\right.\right. \\ & \left.\left. + \frac{\partial P}{\partial x}\sum_j\left(\frac{\partial k_{ro}}{\partial\gamma_j}\,\delta\gamma_j\right)\right]\right\} + \frac{\partial}{\partial y}\left\{\frac{\rho_o K_y}{\mu_o}\left[k_{ro}\frac{\partial\delta P}{\partial y}\right.\right. \\ & \left.\left. + k'_{ro}\frac{\partial P}{\partial y}\,\delta S + \frac{\partial P}{\partial y}\sum_j\left(\frac{\partial k_{ro}}{\partial\gamma_j}\,\delta\gamma_j\right)\right]\right\} \\ & - \sum_m q_m\left[f'\delta S + \sum_j\left(\frac{\partial f}{\partial\gamma_j}\,\delta\gamma_j\right)\right]\delta(x-x_m)\delta(y-y_m)\end{aligned} \tag{F.52}$$

The derivation proceeds analogous to Eqs. F.17-30. Note that the first order variation in the objective function, Eq. F.25, is now given by:

$$\delta J = -2 \int_0^T \int_0^{y_B} \int_0^{x_B} \Bigg\{ \sum_\xi \sum_\theta \sum_\tau \Big[P^{obs}(x_\xi, y_\theta, t_\tau) - P(x_\xi, y_\theta, t_\tau) \Big] \delta P \, \delta(x-x_\xi)\delta(y-y_\theta)\delta(t-t_\tau) + \sum_\beta \sum_\nu \sum_\eta \omega \Big[R^{obs}(x_\beta, y_\nu, t_\eta) - R(x_\beta, y_\nu, t_\eta) \Big] \Big[R' \delta S + \sum_j \frac{\partial R}{\partial \gamma_j} \delta \gamma_j \Big] \delta(x-x_\beta)\delta(y-y_\nu)\delta(t-t_\nu) \Bigg\} dx dy dt \qquad (F.53)$$

With the specification that λ_1 and λ_2 satisfy Eqs. F.31-35, the following relation is obtained for the variation δJ resulting from perturbations in the relative permeability coefficients:

$$\delta J = -\int_0^T \int_0^{y_B} \int_0^{x_B} \sum_j \Bigg\{ \frac{\rho_w}{\mu_w} \frac{\partial k_{rw}}{\partial \gamma_j} \left(K_x \frac{\partial P}{\partial x} \frac{\partial \lambda_1}{\partial x} + K_y \frac{\partial P}{\partial y} \frac{\partial \lambda_1}{\partial y} \right) + \frac{\rho_o}{\mu_o} \frac{\partial k_{ro}}{\partial \gamma_j} \left(K_x \frac{\partial P}{\partial x} \frac{\partial \lambda_2}{\partial x} + K_y \frac{\partial P}{\partial y} \frac{\partial \lambda_2}{\partial y} \right)$$

$$- \sum_m q_m (\lambda_1 - \lambda_2) \frac{\partial f}{\partial \gamma_j} \delta(x-x_m)\delta(y-y_m)$$

$$+ 2 \sum_\beta \sum_\nu \sum_\eta \omega \Big[R^{obs}(x_\beta, y_\nu, t_\eta) - R(x_\beta, y_\nu, t_\eta) \Big] \frac{\partial R}{\partial \gamma_j} \delta(x-x_\beta)\delta(y-y_\nu)$$

$$\delta(t-t_\eta) \Bigg\} \delta \gamma_j \, dx dy dt \qquad (F.54)$$

The derivative of the objective function with respect to the coefficient γ_j is given by:

$$\frac{\delta J}{\delta \gamma_j} = -\int_0^T \int_0^{y_B} \int_0^{x_B} \left\{ \frac{\rho_w}{\mu_w} \frac{\partial k_{rw}}{\partial \gamma_j} \left(K_x \frac{\partial P}{\partial x} \frac{\partial \lambda_1}{\partial x} + K_y \frac{\partial P}{\partial y} \frac{\partial \lambda_1}{\partial y} \right) \right.$$

$$+ \frac{\rho_o}{\mu_o} \left(K_x \frac{\partial P}{\partial x} \frac{\partial \lambda_2}{\partial x} + K_y \frac{\partial P}{\partial y} \frac{\partial \lambda_2}{\partial y} \right)$$

$$+ \sum_m q_m (\lambda_1 - \lambda_2) \frac{\partial f}{\partial \gamma_j} \delta(x-x_m)\delta(y-y_m)$$

$$+ 2 \sum_\beta \sum_\nu \sum_\eta \omega \left[R^{obs}(x_\beta, y_\nu, t_\eta) - R(x_\beta, y_\nu, t_\eta) \right] \frac{\partial R}{\partial \gamma_j}$$

$$\left. \delta(x-x_\beta)\delta(y-y_\nu)\delta(t-t_\eta)\, dxdydt \right\} \qquad \text{(F.55)}$$

APPENDIX G. Derivatives of the Objective Function with Respect to the Reservoir Parameters-Derivation for the Finite-Difference Equation Model

In this appendix we derive expressions for the derivatives of the objective function with respect to the reservoir properties based on the formulation of the reservoir model as finite-difference equations. Using this derivation, the adjoint equations are specified in finite-difference form. In this way, the various approximations made in the solution of the partial differential equations by the method of finite-differences, such as upstream weighting and explicit evaluation of the relative permeabilities, are reflected in the adjoint equations. That is, we need not consider the effects of the method chosen to solve the adjoint system when they are derived as partial differential equations.

For simplicity, the detailed derivation is presented for the one-dimensional reservoir model only. The adjoint system for the two-dimensional model will be specified; the addition of a space dimension to the derivation given here is straightforward.

The objective function given by Eq. 6.2 can be written in the following form:

$$J = \sum_{\xi} \sum_{\tau} [P^{obs}(i_{\xi},n_{\tau}) - P(i_{\xi},n_{\tau})]^2 + \sum_{\beta} \sum_{\theta} \omega[R^{obs}(i_{\beta},n_{\theta}) - R(i_{\beta},n_{\theta})]^2 \qquad (G.1)$$

where the subscripted values of i and n refer to the grid block location and discrete time index which correspond to the location and time of the measurements. The finite-difference equations for the reservoir model form a linear system, specified in Appendix B, which is solved for each

time step in the simulation. The simulator (see Eq. B.4) is thus specified by

$$\underset{\sim}{\underset{\sim}{A}}\underset{\sim}{u} = \underset{\sim}{b} \qquad n=0,1\ldots,N-1 \tag{G.2}$$

where N is the time index which corresponds to the final time for which the pressure and saturation solutions are calculated. For a one-dimensional finite-difference grid of NX grid blocks, we define a vector of adjoint variables, $\underset{\sim}{\Lambda}$, as

$$\underset{\sim}{\Lambda} = [\lambda_1(1,n)\ \lambda_2(1,n)\ \lambda_1(2,n)\ \ldots\ \lambda_1(NX,n)\ \lambda_2(NX,n)]^T$$

We obtain an augmented objective function, $\bar{J}$, as

$$\bar{J} = J + \sum_{n=0}^{N-1} \underset{\sim}{\Lambda}^T(\underset{\sim}{\underset{\sim}{A}}\underset{\sim}{u} - \underset{\sim}{b}) \tag{G.3}$$

The problem of minimizing Eq. G.1, subject to Eq. G.2, is equivalent to minimizing the augmented objective function $\bar{J}$. We consider first the derivation of the derivatives of the objective function $\bar{J}$ with respect to the absolute permeability.

Estimation of the Absolute Permeability

Our objective here is to relate a perturbation in the harmonic average permeability, $\delta K_{i+\frac{1}{2}}$, at the boundary between each grid block to a variation in $\bar{J}$, $\delta\bar{J}$. First, we write the product of the adjoint vector and simulator equations in Eq. G.3 as a sum of the product of elements of the vectors $\underset{\sim}{\Lambda}$, $\underset{\sim}{u}$, and $\underset{\sim}{b}$, and matrix A. Eq. G.3 can thus be written as :

$$\bar{J} = J + \sum_{n=0}^{N-1} \sum_{i=1}^{NX} \left\{ \lambda_1(i,n) \left[\sum_{j=1}^{2NX} a(2i-1,j)u(j) - b(2i-1) \right] \right.$$

$$\left. + \lambda_2(i,n) \left[\sum_{j=1}^{2NX} a(2i,j)u(j) - b(2i) \right] \right\} \qquad (G.4)$$

The term given in the first set of brackets is the finite-difference equation at grid block i and time index n for water, and the term given in the second set of brackets is the corresponding equation for oil. For two-dimensional flow, these are given by Eqs. 4.32 and 4.33. The terms $\Delta_y(T^w \Delta P)$ and $\Delta_y(T^o \Delta P)$ do not appear in the corresponding one-dimensional equations. Expanding the operators defined by Eqs. 4.10 and 4.11, the finite-difference equations 4.32 and 4.33 can be written for one-dimension as:

$$\frac{v}{(t^{n+1}-t^n)} \frac{\phi(i,n)}{B_w(i,n)} (c_r+c_w)\, S(i,n)[P(i,n+1) - P(i,n)]$$

$$+ \frac{v}{(t^{n+1}-t^n)} \frac{\phi(i,n)}{B_w(i,n)} [S(i,n+1) - S(i,n)] - T^w(i+\tfrac{1}{2},n)[P(i+1,n+1) - P(i,n+1)]$$

$$+ T^w(i-\tfrac{1}{2},n)[P(i,n+1) - P(i-1,n+1)] - \sum_m Q_{T_m}^{n+1}\, g_w^{n+1}\, \delta(i,i_m) = 0 \qquad (G.5)$$

$$\frac{v}{(t^{n+1}-t^n)} \frac{\phi(i,n)}{B_o(i,n)} (c_r+c_o)\, [1-S(i,n)]\, [P(i,n+1) - P(i,n)]$$

$$+ \frac{v}{(t^{n+1}-t^n)} \frac{\phi(i,n)}{B_o(i,n)} [S(i,n) - S(i,n+1)] - T^o(i+\tfrac{1}{2},n)\, [P(i+1,n+1) - P(i,n)]$$

$$+ T^o(i-\tfrac{1}{2},n)\, [P(i,n+1) - P(i-1,n+1)] - \sum_m Q_{T_m}^{n+1}\, (1-g_w^{n+1})\, \delta(i,i_m) = 0$$

$$(G.6)$$

where

$$T^{\ell}(1+\tfrac{1}{2},n) = \frac{v}{\Delta x_i}\left(\frac{K\, k^n_{r\ell}}{\mu^n_{\ell}\, B^n_{\ell}}\right)_{i+\frac{1}{2}}$$

$$T^{\ell}(i-\tfrac{1}{2},n) = \frac{v}{\Delta x_i}\left(\frac{K\, k^n_{r\ell}}{\mu^n_{\ell}\, B^n_{\ell}}\right)_{i-\frac{1}{2}}$$

The subscript ℓ refers to the oil or water phase. For simplicity, we have evaluated the quantity g_w at time t^{n+1} rather than the semi-implicit approximation of that value used in Eqs. 4.32 and 4.33.

We now want to relate perturbations in $K_{i+\frac{1}{2}}$ to variations in the pressure and saturation. To simplify notation, we introduce the following variables:

$$M^{\ell}(i,n) = \frac{v}{(t^{n+1}-t^n)}\frac{\phi(i,n)}{B_{\ell}(i,n)}$$

$$F^{\ell}(i+\tfrac{1}{2},n) = \frac{v}{\Delta x_i}\left(\frac{1}{\mu^n_{\ell}\, B^n_{\ell}}\right)_{i+\frac{1}{2}}$$

$$C_w = c_w + c_r$$

$$C_o = c_o + c_r$$

Also, we will write $Q^{n+1}_{T_m}$ as simply Q_m with the understanding that it is to be evaluated at the same time as the multiplying term g_w, and omit the subscript w from g^{n+1}_w.

The perturbation equations corresponding to Eqs. G.5 and G.6 are:

$$M^w(i,n)C_w[S(i,n) + \delta S(i,n)][P(i,n+1) + \delta P(i,n+1) - P(i,n) - \delta P(i,n)]$$

$$+ M^w(i,n)\,[S(i,n+1) + \delta S(i,n+1) - S(i,n) - \delta S(i,n)]$$

$$- F^w(i+\tfrac{1}{2},n)(K_{i+\frac{1}{2}} + \delta K_{i+\frac{1}{2}})[k_{rw}(i+\tfrac{1}{2},n) + \delta k_{rw}(i+\tfrac{1}{2},n)][P(i+1,n+1)$$

$$+ \delta P(i+1,n+1) - P(i,n+1) - \delta P(i,n+1)]$$

$$+ F^w(i-\tfrac{1}{2},n)(K_{i-\frac{1}{2}} + \delta K_{i-\frac{1}{2}})[k_{rw}(i-\tfrac{1}{2},n) + \delta k_{rw}(i-\tfrac{1}{2},n)][P(i,n+1)$$

$$+ \delta P(i,n+1) - P(i-1,n+1) - \delta P(i-1,n+1)] - \sum_m Q_m(g^{n+1} + \delta g^{n+1})\delta(i,i_m)$$

$$= 0 \qquad (G.7)$$

$$M^o(i,n)C_o[1 - S(i,n) - \delta S(i,n)][P(i,n+1) + \delta P(i,n+1) - P(i,n) - \delta P(i,n)]$$

$$+ M^o(i,n)[S(i,n) + \delta S(i,n) - S(i,n+1) - \delta S(i,n+1)]$$

$$- F^o(i+\tfrac{1}{2},n)(K_{i+\frac{1}{2}} + \delta K_{i+\frac{1}{2}})[k_{ro}(i+\tfrac{1}{2},n) + \delta k_{ro}(i+\tfrac{1}{2},n)][P(i+1,n+1)$$

$$+ \delta P(i+1,n+1) - P(i,n+1) - \delta P(i,n+1)]$$

$$+ F^o(i-\tfrac{1}{2},n)(K_{i-\frac{1}{2}} + \delta K_{i-\frac{1}{2}})[k_{ro}(i-\tfrac{1}{2},n) + \delta k_{ro}(i-\tfrac{1}{2},n)][P(i,n+1)$$

$$+ \delta P(i,n+1) - P(i-1,n+1) - \delta P(i-1,n+1)] - \sum_m Q_m(1-g^{n+1} - \delta g^{n+1})\delta(i,i_m)$$

$$= 0 \qquad (G.8)$$

The first-order variational equations are:

$$M^w(i,n)C_w\{S(i,n)[\delta P(i,n+1) - \delta P(i,n)] + \delta S(i,n)\,[P(i,n+1) - P(i,n)]\}$$

$$+\ M^w(i,n)[\delta S(i,n+1) - \delta S(i,n)]$$

$$- F^w(i+\tfrac{1}{2},n)\left\{K_{i+\frac{1}{2}}\ k_{rw}(i+\tfrac{1}{2},n)[\delta P(i+1,n+1) - \delta P(i,n+1)]\right.$$

$$+ K_{i+\frac{1}{2}}\,[P(i+1,n+1) - P(i,n+1)]k'_{rw}(i+\tfrac{1}{2},n)\delta S(i+\tfrac{1}{2},n)$$

$$\left.+ k_{rw}(i+\tfrac{1}{2},n)[P(i+1,n+1) - P(i,n+1)]\delta K_{i+\frac{1}{2}}\right\}$$

$$+ F^w(i-\tfrac{1}{2},n)\left\{K_{i-\frac{1}{2}}\ k_{rw}(i-\tfrac{1}{2},n)[\delta P(i,n+1) - \delta P(i-1,n+1)]\right.$$

$$+ K_{i-\frac{1}{2}}\,[P(i,n+1) - P(i-1,n+1)]k'_{rw}(i-\tfrac{1}{2},n)\delta S(i-\tfrac{1}{2},n)$$

$$\left.+ k_{rw}(i-\tfrac{1}{2},n)[P(i,n+1) - P(i-1,n+1)]\delta K_{i-\frac{1}{2}}\right\}$$

$$- \sum_m Q_m(g')^{n+1}\,\delta S(i,n+1)\delta(i,i_m) = 0 \qquad (G.9)$$

$$M^o(i,n)C_o\{[1-S(i,n)][\delta P(i,n+1) - \delta P(i,n)] - \delta S(i,n)\,[P(i,n+1) - P(i,n)]\}$$

$$+ M^o(i,n)[\delta S(i,n) - \delta S(i,n+1)]$$

$$- F^o(i+\tfrac{1}{2},n)\left\{K_{i+\frac{1}{2}}\ k_{ro}(i+\tfrac{1}{2},n)[\delta P(i+1,n+1) - \delta P(i,n+1)]\right.$$

$$+ K_{i+\frac{1}{2}}[P(i+1,n+1) - P(i,n+1)]k'_{ro}(i+\tfrac{1}{2},n)\delta S(i+\tfrac{1}{2},n)$$

$$\left.+ k_{ro}(i+\tfrac{1}{2},n)[P(i+1,n+1) - P(i,n+1)]\delta K_{i+\frac{1}{2}}\right\}$$

$$+ F^o(i-\tfrac{1}{2},n)\left\{K_{i-\frac{1}{2}}\ k_{ro}(i-\tfrac{1}{2},n)[\delta P(i,n+1) - \delta P(i-1,n+1)]\right.$$

$$+ K_{i-\frac{1}{2}}[P(i,n+1) - P(i-1,n+1)]k'_{ro}(i-\tfrac{1}{2},n)\delta S(i-\tfrac{1}{2},n)$$

$$\left.+ k_{ro}(i-\tfrac{1}{2},n)[P(i,n+1) - P(i-1,n+1)]\delta K_{i-\frac{1}{2}}\right\}$$

$$+ \sum_{m} Q_m (g')^{n+1} \, \delta S(i,n+1)\delta(i,i_m) = 0 \qquad (G.10)$$

where the primes denote the derivatives with respect to saturation.

We now obtain the first-order variation of the quantity J in Eq. G.3. That quantity can be written as the following sum:

$$\delta J = -2 \sum_{n=0}^{n=1} \sum_{i=1}^{NX} \Bigg\{ \sum_{\xi} \sum_{\tau} [P^{obs}(i_\xi, n_\tau) - P(i_\xi, n_\tau)] \delta P(i,n+1) \delta(i,i_\xi) \delta(n+1,n_\tau)$$

$$+ \omega \sum_{\beta} \sum_{\theta} [R^{obs}(i_\beta, n_\theta) - R(i_\beta, n_\theta)] R' \delta S(i,n+1) \delta(i,i_\beta) \delta(n+1,n_\theta) \Bigg\} \qquad (G.11)$$

Using Eqs. G.9 - 11, the following equation can be obtained for the variation $\delta \bar{J}$ of Eq. G.3:

$$\delta \bar{J} = \sum_{n=0}^{N-1} \sum_{i=1}^{NX} \Bigg\{ \lambda_1(i,n) M^w(i,n) C_w S(i,n) + \lambda_2(i,n) M^o(i,n) C_o [1 - S(i,n)]$$

$$+ \lambda_1(i,n)[T^w(i+\tfrac{1}{2},n) + T^w(i-\tfrac{1}{2},n)] + \lambda_2(i,n)[T^o(i+\tfrac{1}{2},n) + T^o(i-\tfrac{1}{2},n)]$$

$$- 2 \sum_{\xi} \sum_{\tau} [P^{obs}(i_\xi, n_\tau) - P(i_\xi, n_\tau)] \delta(i,i_\xi) \delta(n+1,n_\tau) \Bigg\} \delta P(i,n+1)$$

$$- \sum_{n=0}^{N-1} \sum_{i=1}^{NX} \Big\{ \lambda_1(i,n) T^w(i-\tfrac{1}{2},n) + \lambda_2(i,n) T^o(i-\tfrac{1}{2},n) \Big\} \delta P(i-1,n+1)$$

$$- \sum_{n=0}^{N-1} \sum_{i=1}^{NX} \Big\{ \lambda_1(i,n) T^w(i+\tfrac{1}{2},n) + \lambda_2(i,n) T^o(i+\tfrac{1}{2},n) \Big\} \delta P(i+1,n+1)$$

$$- \sum_{n=0}^{N-1} \sum_{i=1}^{NX} \Big\{ \lambda_1(i,n) M^w(i,n) C_w S(i,n) + \lambda_2(i,n) M^o(i,n) C_o [1 - S(i,n)] \Big\} \delta P(i,n)$$

$$
\begin{aligned}
&+\sum_{n=0}^{N-1}\sum_{i=1}^{NX}\Big\{\lambda_1(i,n)M^w(i,n)-\lambda_2(i,n)M^o(i,n)\\
&+\sum_m Q_m[\lambda_2(i,n)-\lambda_1(i,n)](g')^{n+1}\delta(i,i_m)\\
&-2\sum_\beta\sum_\theta[R^{obs}(i_\beta,n_\theta)-R(i_\beta,n_\theta)]R'\delta(i,i_\beta)\delta(n+1,n_\theta)\Big\}\delta S(i,n+1)\\
&+\sum_{n=0}^{N-1}\sum_{i=1}^{NX}\Big\{\lambda_1(i,n)M^w(i,n)\Big[C_w[P(i,n+1)-P(i,n)]-1\Big]\\
&-\lambda_2(i,n)M^o(i,n)\Big[C_o[P(i,n+1)-P(i,n)]-1\Big]\Big\}\delta S(i,n)\\
&+\sum_{n=0}^{N-1}\sum_{i=1}^{NX}\Big\{[P(i,n+1)-P(i-1,n+1)][\lambda_1(i,n)F^w(i-\tfrac{1}{2},n)K_{i-\frac{1}{2}}k'_{rw}(i-\tfrac{1}{2},n)\\
&+\lambda_2(i,n)F^o(i-\tfrac{1}{2},n)K_{i-\frac{1}{2}}k'_{ro}(i-\tfrac{1}{2},n)]\Big\}\delta S(i-\tfrac{1}{2},n)\\
&-\sum_{n=0}^{N-1}\sum_{i=1}^{NX}\Big\{[P(i+1,n+1)-P(i,n+1)][\lambda_1(i,n)F^w(i+\tfrac{1}{2},n)K_{i+\frac{1}{2}}k'_{rw}(i+\tfrac{1}{2},n)\\
&+\lambda_2(i,n)F^o(i+\tfrac{1}{2},n)K_{i+\frac{1}{2}}k'_{ro}(i+\tfrac{1}{2},n)]\Big\}\delta S(i+\tfrac{1}{2},n)\\
&+\sum_{n=0}^{N-1}\sum_{i=1}^{NX}\Big\{[P(i,n+1)-P(i-1,n+1)][\lambda_1(i,n)F^w(i-\tfrac{1}{2},n)k_{rw}(i-\tfrac{1}{2},n)\\
&+\lambda_2(i,n)F^o(i-\tfrac{1}{2},n)k_{ro}(i-\tfrac{1}{2},n)]\Big\}\delta K_{i-\frac{1}{2}}\\
&-\sum_{n=0}^{N-1}\sum_{i=1}^{NX}\Big\{[P(i+1,n+1)-P(i,n+1)][\lambda_1(i,n)F^w(i+\tfrac{1}{2},n)k_{rw}(i+\tfrac{1}{2},n)\\
&+\lambda_2(i,n)F^o(i+\tfrac{1}{2},n)k_{ro}(i+\tfrac{1}{2},n)]\Big\}\delta K_{i+\frac{1}{2}} \qquad (G.12)
\end{aligned}
$$

We will obtain from Eq. G.12 an equation which contains only the variations $\delta P(i,n)$, $\delta S(i,n)$, and $\delta K_{i+\frac{1}{2}}$. We will consider each of the terms in Eq. G.12 which contain perturbations at other values of i and n.

By simply changing the time index in the first term in Eq. G.12, that term can be written as:

$$\sum_{n=1}^{N}\sum_{i=1}^{NX}\Big\{\lambda_1(i,n-1)M^w(i,n-1)C_w S(i,n-1) + \lambda_2(i,n-1)M^o(i,n-1)C_o[1-S(i,n-1)]$$
$$+ \lambda_1(i,n-1)[T^w(i+\tfrac{1}{2},n-1) + T^w(i-\tfrac{1}{2},n-1)]$$
$$+ \lambda_2(i,n-1)[T^o(i+\tfrac{1}{2},n-1) + T^o(i-\tfrac{1}{2},n-1)]$$
$$- 2\sum_{\xi}\sum_{\tau}[P^{obs}(i_\xi,n_\tau) - P(i_\xi,n_\tau)]\delta(i,i_\xi)\delta(n,n_\tau)\Big\}\delta P(i,n) \qquad (G.13)$$

Changing the time and space indices in the second term in Eq. G.12, that term can be written as:

$$\sum_{n=1}^{N}\sum_{i=1}^{NX}\Big\{\lambda_1(i+1,n-1)T^w(i+\tfrac{1}{2},n-1) + \lambda_2(i+1,n-1)T^o(i+\tfrac{1}{2},n-1)\Big\}\delta P(i,n)$$
$$+ \sum_{n=0}^{N-1}\Big\{\lambda_1(1,n)T^w(\tfrac{1}{2},n) + \lambda_2(1,n)T^o(\tfrac{1}{2},n)\Big\}\delta P(0,n+1)$$
$$- \sum_{n=0}^{N-1}\Big\{\lambda_1(NX+1,n)T^w(NX+\tfrac{1}{2},n) + \lambda_2(NX+1,n)T^o(NX+\tfrac{1}{2},n)\Big\}\delta P(NX,n) \qquad (G.14)$$

Similarly, the third term in Eq. G.12 can be written as:

$$\sum_{n=1}^{N}\sum_{i=1}^{NX}\left\{\lambda_1(i-1,n-1)T^w(i-\tfrac{1}{2},n-1)+\lambda_2(i-1,n-1)T^o(i-\tfrac{1}{2},n-1)\right\}\delta P(i,n)$$

$$+\sum_{n=0}^{N-1}\left\{\lambda_1(NX,n)T^w(NX+\tfrac{1}{2},n)+\lambda_2(NX,n)T^o(NX+\tfrac{1}{2},n)\right\}\delta P(NX+1,n+1)$$

$$-\sum_{n=0}^{N-1}\left\{\lambda_1,(0,n)T^w(\tfrac{1}{2},n)+\lambda_2(0,n)T^o(\tfrac{1}{2},n)\right\}\delta P(1,n+1) \qquad (G.15)$$

The fourth term in Eq. G.12 can be written as a sum over n=1,...,N:

$$\sum_{n=1}^{N}\sum_{i=1}^{NX}\left\{\lambda_1,(i,n)M^w(i,n)C_wS(i,n)+\lambda_2(i,n)M^o(i,n)C_o[1-S(i,n)]\right\}\delta P(i,n)$$

$$-\sum_{i=1}^{NX}\left\{\lambda_1,(i,N)M^w(i,N)C^wS(i,N)+\lambda_2(i,N)M^o(i,N)C_o[1-S(i,N)]\right\}\delta P(i,N)$$

$$+\sum_{i=1}^{NX}\left\{\lambda_1(i,0)M^w(i,0)C_wS(i,0)+\lambda_2(i,0)M^o(i,0)C_o[1-S(i,0)]\right\}\delta P(i,0) \qquad (G.16)$$

Variations in the pressure and saturation corresponding to time index n=0 are zero since those values are specified as initial conditions. That is, $\delta P(i,0) = 0$; consequently, the last sum can be omitted from Eq. G.16.

The fifth term can be written as the following sum be simply changing the time index:

$$\sum_{n=1}^{N}\sum_{i=1}^{NX}\left\{\lambda_1(i,n-1)M^w(i,n-1)-\lambda_2(i,n-1)M^o(i,n-1)\right.$$

$$+\sum_{m}Q_m[\lambda_2(i,n-1)-\lambda_1(i,n-1)](g')^n\delta(i,i_m)-2\omega\sum_{\beta}\sum_{\theta}[R^{obs}(i_\beta,n_\theta)$$

$$\left.-R(i_\beta,n_\theta)]R'\delta(i,i_\beta)\delta(n,n_\tau)\right\}\delta S(i,n) \qquad (G.17)$$

The sixth term can be written as

$$\sum_{n=1}^{N}\sum_{i=1}^{NX}\Big\{\lambda_1(i,n)M^w(i,n)\Big[C_w[P(i,n+1)-P(i,n)]-1\Big]$$
$$-\lambda_2(i,n)M^o(i,n)\Big[C_o[P(i,n+1)-P(i,n)]-1\Big]\Big\}\delta S(i,n)$$
$$-\sum_{i=1}^{NX}\Big\{\lambda_1(i,N)M^w(i,N)\Big[C_w[P(i,N+1)-P(i,N)]-1\Big]$$
$$-\lambda_2(i,N)M^o(i,N)\Big[C_o[P(i,N+1)-P(i,N)]-1\Big]\Big\}\delta S(i,N)$$
$$+\sum_{i=1}^{NX}\Big\{\lambda_1(i,0)M^w(i,0)\Big[C_w[P(i,1)-P(i,0)]-1\Big]$$
$$-\lambda_2(i,0)M^o(i,0)\Big[C_o[P(i,1)-P(i,0)]-1\Big]\Big\}\delta S(i,0) \qquad (G.18)$$

Similarly to Eq. G.16, the last term can be omitted since $\delta S(i,0) = 0$.

The variations $\delta S(i-\frac{1}{2},n)$ and $\delta S(i+\frac{1}{2},n)$ in the seventh and eigth terms represent fictitious values since the relative permeabilities are evaluated at the upstream value of saturation. The quantities $\delta S(i-\frac{1}{2},n)$ and $\delta S(i+\frac{1}{2},n)$ are given by:

$$\delta S(i-\tfrac{1}{2},n) = \alpha^n_{i-\frac{1}{2}}\,\delta S(i-1,n) + \left(1-\alpha^n_{i-\frac{1}{2}}\right)\delta S(i,n) \qquad (G.19)$$

$$\delta S(i+\tfrac{1}{2},n) = \alpha^n_{i+\frac{1}{2}}\,\delta S(i,n) + \left(1-\alpha^n_{i+\frac{1}{2}}\right)\delta S(i,n)$$

where $\alpha^n_{i-\frac{1}{2}} = 1$ if $P(i-1,n) \geq P(i,n)$

$= 0$ otherwise.

Using Eq. G.19, the following is obtained for the seventh term in Eq. G.12:

$$\sum_{n=0}^{N-1}\sum_{i=1}^{NX}\left\{[P(i,n+1)-P(i,n+1)]\left[\lambda_1(i,n)F^w(i-\tfrac{1}{2},n)K_{i-\frac{1}{2}}k'_{rw}(i-\tfrac{1}{2},n)\right.\right.$$

$$\left.\left.+\lambda_2(i,n)F^o(i-\tfrac{1}{2},n)K_{i-\frac{1}{2}}k'_{ro}(i-\tfrac{1}{2},n)\right]\right\}\left[\alpha^n_{i-\frac{1}{2}}\delta S(i-1,n)+\left(1-\alpha^n_{i-\frac{1}{2}}\right)\delta S(i,n)\right]$$

$$=\sum_{n=0}^{N-1}\sum_{i=1}^{NX}\left\{[P(i+1,n+1)-P(i,n+1)]\left[\lambda_1(i+1,n)F^w(i+\tfrac{1}{2},n)K_{i+\frac{1}{2}}k'_{rw}(i+\tfrac{1}{2},n)\right.\right.$$

$$\left.+\lambda_2(i+1,n)F^o(i+\tfrac{1}{2},n)K_{i+\frac{1}{2}}k'_{ro}(i+\tfrac{1}{2},n)\right]\alpha^n_{i+\frac{1}{2}}$$

$$+[P(i,n+1)-P(i-1,n+1)]\left[\lambda_1(i,n)F^w(i-\tfrac{1}{2},n)K_{i-\frac{1}{2}}k'_{rw}(i-\tfrac{1}{2},n)\right.$$

$$\left.\left.+\lambda_2(i,n)F^o(i-\tfrac{1}{2},n)K_{i-\frac{1}{2}}k'_{ro}(i-\tfrac{1}{2},n)\right]\left(1-\alpha^n_{i-\frac{1}{2}}\right)\right\}\delta S(i,n)$$

$$+\sum_{n=0}^{N-1}\left\{[P(1,n+1)-P(0,n+1)][\,\cdot\,\cdot\,\cdot\,]\right\}\delta S(0,n)$$

$$-\sum_{n=0}^{N-1}\left\{[P(NX+1,n+1)-P(NX,n+1)][\,\cdot\,\cdot\,\cdot\,]\right\}\delta S(NX,n) \qquad (G.20)$$

The last two sums do not contribute to G.20 since, from the reflection boundary conditions, we obtain:

$$P(1,n) = P(0,n)$$

$$P(NX,n) = P(NX+1,n) \qquad (G.21)$$

for all values n. Noting that $\delta S(i,0) = 0$, the first term on the right-hand side of Eq. G.20 can be written as the sum from n=1,...,N, rather than n=0,...,N-1, as:

$$\sum_{n=0}^{N-1}\sum_{i=1}^{NX}\left\{\qquad\right\}\delta S(i,n) = \sum_{n=1}^{N}\sum_{i=1}^{NX}\left\{\qquad\right\}\delta S(i,n) - \sum_{i=1}^{NX}\left\{\qquad\right\}\Bigg|_{n=N}\delta S(i,n) \tag{G.22}$$

The terms in brackets are identical to those given in Eq. G.20.

Similarly, the following can be obtained for the eigth term in Eq. G.12:

$$\begin{aligned}
&\sum_{n=0}^{N-1}\sum_{i=1}^{NX}\Big\{[P(i,n+1) - P(i-1,n+1)][\lambda_1(i-1,n)F^w(i-\tfrac{1}{2},n)K_{i-\frac{1}{2}}k'_{rw}(i-\tfrac{1}{2},n) \\
&\quad + \lambda_2(i-1,n)F^o(i-\tfrac{1}{2},n)K_{i-\frac{1}{2}}k'_{ro}(i-\tfrac{1}{2},n)]\left(1-\alpha^n_{i-\frac{1}{2}}\right) \\
&\quad + [P(i+1,n+1) - P(i,n+1)][\lambda_1(i,n)F^w(i+\tfrac{1}{2},n)K_{i+\frac{1}{2}}k'_{rw}(i+\tfrac{1}{2},n) \\
&\quad + \lambda_2(i,n)F^o(i+\tfrac{1}{2},n)K_{i+\frac{1}{2}}k'_{ro}(i+\tfrac{1}{2},n)]\alpha^n_{i+\frac{1}{2}}\Big\}\delta S(i,n) \\
&\quad + \sum_{n=0}^{N-1}\Big\{[P(NX+1,n+1) - P(NX,n+1)][\cdots]\Big\}\delta S(NX+1,n) \\
&\quad + \sum_{n=0}^{N-1}\Big\{[P(1,n+1) - P(0,n+1)][\cdots]\Big\}\delta S(1,n) \\
&= \sum_{n=1}^{N}\sum_{i=1}^{NX}\left\{\qquad\right\}\delta S(i,n) - \sum_{i=1}^{NX}\left\{\qquad\right\}\Bigg|_{n=N}\delta S(i,N)
\end{aligned} \tag{G.23}$$

The right-hand side of Eq. G.23 is obtained by the same steps which were used to obtain Eq. G.22 from G.20.

The following can be obtained for the ninth term in Eq. G.12:

$$\sum_{n=0}^{N-1}\sum_{i=1}^{NX}\Big\{[P(i+1,n+1) - P(i,n+1)][\lambda_1(i+1,n)F^w(i+\tfrac{1}{2},n)k_{rw}(i+\tfrac{1}{2},n) + \lambda_2(i+1,n)F^o(i+\tfrac{1}{2},n)k_{ro}(i+\tfrac{1}{2},n)]\Big\}\delta K_{i+\frac{1}{2}}$$

$$- \sum_{n=0}^{N-1}\Big\{[P(NX+1,n+1) - P(NX,n+1)][\cdot\ \cdot\ \cdot]\Big\}\ \delta K_{NX+\frac{1}{2}}$$

$$+ \sum_{n=0}^{N-1}\Big\{[P(1,n+1) - P(0,n+1)][\cdot\ \cdot\ \cdot]\Big\}\ \delta K_{\frac{1}{2}} \qquad (G.24)$$

The final two sums can be eliminated by use of the boundary conditions (see Eq. G.21).

With the changes in the terms in Eq. G.12 given by Eqs. G.13 - 18, 22, 24, Eq. G.12 can be written as:

$$\delta\bar{J} = \sum_{n=1}^{N}\sum_{i=1}^{NX}\Big\{\lambda_1(i,n-1)M^w(i,n-1)C_wS(i,n-1) + \lambda_2(i,n-1)M^o(i,n-1)C_o[1-S(i,n-1)]$$

$$+ \lambda_1(i,n-1)[T^w(i-\tfrac{1}{2},n-1) + T^w(i+\tfrac{1}{2},n-1)]$$

$$+ \lambda_2(i,n-1)[T^o(i-\tfrac{1}{2},n-1) + T^o(i+\tfrac{1}{2},n-1)] - \lambda_1(i+1,n-1)T^w(i+\tfrac{1}{2},n-1)$$

$$- \lambda_2(i+1,n-1)T^o(i+\tfrac{1}{2},n-1) - \lambda_1(i-1,n-1)T^w(i-\tfrac{1}{2},n-1)$$

$$- \lambda_2(i-1,n-1)T^o(i-\tfrac{1}{2},n-1) - \lambda_1(i,n)M^w(i,n)C_wS(i,n)$$

$$- \lambda_2(i,n)M^o(i,n)C_o[1-S(i,n)]$$

$$- 2\sum_{\xi}\sum_{\tau}[P^{obs}(i_\xi,n_\tau) - P(i_\xi,n_\tau)]\delta(i,i_\xi)\delta(n,n_\tau)\Big\}\ \delta P(i,n)$$

$$+\sum_{n=1}^{N}\sum_{i=1}^{NX}\Big\{\lambda_1(i,n)M^w(i,n)\big[C_w[P(i,n+1)-P(i,n)]-1\big]$$

$$-\lambda_2(i,n)M^o(i,n)\big[C_o[P(i,n+1)-P(i,n)]-1\big]+\lambda_1(i,n-1)M^w(i,n-1)$$

$$-\lambda_2(i,n-1)M^o(i,n-1)+\sum_m Q_m(g')^n\,\delta(i,i_m)[\lambda_2(i,n-1)-\lambda_1(i,n-1)]$$

$$+[P(i+1,n+1)-P(i,n+1)]\Big[[\lambda_1(i+1,n)-\lambda_1(i,n)]\,F^w(i+\tfrac{1}{2},n)K_{i+\frac{1}{2}}k'_{rw}(i+\tfrac{1}{2},n)$$

$$+[\lambda_2(i+1,n)-\lambda_2(i,n)]F^o(i+\tfrac{1}{2},n)K_{i+\frac{1}{2}}k'_{ro}(i+\tfrac{1}{2},n)\Big]\alpha^n_{i+\frac{1}{2}}$$

$$+[P(i,n+1)-P(i-1,n+1)]\Big[[\lambda_1(i,n)-\lambda_1(i-1,n)]F^w(i-\tfrac{1}{2},n)K_{i-\frac{1}{2}}k'_{rw}(i-\tfrac{1}{2},n)$$

$$+[\lambda_2(i,n)-\lambda_2(i-1,n)]F^o(i-\tfrac{1}{2},n)K_{i-\frac{1}{2}}k'_{ro}(i-\tfrac{1}{2},n)\Big]\left(1-\alpha^n_{i-\frac{1}{2}}\right)$$

$$-2\omega\sum_\beta\sum_\theta[R^{obs}(i_\beta,n_\theta)-R(i_\beta,n_\theta)]R'\delta(i,i_\beta)\delta(n,n_\theta)\Big\}\,\delta S(i,n)$$

$$+\sum_{n=0}^{N-1}\sum_{i=1}^{NX}\Big\{[P(i+1,n+1)-P(i,n+1)]\Big[[\lambda_1(i+1,n)$$

$$-\lambda_1(i,n)]F^w(i+\tfrac{1}{2},n)k_{rw}(i+\tfrac{1}{2},n)+[\lambda_2(i+1,n)-\lambda_2(i,n)]F^o(i+\tfrac{1}{2},n)$$

$$k_{ro}(i+\tfrac{1}{2},n)\Big]\Big\}\,\delta K_{i+\frac{1}{2}}$$

$$+\sum_{n=0}^{N-1}\Big\{T^w(NX+\tfrac{1}{2},n)[\lambda_1(NX+1,n)-\lambda_1(NX+n)]$$

$$+T^o(NX+\tfrac{1}{2},n)[\lambda_2(NX+1,n)-\lambda_2(NX,n)]\Big\}\,\delta P(NX+1,n+1)$$

$$+\sum_{n=0}^{N-1}\Big\{T^w(\tfrac{1}{2},n)[\lambda_1(0,n)-\lambda_1(1,n)]$$

$$+ T^{o}(\tfrac{1}{2},n)[\lambda_2(0,n) - \lambda_2(1,n)]\Big\}\,\delta P(1,n+1)$$

$$+ \sum_{i=1}^{NX}\Big\{\lambda_1(i,N)M^{w}(i,N)C_w S(i,N) + \lambda_2(i,N)M^{o}(i,N)C_o[1-S(i,N)]\Big\}\delta P(i,N)$$

$$- \sum_{i=1}^{NX}\Big\{\lambda_1(i,N)M^{w}(i,N)\Big[C_w[P(i,N+1) - P(i,N)] - 1\Big]$$

$$- \lambda_2(i,N)M^{o}(i,N)\Big[C_o[P(i,N+1) - P(i,N)] - 1\Big]$$

$$+ [P(i+1,N+1) - P(i,N+1)]\Big[[\lambda_1(i+1,N) - \lambda_1(i,N)]F^{w}(i+\tfrac{1}{2},N)K_{i+\frac{1}{2}}k'_{rw}(i+\tfrac{1}{2},N)$$

$$+ [\lambda_2(i+1,N) - \lambda_2(i,N)]F^{o}(i+\tfrac{1}{2},N)K_{i+\frac{1}{2}}k'_{ro}(i-\tfrac{1}{2},N)\Big]\alpha^{N}_{i+\frac{1}{2}}$$

$$+ [P(i,N+1) - P(i-1,N+1)]\Big[[\lambda_1(i,N) - \lambda_1(i-1,N)]F^{w}(i-\tfrac{1}{2},N)K_{i-\frac{1}{2}}k'_{rw}(i-\tfrac{1}{2},N)$$

$$+ [\lambda_2(i,N) - \lambda_2(i-1,N)]F^{o}(i-\tfrac{1}{2},N)K_{i-\frac{1}{2}}k'_{ro}(i-\tfrac{1}{2},N)\Big]\Big(1-\alpha^{N}_{i-\frac{1}{2}}\Big)\Big\}\,\delta S(i,N)$$

(G.25)

We now specify λ_1 and λ_2 by setting the quantity in braces which multiply each quantity $\delta P(i,n)$ in the first term in Eq. G.25, and each quantity $\delta S(i,n)$ in the second term in Eq. G.25, equal to zero with the following additional conditions:

$$\lambda_1(0,n) = \lambda_1(1,n)\ , \quad n=0,1,\ldots,N-1 \qquad \text{(G.26)}$$

$$\lambda_2(0,n) = \lambda_2(1,n)$$

$$\lambda_1(NX+1,n) = \lambda_1(NX,n)$$

$$\lambda_2(NX,n) = \lambda_2(NX,n)$$

$$\lambda_1(i,N) = \lambda_2(i,N) = 0\ , \quad i=1,\ldots,NX \qquad \text{(G.27)}$$

Using the vector for the adjoint variables defined previously, these conditions can be expressed as the following linear system;

$$\underset{\sim}{\bar{A}}\ \underset{\sim}{\Lambda} = \underset{\sim}{\bar{b}}, \qquad n=N-1,N-2,\ldots,0 \tag{G.28}$$

where the elements of the 2NX x 2NX matrix $\underset{\sim}{\bar{A}}$, and 2NX vector $\underset{\sim}{\bar{b}}$ can be determined from the first two terms in Eq. G.25. The linear system G.28 can thus be solved backwards in time subject to Eq. G.27. The derivative of the objective function with respect to $K_{i+\frac{1}{2}}$ is given by the following expression obtained from Eq. G.25 after Eqs. G.26 - 28 have been used to simplify that expression:

$$\frac{\delta\bar{J}}{\delta K_{i+\frac{1}{2}}} = \sum_{n=0}^{N-1} \Big\{ [P(i+1,n+1) - P(i,n+1)] \Big[[\lambda_1(i+1,n) - \lambda_1(i,n)] F^w(i+\tfrac{1}{2},n) k_{rw}(i+\tfrac{1}{2},n) + [\lambda_2(i+1,n) - \lambda_2(i,n)] F^o(i+\tfrac{1}{2},n) k_{ro}(i+\tfrac{1}{2},n) \Big] \Big\} \tag{G.29}$$

Estimation of the Porosity

The derivation for the derivative of the objective function with respect to the porosity closely parallels the previous derivation. We note the differences here.

The reservoir is taken to be slightly compressible so that we consider only perturbations $\delta\phi(i)$, rather than $\delta\phi(i,n)$. The first-order variational equation will be exactly the same as Eq. G.12 with the exception that the terms which contain perturbations $\delta K_{i+\frac{1}{2}}$ (the ninth and tenth terms in Eq. G.12) will be replaced with a term containing the perturbations $\delta\phi(i)$,

After the adjoint variables are specified as in Eq. G.26 - 28, the following is obtained:

$$\frac{\delta J}{\delta \phi(i)} = \sum_{n=0}^{N-1} \Big\{ \lambda_1(i,n) D^w(i,n) \Big[C_w S(i,n) [P(i,n+1) - P(i,n)] + [S(i,n+1) - S(i,n)] \Big] + \lambda_2(i,n) D^o(i,n) \Big[C_o [1-S(i,n)] [P(i,n+1) - P(i,n)] - [S(i,n+1) - S(i,n)] \Big] \Big\} \tag{G.30}$$

where $$D^{\ell} = \frac{v}{(t^{n+1} - t^n) B_{\ell}(i,n)}$$

Estimation of Relative Permeabilities

The methodology used to estimate the relative permeability parameters γ_j is specified in Appendix F (see Eqs. F.45 and F.46). Note that the variations in k_{rw} and k_{ro} are now given by terms which contain the derivatives of the relative permeability with respect to the parameters γ_j (see Eqs. F.48 and F.49). The perturbation in the function g(i,n) is given by

$$\delta g(i,n) = g'(i,n) \delta S(i,n) + \sum_j \left(\frac{\partial g}{\partial \gamma_j} \delta \gamma_j \right) \tag{G.31}$$

The first-order variation of J in Eq. G.3, previously given by Eq. G.11, will now be:

$$\delta J = -2 \sum_{n=0}^{N-1} \sum_{i=1}^{NX} \Big\{ \sum_{\xi} \sum_{\tau} [P^{obs}(i_\xi, n_\tau) - P(i_\xi, n_\tau)] \delta P(i,n+1) \delta(i,i_\xi) \delta(n+1,n_\tau) + \omega \sum_{\beta} \sum_{\theta} [R^{obs}(i_\beta, n_\theta) - R(i_\beta, n_\theta)] \Big[R' \delta S(i,n+1) + \sum_j \left(\frac{\partial R}{\partial \gamma_j} \delta \gamma_j \right) \Big] \delta(i,i_\beta) \delta(n+1,n_\theta) \Big\} \tag{G.32}$$

The first-order variational equation will be exactly the same as Eq. G.12 with the exception that terms containing perturbations in $\delta K_{i+\frac{1}{2}}$ will be replaced with the following term containing perturbations $\delta\gamma_j$:

$$\sum_{n=0}^{N-1}\sum_{i=1}^{NX}\sum_{j}\Bigg\{\left[\lambda_2(i,n) - \lambda_1(i,n)\right]\sum_{m} Q_m \left(\frac{\partial g^{n+1}}{\partial\gamma_j}\right)\delta(i,i_m)$$

$$- \left[P(i+1,n+1) - P(i,n+1)\right]\Bigg[\lambda_1(i,n)F^w(i+\tfrac{1}{2},n)K_{i+\frac{1}{2}}\frac{\partial k_{rw}(i+\frac{1}{2},n)}{\partial\gamma_j}$$

$$+ \lambda_2(i,n)F^o(i+\tfrac{1}{2},n)K_{i+\frac{1}{2}}\frac{\partial k_{ro}(i+\frac{1}{2},n)}{\partial\gamma_j}\Bigg]$$

$$+ \left[P(i,n+1) - P(i-1,n+1)\right]\Bigg[\lambda_1(i,n)F^w(i-\tfrac{1}{2},n)K_{i-\frac{1}{2}}\frac{\partial k_{rw}(i-\frac{1}{2},n)}{\partial\gamma_j}$$

$$+ \lambda_2(i,n)F^o(i-\tfrac{1}{2},n)K_{i-\frac{1}{2}}\frac{\partial k_{ro}(i-\frac{1}{2},n)}{\partial\gamma_j}\Bigg]$$

$$- 2\omega\sum_{\beta}\sum_{\theta}\left[R^{obs}(i_\beta,n_\theta) - R(i_\beta,n_\theta)\right]\frac{\partial R}{\partial\gamma_j}\,\delta(i,i_\beta)\delta(n+1,n_\theta)\Bigg\}\delta\gamma_j \qquad (G.33)$$

We now rewrite the terms in Eq. G.33 which contain the derivatives of the relative permeabilities in order to specify the grid block for which these terms are evaluated. Similarly to Eq. G.19, we write the following expression for the derivative of the relative permeability:

$$\frac{\partial k_{r\ell}(i-\frac{1}{2},n)}{\partial\gamma_j} = \alpha^n_{i-\frac{1}{2}}\frac{\partial k_{r\ell}(i-1,n)}{\partial\gamma_j} + \left(1-\alpha^n_{i-\frac{1}{2}}\right)\frac{\partial k_{r\ell}(i,n)}{\partial\gamma_j} \qquad (G.34)$$

where $\alpha^n_{i-\frac{1}{2}} = 1$ if $P(i-1,n) \geq P(i,n)$

$= 0$ otherwise

Using Eq. G.34 and the boundary conditions given by Eq. G.21, the following identity is obtained:

$$\sum_{n=0}^{N-1}\sum_{i=1}^{NX}\left\{[P(i,n+1) - P(i-1,n+1)]\left[\lambda_1(i,n)F^w(i-\tfrac{1}{2},n)K_{i-\frac{1}{2}}\frac{\partial k_{rw}(i-\frac{1}{2},n)}{\partial \gamma_j}\right.\right.$$

$$\left.\left. + \lambda_2(i,n)F^o(i-\tfrac{1}{2},n)K_{i-\frac{1}{2}}\frac{\partial k_{ro}(i-\frac{1}{2},n)}{\partial \gamma_j}\right]\right\}$$

$$= \sum_{n=0}^{N-1}\sum_{i=1}^{NX}\left\{[P(i+1,n+1) - P(i,n+1)]\left[\alpha^n_{i+\frac{1}{2}}\lambda_1(i+1,n)F^w(i+\tfrac{1}{2},n)\frac{\partial k_{rw}(i,n)}{\partial \gamma_j}\right.\right.$$

$$\left. + \lambda_2(i+1,n)F^o(i+\tfrac{1}{2},n)\frac{\partial k_{ro}(i,n)}{\partial \gamma_j}\right] + \left(1-\alpha^n_{i+\frac{1}{2}}\right)\left[\lambda_1(i,n)F^w(i-\tfrac{1}{2},n)\frac{\partial k_{rw}(i,n)}{\partial \gamma_j}\right.$$

$$\left.\left. + \lambda_2(i,n)F^o(i-\tfrac{1}{2},n)\frac{\partial k_{ro}(i,n)}{\partial \gamma_j}\right]\right\} \qquad \text{(G.35)}$$

Using Eqs. G.34 and G.35 in Eq. G.33, and specifying that the adjoint variables satisfy Eqs. G.26-G.28, the following expression can be obtained for the derivative of the objective function with respect to the parameter γ_j:

$$\frac{\delta \bar{J}}{\delta \gamma_j} = \sum_{n=0}^{N-1}\sum_{i=1}^{NX}\left\{[\lambda_2(i,n) - \lambda_1(i,n)]\sum_m Q_m\left(\frac{\partial g^{n+1}}{\partial \gamma_j}\right)\delta(i,i_m)\right.$$

$$+ [P(i+1,n+1) - P(i,n+1)]K_{i+\frac{1}{2}}\left[\alpha^n_{i+\frac{1}{2}}[\lambda_1(i+1,n) - \lambda_1(i,n)]F^w(i+\tfrac{1}{2},n)\frac{\partial k_{rw}(i,n)}{\partial \gamma_j}\right.$$

$$+ \alpha^n_{i+\frac{1}{2}}[\lambda_2(i+1,n) - \lambda_2(i,n)]F^o(i+\tfrac{1}{2},n)\frac{\partial k_{ro}(i,n)}{\partial \gamma_j}$$

$$\left. + \left(1-\alpha^n_{i+\frac{1}{2}}\right)[\lambda_1(i+1,n) - \lambda_1(i,n)]F^w(i+\tfrac{1}{2},n)\frac{\partial k_{rw}(i+1,n)}{\partial \gamma_j}\right.$$

$$+\left(1-\alpha^{n}_{i+\frac{1}{2}}\right)\left[\lambda_2(i+1,n)-\lambda_2(i,n)\right]F^{o}(i+\tfrac{1}{2},n)\frac{\partial k_{ro}(i+1,n)}{\partial \gamma_j}\Bigg]$$

$$-2\omega\sum_{\beta}\sum_{\theta}\left[R^{obs}(i_\beta,n_\theta)-R(i_\beta,n_\theta)\right]\frac{\partial R}{\partial \gamma_j}\delta(i,i_\beta)\delta(n+1,n_\theta)\Bigg\} \qquad (G.36)$$

Specification of Adjoint System for Two-Dimensions

Here we specify the system of equations which are used to determine the derivatives of the objective function with respect to the reservoir parameters. First we will specify the linear system which is used to solve for the adjoint variables λ_1 and λ_2.

For a finite-difference grid consisting of NX and NY grid blocks in the x and y directions, respectively, we define a single index k to refer to the grid block at location i,j. The index k is defined by Eq. B.1. Using this index, the linear equations for the adjoint variables λ_1 and λ_2 for grid block k can be written in the following form:

$$CA_k\lambda_1(k,n-1)+CB_k\lambda_2(k,n-1) = C_k \qquad (G.37)$$

$$DA_{k-NX}\lambda_1(k-NX,n-1)+DB_{k-NX}\lambda_2(k-NX,n-1)+DA_{k-1}\lambda_1(k-1,n-1)$$

$$+DB_{k-1}\lambda_2(k-1,n-1)+DA_k\lambda_1(k,n-1)+DB_k\lambda_2(k,n-1)+DA_{k+1}\lambda_1(k+1,n-1)$$

$$+DB_{k+1}\lambda_2(k+1,n-1)+DA_{k+NX}\lambda_1(k+NX,n-1)+DB_{k+NX}\lambda_2(k+NX,n-1)=D_k$$

$$(G.38)$$

Eq. G.37 represents the terms which multiply the variation $\delta S(i,j,n)$ in the equation for two dimensions which is analogous to Eq. G.25. Similarly,

Eq. G.38 are those terms which multiply the variation $\delta P(k,j,n)$. The terms in these equations are as follows:

$$CA_k = M^w(k,n-1) - \sum_m Q_m(g')^n \delta(k,k_m) \tag{G.39}$$

$$CB_k = -M^o(k,n-1) + \sum_m Q_m(g')^n \delta(k,k_m) \tag{G.40}$$

$$\begin{aligned}
C_k = {} & \lambda_2(k,n)M^o(k,n)\left[C_o[P(k,n+1) - P(k,n)] - 1\right] \\
& - \lambda_1(k,n)M^w(k,n)\left[C_w[P(k,n+1 - P(k,n)] - 1\right] \\
& - [P(k+1,n+1) - P(k,n+1)]K_{i+\frac{1}{2},j}\,\alpha^n_{i+\frac{1}{2},j}\Big[[\lambda_1(k+1,n) - \lambda_1(k,n)]F^w(i+\tfrac{1}{2},j,n) \\
& \quad k'_{rw}(k,n) + [\lambda_2(k+1,n) - \lambda_2(k,n)]F^o(i+\tfrac{1}{2},j,n)k'_{ro}(k,n)\Big] \\
& - [P(k,n+1) - P(k-1,n+1)]K_{i-\frac{1}{2},j}\left(1-\alpha^n_{i-\frac{1}{2},j}\right)\Big[[\lambda_1(k,n) - \lambda_1(k-1,n)]F^w(i-\tfrac{1}{2},j,n) \\
& \quad k'_{rw}(k,n) + [\lambda_2(k,n) - \lambda_2(k-1,n)]F^o(i-\tfrac{1}{2},j,n)k'_{ro}(k,n)\Big] \\
& - [P(k+NX,n+1) - P(k,n+1)]K_{i,j+\frac{1}{2}}\,\alpha^n_{i,j+\frac{1}{2}}\Big[[\lambda_1(k+NX,n) \\
& - \lambda_1(k,n)]F^w(i,j+\tfrac{1}{2},n)k'_{rw}(k,n) + [\lambda_2(k+NX,n) - \lambda_2(k,n)]F^o(i,j+\tfrac{1}{2},n)k'_{ro}(k,n)\Big] \\
& - [P(k,n+1) - P(k-NX,n+1)]K_{i,j-\frac{1}{2}}\left(1- \alpha^n_{i,j-\frac{1}{2}}\right)\Big[[\lambda_1(k,n) \\
& - \lambda_1(k-NX,n)]F^w(i,j-\tfrac{1}{2},n)k'_{rw}(k,n) + [\lambda_2(k,n) - \lambda_2(k-NX,n)] \\
& \quad F^o(i,j-\tfrac{1}{2},n)k'_{ro}(k,n)\Big] \\
& - 2\omega \sum_\beta \sum_\theta [R^{obs}(k_\beta,n_\theta) - R(k_\beta,n_\theta)]R'\delta(k,k_\beta)\delta(n,n_\theta)
\end{aligned} \tag{G.41}$$

$$DA_{k-NX} = - T^w(i,j-\tfrac{1}{2},n-1) \tag{G.42}$$

$$DB_{k-NX} = -T^{O}(i,j-\tfrac{1}{2},n-1) \tag{G.43}$$

$$DA_{k-1} = -T^{W}(i-\tfrac{1}{2},j,n-1) \tag{G,44}$$

$$DB_{k-1} = -T^{O}(i-\tfrac{1}{2},j,n-1) \tag{G.45}$$

$$DA_{k} = M^{W}(k,n-1)C_{w}S(k,n-1) + T^{W}(i-\tfrac{1}{2},j,n-1) + T^{W}(i+\tfrac{1}{2},j,n-1) + T^{W}(i,j-\tfrac{1}{2},n-1) + T^{W}(i,j+\tfrac{1}{2},n-1) \tag{G.46}$$

$$DB_{k} = M^{O}(k,n-1)C_{o}[1-S(k,n-1)] + T^{O}(i-\tfrac{1}{2},j,n-1) + T^{O}(i+\tfrac{1}{2},j,n-1) + T^{O}(i,j-\tfrac{1}{2},n-1) + T^{O}(i,j+\tfrac{1}{2},n-1) \tag{G.47}$$

$$DA_{k+1} = -T^{W}(i+\tfrac{1}{2},j,n-1) \tag{G.48}$$

$$DB_{k+1} = -T^{O}(i+\tfrac{1}{2},j,n-1) \tag{G.49}$$

$$DA_{k+NX} = -T^{W}(i,j+\tfrac{1}{2},n-1) \tag{G.50}$$

$$DB_{k+NX} = -T^{O}(i,j+\tfrac{1}{2},n-1) \tag{G.51}$$

$$D_{k} = \lambda_{1}(k,n)M^{W}(k,n)C_{w}S(i,n) + \lambda_{2}(k,n)M^{O}(k,n)C_{o}[1-S(k,n)] + 2\sum_{\xi}\sum_{\tau}[P^{obs}(k_{\xi},n_{\tau}) - P(k_{\xi},n_{\tau})]\delta(k,k_{\xi})\delta(n,n_{\tau}) \tag{G.52}$$

Using the reflection boundary conditions for λ_1 and λ_2, the following system specifies the adjoint variables:

$$\bar{\underset{\sim}{A}}\,\underset{\sim}{\Lambda} = \bar{\underset{\sim}{b}} \qquad n = N-1,N-2,\ldots,= 0 \tag{G.53}$$

The solution vector $\underset{\sim}{\Lambda}$ is given by:

$$\underset{\sim}{\Lambda} = [\lambda_{1}(1,n-1)\ \lambda_{2}(1,n-1)\ \lambda_{1}(2,n-1)\ \cdots\ \lambda_{1}(k,n-1)\ \lambda_{2}(k,n-1)\ \cdots\ \lambda_{1}(NXY,n-1)\ \lambda_{2}(NXY,n-1)]^{T}$$

where NXY is the product of NX and NY. The (2NXY) x (2NXY) matrix $\bar{\underset{\sim}{A}}$ can

be written as:

$$\bar{\bar{A}} = \begin{bmatrix} \alpha_{1,1} & \alpha_{1,2} & \cdots & \alpha_{1,NXY} \\ \alpha_{2,1} & & & \vdots \\ \vdots & & & \\ \alpha_{NXY,1} & & & \alpha_{NXY,NXY} \end{bmatrix}$$

where each $\alpha_{k,\ell}$ is a 2x2 matrix defined as:

$$\alpha_{k,\ell} = \begin{bmatrix} CA_k & CB_k \\ DA_k & DB_k \end{bmatrix} \quad \text{for } \ell = k$$

$$= \begin{bmatrix} 0 & 0 \\ DA_\ell & DB_\ell \end{bmatrix} \quad \text{for } \ell = k+1, k-1, k+NX, \text{ or } k-NX$$

$$= \begin{bmatrix} 0 & 0 \\ 0 & 0 \end{bmatrix} \quad \text{otherwise}$$

The vector $\bar{\bar{b}}$ can be written as :

$$\bar{\bar{b}} = \left[\beta_1 \ \beta_2 \ \cdots \ \beta_{NXY}\right]^T$$

where the β_k are vectors with dimension 2x1 defined as:

$$\beta_k = \begin{bmatrix} C_k \\ D_k \end{bmatrix}$$

The derivatives with respect to the reservoir parameters are given as follows:

$$\frac{\delta \bar{J}}{\delta K_{i+\frac{1}{2},j}} = \sum_{n=0}^{N-1} \Big\{ [P(k+1,n+1) - P(k,n+1)] \left[[\lambda_1(k+1,n) - \lambda_1(k,n)] \right.$$

$$T^w(i+\tfrac{1}{2},j,n)k_{rw}(i+\tfrac{1}{2},j,n) + [\lambda_2(k+1,n) - \lambda_2(k,n)]T^o(i+\tfrac{1}{2},j,n)k_{ro}(i+\tfrac{1}{2},j,n)\Big]\Big\} \tag{G.54}$$

$$\frac{\delta \bar{J}}{\delta K_{i,j+\frac{1}{2}}} = \sum_{n=0}^{N-1} \Big\{[P(k+NX,n+1) - P(k,n+1)]\Big[[\lambda_1(k+NX,n) - \lambda_1(k,n)]$$

$$T^w(i,j+\tfrac{1}{2},n)k_{rw}(i,j+\tfrac{1}{2},n) + [\lambda_2(k+NX,n) - \lambda_2(k,n)]$$

$$T^o(i,j+\tfrac{1}{2},n)k_{ro}(i,j+\tfrac{1}{2},n)\Big]\Big\} \tag{G.55}$$

$$\frac{\delta \bar{J}}{\delta \phi(k)} = \sum_{n=0}^{N-1} \Big\{\lambda_1(k,n)D^w(k,n)\Big[C_w S(k,n)[P(k,n+1) - P(k,n)] + [S(k,n+1) - S(k,n)]\Big]$$

$$+ \lambda_2(k,n)D^o(k,n)\Big[C_o[1-S(k,n)][P(k,n+1) - P(k,n)]$$

$$- [S(k,n+1) - S(k,n)]\Big]\Big\} \tag{G.56}$$

$$\frac{\delta \bar{J}}{\delta \gamma_\ell} = \sum_{n=0}^{N-1}\sum_{k=1}^{NXY}\Big\{[\lambda_2(k,n) - \lambda_1(k,n)]\sum_m Q_m\left(\frac{\partial g^{n+1}}{\partial \gamma_\ell}\right)\delta(k,k_m)$$

$$+ [P(k+1,n+1) - P(k,n+1)]K_{i+\frac{1}{2},j}\Big[\alpha^n_{i+\frac{1}{2},j}[\lambda_1(k+1,n) - \lambda_1(k,n)]$$

$$F^w(i+\tfrac{1}{2},j,n)\frac{\partial k_{rw}(k,n)}{\partial \gamma_\ell} + \alpha^n_{i+\frac{1}{2},j}[\lambda_2(k+1,n) - \lambda_2(k,n)]$$

$$F^o(i+\tfrac{1}{2},j,n)\frac{\partial k_{ro}(k,n)}{\partial \gamma_\ell} + \left(1-\alpha^n_{i+\frac{1}{2},j}\right)[\lambda_1(k+1,n) - \lambda_2(k,n)]$$

$$F^w(i+\tfrac{1}{2},j,n)\frac{\partial k_{rw}(k+1,n)}{\partial \gamma_\ell} + \left(1-\alpha^n_{i+\frac{1}{2},j}\right)[\lambda_2(k+1,n) - \lambda_2(k,n)]$$

$$F^o(i+\tfrac{1}{2},j,n)\frac{\partial k_{ro}(k+1,n)}{\partial \gamma_\ell}\Big]$$

$$+ [P(k+NX,n+1) - P(k,n+1)]K_{i,j+\frac{1}{2}} \left[\alpha^{n}_{i,j+\frac{1}{2}} [\lambda_1(k+NX,n) - \lambda_1(k,n)] \right.$$

$$F^{w}(i,j+\tfrac{1}{2},n) \frac{\partial k_{rw}(k,n)}{\partial \gamma_{\ell}} + \alpha^{n}_{i,j+\frac{1}{2}} [\lambda_2(k+NX,n) - \lambda_2(k,n)]$$

$$F^{o}(k,j+\tfrac{1}{2},n) \frac{\partial k_{ro}(k,n)}{\partial \gamma_{\ell}} + \left(1-\alpha^{n}_{i,j+\frac{1}{2}}\right) [\lambda_1(k+NX,n) - \lambda_2(k,n)]$$

$$F^{w}(i,j+\tfrac{1}{2},n) \frac{\partial k_{rw}(k+NX,n)}{\partial \gamma_{\ell}} + \left(1-\alpha^{n}_{i,j+\frac{1}{2}}\right) [\lambda_2(k+NX,n) - \lambda_2(k,n)]$$

$$\left. F^{o}(i,j+\tfrac{1}{2},n) \frac{\partial k_{ro}(k+NX,n)}{\partial \gamma_{\ell}} \right]$$

$$\left. - 2\omega \sum_{\beta} \sum_{\theta} [R^{obs}(k_{\beta},n_{\tau}) - R(k_{\beta},n_{\theta})] \frac{\partial R}{\partial \gamma_{\ell}} \delta(k,k_{\beta}) \delta(n+1,n_{\theta}) \right\} \qquad (G.57)$$

APPENDIX H. Specification of the Minimization Algorithm

The method of steepest descent is used to iteratively update the parameter estimates. This method is easily demonstrated by the following. We represent the parameters to be estimated as a vector $\underset{\sim}{\pi}$. Expanding the objective function corresponding to the $\ell+1^{th}$ iteration in a first-order Taylor series, the following is obtained:

$$J^{\ell+1}(\underset{\sim}{\pi}) = J^{\ell}(\underset{\sim}{\pi}) + (\underset{\sim}{\pi}^{\ell+1} - \underset{\sim}{\pi}^{\ell})^T \frac{\partial J^{\ell}}{\partial \underset{\sim}{\pi}} \qquad (H.1)$$

Thus, in order to minimize J, the $\ell+1^{th}$ estimate is calculated from the ℓ^{th} estimate by the following relation:

$$\underset{\sim}{\pi}^{\ell+1} = \underset{\sim}{\pi}^{\ell} - \alpha \frac{\partial J^{\ell}}{\partial \underset{\sim}{\pi}} \qquad (H.2)$$

where the positive scaler α is the iteration step size.

For problems in which one type of reservoir parameter is to be estimated — i.e., the permeability alone, the porosity alone, or the relative permeability coefficients alone — the vector $\underset{\sim}{\pi}$ is composed of the reservoir parameter itself. For example, if the values of porosity corresponding to each of M grid blocks are to be estimated, then

$$\underset{\sim}{\pi} = [\phi(1)\ \phi(2)\ \ldots\ \phi(M)]^T$$

The evaluation of the gradient $\frac{\partial J}{\partial \underset{\sim}{\pi}}$ is specified in Appendix G. To use zonation, the vector $\underset{\sim}{\pi}$ consists of one parameter value corresponding to each zone. The derivative of the objective function with respect to each zone is the sum of the derivatives for each grid block in that zone.

For problems in which different types of reservoir parameters are estimated, dimensionless parameters are estimated. These parameters are the values of the reservoir properties normalized by the ℓ^{th} estimate.

For example, the dimensionless parameter η_i associated with the value of porosity at the i^{th} grid block would be defined as:

$$\eta_i = \frac{\phi(i)}{\phi(i)^{\ell}} \tag{H.3}$$

From Eq. H.2, the following is obtained for the calculation of the parameter τ_i at the $\ell+1^{th}$ iteration:

$$\eta_i^{\ell+1} = \eta_i^{\ell} - \alpha \frac{\partial J^{\ell}}{\partial \eta} \tag{H.4}$$

Multiplying Eq. H.4 by the value $\phi(i)^{\ell}$, we obtain the following expression to update the parameter $\phi(i)$:

$$\phi(i)^{\ell+1} = \phi(i)^{\ell} - \alpha[\phi(i)^{\ell}]^2 \frac{\partial J^{\ell}}{\partial \phi(i)} \tag{H.5}$$

We note that the estimation of dimensionless parameters which can be defined similarly to that given here have been used by Jahns[24] for a single-phase problem.

The iteration step size α is chosen so that the largest change in any reservoir parameter value is the fraction β, which is initially specified as 0.1. When new parameter values lead to an increase in the objective function, β is multiplied by 0.6, and the new parameter estimates are then recalculated.

We now summarize the steps taken for one iteration of the algorithm:

(1) Solve the simulator equations using the ℓ^{th} estimate of the reservoir parameters,

(2) Calculate J^{ℓ},

(3) Solve the adjoint system and evaluate the gradient of J, and

(4) Update the parameter estimates using the method of steepest descent.

These steps are repeated until some termination criterion is met. The criterion used is a minimum acceptable value of J, or a total number of iterations.